Report
P-17-30
April 2020

Task description of Task 9B – Modelling of LTDE-SD performed at Äspö HRL

Task 9 of SKB Task Force GWFTS – Increasing the realism in solute transport modelling based on the field experiments REPRO and LTDE-SD

Martin Löfgren
Kersti Nilsson

SVENSK KÄRNBRÄNSLEHANTERING AB

SWEDISH NUCLEAR FUEL
AND WASTE MANAGEMENT CO

Box 3091, SE-169 03 Solna
Phone +46 8 459 84 00
skb.se

SVENSK KÄRNBRÄNSLEHANTERING

ISSN 1651-4416
SKB P-17-30
ID 1628769

April 2020

Task description of Task 9B – Modelling of LTDE-SD performed at Äspö HRL

Task 9 of SKB Task Force GWFTS – Increasing the realism in solute transport modelling based on the field experiments REPRO and LTDE-SD

Martin Löfgren, Niressa AB

Kersti Nilsson, Geosigma AB

Keywords: Taskforce GWFTS, LTDE-SD, Äspö Hard Rock Laboratory, Matrix diffusion, Sorption, Rock matrix.

This report concerns a study which was conducted for Svensk Kärnbränslehantering AB (SKB). The conclusions and viewpoints presented in the report are those of the authors. SKB may draw modified conclusions, based on additional literature sources and/or expert opinions.

Data in SKB's database can be changed for different reasons. Minor changes in SKB's database will not necessarily result in a revised report. Data revisions may also be presented as supplements, available at www.skb.se.

A pdf version of this document can be downloaded from www.skb.se.

© 2020 Svensk Kärnbränslehantering AB

Abstract

This report concerns Task 9 of the SKB Task Force GWFTS – Increasing the realism in solute transport modelling – Modelling the field experiments of REPRO and LTDE-SD. The purpose of this report is to publish the suite of Task 9B descriptions, as well as accompanying data deliveries, in the open literature. These documents have previously been distributed to the modelling groups of Task 9.

Task 9B concerns the inverse and predictive modelling of tracer penetration profiles of the Long-Term Diffusion Experiment – Sorption Diffusion (LTDE-SD). This in-situ tracer test was carried out within Äspö Hard Rock Laboratory, at about 410 m depth, by SKB and contractors. The main in-situ test was carried out in years 2006-2007. The suite of Task 9B descriptions gives the prerequisites of the experiments; accompanying in-situ and laboratory data on rock properties; and guidance on the inverse and predictive modelling of the tracer penetration profiles. The actual modelling within Task 9B is not presented here but is reported in separate publications.

Sammanfattning

Den här rapporten behandlar Task 9 inom ramen för SKB Task Force GWFTS – Förbättring av realismen vid transportmodellering av lösta ämnen – Modellering av fältexperimenten REPRO och LTDE-SD. Syftet med denna rapport är att publicera en serie modelleringsbeskrivningar för Task 9B, samt de medföljande dataleveranserna, i den öppna litteraturen. Dessa dokument har tidigare distribuerats till modelleringsgrupperna i Task 9.

Task 9B berör invers och prediktiv modellering av penetrationsprofilera i in-situ experimentet LTDE-SD (Long-Term Diffusion Experiment – Sorption Diffusion). Detta spårämnesförsök har utförts i Äspölaboratoriet på ca 410 m djup, av SKB och konsulter. Huvudförsöket ägde rum in-situ mellan år 2006 och 2007. Serien av modelleringsbeskrivningar för Task 9B ger förutsättningarna för experimenten, kompletterande in-situ och laborativa data gällande berget, samt vägledning angående den inversa och prediktiva modelleringen av penetrationsprofilerna. Den faktiska modelleringen inom Task 9B presenteras inte här utan i separata publikationer.

Contents

1 Introduction

1.1 Background to Task 9B

Task 9 is part of the SKB Task Force on Modelling of Groundwater Flow and Transport of Solutes (Task Force GWFTS), which focuses on the fractured crystalline host rock surrounding present and future repositories for spent fuel and other radioactive waste. Special interest is taken in work on fracture flow and solute transport made at the Äspö Hard Rock Laboratory (HRL) in Sweden.

The title of Task 9 is "Increasing the realism in solute transport modelling – Modelling the field experiments of REPRO and LTDE-SD". The task focuses on the realistic modelling of coupled matrix diffusion and sorption in the heterogeneous crystalline rock matrix at depth. This is done in the context of inverse and predictive modelling of tracer concentrations of the in-situ experiments performed within LTDE-SD at the Äspö HRL in Sweden, as well as within the REPRO project at ONKALO in Finland, focusing on sorption and diffusion. The ultimate aim is to develop models that in a more realistic way represent retardation in the natural rock matrix at depth. The following waste management organisations are part of Task 9:

- Svensk Kärnbränslehantering AB, SKB, Sweden
- Bundesministerium für Wirtschaft und Technologie, BMWi, Germany
- Japan Atomic Energy Agency, JAEA, Japan
- Korea Atomic Energy Research Institute. KAERI, South Korea
- Posiva Oy, Finland
- Department of Energy, DOE, USA
- Radioactive Waste Repository Authority (RAWRA), SURAO, Czech Republic

These waste management organisations assign modelling groups that perform the actual modelling within Task 9.

Task 9B is the second subtask within Task 9 and focuses on inverse and predictive modelling of experimental results from the in-situ tracer test LTDE-SD. The experiment was carried out using radioactive tracers at a depth of about 410 m below sea level within the Äspö Hard Rock Laboratory in Sweden by Geosigma AB, under the conduit of SKB. It is one of few recent in-situ studies focusing on tracer transport in the stagnant pore water of the crystalline rock matrix.

Task 9B was initiated at the Task Force meeting #33 in Kalmar, Sweden, in October 2015. It has been organised into the inverse modelling subtasks Task 9B-1 and 9B-2, as well as in the predictive modelling subtask Task 9B-3. The framework of Task 9B was first established by the Technical Committee of Task 9, including:

- Jan-Olof Selroos, Svensk Kärnbränslehantering AB,
- Björn Gylling, Svensk Kärnbränslehantering AB,
- Lasse Koskinen, Posiva Oy,
- Martin Löfgren, Niressa AB,
- Kersti Nilsson, Geosigma AB,
- Antti Poteri, VTT Technical Research Centre of Finland.

The Scientific Chairman of Task 9:

- Bill Lanyon, Fracture Systems Ltd.

has also been included in the discussion when setting up the framework. The subtasks were thereafter detailed in a suite of three task descriptions, with accompanying data deliveries. These documents are primarily authored by the Principal Investigators Martin Löfgren and Kersti Nilsson but with

valuable input from the technical committee; Bill Lanyon; Johan Byegård; Erik Gustafsson; and Henrik Drake. The setup of Task 9B, and the modelling groups' work on the subtasks, is evaluated by the Task 9 Evaluator:

- Josep Maria Soler Matamala, IDAEA-CSIC

The outcome of Task 9B is reported in separate SKB reports, and/or other publications, prepared by the modelling groups and the Task 9 Evaluator.

1.2 Guide to this report

This report compiles the suite of task descriptions of Task 9B, as well as their appendices and accompanying data deliveries. The five main chapters of the Task 9B-1 description are found in Chapters 2 to 6 of this present report. The main chapters of the Task 9B-2 and 9B-3 descriptions are found in Chapters 7 to 9 and Chapters 10 to 13, respectively. Appendices and accompanying data deliveries that are partly or fully included in Appendices 1 to 9 are indicated in Table 1-1.

Table 1-1. Mapping of task descriptions and data deliveries included in this report.

Delivery number	Description of data delivery	Degree of inclusion	Chapter or appendix in this report, and comment
#1	Task 9B-1 description, main chapters	Fully included, with revisions	Chapters 2 to 6, with revisions according to delivery #7 and #11.
#11	Task 9B-2 description, main chapters	Fully included	Chapters 7 to 9.
#16	Task 9B-3 description, main chapters	Fully included	Chapters 10 to 13.
#7	Errata for Task Description 9B-1	Revisions included	Revisions incorporated directly in Table 4-7, Table 4-14 and Table 4-15.
#8	Task 9B-1: Additional information on timeline, core storage and decay correction.	Fully included	Appendix 1
#11	Task 9B-2: Rock matrix data	Partly included	Appendix 2. Data tabulated in Chapter 4 (not revised) are duplicated from revision in delivery #29.
#11	Task 9B-2: Tracer cocktail data	Fully included	Appendix 3.
#11	Task 9B-2: Accompanying data	Fully included	Appendix 4
#12	Task 9B-2: Geological characterisation of D-cores	Partly included	Appendix 5. Only D6 included, as all other D-cores are reported in Nilsson et al. (2010).
#14	Task 9B-2: Geological description of a piece of rock from the LTDE-SD site.	Fully included	Appendix 6
#17	Task 9B-2: Update on injected activity of Na-22	Fully included	Appendix 7
#16	Task 9B-3 description, Appendix 1	Fully included	Appendix 8. Geological characterisation of core samples A4, A11, A13, D15, and D16.
#21	Task 9B: Discussion on artefacts in LTDE-SD	Fully included	Appendix 9
#24	Task 9B-2: Accompanying data	Fully included	Appendix 4, Tables A4-2 to A4-7
#29	Memo part 1: Updated reporting and detection limits	Partly included	All revised data are included in Appendix 2
#33	Updated Rock Matrix data	Fully included	Appendix 2
#35	Memo part 2: Risk of contamination during rock sampling in the LTDE-SD experiment	Fully included	Appendix 12
#40	Updated Rock Matrix data	Fully included	Appendix 2

A number of appendices or data deliveries have been omitted from this report, as indicated in Table 1-2. The omitted information concerns:

- Geological characterisations of the LTDE-SD core samples that are already published in Nilsson et al. (2010, Appendix 3).
- Tabulated data of a great number of rows (but where plots of the data are reported).
- Preliminary versions of documents, where the final versions are provided in this report.
- Information of administrative character.

Table 1-2. Documents and data deliveries omitted from report.

Delivery number	Description of data delivery	Degree of inclusion	Comment
#1	Task 9B-1 description, Appendix A	Not included	This concerns a list of revision from an early draft of the Task 9B-1 description.
#5	Task Description 9B-1 Appendix 1	Not included	Geological characterisations of core sample A6, A9, D12, and D13 that are already reported in Nilsson et al. 2010).
#6	Evolution of pH and Eh in LTDE-SD	Not included	34 172 rows of tabulated Eh and pH data of the tracer cocktail vs. experimental time. Plots of the data are reported in Widestrand et al. (2010b, Figures A7-1 and A7-2).
#9	Task 9B-2 description, preliminary version	Not included	The final version of data delivery #11 is instead included.
#12	Task 9B-2. Geological characterisation of A-cores.	Not included	Geological characterisations of A-cores that are already reported in Nilsson et al. (2010).
#13	Instructions for producing manuscript	Not included	Information of administrative nature.
#27	Draft SKB Report P-16-12	Not included	Data delivery due to difficulty to know when the report was to be published
#28	Pre-memo Revised background tracer concentrations	Not included	New information about background concentrations included in data tables at delivery #29

The pieces of information in Table 1-1 and Table 1-2 have been delivered at different times to the modellers. This has been done via data deliveries on the SKB Task Force website, where each data delivery is numbered. A few of the delivered documents feature separate reference lists. In this present report, however, a single reference list is compiled.

Three more deliveries and corrected data have been added to this Task Description:

- A measure of the length of the PU cylinder has been added in Appendix 4, Figure A4-3.
- Figures of the pressures in the experiment and surrounding drillhole sections have been added in Appendix 10.
- Appendix 11, Concerning mass balances in LTDE-SD and potentially underestimated sorption.
- Data for activities in PEEK tubings have been updated in Table A4-3 of Appendix 4.

The main chapters of the task descriptions have been left mostly unedited, even though they may contain information that is no longer relevant. At the end of concerned sections or chapters, and sometimes even between paragraphs, text boxes with grey background colour are inserted. Within these text boxes, comments on the original text are provided. The text boxes may also contain complementary information and/or links or references to updated information. Allowed changes in the original text of the main chapters generally concern the numbering of chapters, sections, tables, and figures. Revisions have, however, been made in Table 4-7, Table 4-14 and Table 4-15 to reflect the errata in data delivery #7.

The reason for not editing directly in the original text is that the task descriptions can be seen as a set of rules, which have influenced the modellers' decisions in their efforts to carry out Task 9B. Changing the original text can, accordingly, be seen as changing the rules retrospectively.

The information of some data deliveries, for example if consisting of tabulated data in Excel files, has been lightly edited. This has been done with regard to its layout and sometimes by adding some explanatory text. No modifications have been made, however, in regard to the scientific content or the numerical data. However, substituted numerical data are marked in yellow and comments have been added in data tables.

2 9B-1: Introduction

Task 9B will be the second subtask of the Task Force GWFTS Task 9 and will focus on the inverse modelling of experimental results from the in-situ tracer test LTDE-SD (Long Term Sorption Diffusion Experiment). The experiment was carried out using radioactive tracers at a depth of about 410 m below sea level within the Äspö Hard Rock Laboratory in Sweden by Geosigma AB, under the conduit of SKB. It is one of few recent in-situ studies focusing on tracer transport in the stagnant pore water of the crystalline rock matrix.

Task 9B was initiated at the Task Force meeting #33 in Kalmar, Sweden, between the 20th and 22nd of October, 2015. At the same meeting, the first results of Task 9A were presented. As anticipated, different modelling groups had made different progress with Task 9A up until the Kalmar meeting, mainly relating to the point in time when they could start their assignment. Accordingly we assume that some groups are ready to start with Task 9B in late October or early November while others still have substantial work ahead of them with Task 9A prior to initiating Task 9B. For this reason we have decided to divide Task 9B into two parts; Task 9B-1 and 9B-2. While the modelling of Task 9B-1 was formally initiated at the Kalmar meeting, the modelling of Task 9B-2 will have to wait until after the Task Force spring meeting in May, 2016. Most groups should go ahead with the modelling of Task 9B-1 while some groups may need to fully focus on the modelling of Task 9A up until the spring meeting. If more convenient, and in the interest of not falling too far behind, there is also the possibility for newly formed groups to start the entire Task 9 by modelling Task 9B-1.

Comment:
At a later stage the predictive modelling subtask 9B-3 was added.

In any respect, Task 9B-1 will be a subpart of Task 9B-2 and only a limited part of the LTDE-SD experiment is intended to be modelled. The focus will be on the small-scale penetration pattern of a handful of tracers, all which have diffused into the fracture coating and/or the rock matrix surrounding the experimental sections of the LTDE-SD borehole during the ~200 days of exposure to the tracer cocktail. As described in Chapter 3, the rock surrounding the injection hole was over-cored after termination of the experiment and a large number of small core samples were drilled from the over-cored rock volume and analysed with respect to their tracer content. So called A-core samples were drilled from the exposed fracture surface, thus sampling the fracture coating, alteration rim, and underlying rock matrix (see Figure 2-1). So called D-core samples were drilled to intersect the slim hole, thus sampling the unaltered rock matrix.

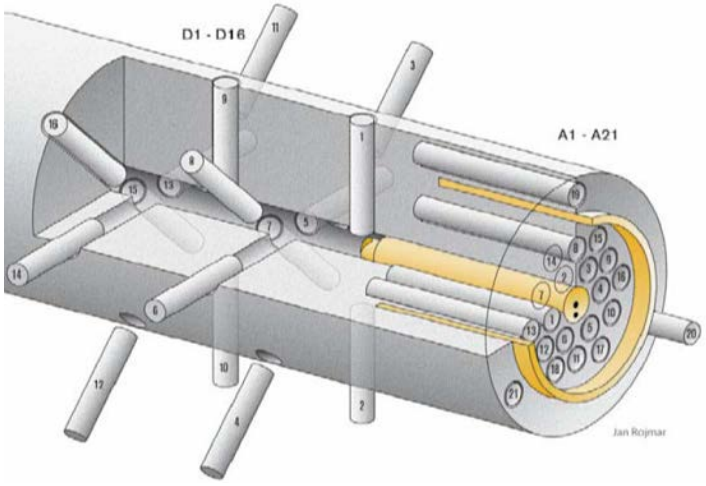

Figure 2-1. *Illustration of drill core samples drilled from the over-cored rock volume. The A-core samples are drilled from the target fracture and the D-core samples correspond to the slim hole.*

Task 9B-1 will focus on only a few of these drill core samples and the inverse modelling of their penetration profiles; extending a few centimetres into the rock matrix. In this respect, the overall scale of the modelling task will be on the mm- to cm-scale. However, considering the heterogeneity of the rock matrix and fracture coating, one could envision setting up models with important structures (pores and minerals grains) on a much smaller scale. In addition, important processes may act on much smaller scales.

The outline of this document is as following. In Chapter 3 we provide a guide to the LTDE-SD campaign and give detailed references to the comprehensive suite of LTDE-SD reports. Chapter 4 provides specifics of Task 9B-1 such as the objectives and critical input data. In addition to this, Chapter 5 provides supporting information and data. In Chapter 6 we look ahead at some tentative objectives of Task 9B-2.

3 9B-1: Guide to the LTDE-SD campaign

The initial planning of the LTDE-SD tracer test was carried out in the late 1990's. Thereafter a few years followed with focus on site characterisation, drilling of boreholes, and pre-testing. The main in-situ tracer test was carried out in 2006-2007 and timelines of the main events are given in Widestrand et al. (2010b, Appendix 4) and Nilsson et al. (2010, Appendix 1). In parallel with the in-situ activities, an extensive laboratory program has been carried through. The LTDE-SD results were finally reported in 2010.

3.1 Planning and preparatory work for the in-situ tracer test

The initial planning of the LTDE-SD tracer test, called LTDE at the time, is outlined in Byegård et al. (1999). The initial objectives were to:

- To investigate the magnitude and extent of diffusion into matrix rock from a natural fracture in situ under natural rock stress conditions and hydraulic pressure and groundwater chemical conditions.
- To obtain data on sorption properties and processes of individual radionuclides on natural fracture surfaces and internal surfaces in the matrix.
- To compare laboratory derived diffusion constants and sorption coefficients for the investigated rock fracture system with the sorption behaviour observed in situ at natural conditions, and to evaluate if laboratory scale sorption results are representative also for larger scales.
- To achieve the above listed objectives a number of prerequisites were listed for the target fracture. This led to the identification of a stable hydraulically conductive fracture (or splay fracture) at a distance of about 10 m from the Äspö HRL tunnel (Winberg et al. 2000, 2003). The fracture identification was made by using the pilot hole KA3065A02.

Thereafter the LTDE-SD experimental borehole KA3065A03 was drilled in close proximity to the pilot borehole (see Figure 3-1). Due to spatial demands of the in-hole equipment, a telescoped experimental borehole was drilled with decreasing diameter, starting with a diameter of 300 mm, which was decreased to 196.5 mm before approaching the target fracture. The approximate location of the target fracture in the experimental borehole had been predicted prior to its drilling based on a structural model and geometric considerations. During the drilling of the experimental borehole, when approaching the target fracture, a number of measurements and observations were made with the aim at reaching the target fracture according to plan (cf. Winberg et al. 2003, Chapter 3). The aim was to drill 50 mm past the fracture surface, thus creating a short core stub. This stub was required in order to pack-off a section of the fracture plane, using a special cup-shaped device, for subsequent performance of the tracer test. However, due to various reasons the drilling continued too far beyond the target fracture, leaving a 16 cm long core stub. The stub surface is located at the borehole length 10.72 m (Winberg et al. 2003, Section 3.2.1).

Based on the concern that the rock matrix in the core stub had become substantially stress released, at least at penetration depths relevant for the experiment, experimental redesigning took place. It was decided to drill a Ø36 mm slim hole through the centre of the core stub. By finding a non-fractured section at a reasonable distance beyond the target fracture, a radial in-diffusion test was planned with diffusion into the unaltered rock matrix (Winberg et al. 2003, Chapter 3). Stress-released conditions in the rock surrounding the slim hole were projected for a narrow rim extending into the borehole wall. This rim was also suspected to be mechanically damaged by the drilling. Such mechanical damaged was observed in the drill core from the 196.5 mm part of the borehole (Li 2001). Later on in the main tracer test, the tracer injection occurred from a 300 mm long packed-off section of the slim hole (Widestrand et al 2010b). The telescoped borehole and its packer systems and tubing are illustrated in Figure 3-2.

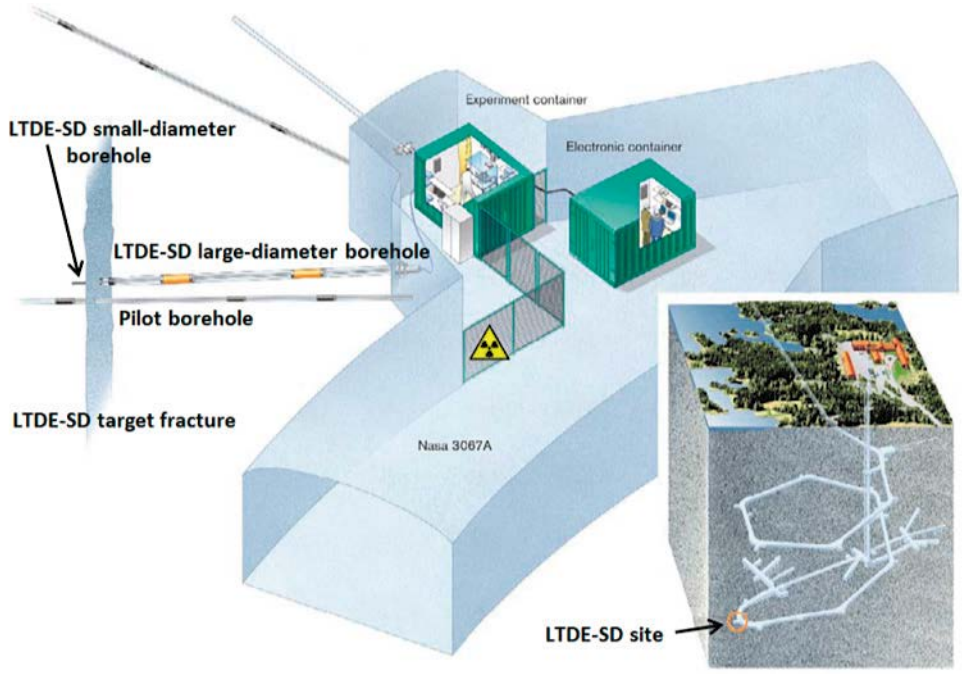

Figure 3-1. *Illustration of the LTDE-SD experimental site showing the pilot and experimental holes.*

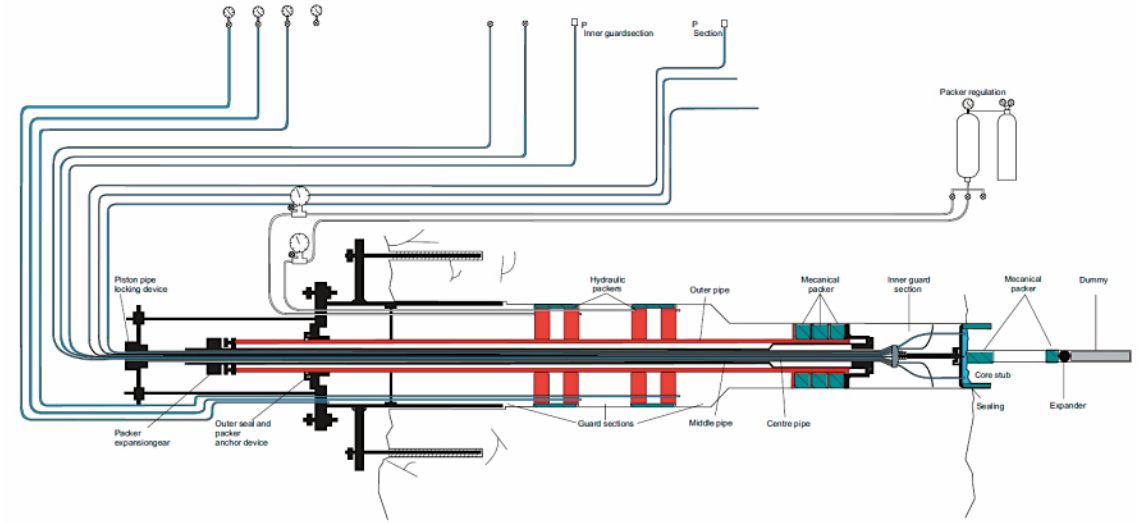

Figure 3-2. *Schematic diagram of the LTDE-SD experimental setup, showing the telescoped borehole of different diameters, as well as the packer system and tubing. The target fracture is indicated by a light blue water mass between the core stub and cup-shaped sealing (reproduced from Widestrand et al. 2010b, Figure 2-1).*

Due to the fact that a slim hole needed to be drilled, and also that hydraulic responses were evident in the target fracture when performing other activities at the Äspö HRL (cf. Wass 2005), the start-up of the main tracer test was delayed as compared to in the original plan. During this delay, a greater consensus came about within the scientific community that matrix diffusion does occur in-situ; also over considerable scales. The importance of demonstrating this within LTDE was hence decreased. As a result, the originally planned duration of the tracer injection of 4 years (Byegård et al. 1999) could be decreased. During the course of planning, an increased focus on in-situ sorption emerged that also included the demonstration that sorption of important radionuclides in a Swedish KBS-3 repository takes place in-situ. Hence, a number of tracers, especially sorbing tracers, were added to the tracer cocktail.

Prior to the main tracer test, between years 2000 and 2004, a number of hydraulic test were performed in the local rock volume; also using stable tracers in dilution and breakthrough tests (cf. Wass 2005). Thereafter a functionality test was carried out in 2005, using a number of short-lived radionuclides (Widestrand et al. 2006). This test had a primary focus on demonstrating that the experimental setup and equipment worked properly.

3.2 The main in-situ tracer test

In the main in-situ tracer test, a cocktail of both sorbing and non-sorbing tracers was allowed to contact the natural fracture surface of the target fracture, as well as the unaltered rock matrix surrounding the slim hole, for a time period of 198 days. The tracer cocktail contained the 22 radionuclides Na-22, S-35, Cl-36, Co-57, Ni-63, Se-75, Sr-85, Nb-95, Zr-95, Tc-99, Pd-102, Cd 109, Ag-110, Sn-113, Ba-133, Cs-137, Gd-153, Hf-175, Ra-226, Pa-233, U-236, and Np-237. The injection proceeded as described in Widestrand et al. (2010b, Chapter 2) and took place on the 27th of September 2006.

PEEK tubing connected the contact sections in the slim hole and at the target fracture, and as the system was circulated one may approximate that the tracer concentrations are the same in the two contact sections, for each time step. The exception is for the very beginning of the experiment, as the tracer cocktail was allowed to contact the target fracture for two hours prior to also filling the packed-off section of the slim hole (Widestrand et al. 2010b, Appendix 3). PEEK tubing also connected the tracer cocktail with experimental equipment in the tunnel. Hence, the decreasing tracer concentrations could be monitored, together with environmental parameters, as the tracer test progressed. Tracer cocktail sampling was typically performed with an about two week interval. However, more frequent sampling was made during the first few days after injection (Widestrand et al. 2010b, Appendix 4). Examples of the tracer concentration decline in the tracer cocktail are shown for Cl-36 and Cs-137 in Figure 3-3.

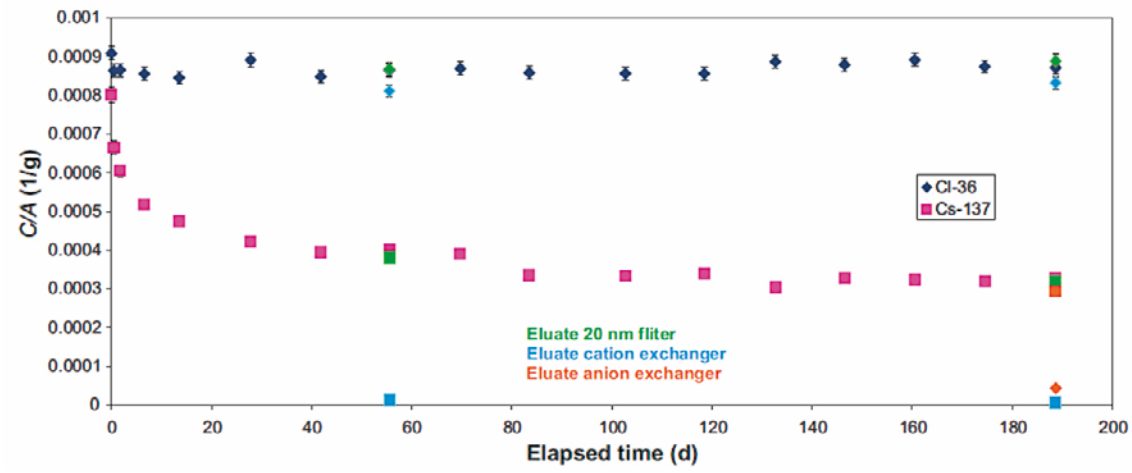

Figure 3-3. *Example of declining tracer concentrations in the tracer cocktail during the course of the in-situ experiment. Reproduced from Widestrand et al. (2010b, Figure 3-12).*

A main consideration of the experiment was to maintain natural chemical conditions in the experiment and therefore avoid increasing concentration of the elements used as tracer. By the use of radioisotopes with high specific activity, the combination of large amounts of radioactivity and low or no increase of the chemical concentrations could be achieved. Even so there were limitations when obtaining tracer penetration profiles in the rock for some radionuclides, due to e.g. detection limits and relatively short half-lives.

The in-diffusion part of the tracer experiment was terminated by expelling the tracer cocktail from the borehole system on the 12th of April 2007. This was done by rinsing the system with isopropyl alcohol. Thereafter an Epoxy resin was injected in order to increase the mechanical strength of the rock prior to over-coring. An additional objective was to protect the water-rock interface of the stub and slim hole test section from flushing water used in the over-core drilling. The tracer content of the outgoing isopropyl alcohol (later with inmixing of epoxy) was monitored (Nilsson et al. 2010, Appendix 2).

3.3 Rock sampling and analysis after the in-situ tracer test

After termination of the in-situ tracer test, the rock volume surrounding the contact sections was over-cored and subsequently drilled and sawn into numerous subsamples, which is described in detail in Nilsson et al. (2010, Chapter 2).

The over-coring was performed over a number days, from the 26th of April 2007 to the 3rd of May 2007, producing a Ø278 mm large core. During the over-coring the tracer activity in the flushing water was controlled. However, a critical incident during the over-coring gave rise to a situation where the PEEK lid packer and epoxy resin, protecting the core stub, accidently loosened. Thereby the fracture surface was exposed to flushing water, causing some minor amounts of desorption of tracers. The slim hole/rock interface should not have been affected by this. On the 4th of May the large core was transported to the Clab facility[1]. Here it was covered with heavy plastic foil to prevent drying. About a month thereafter scaling and geological mapping commenced. After about another month, on the 3rd of August, the large core was covered by a 1-2 mm thick layer of clear epoxy resin. This was primarily done to prevent contamination during further sample preparation, but the resin also prevented drying. On the 6th of August the exposed part of the core was sawn off from the remaining part of the over-cored rock. Between the 8th to the 13th of August a large number of smaller core samples were drilled from the over-cored rock volume (see Figure 2-1 of Chapter 2 and Figure 3-4).

These smaller core samples, having a diameter of 24 mm, were divided into the subclasses A, C, and D[2], depending on their location. A-cores correspond to the rock at the target fracture while D-cores correspond to rock at the slim hole section. During the drilling of the smaller core samples, cooling water and debris were collected (see Figure 3-4) and controlled with respect to their tracer content.

It should be noted that a significant time period, about 120 days, went by between the termination of the in-situ tracer test and the drilling of smaller core samples. During this time the over-cored rock volume was reasonably well protected by heavy plastic foil to prevent it from drying. Hence one could speculate that the exposed parts of the rock were fully, or at least partly, saturated long after the over-cored rock was bought to the laboratory. Hence, further water phase matrix diffusion could have occurred.

[1] This is SKBs interim storage facility for spent nuclear fuel, where handling of the exposed rock material took place.

[2] B-cores were drilled from the epoxy coated PEEK lid as “mirror images” of the corresponding A-cores, see Section 5.3. C-samples were not further analysed.

Figure 3-4. *Drilling of core samples from the over-cored rock volume. This image also demonstrates the scale of the exposed rock volume in the experiment. Reproduced from Nilsson et al. (2010, Figure 2-4).*

After the drilling of the small core samples, their surfaces were not covered by an epoxy layer. The rational for not doing this was to facilitate the subsequent cutting into slices and to allow for further mineralogical analysis and determination of radionuclide content. However, the core samples were stored in small individual plastics bags, which were reasonably tight, until they were sawed into slices.

This should have prevented, or at least delayed, the drying of the pore water. Physical separation of the core slices was not performed until December 2007 to January 2008 (Nilsson et al. 2010, Appendix 1). If assuming that the core samples were fully or at least partly saturated up until the slicing, this would have added between ~240 to ~290 days of time during which liquid phase matrix diffusion could have occurred, after the termination of the LTDE-SD in-situ part. It should be noted that this time exceeds that of the in-situ in-diffusion phase.

If assuming that the core samples had dried completely or partly during the storing period up until slicing was commenced, there may be a need to consider solute mass transfer processes occurring during drying. A few processes and events that may have occurred are:

- Receding drying fronts starting at the core sample surfaces, where water vaporisation occurs, and moving towards its centre.
- Up-concentration of solutes in the water phase at the drying front, which is counteracted by increased diffusion towards the sample centre and by sorption. The up-concentration may possibly also result in aqueous phase reaction and re-speciation.
- The drying front and its sharpness may be counteracted by capillary forces, resulting in minute flows of bulk water. This would generally cause redistribution of water from micropores of large aperture to those of small aperture.

As mentioned earlier, a large number of the small core samples that were drilled from the over-cored rock volume were cut into slices, to facilitate subsequent analysis of their radionuclide content. A partition diagram of a typical sawing of a core sample is shown in Figure 3-5.

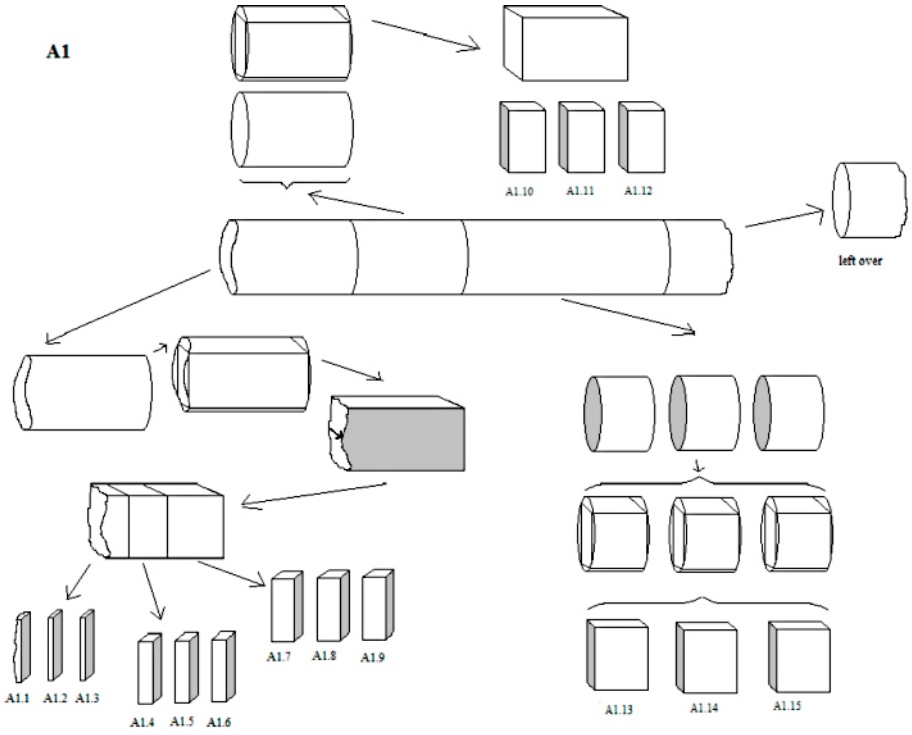

Figure 3-5. *Illustration of the sampling of the A1-core from the over-cored rock volume in LTDE-SD. Reproduced from Nilsson et al. (2010, Figure 2-10).*

It should be noted that most subsamples were sawn into cuboids prior to the slicing, hence removing the outer cylindrical mantel that could have been subjected to contamination during the core drilling at Clab. The first three slices closest to the tracer cocktail/rock interface were sawn into a thickness of ~ 1 mm, with the discrepancy that the very first slice in a few cases was significantly larger. This is due to fracture surface roughness for A-cores and the curvature of the slim hole for D-cores. For example, mean thicknesses of the first slice for A-cores vary from one to several millimetres (cf. Nilsson et al. 2010, Figure 3-10). The next three slices were sawn with a thickness of ~ 3 mm; the following three slices were ~ 5 mm thick; the following three slices were 10 mm thick; and the last three slices had a thickness of 20 mm. The thickness of the sawing blade was 0.25 mm which gave a loss of rock matrix of about 0.3 mm between each slice (Nilsson et al. 2010, Section 2.3).

Tracer concentrations (or activities) in the rock sample were obtained by a number of analysis methods. These include autoradiography on intact samples; direct activity measurements on intact and crushed samples; and leaching or dissolution of intact and crushed samples, followed by water phase measurements. Analysis methods giving rise to individual trace concentrations were HPGe (High-Purity Germanium detector), ICP-SFMS (Inductively Coupled Plasma-Sector Field Mass Spectrometry) and LSC (Liquid Scintillation Counter). A list of what core samples were subjected to what sample preparation and analysis methods is provided in Nilsson et al. (2010, Table 2-2). Sample preparation and analysis methods are described briefly[3] in Nilsson et al. (2010, Sections 2.7 and 2.8).

Comment:
A more detailed timeline of events at, and after, termination of the in-situ experiment is given in Appendix 1.

[3] Applied analysis methods are described in detail in the SKB international technical document SKB ITD-10-02, which can be made available upon request.

3.4 Penetration profiles deviating from those predicted

The LTDE-SD campaign has produced numerous interesting results, but there is one observation in particular that is of interest for Task 9B. This concerns the tracer penetration profiles in the rock matrix. In Widestrand et al. (2010a) predictive modelling was made for the tracer penetration profiles, based on laboratory data, and in Nilsson et al. (2010) inverse modelling was made based on the obtained in-situ data. Regardless of the chosen parameters, the discrepancies between the modelled and observed profiles were more pronounced than the similarities. This apply both for penetration profiles at the natural fracture surface and in the unaltered rock matrix. Figure 3-6 shows the experimental concentration profiles of the tracers Na-22 and Cl-36 by diamonds, as well as the modelled profiles by the solid curves. Here the discrepancy in the curve shapes should be highlighted, whereas the discrepancy in relative curve positions is perhaps of lesser importance. The modelling performed in Widestrand et al. (2010a) and Nilsson et al. (2010) had the assumption of Fickian diffusion in a homogenous medium, with linear equilibrium sorption and no speciation reactions (other than equilibrium sorption partitioning) in the pore water of the matrix.

The heterogeneous nature of the rock matrix, in terms of both the microporous network and mineral surfaces available for sorption, has been qualitatively offered as an explanation for the discrepancy (Nilsson et al. 2010). However, other features, events, processes and artefacts that are traditionally not included in such modelling may add to the observed discrepancy. It may also be that using the fundamental prerequisites of the modelling, that is the Fickian diffusion equations and the linear equilibrium sorption approach, may add to the discrepancy.

3.5 Complementary laboratory programme

During the course of the LTDE-SD campaign, a number of laboratory examinations and experiments have been performed on rock samples from the LTDE-SD site. These include geological, mineralogical and microstructural characterisations as well as characterisation of the rock's migration and retention properties (e.g. Li 2001, Winberg et al. 2003, Vilks et al. 2005, Widestrand et al. 2010a).

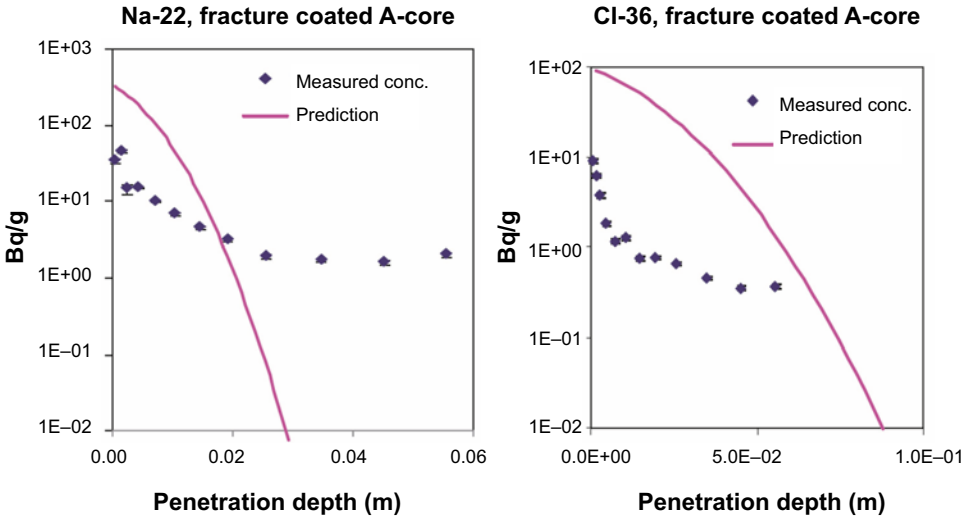

Figure 3-6. *Results from the in-situ in-diffusion experiment LTDE-SD through a natural fracture surface. Modelled Na-22 and Cl-36 penetration profiles (solid curves) in comparison with the measured profiles (diamonds). Na-22 activities in the rock matrix were obtained on intact or crushed rock slices and Cl-36 activities were obtained by leaching of intact or crushed slices. Excerpts from Nilsson et al. (2010, Figures 4-1a and 4-2a).*

Two laboratory campaigns have been undertaken with the aim at obtaining migration and retention parameters for the rock; such as the porosity, diffusivity, and sorption partitioning coefficients. These were performed in Sweden and Finland under the conduit of SKB and in Canada under the conduit of Atomic Energy of Canada Limited (AECL). In both campaigns, drill core samples from the pilot hole (KA3065A02) and experimental hole (KA3065A03) were used. It should be noted that this rock material had not been previously exposed to tracer contact in-situ, and that this section does not concern rock samples from the over-cored rock volume surrounding the experimental borehole.

3.5.1 The SKB laboratory campaign

In the SKB laboratory campaign, different experimental procedures were used on 19 rock samples from the LTDE-SD site, although not all samples were subjected to all procedures. Table 3-1 shows which samples were subjected to which experiments. An account of the original positions of the rock samples in the two boreholes is given in Widestrand et al. (2010a, Appendix 2 and 13), together with descriptions of the rock samples. It should be noted that the rock samples from the experimental borehole were taken from the drill core of the slim hole at, and at some distance from, the target fracture. An account of the experimental procedures is given in Widestrand et al. (2010a, Chapter 3). Short notes on the campaign are given below.

Table 3-1. Overview of the rock samples versus the different methods. The samples have been divided into three general types: 1, matrix rock; 2, matrix rock with fracture surface; 3, mainly fracture mineralizations, in addition to mylonitic/cataclastic rock matrix; 4, strongly altered bedrock. Reproduced from excerpt of Widestrand et al. (2010a, Table 3-1).

Sample ID	Type of sample	Porosity. water saturation	PMMA porosity	Electrical resistivity	Through-diffusion	Sorption/ diffusion	BET, specific surface area	Batch sorption, crushed rock
LTDE-SD rock samples:								
A02:1	2						X	X
A02:2	2–3						X	X
A02:4	1	X			X			
A02:5	1	X		X				
A02:6	1						X	X
A02:7	1	X		X				
A02:8	1	X			X			
A03:1	1						X	X
A03:2	1						X	X
A03:3	2	X			X	X		
A03:4	1	X			X	X		
A03:5	1	X			X	X		
A03:6	1	X			X	X		
A03:7	1	X	X					
A03:8	1	X	X					
A03:9	3						X	X
A03:10	3/4	X	X					
A03:11	3	X	X					
A19	2		X					

Three different methods were used to measure the rock samples porosity. The most frequently used method was the water saturation, which is also called the water immersion, technique. In addition the porosity distribution was estimated using a ^{14}C-PMMA impregnation technique (Widestrand et al. 2010a, Section 3.1). Furthermore, the rock capacity factor a (–) was obtained in through-diffusion experiments using the non-sorbing tracer HTO (Widestrand et al. 2010a, Section 3.2). The rock capacity factor should be equivalent to the connected porosity for non-sorbing solutes that suffer no exclusion effects. As can be seen from Table 3-1, porosity measurements with at least one of the methods were done on 13 of the studied samples from the LTDE-SD site.

The effective diffusivity of the rock matrix, or its formation factor, was estimated by two methods. From through-diffusion measurements, using HTO and sometimes Cl-36 as the tracers, the effective diffusivity could be estimated directly by fitting the resulting breakthrough curves with Fick's first and/or second laws. This was done for six different samples from the local site. Five of the samples had a length of 30 mm and one sample a length of 70 mm. Results were obtained for four of the 30 mm samples.

The effective diffusivity can also be estimated from electrical measurements (Widestrand et al. 2010a, Section 3.2.2). Such measurements are based on the Einstein relation between diffusion and electromigration (e.g. Löfgren and Neretnieks 2006). Further assumptions made were that a low frequency alternating field well represents a direct field and that surface conduction is of insignificant consequence at the experimental conditions. When obtaining the effective diffusivity from such measurements, the diffusivity in free solution of the average current bearing ion in the pore water can be assumed to be around $1 \cdot 10^{-9}$ to $2 \cdot 10^{-9}$ m^2/s. Electrical measurements were performed on two of the LTDE-SD samples.

Information on the diffusivity was also obtained from in-diffusion experiments, also called sorption-diffusion experiments, on intact cores in the laboratory. This was done on four samples using the tracers HTO, Na-22, Co-57, Se-75, Sr-85, Cd-109, Ag-110m, Sn-113, Ba-133, Cs-137, Hf-175, U-236, and Np-237 (Widestrand et al. 2010a, Section 3.4 and Appendix 6). Extracting results from these experiments requires modelling that is similar to that envisioned in Task 9B-1, where several modelling assumptions are required. As identified in Widestrand et al. (2010a), individual fittings of the rock capacity factor and the formation factor (or effective diffusivity) cannot be made based solely on data on the decreasing tracer concentrations in the surrounding tracer cocktail. Instead Widestrand et al. (2010a) estimated the parameter group $K_d \cdot F_f$.

Sorption data were also obtained from batch sorption and BET surface area measurements on five samples (Widestrand et al. 2010a, Section 3.3). In both these methods the rock samples were crushed and sieved. Batch sorption measurements were performed on the size fractions 0.063–0.125, 0.25–0.5, and 1–2 mm and BET measurements were performed on the size fractions 0.063–0.125 and 2–4 mm. In the batch sorption measurements, the tracers Na-22, Cl-36, Co-57, Ni-63, Se-75, Tc-99, Cd-109, Ag-110m, Ba-133, Cs-137, Gd-153, Ra-226, U-236, and Np-237 were used.

3.5.2 The AECL laboratory campaign

In the Canadian campaign, reported in Vilks et al. (2005), rock samples were taken from two drill core sections from the outer telescopic section (Ø270 mm core from Ø300 mm borehole) of the LTDE-SD experimental hole (cf. Figure 3-2). This means that the rock samples originated a couple of meters from the target fracture. The drill core sections neighboured each side of a natural fracture at the borehole depth 8.329 m (cf. Winberg et al. 2003, Table 3-1). From one section, 18 smaller core samples were extracted for further analysis. The axis of 12 of the samples was parallel to the borehole axis, while that of the remaining six samples was normal to the borehole axis. In this way rock matrix anisotropy could be investigated. All of these samples were subjected to water immersion porosity measurements and 16 of the samples were subjected to through-diffusion measurements using both iodide and HTO as tracers (Vilks et al. 2005, Section 2.1). An extraction diagram of smaller core samples is displayed in Figure 3-7 (left). Samples used for porosity and diffusivity measurements come from cores A, E, F, M1, M2, and M3.

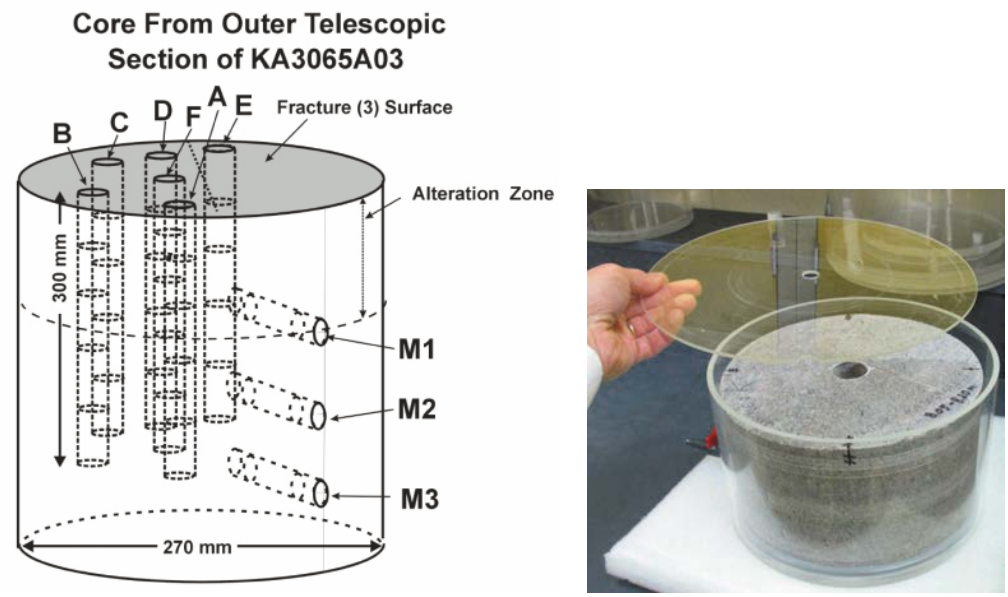

Figure 3-7. *Left: Schematic diagram of core sample extraction. Subsequent analysis was made on four samples from the each of the A, E and F cores. Two samples were taken for each of the M1, M2, and M3 cores. Right: Setup of the radial diffusion experiment. Reproduced from Vilks et al. (2005, Figures 5 and 10).*

For a single sample from core D, the rock's permeability was measured by placing a pressure gradient over it and measuring the flow of deionised water through it (Vilks et al. 2005, Section 3.3).

For the other drill core section, taken from the opposite side of the natural fracture, the edges were trimmed so that it represented unaltered rock. A small hole was drilled through its axis and a radial through-diffusion experiment commenced that in part mimicked that around the slim hole of the main LTDE-SD tracer test (see Figure 3-7, right). Iodide, lithium and uranine were used as tracers (Vilks et al. 2005, Section 2.2), although no results are reported for lithium. Iodide and uranine produced breakthrough curves that could be used to estimate the average effective diffusivity of the drill core (Vilks et al. 2005, Section 3.2). Upon termination of the radial diffusion experiment, nine smaller drill cores were drilled into the affected rock mass. These smaller drill cores were sliced and the slices were leached. In this way, penetration profiles from the slim hole could be obtained.

3.6 LTDE-SD publications

The LTDE-SD campaign has been thoroughly reported and important references within the LTDE-SD suite of reports are shown in Table 3-2, in chronological order. It should be noted that only a fraction of the published material is of direct interest for Task 9B-1. A short note on the report's content is provided in the second column where also some (subjective) comments on the report's applicability for TASK 9B-1 are provided in italic.

Table 3-2. Important documents in the LTDE-SD suite.

Reference, title and report number	Comment
Byegård et al. 1999. Test plan for the long term diffusion experiment. SKB IPR-99-36.	The first planning document for the LTDE experiment. Here important processes and features to be investigated are listed. Some scoping calculations are made. Also, experimental prerequisites such as the tracers to use are suggested. *Some sections can be browsed for orientation.*
Winberg et al. 2000. Evaluation of fracture candidates in boreholes KA2865A01 and KA3065A02. Location of experimental site for the long term diffusion experiment. SKB IPR-00-27.	Here different fracture candidates for LTDE, in different boreholes, are evaluated. The report contains some fracture mineralogy information and structural models of the investigated fracture system, as well as flow data from hydraulic logging. *Of lesser interest for Task 9B-1. Relevant information is found in Winberg et al. (2003).*
Li 2001. Long-Term Diffusion Experiment. Microscopic observation of disturbance in drill core samples from KA3065A02 and KA3065A03. SKB IPR-01-03.	Investigates possible microcracking in the drill cores, as result of the core drilling. *Is recommended if setting up a microstructural model for a mechanically disturbed zone around the borehole, affecting the diffusion profiles in Task 9B-1.*
Winberg et al. 2003. Long-Term Diffusion Experiment. Structural model of the LTDE site and detailed description of the characteristics of the experimental volume including target structure and intact rock section. SKB IPR-03-51.	Is a summary of previously performed work, and also provides updated structural models etc. *Contains a detailed structural model of the target fracture and surrounding fracture system, as well as mineralogical information on the fracture surface. There is also an assessment of sample disturbance. Parts could be of interest for Task 9B-1, depending on the model's microstructural resolution.*
Vilks et al. 2005. Laboratory program supporting SKB's Long Term Diffusion Experiment. Report 06819-REP-01300-10111-R00, Atomic Energy of Canada Limited.	Reports the laboratory porosity and diffusion experiments (with HTO, iodide and uranine) made by AECL on the large diameter drill core from the LTDE-SD borehole. *Of high interest for Task 9B-1.*
Wass 2005. LTDE Long-Term Diffusion Experiment. Hydraulic conditions of the LTDE experimental volume – results from Pre-Tests 0.1–6. SKB IPR-05-25.	Reports hydraulic testing, including dilution tests and tracer breakthrough tests, in the flowing system at the LTDE-SD site. *Of lesser interest for Task 9B-1.*
Widestrand et al. 2006. LTDE Long-Term Diffusion Experiment. Functionality tests with short-lived radionuclides 2005. SKB IPR-06-05.	Reports a functionality tests with short-lived radionuclides at the LTDE-SD site, focusing on practical issues concerning injection, analyses etc. *Of lesser interest for Task 9B-1.*
Widestrand et al. 2010a. Long Term Sorption Diffusion Experiment (LTDE-SD). Supporting laboratory program – Sorption diffusion experiments and rock material characterisation. With supplement of adsorption studies on intact rock samples from the Forsmark and Laxemar site investigations. SKB R-10-66.	One of the main reports of the campaign, focusing on sorption and diffusion results from the LTDE-SD laboratory program. Also geological and micro-structural information of the relevant rock types is given. *Of high interest for Task 9B-1.*
Widestrand et al. 2010b. Long Term Sorption Diffusion Experiment (LTDE-SD). Performance of main in-situ experiment and results from water phase measurements. SKB R-10-67.	One of the main reports of the campaign, focusing on the decline in tracer concentrations in the injection borehole. *In Task 9B-1, tracer concentrations in the cocktail are used as boundary conditions. The report also contains water chemistry data and speciation considerations of interest for Task 9B-1, if focusing on the effect of speciation.*
Nilsson et al. 2010. Long Term Sorption Diffusion Experiment (LTDE-SD). Results from rock sample analyses and modelling. SKB R-10-68.	One of the main reports of the campaign, focusing on the tracer penetration profiles in the rock surrounding the injection hole. Also gives fracture surface activities, and sample specific characterisations and autoradiography. *Of high interest for Task 9B-1, as it reports the profiles to be inversely modelled.*

All of these reports can be downloaded from the SKB website, with the exception of Vilks et al. (2005) that will be made available for the Task 9 modelling groups. It should be noted that there are also a few international technical documents (SKB ITD) prepared within the LTDE-SD campaign, which are no longer publically available. Upon request, such documents can be made available. However, such documents would probably be of more interest for Task 9B-2.

In this present document we strive to reference to appropriate sections of the background reports, with a short summary on the content of the section, rather than reproducing the full information.

4 9B-1: Specifics of Task 9B-1

4.1 General considerations

Generally speaking, Task 9B-1 is intended to include the inverse modelling of a limited number of penetration profiles for a few tracers into a few core samples. Out of the 22 tracers used in the experiment, only the tracers Na-22, Cl-36, Co-57, Ni-63, Ba-133, and Cs-137 produced detectable penetration profiles into the rock of three data points or more. This means that the remaining 16 radionuclides were not found beyond the second slice in the rock. In some cases their absence in more deeply lying slices can be explained by their strong sorption in the first slice, if found there, but in other cases short-lived radionuclides decayed before analysis was performed, or the detection limit of the analytic method was relatively high.

The penetration profiles of the six above listed radionuclides are suggested to be inversely modelled in Task 9B-1, but the individual modelling groups have the freedom to model penetration profiles of Ba-133 in Task 9B-2 instead of in Task 9B-1. The reason for giving this option is based on nothing else than the possible desire to reduce the number of inversely modelled penetration profiles in Task 9B-1. Each tracer will represent different migration, retention and speciation features as is further discussed in Section 4.4. Improving the understanding of such features could be of importance both for tracer test evaluation and for performance assessment considerations.

To further reduce the number of inversely modelled penetration profiles in Task 9B-1, it has been decided to choose only four core samples for the subtask. This also reduces the quantity of sample specific information on geometry, petrology, micro-fractures etc. that needs to be assimilated by the modelling groups. A short presentation of the drill cores, as well as the rationale behind the choice of drill cores, is given in Section 4.3.

4.2 Objectives of Task 9B-1

An overall objective of Task 9 is to increase the realism in solute transport modelling in the rock mass. Performing detailed inverse modelling of experimental results from the LTDE-SD main tracer test is an integrated part of achieving this overall objective. As a separate subtask, Task 9B-1 has both qualitative and quantitative objectives. A set of general objectives are listed below:

- To get familiar with the LTDE-SD campaign and documentation.
- To focus on the inverse modelling of a subset of the experimentally obtained penetration profiles, for a few tracers in a few core samples. Extra attention should be given to small-scale heterogeneity and transport patterns in the rock.
- To focus on the most prominent features, events, processes and/or experimental artefacts that create a discrepancy in the experimentally obtained penetration profiles from what is expected from typical diffusion models in a homogenous medium (i.e. using Fickian diffusion, linear equilibrium sorption, and no aqueous reactions). Such penetration profiles are shown in Figure 3-6.
- To address sorption/reaction/speciation of tracers in the pore water and at mineral surfaces in the rock.

A set of specific objectives for each modelling group is:

1. To provide a general discussion on small-scale features of the fracture coating, alteration rim/borehole disturbed zone, and rock matrix that may impact the tracer migration in the rock.
2. To provide a general discussion on different migration processes that may impact the tracer penetration into the rock, in relation to the spatial and temporal scales of the experiment.
3. To provide a general discussion on sorption/reaction/speciation, and associated processes, that may impact the tracer penetration into the rock, in relation to the spatial and temporal scales of the experiment.

4. To choose the most important ones of the above discussed features, events, and processes and incorporate them in a refined transport code that can produce penetration profiles or even penetration patterns. Different modelling groups may implement different features, events, and processes.
5. To, by inverse modelling, reproduce the penetration profiles of up to six different tracers (Na-22, Cl-36, Co-57, Ni-63, Ba-133, and Cs-137) in four different drill core samples (A6, A9, D12, and D13) from the over-cored rock volume.
    a. To produce a central case where the profiles are reproduced using justifiable input data as well as justifiable features, events, and processes. There should be internal consistency in the approach used to fit one profile compared to the others. There should also be internal consistency in the used sets of input data. In Task 9B-1, no formal demands are made on how to produce the central case.
    b. It is possible to propagate more than one model as the central case, for example if they are conceptually different. Another example is if the models assume different chains of events in the experimental procedures, in case there is a gap in experimental records and where one chain of events is not more likely than the other.
    c. To produce variant cases, uncertainty assessments, or sensitivity studies, to explore ranges of input data or the impact of more or less likely features, events, and processes. In Task 9B-1, no formal demands are made on how to produce these alternative cases.
6. It is probably not within the grasp of Task 9B-1 to model all the impacts on the penetration profiles that may have been introduced as experimental artefacts, due to the experimental procedures. However, it is recommended to recognise that solute transport may have continued within the rock samples even after the in-situ experiment was terminated, in case the porous system of the excavated rock samples was saturated (see Section 3.3). There are large uncertainties associated with the drying of the samples and with the additional time during which matrix diffusion could have occurred. This warrants sensitivity studies.

4.3 The rock samples in Task 9B-1

As already mentioned in the section above, the four core samples A6, A9, D12, and D13 will be the focus of attention in Task 9B-1. The locations of these core samples are indicated in Figure 4-1.

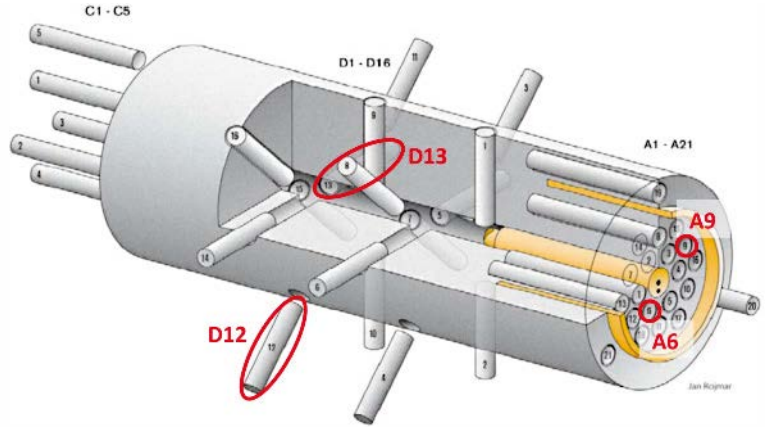

Figure 4-1. *Location of drill cores A6, A9, D12 and D13.*

4.3.1 Rationale for choice of core samples

The rationale for using only a limited number of cores is that less information on mineralogy, petrology, etc., needs to be given to, and assimilated by, the modelling groups. This is intended to give a proper balance between the focus on small-scale features of the rock and processes occurring in the pore water or at mineral surfaces.

Penetration depth

Concerning the choice of all four core samples, a prerequisite is that most of the chosen tracers should have demonstrated significant penetration. Not all A- and D-cores feature significant penetration and from this perspective, the chosen subset of core samples is not entirely representative for the LTDE-SD experiment.

Fracture coating

Concerning the A-cores, a preference is that one core should feature a relatively thick fracture coating while the other should only feature a partial and thin fracture coating. The type of alteration rim was not an issue in the choice. D-cores feature no fracture coating and no alteration rim (although a mechanically disturbed zone is conceivable).

Thickness of first slice

As indicated in Figure 3-5, each core sample is sawn into slices. The first slice of A-cores, including the fracture surface, is irregular in shape. Accordingly its mean thickness varies. A preference in the choice was that the mean thickness should be as small as possible. Otherwise, much of the concentration decrease in the rock would be contained in the first slice and the penetration profile would in that case be described with a smaller resolution.

Geological and microstructural information

Some A- and D-cores are associated with more thorough mineralogical and microstructural analyses. There may also be more or less information from autoradiography etc. for different cores. Drill cores having a broader range of additional information have been prioritised in the choice.

Coherence with penetration profiles by "traditional" modelling

Inverse modelling of penetration profiles in Nilsson et al. (2010) indicated that for some samples and tracers, a good fit could be achieved also when using a diffusion model for homogenous medium. However, for other samples and tracers there were severe discrepancies (cf. Figure 3-6). To study both possibilities, one D-core is chosen where a reasonable match was achieved in Nilsson et al. (2010), at least for some tracers. The other D-core should feature penetration profiles indicating "anomalous" diffusion. The reason for choosing from the pool of D-cores and not including the A-cores, in regard to this particular aspect, is that D-cores should not feature obvious heterogeneity in terms of layers of fracture coatings and altered rock (although a mechanical disturbed rim around the borehole is a possibility).

Loss of tracer to epoxy

Another issue that may deserve some attention originates in the performance of the experiment. When terminating the in-situ tracer test, an epoxy resin was injected that should, upon curing, protect the rock during over-coring. It has been hypothesised that some of the tracers transferred from the rock to the epoxy resin, by one or another mechanism. In some cases, tracer activities were analysed in so called B-cores drilled in the epoxy resin, at locations directly facing A-cores (cf. Section 5.3). Cases where such information is available are prioritised in the choice of A-cores.

4.3.2 Presentation of the core samples

The rock type of the four selected core samples is interpreted as Ävrö granodiorite. The same applies for all other unaltered core samples taken from the pilot and experimental boreholes KA306502 and KA3065A03, the average density of the rock at the LTDE-SD site is 2.66 g/cm^3 (Widestrand et al. 2010a, Section 2.2). A geological characterisation is reported for each core sample in Nilsson et al. (2010, Appendix 3), together with close-up photos and other information. The photos in Figure 4-2 to Figure 4-5 show the four cores from the side.

Figure 4-2. *Photo of core sample A6, above a cm-ruler. The target fracture is on the right-hand side. Reproduced from Nilsson et al. (2010, Appendix 3).*

Figure 4-3. *Photo of core sample A9, above a cm-ruler. The target fracture is on the right-hand side. Reproduced from Nilsson et al. (2010, Appendix 3).*

Figure 4-4. *Photo of core sample D12, above a cm-ruler. The slim hole surface is on the right-hand side. Reproduced from Nilsson et al. (2010, Appendix 3)*

Figure 4-5. *Photo of core sample D13, above a cm-ruler. The slim hole surface is on the right-hand side. Reproduced from Nilsson et al. (2010, Appendix 3).*

The edge of core sample A6, which corresponds to the target fracture, is to a large part (95 %) coated by a varying layer of calcite, chlorite, epidote and minor amount of chalcopyrite, with or without quartz. The coating thickness varies from 0 to 2 mm. The corresponding edge of sample A9 is coated by a thin layer (≤ 0.5 mm) of calcite with minor amounts of chlorite, with or without epidote, covering about 50 % of the surface area. This means that the fracture surface is uncoated for 5 % for core sample A6 and 50 % for core sample A9.

Wall rock alteration for core sample A6 (cf. Figure 4-2) displays a faint to medium (possibly strong) degree of oxidation, i.e. red-staining. For core sample A9 (cf. Figure 4-3), the wall rock alteration is described as red-staining with faint to medium degree, increasing towards the fracture surface. Core sample D12 (cf. Figure 4-4) shows nearly no signs of alteration while sample D13 (cf. Figure 4-5) shows red-staining, but only around sealed fractures.

4.3.3 Partitioning diagrams and data for cores

The partitioning of core samples into cylindrical or square slices generally took place according to the partitioning scheme of Figure 3-5. The core loss between the slices, i.e. the gap formed between the slices as result of the sawing, was estimated to be 0.3 mm. More information on the sawing is available in Nilsson et al. (2010, Section 2.3). For the tracers of interest for Task 9B-1, except for Ni-63, analyses were generally performed on the first twelve slices. For Ni-63 only the first five slices were analysed. Table 4-1 to Table 4-4 show the slices' individual weights, mean lengths, and distances of the samples' centre to the exposed rock surface. Length data come from the Sicada database. Weights come from experimental records of Geosigma.

Table 4-1. Information on the partitioning of core sample A6.

Slice	Weight (g)	Mean length (mm)	Centre distance to surface (mm)
A6.1	1.2112	0.97	0.48
A6.2	0,2507	0.65	1.59
A6.3	0.1595	0.57	2.50
A6.4	1.5514	2.52	4.35
A6.5	1.6377	2.57	7.20
A6.6	2.0157	3.22	10.39
A6.7	3.2038	4.47	14.54
A6.8	3.0193	4.29	19.21
A6.9	5.0723	7.76	25.54
A6.10	6.8373	10.0	34.72
A6.11	7.5367	10.0	45.02
A6.12	5.8941	10.0	55.32

Table 4-2. Information on the partitioning of core sample A9.

Slice	Weight (g)	Mean length (mm)	Centre distance to surface (mm)
A9.1	0.4500	1.95	0.97
A9.2	0.2442	1.00	2.75
A9.3	0.1738	0.94	4.02
A9.4	1.5824	3.44	6.51
A9.5	0.8032	2.24	9.65
A9.6	1.2429	2.82	12.48
A9.7	3.0619	5.46	16.92
A9.8	2.7546	5.25	22.57
A9.9	2.6666	5.73	28.36
A9.10	6.9893	10.0	36.53
A9.11	6.6689	10.0	46.83
A9.12	5.3814	10.0	57.13

Table 4-3. Information on the partitioning of core sample D12.

Slice	Weight (g)	Mean length (mm)	Centre distance to surface (mm)
D12.1	0.6106	1.30	0.65
D12.2	0.3842	0.93	2.06
D12.3	0.6103	1.23	3.44
D12.4	1.1548	2.38	5.55
D12.5	0.9940	2.27	8.18
D12.6	0.9462	2.19	10.71
D12.7	2.4208	4.25	14.22
D12.8	2.4073	4.07	18.68
D12.9	2.8442	5.18	23.61
D12.10	6.4697	10.0	31.50
D12.11	4.9725	10.0	41.80
D12.12	5.6462	10.0	52.10

Table 4-4. Information on the partitioning of core sample D13.

Slice	Weight (g)	Mean length (mm)	Centre distance to surface (mm)
D13.1	0.7043	1.56	0.78
D13.2	0.0029*	0.64	2.18
D13.3	0.2051	0.77	3.19
D13.4	1.2136	2.53	5.13
D13.5	1.3734	2.60	8.00
D13.6	1.4916	2.79	10.99
D13.7	2.1806	4.84	15.11
D13.8	1.7642	4.26	19.96
D13.9	5.2101	8.17	26.48
D13.10	5.6486	10.0	35.86
D13.11	4.8526	10.0	46.16
D13.12	6.6632	10.0	56.46

* The sample size was very small and the sample has not been analysed

4.4 Tracers of Task 9B-1

4.4.1 Description of tracers

The tracers used in the LTDE-SD main tracer test are described in Widestrand et al. (2010b, Sections 2.2 and 2.3). Half-lives of the tracers are found in Nilsson et al. (2010, Table 1-1), together with their analysis methods. For the five mandatory tracers of Task 9B-1, as well as for the optional tracer Ba-133, half-lives are reproduced in Table 4-5.

Table 4-5. Half-lives of tracers in Task 9B. Data reproduced from Nilsson et al. (2010, Table 1-1).

Radionuclide	Half-life
Na-22	2.6 years
Cl-36	$3.0 \cdot 10^5$ years
Co-57	272 days
Ni-63	100 years
Ba-133	10.5 years
Cs-137	30 years

Na-22

Sodium is a weakly sorbing tracer that is expected to sorb by ion exchange reactions. From aqueous speciation calculations made in Widestrand et al. (2010b, Table 3-3), excluding the effect of functional groups of the mineral surfaces, sodium is expected to predominately exist as cationic Na^+ during relevant experimental conditions. As Na-22 is weakly sorbing, it has generally penetrated a fair distance into the rock matrix during the course of the LTDE-SD main tracer test. It is therefore a good marker when examining the geometric/volumetric extension of the microporous network in the rock.

Cl-36

This tracer is traditionally treated as a non-sorbing. From aqueous speciation calculations it is expected to predominately exist as anionic Cl^- during relevant experimental conditions. As chloride is non-sorbing, it has generally penetrated a fair distance into the rock matrix during the course of the experiment. It is therefore a good marker when examining the geometric/volumetric extension of the microporous network in the rock. Due to its anionic form it is also a good marker for anion exclusion effects that, in some performance assessments, may be troublesome. The Cl-36 profiles will be analysed in a few spare core samples from the over-cored LTDE-SD rock. Accordingly predictive modelling could be performed at a later stage.

Co-57

Cobalt is a tracer that shows clear signs of sorption in the LTDE-SD main tracer test. This tracer is of interest from a speciation point of view. Aqueous speciation calculations made by PHREEQC in Widestrand et al. (2010b, Table 3-3) suggest that relevant fractions of Co-57 could be present in both anionic and cationic forms[4]. If one would (overly-pessimistically) assume that Co is in its anionic form in PA calculations, this may result in the assumption of non-sorbing behaviour which could be clearly unfavourable for some repository concepts. On the contrary, evidence from LTDE-SD points to the fact that in many rock samples, the tracer does not penetrate beyond the first rock slice. This is perhaps consistent with surface complexation behaviour that is expected for the divalent cationic species Co^{2+}. However, in other rock samples, significant penetration occurs which suggests weaker sorption behaviour.

[4] For Task 9B-1, it could be an additional objective to perform aqueous speciation calculations and compare the results with those from the PHREEQC modelling made in Widestrand et al. (2010b, Table 3-3). Concerning Co in particular, there are some identified question marks relating to the database used for thermodynamic constants in Widestrand et al. (2010b, Table 3-3).

Ni-63

Nickel is a tracer that is expected to sorb to mineral surfaces and evidence from LTDE-SD supports this notion. Aqueous speciation calculations in Widestrand et al. (2010b, Table 3-3) suggest that it exists mostly in the divalent cationic form Ni^{2+} (to a degree of 96 %). This species is expected to sorb by surface complexation to mineral phases common in the rock matrix. However, the speciation calculations suggest that a fraction (3 %) reacts with sulphate to form the neutral specie $NiSO_4$ (aq). Ni-63 is also of interest for Task 9B-2, as a few spare core samples from the over-cored LTDE-SD rock volume will be analysed with respect to Ni-63. Accordingly predictive modelling could be performed.

Ba-133

Ba-133 is a tracer that is representative for divalent alkaline earth elements. Barium is expected to sorb moderately well to mineral surfaces and evidence from LTDE-SD supports this notion. Aqueous speciation calculations in Widestrand et al. (2010b, Table 3-3) suggest that it exists mostly in the divalent cationic form Ba^{2+} (to a degree of 99 %). Barium is reported to sorb by ion exchange to minerals. The Ba-133 profiles will be analysed in a few spare core samples from the over-cored LTDE-SD rock. Unless the potentially present Ba-133 has decayed below the detection limit, predictive modelling of the radionuclide can be performed at a later stage.

Cs-137

Caesium is a common tracer that exhibits weak to moderately sorbing behaviour, where the sorption mechanism is suggested to be ion exchange. Caesium is also (sometimes) suggested to be affected by surface enhanced diffusion (also called surface diffusion). Aqueous speciation calculations in Widestrand et al. (2010b, Table 3-3) suggest that it predominately exists in cationic form; Cs^{+} (to a degree of 95 %). However, the speciation calculations suggest that a fraction (5 %) reacts with chloride to form the neutral specie CsCl (aq). In the LTDE-SD experiment, caesium penetration is generally extensive. The Cs-137 profiles will be analysed in a few spare core samples from the over-cored LTDE-SD rock. Accordingly predictive modelling could be performed at a later stage.

4.4.2 Tracer penetration profiles

Penetration profiles are available for the core samples in terms of tracer specific activity per mass weight of the rock slice (Bq/g). This is illustrated in Figure 4-6 for Na-22 penetration into the A-cores.

The tracer activities for the six different tracers in individual slices of the four chosen core samples are provided in Table 4-6 to Table 4-13. These data form the penetration profiles that should be inversely modelled in a quantitative fashion within Task 9B-1. There are no porosity data available for the individual slices on which the tracer activities were analysed. Hence a translation into tracer concentrations in the pore water needs to rely on assumed porosities (cf. Section 5.2.1).

Comment:
Data in Tables 4-6 to 4-13 have been revised and correct data are presented in Appendix 2.

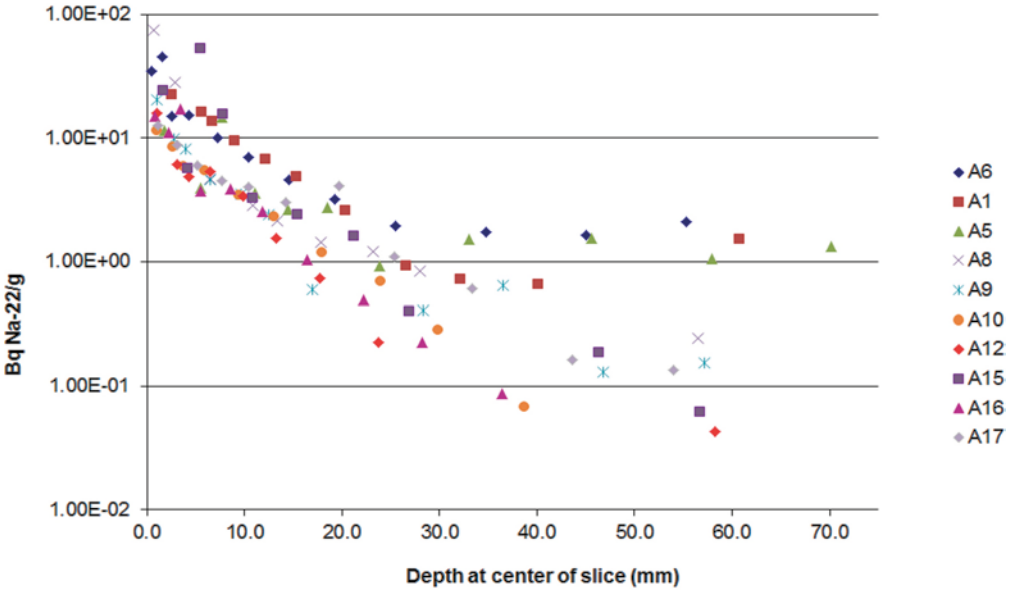

Figure 4-6. *Na-22 activity versus penetration depth in the first 75 mm of A-cores. Data from slices with tracer activity under detection limit are excluded from the graph. Reproduced from Nilsson et al. (2010, Figure 3-9).*

Table 4-6. Tracer activity in slices from the A6 core, per grams of rock. Data recalculated from Sicada (SKB:s primary database). All activities are decay corrected to the tracer injection date. The uncertainty is reported as 2δ, except for Cl-36 for which the method uncertainty (m.u.) from the leaching procedure is included.

Slice	Na-22 (Bq/g)	Na-22 2δ (Bq/g)	Cl-36 (Bq/g)	Cl-36 m.u. (Bq/g)	Co-57 (Bq/g)	Co-57 2δ (Bq/g)
A6.1	3.47E+01	2.08E+00	9.33E+00	5.14E−01	2.28E+03	2.06E+01
A6.2	4.57E+01	2.07E+00	6.36E+00	3.56E−01	9.24E+01	8.79E+00
A6.3	1.49E+01	2.33E+00	3.88E+00	2.31E−01	<1.33E1	
A6.4	1.53E+01	5.08E−01	1.89E+00	1.05E−01	<1.27E0	
A6.5	1.01E+01	4.08E−01	1.18E+00	6.61E−02	<1.20E0	
A6.6	6.96E+00	3.21E−01	1.31E+00	7.29E−02	<1.20E0	
A6.7	4.61E+00	2.03E−01	7.69E−01	4.29E−02	<3.82E−1	
A6.8	3.18E+00	1.78E−01	7.83E−01	4.37E−02	1.14E+00	3.13E−01
A6.9	1.96E+00	1.09E−01	6.71E−01	3.72E−02	<3.74E−1	
A6.10	1.75E+00	9.81E−02	4.65E−01	2.59E−02	<3.70E−1	
A6.11	1.64E+00	9.74E−02	3.55E−01	1.98E−02	<4.49E−1	
A6.12	2.08E+00	1.18E−01	3.73E−01	2.10E−02	<5.66E−1	

Table 4-7. Tracer activity in slices from the A6 core, per grams of rock. Data recalculated from Sicada. All activities are decay corrected to the tracer injection date. The uncertainty is reported as 2δ, except for Ni-63 for which the method uncertainty (m.u.) from the dissolution procedure is included. Some slices were not analysed for Ni-63 (n.a.).

Slice	Ni-63 (Bq/g)	Ni-63 m.u. (Bq/g)	Ba-133 (Bq/g)	Ba-133 2δ (Bq/g)	Cs-137 (Bq/g)	Cs-137 2δ (Bq/g)
A6.1	1.28E+04	1.14E+03	8.95E+02	7.74E+00	2.53E+04	2.99E+01
A6.2	1.31E+03	1.17E+02	5.41E+01	3.60E+00	7.82E+03	1.46E+01
A6.3	1.63E+01	2.74E+00	2.59E+00	1.31E+00	1.55E+02	3.00E+00
A6.4	4.48E+00	5.82E−01	1.95E+00	1.53E−01	1.67E+00	1.39E−01
A6.5	<4		<2.47E−01		8.00E−01	1.13E−01
A6.6	n.a.		<1.85E−01		5.49E−01	9.73E−02
A6.7	n.a.		<1.24E−01		5.12E−01	6.20E−02
A6.8	n.a.		1.52E−01	6.42E−02	1.82E+00	9.04E−02
A6.9	n.a.		<7.93E−02		3.93E−01	3.99E−02
A6.10	n.a.		<8.33E−02		3.03E−01	3.56E−02
A6.11	n.a.		<7.73E−02		1.83E−01	2.42E−02
A6.12	n.a.		1.35E−01	4.85E−2	3.52E−01	3.30E−02

Table 4-8. Tracer activity in slices from the A9 core, per grams of rock. Data recalculated from Sicada. All activities are decay corrected to the tracer injection date. The uncertainty is reported as 2δ, except for Cl-36 for which the method uncertainty (m.u.) from the leaching procedure is included.

Slice	Na-22 (Bq/g)	Na-22 2δ (Bq/g)	Cl-36 (Bq/g)	Cl-36 m.u. (Bq/g)	Co-57 (Bq/g)	Co-57 2δ (Bq/g)
A9.1	2.03E+01	2.84E+00	8.30E+00	4.61E-01	2.43E+03	2.89E+01
A9.2	9.92E+00	4.32E-01	1.62E+00	2.85E-01	<5.32E+00	
A9.3	8.10E+00	1.62E+00	1.09E+00	9.79E-02	<1.31E+01	
A9.4	4.58E+00	2.83E-01	7.66E-01	6.33E-02	<8.53E-01	
A9.5	3.51E+00	3.79E-01	5.50E-01	3.64E-02	<1.73E+00	
A9.6	2.40E+00	2.55E-01	4.38E-01	5.63E-02	<1.15E+00	
A9.7	6.00E-01	2.35E-01	4.35E-01	2.50E-02	<1.12E+00	
A9.8	<1.26E-1		3.15E-01	2.14E-02	<1.24E+00	
A9.9	4.07E-01	2.47E-01	4.34E-01	2.52E-02	1.32E+00	6.08E-01
A9.10	6.42E-01	7.17E-02	3.11E-01	1.85E-02	<5.68E-01	
A9.11	1.30E-01	4.93E-02	1.57E-01	9.32E-03	<5.38E-01	
A9.12	<1.54E-1		9.34E-02	8.43E-03	<8.46E-01	

Table 4-9. Tracer activity in slices from the A9 core, per grams of rock. Data recalculated from Sicada. All activities are decay corrected to the tracer injection date. The uncertainty is reported as 2δ, except for Ni-63 for which the method uncertainty (m.u.) from the dissolution procedure is included. Some slices were not analysed for Ni-63 (n.a.).

Slice	Ni-63 (Bq/g)	Ni-63 m.u. (Bq/g)	Ba-133 (Bq/g)	Ba-133 2δ (Bq/g)	Cs-137 (Bq/g)	Cs-137 2δ (Bq/g)
A9.1	1.56E+04	1.39E+03	7.18E+02	9.86E+00	1.16E+04	3.26E+01
A9.2	<8		2.48E+01	1.04E+00	1.79E+02	2.30E+00
A9.3	<8		5.97E+00	9.65E-01	1.24E+01	1.22E+00
A9.4	n.a.		2.75E-01	8.90E-02	7.13E-01	8.64E-02
A9.5	n.a.		<3.41E-01		6.96E-01	1.47E-01
A9.6	n.a.		<1.95E-01		5.23E-01	9.98E-02
A9.7	n.a.		<9.74E-02		2.69E-01	5.28E-03
A9.8	n.a.		1.04E-01	4.23E-03	3.27E-01	6.35E-03
A9.9	n.a.		<1.13E-01		3.16E-01	4.60E-03
A9.10	n.a.		<5.89E-02		9.15E-02	4.26E-03
A9.11	n.a.		<6.90E-02		9.29E-02	2.41E-02
A9.12	n.a.		8.03E-02	3.98E-02	5.83E-01	5.18E-02

Table 4-10. Tracer activity in slices from the D12 core, per grams of rock. Data recalculated from Sicada. All activities are decay corrected to the tracer injection date. The uncertainty is reported as 2δ. Cl-36 was not analysed for this core (n.a.).

Slice	Na-22 (Bq/g)	Na-22 2δ (Bq/g)	Cl-36 (Bq/g)	Cl-36 m.u. (Bq/g)	Co-57 (Bq/g)	Co-57 2δ (Bq/g)
D12.1	2.25E+01	1.03E+00	n.a.		5.13E+03	2.69E+01
D12.2	1.88E+01	9.72E-01	n.a.		7.43E+01	8.05E+00
D12.3	1.52E+01	6.70E-01	n.a.		1.71E+01	3.29E+00
D12.4	1.40E+01	4.91E-01	n.a.		7.00E+00	1.76E+00
D12.5	1.41E+01	5.56E-01	n.a.		<3.68E+00	
D12.6	9.65E+00	4.72E-01	n.a.		<3.93E+00	
D12.7	7.31E+00	2.58E-01	n.a.		<1.60E+00	
D12.8	3.71E+00	1.97E-01	n.a.		<1.62E+00	
D12.9	1.74E+00	1.32E-01	n.a.		<1.32E+00	
D12.10	7.00E-01	9.14E-02	n.a.		<1.29E+00	
D12.11	<1.87E-01		n.a.		<1.43E+00	
D12.12	<1.55E-01		n.a.		<1.38E+00	

Table 4-11. Tracer activity in slices from the D12 core, per grams of rock. Data recalculated from Sicada. All activities are decay corrected to the tracer injection date. The uncertainty is reported as 2δ, except for Ni-63 for which the method uncertainty (m.u.) from the dissolution procedure is included. Some slices were not analysed for Ni-63 (n.a.).

Slice	Ni-63 (Bq/g)	Ni-63 m.u. (Bq/g)	Ba-133 (Bq/g)	Ba-133 2δ (Bq/g)	Cs-137 (Bq/g)	Cs-137 2δ (Bq/g)
D12.1	6.72E+03	5.99E+02	9.97E+02	4.14E+00	1.65E+04	1.41E+01
D12.2	2.53E+02	2.39E+01	9.64E+01	1.46E+00	1.17E+03	4.17E+00
D12.3	3.71E+01	4.41E+00	2.05E+01	5.72E-01	2.69E+02	1.57E+00
D12.4	1.32E+01	1.31E+00	2.21E+00	2.14E-01	3.41E+01	4.85E-01
D12.5	8.61E+00	9.11E-01	<3.30E-01		9.79E-01	1.42E-01
D12.6	n.a.		<3.54E-01		5.62E-01	1.39E-01
D12.7	n.a.		<1.79E-01		3.04E-01	6.13E-02
D12.8	n.a.		<1.94E-01		1.96E-01	6.09E-02
D12.9	n.a.		<1.46E-01		2.27E-01	5.25E-02
D12.10	n.a.		<1.38E-01		1.17E-01	4.74E-02
D12.11	n.a.		<1.78E-01		7.28E-01	7.05E-02
D12.12	n.a.		<1.53E-01		2.27E-01	5.49E-02

Table 4-12. Tracer activity in slices from the D13 core, per grams of rock. Data recalculated from Sicada. All activities are decay corrected to the tracer injection date. The uncertainty is reported as 2δ, except for Cl-36 for which the method uncertainty (m.u.) from the leaching procedure is included. One slice was not analysed (n.a.).

Slice	Na-22 (Bq/g)	Na-22 2δ (Bq/g)	Cl-36 (Bq/g)	Cl-36 m.u. (Bq/g)	Co-57 (Bq/g)	Co-57 2δ (Bq/g)
D13.1	2.58E+01	2.28E+00	8.74E-01	5.21E-02	1.45E+03	1.93E+01
D13.2	n.a.		n.a.		n.a.	
D13.3	1.87E+01	1.67E+00	5.44E-01	6.50E-02	1.38E+01	3.83E+00
D13.4	1.65E+01	6.29E-01	6.31E-01	3.72E-02	<3.42E+00	
D13.5	1.38E+01	5.09E-01	6.90E-01	4.10E-02	<1.42E+00	
D13.6	1.06E+01	4.33E-01	5.47E-01	3.20E-02	<1.19E+00	
D13.7	6.69E+00	2.90E-01	5.12E-01	2.96E-02	<7.76E-01	
D13.8	3.56E+00	2.60E-01	5.09E-01	3.00E-02	<9.22E-01	
D13.9	1.16E+00	8.75E-02	2.86E-01	1.66E-02	<3.54E-01	
D13.10	1.63E-01	4.82E-02	1.61E-01	1.01E-02	<3.92E-01	
D13.11	<8.19E-02		1.77E-01	1.13E-02	<6.12E-01	
D13.12	3.55E-01	5.92E-02	2.75E-01	1.59E-02	<3.14E-01	

Table 4-13. Tracer activity in slices from the D13 core, per grams of rock. Data recalculated from Sicada. All activities are decay corrected to the tracer injection date. The uncertainty is reported as 2δ, except for Ni-63 for which the method uncertainty (m.u.) from the dissolution procedure is included. Some slices were not analysed for all tracers (n.a.).

Slice	Ni-63 (Bq/g)	Ni-63 m.u. (Bq/g)	Ba-133 (Bq/g)	Ba-133 2δ (Bq/g)	Cs-137 (Bq/g)	Cs-137 2δ (Bq/g)
D13.1	6.41E+03	5.71E+02	8.16E+02	7.89E+00	9.29E+03	2.43E+01
D13.2	3.28E+03	3.04E+01	n.a.		n.a.	
D13.3	7.44E+01	7.39E+00	5.14E+01	1.61E-02	6.84E+02	4.80E+00
D13.4	1.60E+01	1.54E+00	9.83E+00	4.28E-01	2.66E+02	1.65E+00
D13.5	7.01E+00	8.15E-01	4.13E-01	1.42E-01	8.81E+00	2.68E-01
D13.6	n.a.		<2.72E-01		1.17E+00	1.29E-01
D13.7	n.a.		<1.85E-01		6.77E-01	8.35E-02
D13.8	n.a.		<2.14E-01		1.01E+00	1.13E-01
D13.9	n.a.		9.32E-02	3.49E-02	7.18E-01	4.60E-02
D13.10	n.a.		<7.00E-02		3.05E-01	3.51E-02
D13.11	n.a.		<5.15E-02		2.04E-01	2.69E-02
D13.12	n.a.		1.08E-01	3.96E-02	3.20E-01	2.01E-02

4.4.3 Tracer concentrations in the tracer cocktail

Throughout the LTDE-SD main tracer test, tracer concentrations in the tracer cocktail that contacted the rock were measured (Widestrand et al. 2010b). The diffusion of tracers into the rock matrix, together with sorption on mineral surfaces and on the laboratory equipment, led to a decrease in tracer concentrations with time. Such declining tracer concentrations are exemplified in Figure 4-7 for Cl-36 and Cs-137.

Tracer concentrations in the water phase will be used as boundary conditions without further scrutinising in Task 9B-1. Hence, there will be little focus on experimental details such as the manner of injection, tracer interactions with experimental equipment, discrepancies in the experimental performance, etc., causing specific patterns in the evolving tracer concentrations in the water phase. Such issues will be returned to in Task 9B-2. For Task 9B-1 it may be assumed that the measured tracer concentrations represent the contacting tracer cocktail both at the target fracture and in the slim hole, at the corresponding time. Measured tracer concentrations are provided in Table 4-14 and Table 4-15.

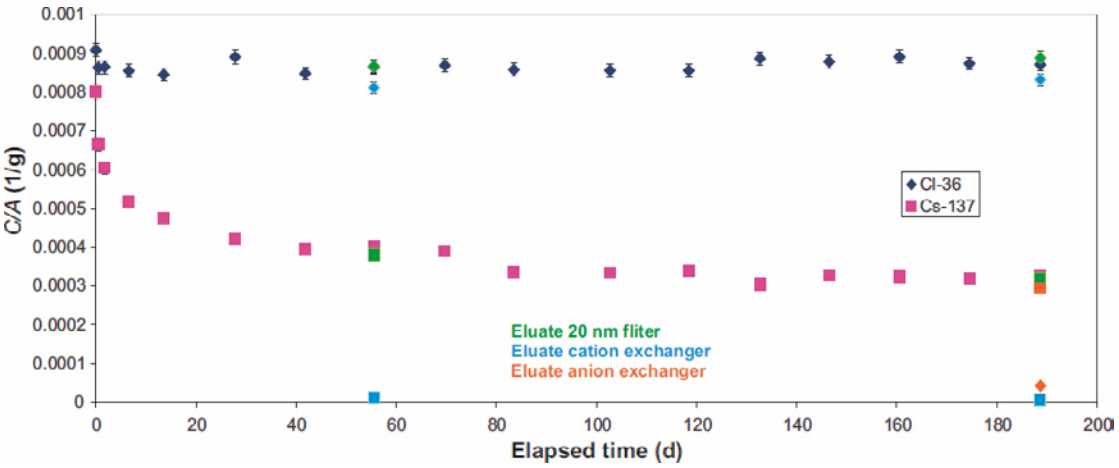

Figure 4-7. *Example of declining tracer concentrations in the tracer cocktail during the course of the main tracer test. Reproduced from Widestrand et al. (2010b, Figure 3-12).*

Table 4-14. Activities in the contacting tracer solution per mL of water, during the evolution of LTDE-SD. Data recalculated from Sicada. All activities are decay corrected to the tracer injection date.

Time after injection (h/d)	Na-22 (Bq/mL)	Na-22 2δ (Bq/mL)	Cl-36 (Bq/mL)	Cl-36 2δ (Bq/mL)	Co-57 (Bq/mL)	Co-57 2δ (Bq/mL)
2 h	3.20E+03	1.01E+02	5.35E+03	1.03E+02	1.36E+04	3.35E+02
14 h	3.14E+03	9.89E+01	5.09E+03	9.78E+01	7.03E+03	1.75E+02
44 h	3.10E+03	9.76E+01	5.09E+03	9.84E+01	3.62E+03	9.14E+01
7 d	3.02E+03	9.54E+01	5.04E+03	9.72E+01	2.63E+02	1.35E+01
14 d	3.03E+03	9.57E+01	4.98E+03	9.60E+01	1.71E+02	1.21E+01
28 d	2.96E+03	9.35E+01	5.25E+03	1.01E+02	9.83E+01	1.11E+01
42 d	2.86E+03	9.03E+01	5.00E+03	9.60E+01	8.87E+01	1.08E+01
56 d	2.66E+03	8.59E+01	5.09E+03	9.78E+01	8.70E+01	1.12E+01
70 d	3.09E+03	9.76E+01	5.12E+03	9.84E+01	1.00E+02	1.14E+01
84 d	2.70E+03	8.53E+01	5.06E+03	9.72E+01	8.94E+01	1.00E+01
103 d	2.74E+03	8.65E+01	5.05E+03	9.72E+01	9.90E+01	1.02E+01
119 d	2.81E+03	8.88E+01	5.04E+03	9.72E+01	1.10E+02	1.05E+01
133 d	2.60E+03	8.27E+01	5.22E+03	1.00E+02	1.22E+02	1.01E+01
147 d	2.89E+03	9.19E+01	5.18E+03	9.90E+01	1.36E+02	1.14E+01
161 d	2.88E+03	9.16E+01	5.25E+03	1.01E+01	1.47E+02	1.14E+01
175 d	2.83E+03	9.03E+01	5.15E+03	9.84E+01	1.52E+02	1.16E+01
189 d	2.94E+03	9.35E+01	5.13E+03	9.84E+01	1.61E+02	1.18E+01

Table 4-15. Activities in the contacting tracer solution per mL of water, during the evolution of LTDE-SD. Data recalculated from Sicada. All activities are decay corrected to the tracer injection date.

Time after injection (h/d)	Ni-63 (Bq/mL)	Ni-63 2δ (Bq/mL)	Ba-133 (Bq/mL)	Ba-133 2δ (Bq/mL)	Cs-137 (Bq/mL)	Cs-137 2δ (Bq/mL)
2 h	2.22E+04	2.16E+01	1.45E+03	3.47E+01	7.07E+03	1.78E+02
14 h	1.53E+04	1.80E+01	1.39E+03	3.36E+01	5.87E+03	1.48E+02
44 h	1.49E+04	1.77E+01	1.30E+03	3.13E+01	5.33E+03	1.35E+02
7 d	1.40E+04	1.71E+01	1.23E+03	2.97E+01	4.56E+03	1.16E+02
14 d	1.33E+04	1.68E+01	1.21E+03	2.95E+01	4.18E+03	1.06E+02
28 d	9.70E+03	1.43E+01	1.18E+03	2.92E+01	3.72E+03	9.50E+01
42 d	1.19E+04	1.58E+01	1.13E+03	2.78E+01	3.48E+03	8.89E+01
56 d	1.17E+04	1.57E+01	1.24E+03	3.38E+01	3.53E+03	9.06E+01
70 d	1.15E+04	1.56E+01	1.19E+03	2.90E+01	3.44E+03	8.89E+01
84 d	1.08E+04	1.51E+01	1.06E+03	2.60E+01	2.96E+03	7.61E+01
103 d	1.06E+04	1.50E+01	1.01E+03	2.51E+01	2.94E+03	7.58E+01
119 d	1.01E+04	1.46E+01	1.09E+03	2.69E+01	2.99E+03	7.71E+01
133 d	9.24E+03	5.32E+00	9.60E+02	2.33E+01	2.68E+03	6.93E+01
147 d	8.91E+03	5.50E+00	1.06E+03	2.62E+01	2.89E+03	7.49E+01
161 d	8.72E+03	5.17E+00	1.01E+03	2.51E+01	2.86E+03	7.41E+01
175 d	8.39E+03	5.08E+00	1.01E+03	2.51E+01	2.82E+03	7.33E+01
189 d	7.90E+03	4.92E+00	1.03E+03	2.55E+01	2.90E+03	7.52E+01

Comment:

The data in Table 4-14 and Table 4-15 were partly erroneous in the original text and also in the errata in data delivery #7. This was corrected for in data delivery #11. The revised data displayed in Table 4-14 and Table 4-15 are copied from data delivery #11 (provided in Appendix 3).

Autoradiographs and microstructural information

For the analysed core samples, for rock pieces and slices, autoradiographs were made. Two types of autoradiographs were used; film autoradiography and digital (FLA) autoradiography. The experimental method by which the autoradiography was performed is described briefly in Nilsson et al. (2010, Section 2.8).

Resulting autoradiographs are shown in Nilsson et al. (2010, Appendix 3) where each autoradiograph is paired with a photo of the same rock piece or slice. Autoradiographs were generally taken on surfaces of the slices (cf. Figure 4-8), that is parallel to the tracer cocktail/rock interface. However, autoradiographs were also taken normal to the tracer cocktail/rock interface on some cuboidal samples (prior to further sawing into slices, cf. Figure 3-5). An example of such an autoradiograph is shown in Figure 4-9

For Task 9B-1, the autoradiographs as well as photos will be delivered in higher resolution than in Nilsson et al. (2010) as a complementary data delivery. This information may be used by the modelling group to set up a small-scale structural model of the rock and its tracer migration pattern.

Comment:
Such high resolution images are found in data delivery #12 but are not included in this report.

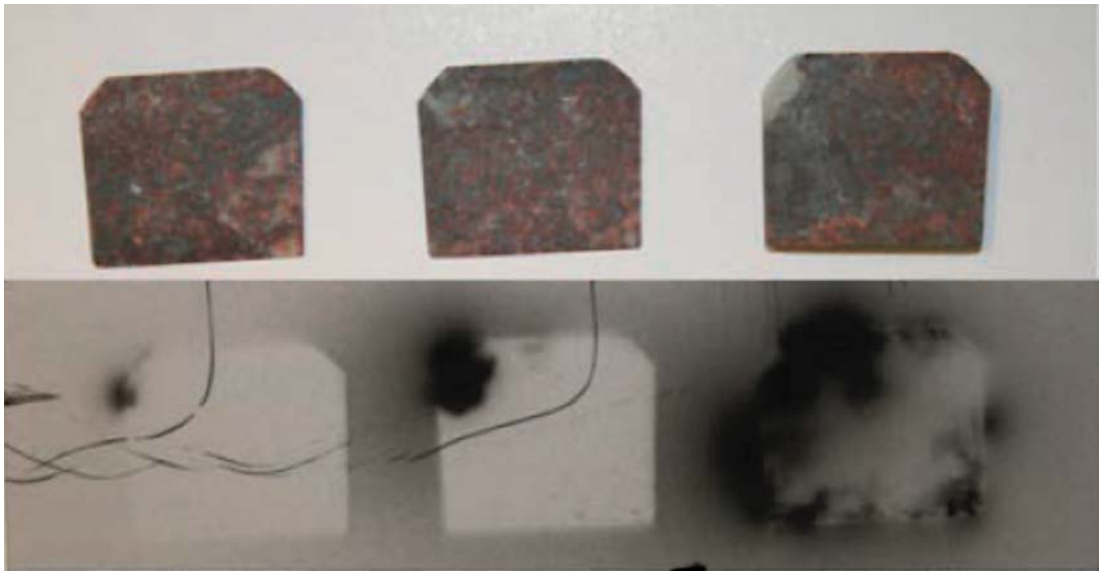

Figure 4-8, Autoradiographs of slice A6.1 (right) to A6.3 (left). *The base of the slice is approximately 16 mm.*

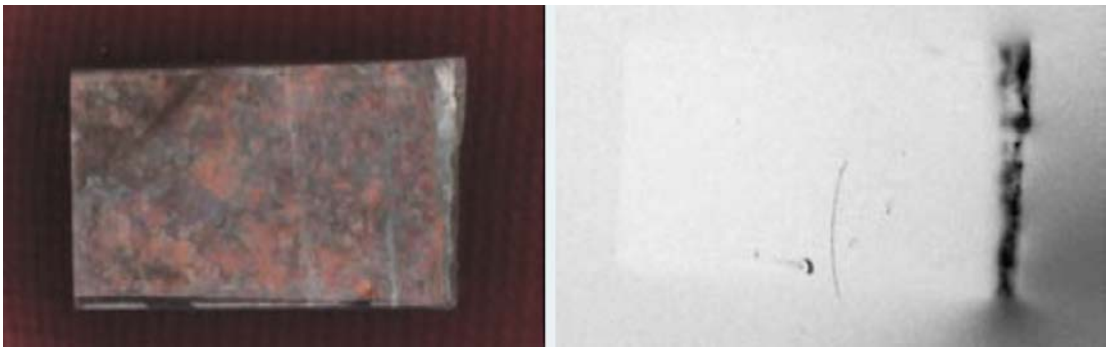

Figure 4-9. *Autoradiograph of the first few centimetres of the cuboid sawn rock core A6, prior to further sawing into slices A6.1 to A6.9. The size of the rock sample is approximately 27×16 mm.*

4.5 Deliverables and reporting of Task 9B-1

4.5.1 Deliverables and performance measures

It was discussed at the Kalmar meeting whether or not we should define a detailed framework for the deliverables of Task 9B-1, and also if we should define a number of numerical performance measures for the subtask. However, there was consensus that for this particular subtask, the modellers should be given a certain degree of freedom to define their own deliverables and performance measures, as long as they include results from the inverse modelling of the provided penetration profiles.

The specific objectives of Task 9B-1 that are outlined in Section 4.2 (i.e. item 1 to 6 of the second list), can be seen as a general framework that the modellers can use when defining their deliverables and performance measures. Even though the opportunity of defining the details of individual deliverables is given, it is within the interest of the overall Task 9 project if comparable results are presented from the different groups. It is also required that each modelling group documents their rationales and decisions behind their deliverables.

4.5.2 Description of the model and the handling of processes, features, etc.

The description of the model in Task 9B follows the same guidelines as in Task 9A. The conceptual model used, and how it is incorporated in the computational code, should be described in a transparent manner. It is encouraged to make detailed references to documents providing a comprehensive background on such issues, if such are available.

A very important part of the reporting is presenting how the model has handled different processes, events, and features. These include the experimental conditions; the perceived chain of events in the tracer test; supporting data; etc. In most modelling, a simplified representation of the reality is incorporated. Typical simplifications are neglecting processes, events and features, or streamlining them so that they fit in a reasonably simple mathematical representation. Other efforts may involve simplifying geometrical constraints; boundary conditions; the initial state; supporting data; etc.

In this respect it is important to both describe processes, conditions, data, and other features that are incorporated in the models, as well as describing those which are knowingly neglected or simplified. Unless the handling is self-evident, steps taken when simplifying the real system should be justified and the impact of the simplification should be discussed.

4.5.3 Reporting and tentative timeline for Task 9B-1

Preliminary results from Task 9B-1 are to be presented at the Task Force spring meeting in May, 2016. Tentatively this spring meeting will be held in Prague, Czech Republic. Preliminary reporting will be on the form of oral presentations at the meeting, accompanied by numerical data in Excel spread sheets submitted prior to the meeting. In the presentations, do not forget to outline your conceptual model and the major modelling decisions your group has taken in transferring this conceptual model into a numerical model. Concerning the Excel spread sheets; these should be sent to the task evaluator no later than two week prior to the spring meeting and:

- Provide numerical data on the decay corrected activity per mass of each rock slice (Bq/g) for the central modelling case, for the concerned tracers and core samples.
- Provide numerical data on the decay corrected activity per mass of each rock slice (Bq/g) for possible alternative cases, sensitivity studies, and/or uncertainty assessments, for the concerned tracers and core samples (if your results can be represented in this way).

It has not yet been decided how Task 9B-1 should be finally reported. A decision on this will have to be taken at the spring meeting. What can be presently said is that there are two main choices to make regarding the reporting of Task 9B:

1. Should Task 9B-1 and 9B-2 be reported separately or together?
2. Should there be a compilation report, as for Task 9A, or should the modelling team produce individual reports?

Until it has been decided which path to choose, the modelling groups could use the Microsoft Word template that has been distributed earlier for the reporting of Task 9A for their preliminary documentation. Other ways to proceed in making preliminary notes are also possible, at the discretion of the modelling groups. In general the final document should describe:

- The conceptual model implemented; including the significant assumptions underlying the model.
- The results of key simulations.
- Sensitivity studies and discussion of uncertainty.
- The assessment of each modelling group of their own model.

However, there is no demand on summiting the documentation prior to, or shortly after, the spring meeting. At the earliest, final reports should be summited in fall of 2016.

The modelling of Task 9B-2 is scheduled to be initiated at the spring meeting and continue for the remaining of 2016. An event that may upset this time plan is if there is an urgent need to perform predictive modelling of the TDE (through-diffusion experiment) within the REPRO project. Presently, however, it is foreseen that such modelling will not commence before fall 2016.

Modelling groups are of course free to produce additional more detailed reports or to publish in the open literature. Please provide a copy of any paper submitted to the Task Force Secretary so that publications of the different modelling groups and experimenters can be coordinated.

Comment:
The actual time plan of Task 9B has been updated. Moreover, modelling groups will present individual reports or publications, spanning over the entire Task 9B.

4.6 Additional data, documentation, and information

During the course of Task 9, additional data and documentation, as well as presentations held at meetings and workshops, will be uploaded to the member area of the SKB Task Force website (www.skb.se/taskforce). During the end of 2015 the following Task 9B-1 documents will be uploaded:

- This version of the task description.
- A word document containing some additional descriptions of the rock samples; including photos and autoradiographs of high resolution.
- A Microsoft Excel template, with short instructions, that should be used by the modelling groups for delivering numerical data within Task 9B-1 concerning penetration profiles.
- Numerical data on the redox and pH evolution in the tracer cocktail, in a Microsoft Excel spreadsheet.
- The report by Vilks et al. (2005), as a pdf-file.

In January 2016 a supplement, or appendix, to this task description will be uploaded containing:

- Some explanations on the procedure in producing decay corrected activities, and a refined timeline of the experimental chain of events leading up to the slicing of individual core samples. This time line could be used, if needed, to undo/recalculate the decay correction in the delivered results in Table 4-6 to Table 4-15.

At the Kalmar meeting it was requested that further information on the experimental chain of events should be provided, including detailed numerical information facilitating careful bookkeeping of the tracers so that a reliable mass balance could be made. However, it has later been decided to adhere to the original planning and instead provide such data in the task description to Task 9B-2. However, a preliminary version of that task description, focusing on the mass balance issue for the six tracers of Task 9B-1, is planned to be distributed in late February 2016.

For requesting additional information please send an e-mail to both

- Martin Löfgren (martin.lofgren@niressa.se), and
- Kersti Nilsson (Kersti.Nilsson@geosigma.se).

Please do not hesitate to ask questions, as we have been assigned to deal with such requests. You may also request a telephone meeting in order to receive additional explanations or help.

5 9B-1: Supporting information and data

5.1 General geological and geochemical characterisation

5.1.1 Geology

A general geological characterisation of the local LTDE-SD site is reported in Winberg et al. (2003). This characterisation includes a structural fracture model of the local site. It also includes a characterisation of fracture minerals for the different fractures (cf. Winberg et al. 2003, Section 4.3). The target fracture for LTDE-SD is a splay fracture that includes fractures #10a and #10b. A mylonitic/cataclastic lens exists between the fractures, which are separated by a distance of 5 to 17 mm. The drillhole was drilled past the splay fracture and the mylonitic/cataclastic lens was removed from the borehole. As drilling continued into the underlying rock matrix, a core stub was created and the stub surface is the far side of fracture #10a. The removed rock material (i.e. the lens) is shown in Figure 5-1.

Based on borehole camera images, an illustration of the fracture coating of the target fracture surface could be made (Winberg et al. 2003, Section 4.5). This illustration is reproduced in Figure 5-2. The upper part of the illustration portrays the fracture surface contacted by the tracer solution in the in-situ tracer test. The lower part portrays the borehole walls around the target fracture, as seen from the inside of the borehole.

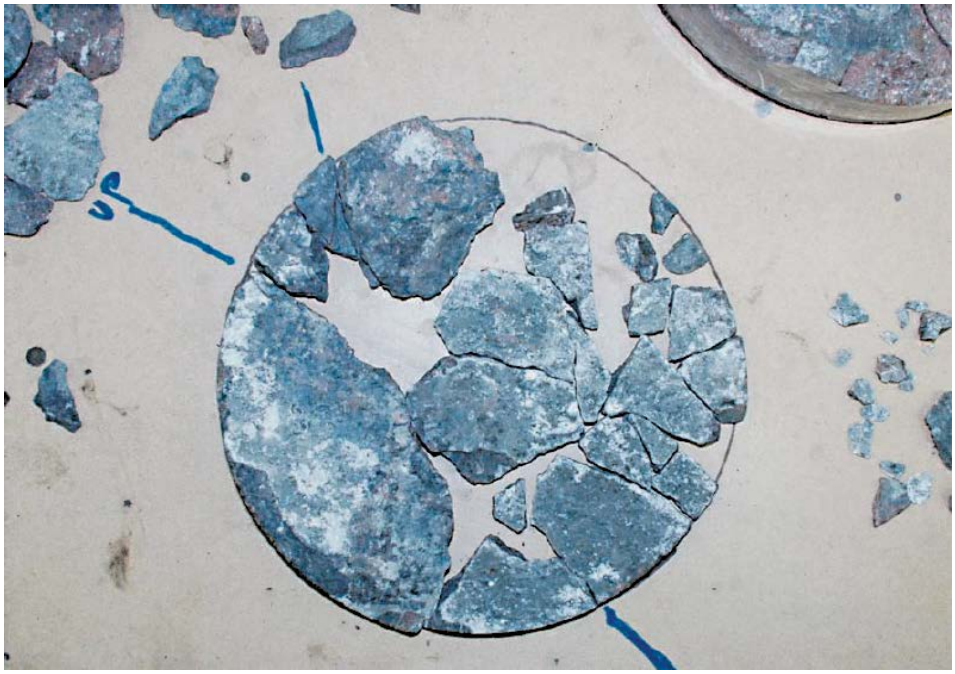

Figure 5-1. *The matching surface to the target fracture. The major part of the surface is covered by a mm-thick layer of calcite as can be inferred from the borehole wall next to the stub. The main fault is extensively deformed and shows strike slip behaviour. Reproduced from Winberg et al. (2003, Figure 4-13).*

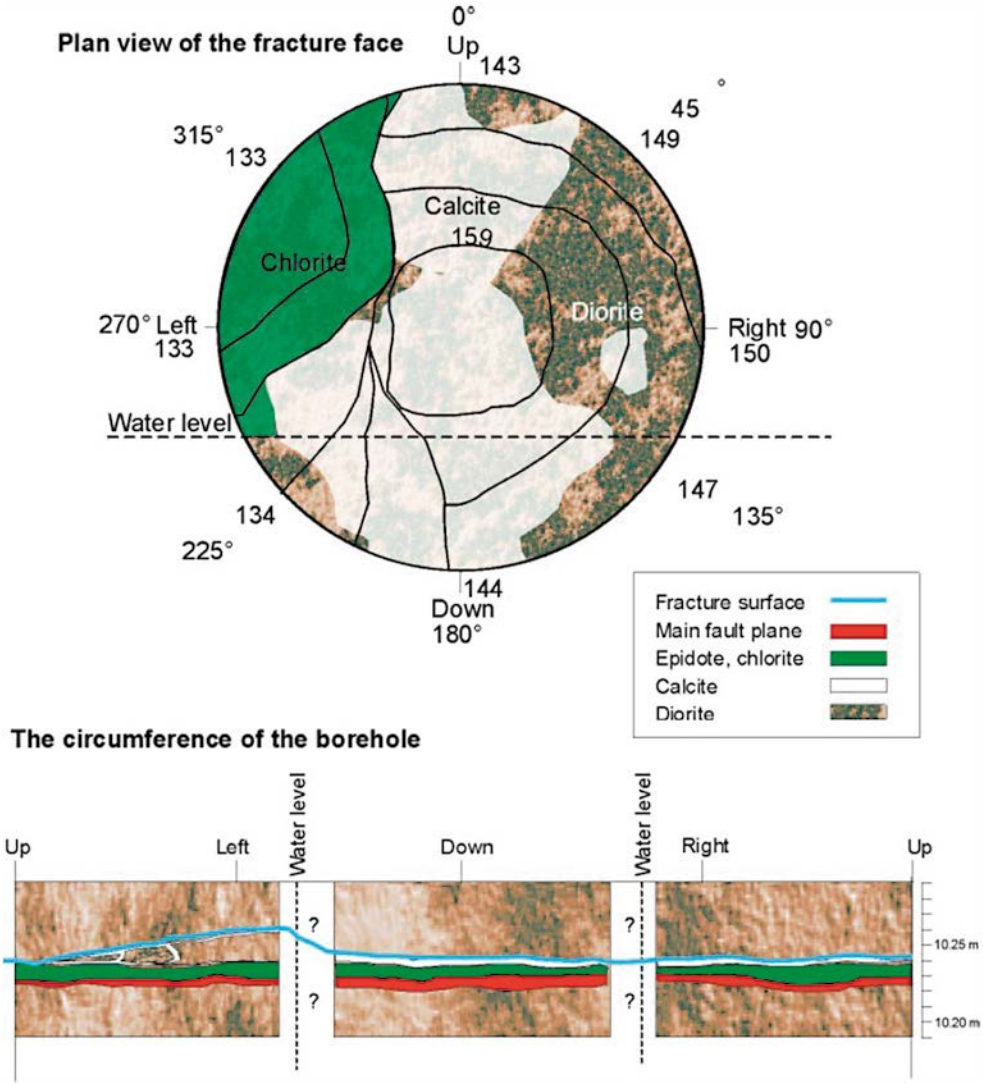

Figure 5-2. *Illustration of the face of the target fracture and the circumference of the target structure around the borehole. Based on borehole camera that also filmed/photographed in the slot around the stub. The hatched line indicates the part of the face that was covered by water during the inspection. Reproduced from Winberg et al. (2003, Figure 4-10).*

Concerning the uncoated parts of the target fracture in Figure 5-2, labelled as diorite, it should be noted that since the publication of Winberg et al. (2003), the rock type has been reclassified to granodiorite.

A photo of the stub surface, after being extracted in the over-coring, is shown in Figure 5-3. Beside the drill core one can see the PEEK plate that was used to pack-off the stub. The yellow material on the plate is the epoxy that was injected upon termination of the in-diffusion phase. As can be seen, spots of fracture minerals cling to the epoxy.

Concerning the underlying rock matrix, a chemical analysis of the rock type is provided in Widestrand et al. (2010a, Table 2-1 and Appendix 1). This analysis provides both percentages of main minerals and total content of elements. Table 2-1 of Widestrand et al. (2010a) is reproduced below.

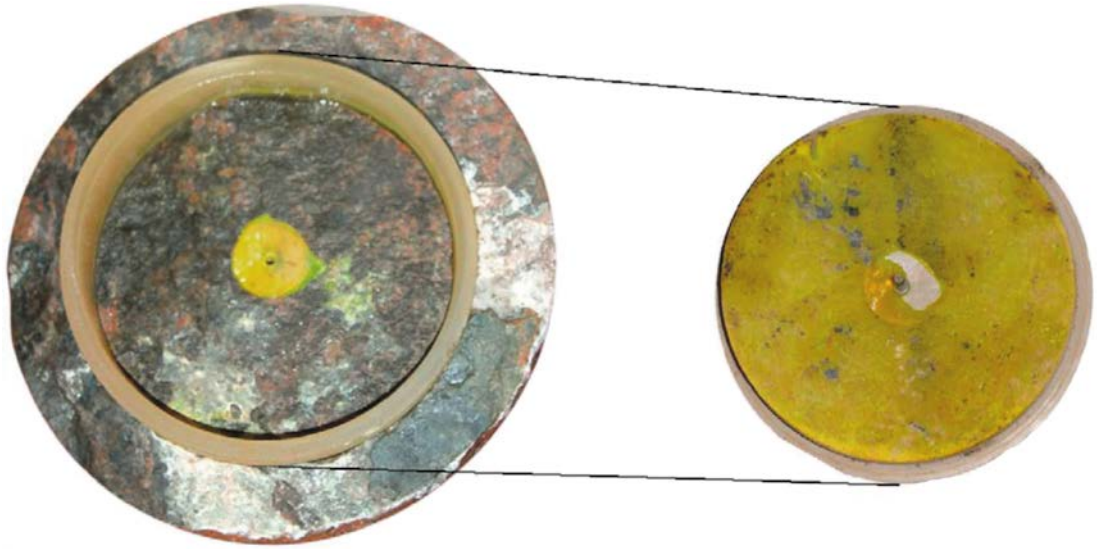

Figure 5-3. *Photograph of the stub to the left and the PEEK-epoxy plate to the right. It is the area inside the polyurethane cylinder that has been exposed to the tracer solution. The PEEK-epoxy plate has been reversed in order to simplify the comparison with the stub surface. Most of the grey spots visible at the yellow surface are remaining rock material, primarily fracture minerals. The alignment of the core in the photo is in accordance with that of Figure 5-2. Reproduced from Nilsson et al. (2010, Figure 3-1).*

Table 5-1. Mineralogical composition and distribution of three thin sections, representing rock samples from KA3065A02 and KA3065A03, determined by thin section analysis (so-called point counting). Mean value of Ävrö granodiorites included in the Transport laboratory programme (SKB Site Investigation) is given as a comparison. Reproduced from Widestrand et al. (2010a, Table 2-1).

Mineral	A02, Unaltered rock sample of Ävrö granodiorite (adjacent to rock sample A02:5) vol.%	A03 #10, strongly altered rock (Ävrö granodiorite), mylonitic/cataclasitic rock and fracture coating vol.%	A03 #14, slightly red-stained Ävrö granodiorite vol.%	Ävrö granodiorite within the Transport laboratory programme* vol.%
Quartz	30.6	33.2	35.2	30.4
Plagioclase	3.0		13.0	33.2***
Sauss. Plag.	27.6		13.2	
Sericitised Plag*		16.3		
K-feldspar	28.6	30.8	31.8	25.8
Biotite	5.8		3.0	2.2
Chlorite	1.8	3.6	2.0	3.6
Titanite	1.0		0.4	0.4
Epidote	0.6	13.1	0.6	2.8
Opaque	1.0		0.6	0.4
Hornblende				0.6
Apatite	– **	0.2	0.2	
Calcite		2.6		
Allanite		0.2		

* Data from rock sample KLX02 753.80 (Oskarshamn Site Investigation).
** less than 0.2 percent.
*** The plagioclase is to some extent saussuritized, although not determined in percentage.

A general geological description of the extracted drill cores of the telescoped experimental borehole is given in Widestrand et al. (2010a, Chapter 2). This description includes various photos and information from thin section analysis etc. Detailed geological information is also given in Nilsson et al. (2010, Appendix 3) for each of the core samples extracted from the over-cored rock volume and used for subsequent radionuclide content analysis.

5.1.2 Hydrogeochemistry

Groundwater chemistry measurements at the LTDE-SD site were performed in 2005 and composition data are reported in Widestrand et al. (2006, Section 3.3 and Appendices D and E). Groundwater sampling was also performed three months prior to tracer injection in the main tracer test in 2006 and composition data are reported in Widestrand et al. (2010b, Appendix 5). The background solution for the tracer cocktail, in which tracers were injected in the main tracer test, was natural groundwater withdrawn from the surrounding rock. The main water composition was hence assumed to be compatible with the ambient groundwater composition (save for the redox conditions).

During the main tracer test, groundwater and environmental parameters such as temperature, pH and Eh were measured which is described in Widestrand et al. (2010b, Sections 2 and 3.1, Appendices 6 to 8). The pH kept fairly stable around 7 during the major part of the experiment, save for directly upon tracer injection when a spread between ~6 to ~8 was observed (cf. Figure 5-4). After stabilisation the data were in line with those previously measured in groundwater at the local site. Regarding Eh there was a fluctuation upon injection, as is shown in Figure 5-4. Importantly, the Eh of about +470 mV in the tracer cocktail, upon stabilisation, indicates oxidising conditions. This does not match the expected Eh of the surrounding groundwater. Three months prior to the tracer injection, a reducing Eh of –90 mV was measured in the surrounding groundwater (Widestrand et al. 2010b, Section 3.1).

An inability to keep reducing conditions in the tracer cocktail was also observed in the functionality test (Widestrand et al. 2006). Aqueous speciation calculations made prior to the main tracer test are reported in Widestrand et al. (2010b, Section 3.1) for both oxidising and reducing conditions. The synthetic groundwater composition used as background solution in the laboratory is provided in Widestrand et al. (2010a, Section 2.5).

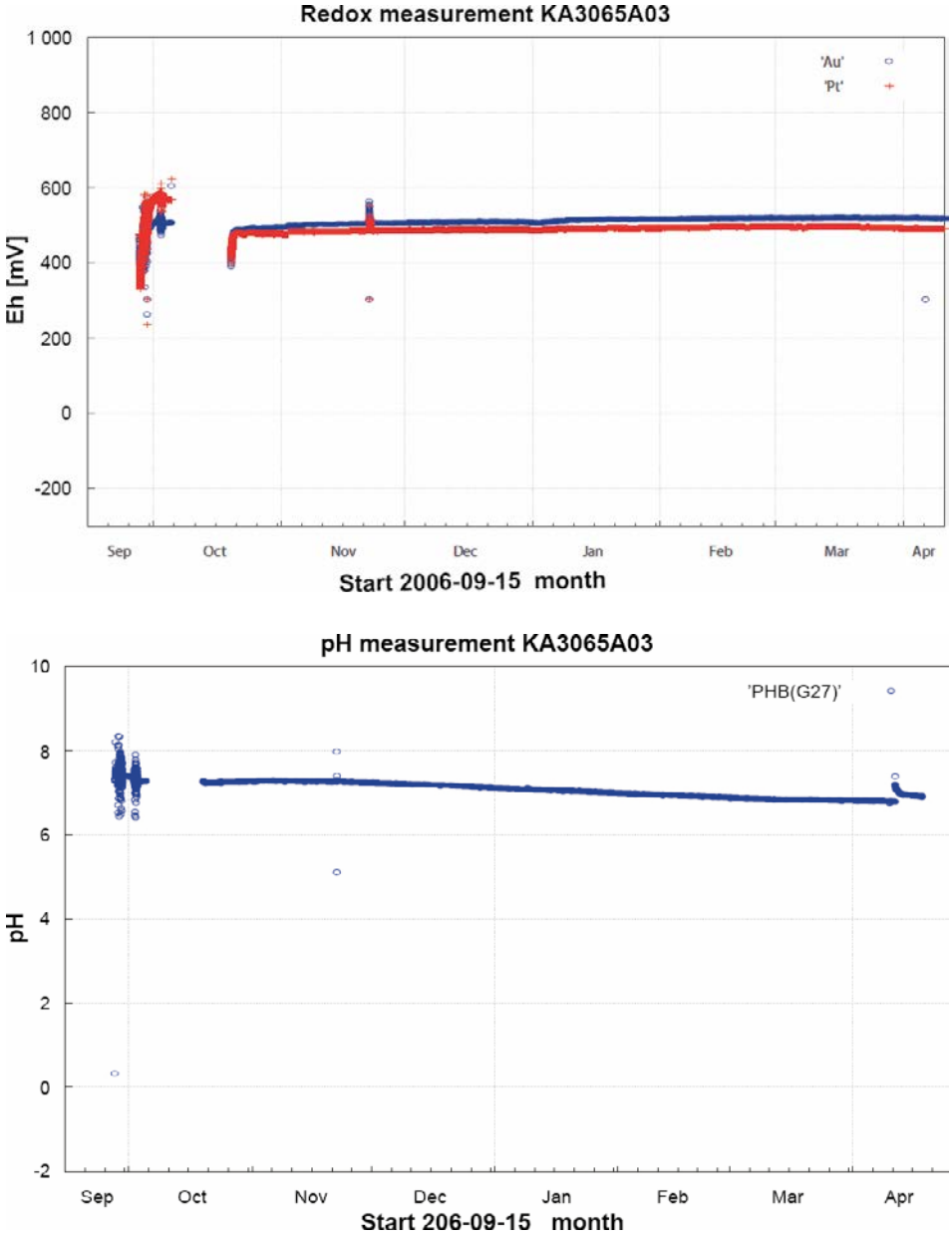

Figure 5-4. *Development in Eh and pH as detected by on-line measurements in the LTDE-SD loop. Reproduced from Widestrand et al. (2010b, Appendix 7).*

5.2 Laboratory migration data from the LTDE-SD site

5.2.1 Porosity

This section provides references to porosities found in tables, graphs and figures in Widestrand et al. (2010a) and Vilks et al. (2005). Porosity data come from water immersion and ^{14}C-PMMA impregnation techniques. Rock capacity factors come from through-diffusion measurements.

A compilation of water immersion and ^{14}C-PMMA impregnation porosities obtained in the SKB laboratory camping is provided in Widestrand et al. (2010a, Table 4-1). A compilation of the water immersion porosities obtained in the AECL laboratory camping is provided in Vilks et al. (2005, Table 1) and is duplicated in Vilks et al. (2005, Table 2).

Detailed information on the porosity distribution, as obtained by ^{14}C-PMMA impregnation, is given for samples adjacent to, and distant from, natural fractures in Widestrand et al. (2010a, Appendix 3).

A compilation of the (only two) rock capacity factors for HTO found in the SKB laboratory camping is provided in Widestrand et al. (2010a, Appendix A). Compilations of the HTO and iodide rock capacity factors found in the AECL laboratory camping are provided in Vilks et al. (2005, Tables 1 and 2).

There are also data on the frequency of micro-fractures in drill cores, from the centre to the mantel area of core samples, which can be used to estimate mechanically induced excavation damages. Such data are found in Li (2001, Chapter 4) indicating that excavation damage may be an important factor for certain samples. However, associated porosities or fracture apertures are not provided.

5.2.2 Effective diffusivity and formation factor

This section provides references to effective diffusivities and formation factors found in tables and figures in Widestrand et al. (2010a) and Vilks et al. (2005).

A compilation of the effective diffusivities obtained in through-diffusion experiments in the SKB laboratory camping is provided in Widestrand et al. (2010a, Table 4-2). Four sets of data are presented for HTO and one for Cl-36. This table also includes two formation factors obtained by electrical methods.

A compilation of the effective diffusivities obtained in through-diffusion experiments on small core samples in the AECL laboratory camping is provided in Vilks et al. (2005, Tables 1 and 2) for HTO and iodide. Effective diffusivities derived from the radial diffusion experiments are provided in Vilks et al. (2005, Tables 3 and 4) for iodide and uranine. Tracer penetration profiles, similar to those of the LTDE-SD main tracer test in-situ, are found in Vilks et al. (2005, Figure 21).

5.2.3 The parameter group $K_d \cdot F_f$

Concerning the results from the laboratory in-diffusion experiments, also called sorption-diffusion experiments, this is discussed in Widestrand et al. (2010a, Section 4.3). In Widestrand et al. (2010a, Table 4-4) the parameter group $K_d \cdot F_f$ is provided for the tracers Na-22, Co-57, Ni-63, and Cs-137 based on experiments in two different samples. In addition data are given for Cd-109 and Ba-133 but these tracers are not modelled in Task 9B-1. Raw data on the decrease in tracer concentrations in the tracer cocktail are plotted in Widestrand et al. (2010a, Appendix 5). The corresponding numerical data can be provided upon request.

5.2.4 Anion exclusion

Data on anion exclusion can be derived if comparing effective diffusivities and rock capacity factors from through-diffusion experiments using iodide and HTO on the same rock sample. Such experiments were predominately made within the AECL laboratory campaign and anion exclusion factors can be derived from data from the same samples in Vilks et al. (2005, Tables 1 and 2). In the SKB laboratory campaign, quantitative results could be derived from a single through-diffusion experiment using HTO and Cl-36 on the same sample (Widestrand et al. 2010a, Appendix 4). In general, the anion exclusion appears to be limited for the site specific rock samples, at least at destressed conditions in the laboratory.

5.2.5 Sorption partitioning coefficients and BET surface areas

Results from batch sorption experiments are provided in Widestrand et al. (2010a, Appendix 11). Here the R_d data are given for different contact times, for different size fractions, and for different replicates. For information on how to identify what sample, size fraction, and replicate that the data point represents, Widestrand et al. (2010a, Tables 4-9 and 4-10) are recommended. The K_d value of each sample was assumed to correspond to the R_d value at the longest contact time and for the largest size fraction in the batch sorption experiments. K_d values are given in Widestrand et al. (2010a, Table 4-11 and Figures 4-26 and 4-27).

BET surface areas are given for different samples, size fractions and replicates in Widestrand et al. (2010a, Table 4-12).

5.3 Tracer activities in B-samples

Upon termination of the LTDE-SD main tracer test, the tracer cocktail was expelled using an isopropanol solution. Thereafter an epoxy resin was injected to protect the target fracture from the influence of over-coring. As can be seen in Figure 5-3, some of the fracture coatings cling to the epoxy when removing it from the core stub in the laboratory. For this and other reasons, circular disks of the epoxy resin were extracted in a fashion so that they corresponded to the surface of the A-cores (cf. Figure 5-5). These discs were called B-cores and were analysed with respect to their radionuclide content (Nilsson et al. 2010, Section 3.5).

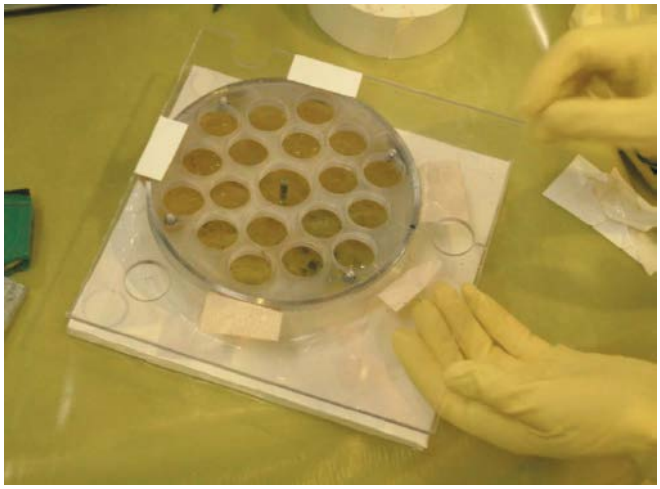

Figure 5-5. *Preparations before drilling of the B-core samples using a jig attached to the epoxy coated PEEK lid for achieving their appropriate positions. At this stage a protective coating of clear epoxy resin had been applied on the first yellow coloured layer of epoxy. Reproduced from Nilsson et al. (2010, Figure 2-8).*

A surprisingly large amount of radioactivity was found in the B-samples, compared to what was found in the A-samples. The amounts in Becquerels found in the first slice of the A-core and the corresponding B-samples, for different tracers, are shown in Table 5-2. Transfer of tracers to the epoxy resin could have occurred from the contacting rock or from remnants of the tracer cocktail upon terminating the experiment.

Table 5-2. Estimation of tracer distribution between Epoxy (B-samples) and the first A-core slice, results from γ-measurements. The sum of the tracer activity in Slice 1 and the tracer activity measured in Epoxy piece/pieces with adhered rock material is presented as the total surface activity. The part of that total activity which was found in the Epoxy is also given in the table. Reproduced from Nilsson et al. (2010, Table 3-4).

Sample		^{22}Na	^{57}Co	^{109}Cd	^{110m}Ag	^{133}Ba	^{137}Cs	^{153}Gd
A1/B1	Sum activity, rock slice 1 + Epoxy (Bq)	62	27,000	16,000	3,800	1,400	14,600	3,800
	Part in the epoxy	50%	93%	55%	92%	21%	6%	82%
A6/B6	Sum activity, rock slice 1 + Epoxy (Bq)	94	13,000	11,000	3,600	1,200	31,600	2,100
	Part in the epoxy	55%	78%	29%	93%	12%	3%	49%
A8/B8	Sum activity, rock slice 1 + Epoxy (Bq)	47	15,000	4,000	625	190	2,400	1,170
	Part in the epoxy	26%	99.5%	90%	<100% [1)]	47%	13%	<100% [1)]
A9/B9	Sum activity, rock slice 1 + Epoxy (Bq)	37	10,000	5,900	870	400	5,300	1,200
	Part in the epoxy	76%	89%	52%	79%	19%	2%	57%
A17/B17	Sum activity, rock slice 1 + Epoxy (Bq)	98	14,000	16,000	6,700	570	6,300	2,200
	Part in the epoxy	83%	89%	30%	95%	19%	3%	62%
Concentration in the solution containing the excess of epoxy obtained at the epoxy injection (Bq/mL)		480	80	470	<2	100	480	<4

[1)] No tracer found in the surface sample of the rock, tracer only measured in the epoxy sample.

Comment:
Numerical data on activities in the epoxy resin are provided in Appendix 4.

6 9B-1: Looking ahead – tentative focus of Task 9B-2

Although the objective of Task 9B-2 may be revised along the way, some tentative objectives of Task 9B-2 are listed below:

To use, or improve, the Task 9B-1 model with regard to small-scale rock characteristics and migration/retention/reaction processes with the aim at explaining the observed range of tracer behaviour.

To model the entire LTDE-SD in-situ experiment, including the decline of tracer activities in the tracer cocktail and the migration of tracers into the entire rock volume surrounding the experimental sections of the injection hole. Also tracer amounts sticking to the experimental equipment etc. should be accounted for, to facilitate a mass balance approach.

Three A-cores and two D-cores from the over-cored LTDE-SD rock volume, not previously analysed, will be revisited and analysed in respect to Cl-36, Ni-63, Ba-133, and Cs-137. The model of the entire LTDE-SD in-situ experiment can, accordingly, be used to predict their penetration profiles.

Comment:
The predictive modelling is carried out in Task 9B-3.

- To model an extended set of tracers used in the experiment compared to the ones considered in Task 9B-1, mainly regarding more strongly sorbing tracers. Also, if any modelling group choose not to model Ba-133 in Task 9B-1, it will be modelled in Task 9B-2.
- To discuss if penetration profiles of sufficient accuracy and resolution can be obtained with the used experimental procedures, from the perspective of inverse modelling and the quantification of retention parameters. If not, are there modified experimental procedures that could have improved the accuracy and resolution?
- To discuss, but perhaps not to model within this particular subtask, the implication of the improved models for understanding future in-situ tracer tests and also for improving long-term and large-scale performance assessment.
- After the Task Force spring meeting in 2016 there is room for incorporating ideas presented by other modelling groups.

In addition, it is planned to perform X-ray microtomography on one or a few rock samples from the LTDE-SD site and also from the REPRO site at ONKALO during 2016. Such detailed microstructural information would benefit Task 9B-2, as one may gain fine-scale information on the spatial distribution of the pore space and mineral grains. More information on X-ray computed microtomography is found in Voutilainen et al. (2012).

7 9B-2: Introduction

Task 9B-2 is a continuation of Task 9B-1. Together these two subtasks form Task 9B, which concerns the in-situ experiment LTDE-SD carried out at the Äspö Hard Rock Laboratory in Sweden. In the Task 9B suite of subtasks there will also be a future Task 9B-3 that concerns predictive modelling of new LTDE-SD penetration profiles. A detailed description of the LTDE-SD experiment is provided in the task description of Task 9B-1 (dated 2015-11-26) and references therein. Only a minimum of information already given in that task description is repeated in this present document.

While Task 9B-1 only focused on the inverse modelling of a limited part of the LTDE-SD experiment, Task 9B-2 includes the inverse modelling of the major part of the experiment. This includes the modelling of an expanded set of radionuclides; in total 11 out of the 22 injected tracers. For the chosen radionuclides, the entire set of tracer concentration data obtained within the experiment is provided. In addition we provide an extended set of experimental records and data needed in making tracer mass balances for the experiment. As such, Task 9B-2 concerns the inverse modelling of the fate of the chosen radionuclides in the LTDE-SD system, and not only the modelling of their penetration into the rock matrix. Generally speaking radionuclides could have:

- stayed dissolved in the tracer cocktail in the LTDE-SD borehole until experimental termination;
- diffused into the surrounding rock matrix and become sorbed on its mineral surfaces;
- become attached to the experimental equipment;
- leaked from the system;
- been removed by water sampling.

Although the main focus of Task 9B is to explain the anomalous penetration profiles in LTDE-SD, calculating the mass balances and understanding the experimental conditions strengthen (or weaken) the notion that the anomalous penetration profiles are caused by natural processes and not by experimental artefacts. For some tracers featuring very shallow penetration, which is the case for the new radionuclides of Task 9B-2, data can still be used to evaluate their sorption properties.

8 9B-2: Specifics of Task 9B-2

8.1 Objectives of Task 9B-2

The objectives presented in the task description for Task 9B-1 generally apply for the entire Task 9B. Additional objectives of Task 9B-2, directly related to the new data of this task description, are as following:

1. In Task 9B-1, the radionuclides Na-22, Cl-36, Co-57, Ni-63, and Cs-137 were included. Furthermore, it was optional to include Ba-133 in the subtask. All of these radionuclides penetrated into the surrounding rock matrix and activities could be quantitatively recorded in, at minimum, three rock slices.

   In Task 9B-2, the radionuclides Cd-109, Ag-110m, Gd-153, Ra-226 and Np-237 will also be modelled. The activities of these radionuclides have been quantitatively recorded in the first rock slice and in some instances also in the second rock slice. For these radionuclides the focus is primarily on the distribution between the tracer cocktail and rock matrix and secondarily on anomalous penetration profiles. For the modelling groups that did not include Ba-133 in Task 9B-1, this nuclide will be included in Task 9B-2.

2. In Task 9B-1, the time dependent data on the evolution of the tracer concentrations in the tracer cocktail were assumed to be accurate without further scrutinising.

   In Task 9B-2, the overall mass balances of the experiment are evaluated, for all included radionuclide. This includes keeping track of the amounts of tracers injected into the borehole; withdrawn from the borehole at sampling and experimental termination; attached to experimental equipment and in the epoxy resin; carried away by leakages; and transported into the rock matrix of the overcored rock volume. Mass balance calculations provide an opportunity to scrutinise the reliability of the tracer concentration data in the cocktail (and rock slices).

3. In Task 9B-1 penetration profiles and supporting geological data were only provided for four of the drill core samples from the overcored rock volume, i.e. A6, A9, D12, and D13. These four drill core samples were selected as they display significant tracer penetration. Accordingly, there may be a bias towards larger porosities and diffusivities and/or lower or heterogeneous sorption properties.

   In Task 9B-2, penetration profiles and supporting geological data will be supplied for all analysed A- and D-cores. Penetration profiles are available for ten A-cores and eight D-cores, although not necessarily for all tracers. The extended set of penetration profiles will provide a less biased representation of rock surrounding the test sections, compared to in Task 9B-1. Such data can be used to better estimate the tracer amounts that have penetrated into the entire rock volume surrounding the test sections. The extended set of data can also be used to evaluate the variability in the tracer penetration pattern.

8.2 The rock samples in Task 9B

8.2.1 Core samples

From the overcored rock volume, in total 21 A-cores and 16 D-cores have been drilled. 18 of the A-cores (A1-A18) were positioned inside the polyurethane/PEEK cup (see outer yellow ring in Figure 8-1) and where hence directly exposed to the tracer cocktail. Cores A19-A21 were positioned outside the cup but may have been indirectly exposed. The (entire) cores were all measured with gamma spectrometry in October 2007 before they were sliced, although not under well calibrated conditions. The results are presented in Nilsson et al. (2010, Appendix 8).

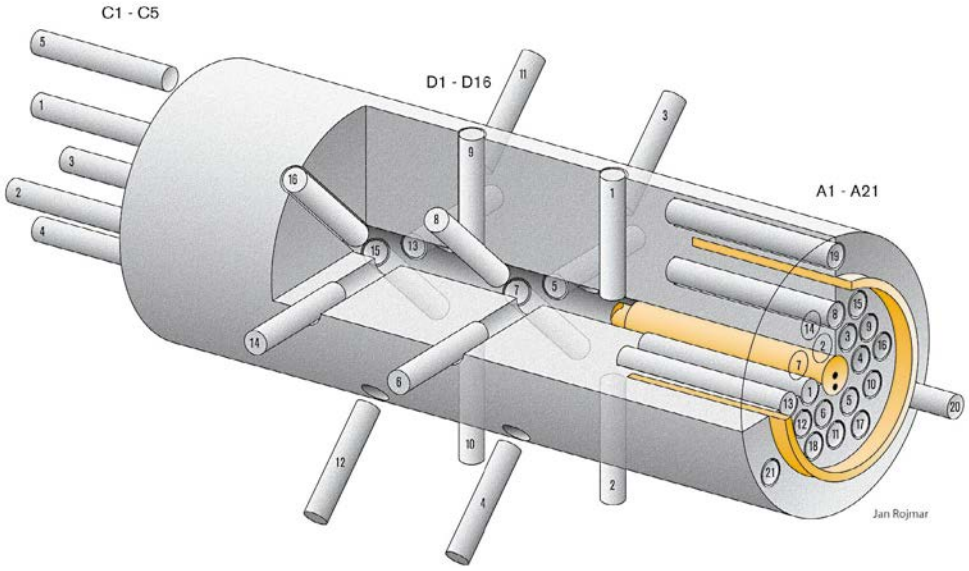

Figure 8-1. *Illustration of the sampling of the overcored rock volume in LTDE-SD. Polyurethane cylinder and packer are shown in yellow. Together with a PEEK lid the cylinder formed a cup-like packer. The slim hole section contained a PEEK dummy in order to reduce the test volume. The dummy is not displayed in the figure.*

All A-cores directly exposed to the tracer cocktail, as well as core A20, were sliced to facilitate further activity analysis. However, such analysis was only performed on eleven of the A-cores (cf. Table 8-1; Nilsson et al. 2010, Table 2-2), including core A20 which proved to be almost uncontaminated by tracers (Nilsson et al. 2010, Appendix 11). All D-cores were sliced in the same fashion, and the tracer activities of eight cores were analysed.

Table 8-1. Cores that have been sliced and where tracer activities have been quantitatively measured.

	Task 9B-1	Task 9B-2, additional cores	Task 9B-3, predictive modelling
A-cores	A6, A9	A1, A5, A8, A10, A12, A15, A16, A17, A20	A4, A11, A13
D-cores	D12, D13	D1, D5, D6, D7, D8, D14	D15, D16

The weights and thicknesses of the individual slices of the core samples of Task 9B-2 are provided in an accompanying Excel file, as part of the Task 9B-2 data delivery:

- Excel file: Task 9B-2 Rock matrix data, Spreadsheet: Partitioning

This Excel file is on the same format as provided in the Task 9B-1 task description (Tables 3-1 to 3-4) for the Task 9B-1 cores. Geological descriptions of these core samples, with the exception of core A20, are provided in Nilsson et al. (2010, Appendices 3 and 4). These appendices also provide photos of the cores and individual slices, as well as autoradiographs. The corresponding photos and autoradiographs will be provided with higher resolution in an accompanying Word file as part of the Task 9B-2 data delivery.

Comment:
Data on the partitioning of the cores are provided in Appendix 2. High resolution photos are not incorporated in this report.

8.3 Tracers of Task 9B-2

8.3.1 Description of tracers

The tracers used in the LTDE-SD main tracer test are described in Widestrand et al. (2010b, Sections 2.2 and 2.3). Tracers included in Task 9B-2 are the six tracers of Task 9B-1 and in addition Cd-109, Ag-110m, Gd-153, Ra-226 and Np-237. Half-lives of these eleven tracers are reproduced from Nilsson et al. (2010, Table 1-1) in Table 4-5.

Table 8-2. Half-lives of tracers in Task 9B-2. Data reproduced from Nilsson et al. (2010, Table 1-1).

Radionuclide	Half-life
Na-22	2.6 years
Cl-36	$3.0 \cdot 10^5$ years
Co-57	272 days
Ni-63	100 years
Cd-109	463 days
Ag-110m	250 days
Ba-133	10.5 years
Cs-137	30 years
Gd-153	240 days
Ra-226	1600 years
Np-237	$2.1 \cdot 10^6$ years

A few notes on each radionuclide included in Task 9B-1 are provided in the Task 9B-1 task description (Section 4.4). Corresponding notes are provided below for the remaining Task 9B-2 radionuclides.

Cd-109

In Widestrand et al. (2010b) speciation calculations have been made in PHREEQC that should reflect the cadmium speciation in the tracer cocktail in the LTDE-SD borehole. In these calculations the impact of the surrounding rock has been neglected. In the water phase, cadmium is proposed to primarily associate with chloride and exist as $CdCl^+$ (71 %) and dissolved $CdCl_2$ (25 %). Only 3 % is proposed to be in the form of divalent Cd^{2+} while 1 % is anionic $CdCl_3^-$. The suggested mechanism for sorption (for Cd^{2+}) is surface complexation (Widestrand et al. 2010b, Table 2-1). Sorption studies in the laboratory (Widestrand et al. 2010a, Table 4-11) show moderate sorption partitioning coefficients of cadmium. This is consistent with the fact that Cd-109 was only found in quantitative amounts in the first slice, or the first two slices, of the A- and D-cores (Nilsson et al. 2010, Appendix 6). This suggests that the reactive sites on the mineral surfaces would have had a significant impact on the speciation calculations, should they have been included. The same may also apply for the below discussed radioelements. Cadmium attached both to anion and cation exchangers at high amounts (Widestrand et al. 2010a, Table 4-11), which further supports the notion that functional groups of reactive materials alter the cadmium speciation.

Ag-110m

Silver is also proposed to associate with chloride in the PHREEQC calculations of Widestrand et al. (2010b), where the majority of the dissolved silver forms the anionic species $AgCl_2^-$ (74 %) and $AgCl_3^{2-}$ (21 %). Only 4 % is dissolved as non-charged AgCl (aq). The suggested mechanism for sorption (for Ag^+) is surface complexation (Widestrand et al. 2010b, Table 2-1). The absence of a penetration profile for Ag-110m does not necessarily point to the fact that the various species do not penetrate into the rock matrix, or sorb very strongly in the first slice, but may be due to the detection limit of the analysis method. However, in batch sorption experiments in the laboratory, Ag-110m sorbed relatively well (Widestrand et al. 2010a, Table 4-11), although one may want to examine if precipitation had a role in the experiments. In the in-situ experiment Ag-110m did not behave as, for example, the non-sorbing anion Cl-36 in the water phase, which is sometimes assumed in safety assessment. This is as virtually no (dissolved) Ag-110m remained in the tracer cocktail at the end of the experiment (Widestrand et al. 2010b, Table 3-11).

Gd-153

Gadolinium is another element that is proposed to have complex speciation chemistry at the groundwater composition of LTDE-SD (Widestrand et al. 2010b, Table 3-3). The majority of Gd-153 is proposed to be the monovalent cation $GdCO_3^+$ (59 %) but a significant fraction is as the trivalent cation Gd^{3+} (26 %). Other species are GdF^{2+} (9 %), $CdCl^{2+}$ (1 %), $GdOH^{2+}$ (1 %) and the anion $Gd(CO_3)_2^-$ (3 %). The suggested mechanism for sorption, for Gd(III), is surface complexation (Widestrand et al. 2010b, Table 2-1). In laboratory batch sorption experiments, good sorption was achieved (Widestrand et al. 2010a, Table 4-11). Only minute amounts of the tracer remained in the tracer cocktail at the end of the in-situ experiment (Widestrand et al. 2010b, Table 3-11).

Ra-226

Ra-226 is one of the most important radionuclides when assessing the radiological risk from a geological repository for spent fuel. In the speciation calculations of Widestrand et al. (2010b), 100 % of the dissolved radium was proposed to be as Ra^{2+}. The suggested mechanism for sorption, for Ra^{2+}, is cation exchange (Widestrand et al. 2010b, Table 2-1). Sorption studies in the laboratory (Widestrand et al. 2010a, Table 4-11) show moderate sorption partitioning coefficients of the radioelement. This is consistent with the fact that Ra-226 was only found in quantitative amounts in the first slice, or the first two slices, in the A- and D-cores. A fairly good portion of the tracer remained in the tracer cocktail at the end of the experiment (Widestrand et al. 2010b, Table 3-11). The tracer became attached to cation exchanger at high amounts but not to anion exchanger (Widestrand et al. 2010a, Table 4-11).

Np-237

Neptunium is sensitive to the redox potential. At relatively oxidising conditions, which likely existed in the tracer cocktail in the borehole, 96 % of neptunium is as NpO_2^+ while 3 % is either as dissolved NpO_2Cl or NpO_2OH (Widestrand et al. 2010b). Under reducing conditions, corresponding to those of the undisturbed host rock at depth, 100 % of the radioelement is proposed to be as $Np(OH)_4$ (aq). The suggested mechanism for sorption, for NpO_2^+, is surface complexation (Widestrand et al. 2010b, Table 2-1). In laboratory batch sorption experiments Np did sorb rather weakly (Widestrand et al. 2010a, Table 4-11). In the in-situ experiment the radioelement was found in quantitative amounts in the first slice in a few instances, and not found at all in other instances. A fairly good portion of the tracer remained in the tracer cocktail at the end of the experiment (Widestrand et al. 2010b, Table 3-11).

8.4 Distribution of tracers in experiment

8.4.1 Tracer penetration data – activities in the rock

The tracer activities in A- and D-cores are discussed and penetration profiles are plotted in Nilsson et al. (2010). In Table 3-6 to 3-13 of the Task 9B-1 task description (dated 2015-11-26), tracer activities in the four A- and D-cores of Task 9B-1 are given for Na-22, Cl-36, Co-57, Ni-63, Ba-133 and Cs-137. Data are given as Bq/g for each analysed slice. One data point regarding Ba-133 in slice A6 was unfortunately in error and an errata (dated 2016-04-19) has been distributed.

The tracer activities in all analysed A- and D-cores of Task 9B-2 are provided in the Excel file:

- Excel file: Task 9B-2 Rock matrix data, Spreadsheet: Tracer amounts

The file also contains the updated data set for Task 9B-1 and thereby replaces the corresponding data of the Task 9B-1 task description (dated 2015-11-26), as well as the distributed errata.

Comment:
These data are provided in Appendix 2.

8.4.2 Tracer amounts in the tracer cocktail

Injected amounts

The injected activities in the LTDE-SD main tracer test are provided in Table 8-3. Note that the mass of Np-237 is given in the table, and not the activity. The reason is that data were given in this way in Widestrand et al. (2010b, Table 2-1). The same data are provided, with additional decimals and uncertainty intervals, in the Excel file:

- Excel file: Task 9B-2 Tracer cocktail data, Spreadsheet: Injected amounts

Table 8-3. Injected amounts of the LTDE-SD main tracer test, for the tracers included in Task 9B-2. All activities are decay corrected to the injection date 2006-09-27. Data are based on Widestrand et al. (2010b, Table 2-1) but the value for Ag-110m has been corrected with an extra decimal.

Na-22	Cl-36	Co-57	Ni-63	Cd-109	Ag-110m
3.2 MBq	5.9 MBq	19 MBq	30 MBq	27 MBq	0.47 MBq
Ba-133	Cs-137	Gd-153	Ra-226	Np-237	
1.8 MBq	8.8 MBq	4.3 MBq	0.15 MBq	$3.1 \cdot 10^{-7}$ kg	

For converting the injected activity to number of injected moles; take the activity (Bq) times the half-life (in seconds) in Table 4-5 divided by ln(2) and Avogadro's number. Similar steps can be taken to calculate the injected activity of Np-237.

Injection took place on the 27th of September 2006 and all activity data are decay corrected to this date. Injection was made by connecting a loop of acidic stock solution (~20 mL) to the system. One minute after tracer injection, a loop of NaOH solution (~20 mL) was connected to the system to neutralise the first acidic injection (Widestrand et al. 2010b, Sections 2.3.1 and 2.3.2).

Comment:
The injected activity of Na-22 is updated to 3.8 MBq, according to Appendix 7.

Volumes of the tracer cocktail

Based on equipment data (i.e. geometries) the experimental volume was estimated to be 1 150 ± 50 mL at the initiation of the tracer test (Widestrand et al. 2010b, Section 3.2.2). Based on the concentration of the non-sorbing tracer Cl-36 and its injected activity, the initial experimental volume was calculated to be 1 140 ± 50 mL, which is in good agreement with the former estimate (Widestrand et al. 2010b, Section 3.5.2). A pressure regulator cylinder, which initially contained about 400 mL, was incorporated in the experimental system in which the tracer cocktail was circulated. When a sample was collected, the piston of the cylinder was moved to compensate for the removed sample volume. Accordingly the total tracer cocktail volume was reduced each time a sample was collected by 1 to 10 mL, corresponding to the sampled volume. In Widestrand et al. (2010b, Appendix 4) approximate volumes of each of the 26 collected samples[5] are provided. Exact values of the sample masses are provided in the Excel file:

- Excel file: Task 9B-2 Tracer cocktail data, Spreadsheet: Sample masses

The Excel file also provides the date of sampling. The total volume of removed samples summarises to 204 mL, based on piston movements in the pressure regulator cylinder, from 50 mm to about 320 mm (before the piston was emptied at termination), its volume was reduced by about 240 mL (Widestrand et al. 2010b, Appendix 6). This corresponds fairly well with the removed sample volume, which indicates no or small leakages from the test sections.

[5] Not all samples were analysed in respect of tracer concentration. Two samples of 1 mL each (#2 and #4) were collected but not analysed. One sample (not numbered) was only used for pH measurement. Two sample vessels were numbered (#20 and #22) but no sample was collected.

The volume of the slim hole was estimated to be 148 mL, based on the geometry of the borehole and of the dummy used to reduce the volume (data taken from experimental records at Geosigma). It should be noted that for the first two hours after tracer injection, the slim hole was bypassed (Widestrand et al. 2010b, Section 3.2.2). Hence, during this period the experimental volume was about 1.0 L.

The combined length of the tubing to and from the two test sections (i.e. the stub section and the slim hole section) and the equipment in the Äspö tunnel is estimated to be 140 m. The inner diameter of the tubing was 2 mm and, accordingly, the total volume of the tubing is estimated to 440 mL. Other equipment in the tracer cocktail circulation loop added about 30 mL. The average slot width between the PEEK lid of the cup like packer and the fracture surface was 3.25 mm (the slot width varied between 2 and 4 mm) and the volume of the stub section can be estimated to 80 mL. The dimensions of the test sections, as well as dimensions and/or volumes of other parts of the experimental setup, packer locations, A-core and D-core locations and inlet and outlet locations are compiled in the Excel file:

- Excel file: Task 9B-2 Accompanying data, Spreadsheet: Experimental geometries

Comment:
Experimental geometry data are provided in Appendix 4.

Tracer amounts

Throughout the LTDE-SD main tracer test, the declining tracer concentrations in the tracer cocktail were measured (Widestrand et al. 2010b, Section 3.5). Samplings for analysis of aqueous phase tracer concentrations were made on 18 occasions, including one sampling prior to tracer injection. Sampling was performed with greater intensity in the early part of the in-situ phase and more sparsely as the experiment progressed. Additional sampling was made for investigations with cation and anion exchange resins (Widestrand et al. 2010b, Section 3.6), as well as filtered samples using a 20 nm filter (Widestrand et al. 2010b, Section 3.7).

In Table 3-14 and 3-15 of the task description for Task 9B-1 (dated 2015-11-26) the declining tracer concentrations are given for the nuclides Na-22, Cl-36, Co-57, Ni-63, Ba-133 and Cs-137. Unfortunately there a number of errors in those tables and an errata (dated 2016-04-19) has been distributed.

In an Excel file of the Task 9B-2 data delivery, tracer concentrations for all of the 11 tracers of Task 9B-2 are provided.

- Excel file: Task 9B-2 Tracer cocktail data, Spreadsheet: Tracer amounts

The Excel file also contains updated data for the radionuclides of Task 9B-1. Accordingly, it replaces the data of the Task 9B-1 task description dated 2015-11-26, and reproduces the data of the distributed errata. In the Excel file, decay corrected activities (with time zero at injection) are given of sampled tracer solution.

Comment:
The tracer cocktail data in the Excel file referred to above are provided in Appendix 3. Table 3-14 and 3-15 of the task description for Task 9B-1 corresponds to Table 4-14 and Table 4-15 of this present report. The original data in these tables have been replaced by the revised data copied from data delivery #11 (provided in Appendix 3).

Tracer activities were also obtained in online HPGe measurements. This facilitated a detailed monitoring of the behaviour of the injected pulse circulating in the system during the first few hours before good mixing was achieved (cf. Figure 8-2). As can be seen, first tracer peak arrival occurs after about 35 minutes. With a flowrate of 15 mL/min (Widestrand et al. 2010b, Table 3-6) this suggests an effective experimental volume of about 0.5 L. This should be compared to the actual experimental volume of 0.6 L between the tracer injection and the HPGe measurements in the first lap. The difference in volumes indicates some initial channelling in the system. Here it should be noted that the HPGe measurements were made prior to the pressure regulator cylinder and that the initial volume of this cylinder makes up the difference between the volume 0.6 L and the total experimental volume of 1.0 L for the first lap (prior to connecting the slim hole). After four circulations, or about 4 hours, well mixed conditions in the entire experimental system can be assumed.

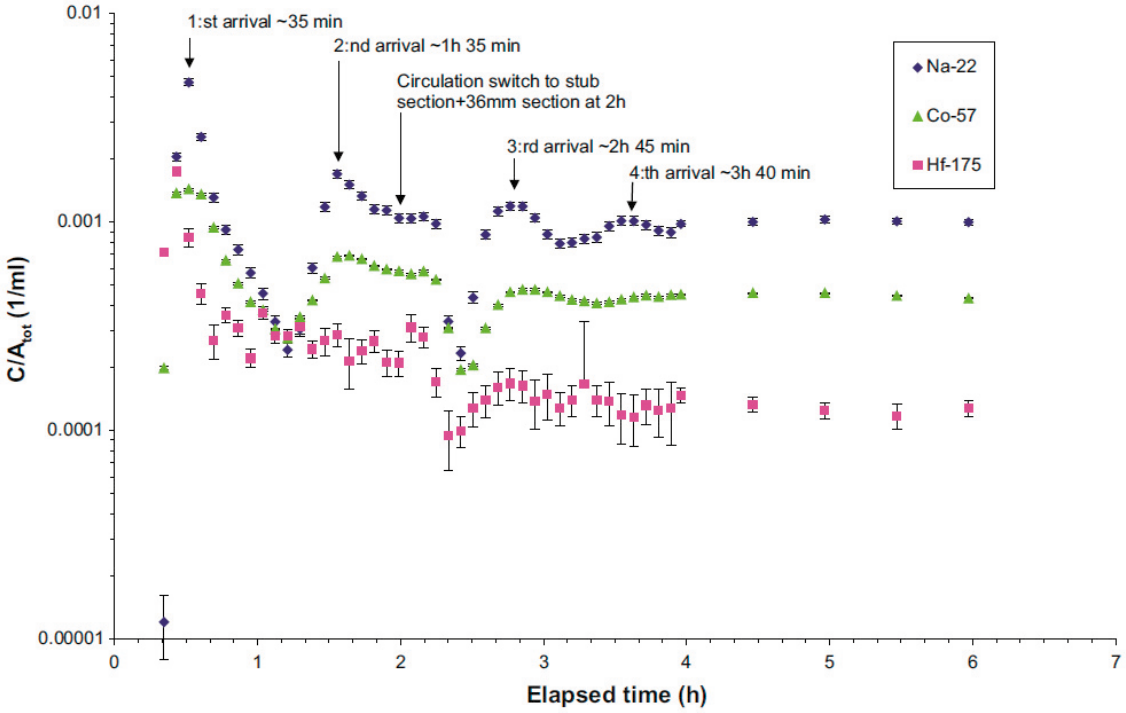

Figure 8-2. *Increases and declines in the normalised tracer activity as the injected tracer pulse is circulated in the system. Reproduced from Widestrand et al. (2010b, Figure 3-1).*

8.4.3 Rock areas in contact with the tracer cocktail

The rock surfaces that have been in contact with the tracer cocktail solution comprise the stub section and the slim hole section. The dimensions of these areas are provided in the Excel file:

- Excel file: Task 9B-2 Accompanying data, Spreadsheet: Experimental geometries

8.4.4 Tracer amounts removed by sampling

The amount of tracer removed in the sampling at different times can be estimated from the Excel file providing volumes of all 25 samples collected after injection and the tracer activities of 17 of these samples:

- Excel file: Task 9B-2 Tracer cocktail data, Spreadsheets: Sample masses
- Excel file: Task 9B-2 Tracer cocktail data, Spreadsheets: Tracer amounts

Comment:
The declining volume of the tracer cocktail is provided in Appendix 3.

As the tracer activities have not been measured in all extracted samples, interpolation is needed at the discretion of the modelling groups.

8.4.5 Information from the environmental radioactivity monitoring program

Due to the risk of radionuclide leakages in the facture system surrounding the LTDE-SD borehole, tracer activities were sampled at regular intervals in the guard section of the LTDE-SD borehole, as well as in section KA3065A02:3 of the nearby pilot borehole that is intersected by the target fracture. In addition, environmental monitoring was made in two other sections of the pilot borehole and at nine other locations in the tunnel close to the site (Widestrand et al. 2010b, Section 2.3.7). No radionuclides relating to the experiment were detected (Widestrand et al. 2010b, Section 3.4.3), strongly

suggesting that insignificant amounts of (dissolved) radionuclides escaped from the system in leaks. After termination of the experiment (see also Section 8.4.6), smear tests and environmental samples showed measured activities below the detection limit (Nilsson et al. 2010, Appendix 2).

8.4.6 Tracer amounts retrieved at termination

On April 11th 2007, the pressure regulator cylinder was emptied to its minimum volume and the equipment loops were disconnected from the flow line and emptied (Widestrand et al. 2010b, Appendix 4). The excess of tracer cocktail was collected and its activity was measured. The amounts of tracers retrieved in this step are tabulated in the Excel file:

- Excel file: Task 9B-2 Accompanying data, Spreadsheet: Activity at termination

Comment:
Activities at termination are provided in Appendix 4.

It should be noted that the test sections were still filled with tracer cocktail, and that tracer circulation was maintained until the following day.

The in-diffusion part of the tracer experiment was terminated on the 12th of April 2007 by exchanging the tracer cocktail by a surplus of isopropanol (isopropyl alcohol). This resulted in an outgoing mixture of tracer cocktail and isopropanol, which was sampled 11 times with respect to tracer content. In addition the exchange was followed online with both HPGe detector and RNI-instruments and amounts are reported for a few radionuclides (cf. Figure 8-3). Isopropanol was added to the system until the outgoing mixture contained only small amounts of tracers.

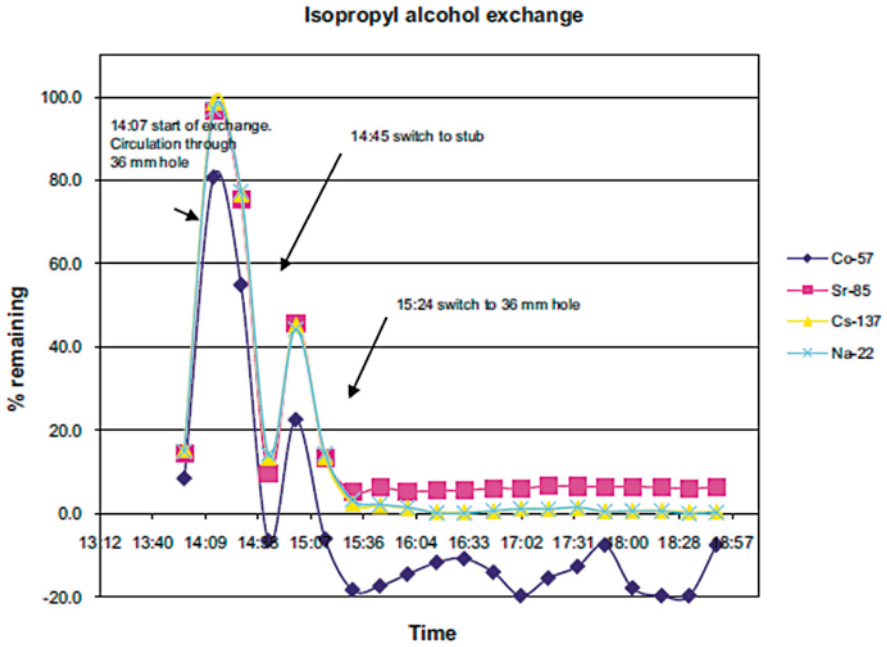

Figure 8-3. *Remaining Co-57, Sr-85, Cs-137 and Na-22 in outflowing isopropyl alcohol relative to the concentrations in the tracer cocktail just before the exchange began. Activity resulting from Co-57 adsorbed on the tubes has been subtracted. Reproduced from Nilsson et al. (2010, Figure A2-1).*

The total tracer amounts in the outgoing mixture of tracer cocktail and isopropanol are given in the Excel file:

- File: Task 9B-2 Accompanying data, Spreadsheet: Activity at termination

After the isopropanol exchange was completed an epoxy resin was injected into the test sections. This was done to increase the mechanical strength at the exposed rock surfaces prior to overcoring and to protect the exposed rock surfaces from flushing water during overcoring. The injection commenced until the flow resistance of the system became too great. During this period a mixture, or slurry, of isopropanol and epoxy resin was retrieved and analysed with respect to tracer content. For some tracers small amounts were found while for other tracers the slurry held insignificant amounts (cf. Widestrand et al. 2010b, Table 3-11). Although it is conceivable that part of the tracers found in the slurry desorbed from rock surfaces upon epoxy injection, one may find it more likely that a complete exchange of tracer cocktail by isopropanol was not achieved, and that a majority of the tracers found in the slurry were present in the tracer cocktail just prior to terminating the experiment. An indication of the total amounts of tracer in the outgoing isopropanol/epoxy slurry is given in the Excel file:

- File: Task 9B-2 Accompanying data, Spreadsheet: Activity at termination

It should be reminded that some isopropanol/epoxy slurry, which may have been contaminated, remained in the outgoing tubing from the experimental sections as the epoxy cured. In addition, the collected isopropanol/epoxy slurry stratified and only the upper phase was measured upon.

8.4.7 Tracer residues on PEEK tubing and cured epoxy resin

During the course of the experiment, radionuclides became attached to PEEK tubes and possibly to other experimental equipment surfaces, such as the PEEK lid of the cup like packer. In this section the word “sorbed” is used in its widest meaning, as the mechanism for the attachment/immobilisation is not known. In Widestrand et al. (2010b, Section 3.5.3), precipitation of iron at PEEK surfaces is postulated, followed by tracer interaction with the precipitate. After dismantling of the experiment the tracer contamination on the tubing was examined, although not for all tracers. Parts of the tubing were leached and the leachates were analysed for gamma emitters. The estimated fractions of the total injected tracer amount that sorbed to the tubing, for the gamma emitters of Task 9B-2, are given in Table 8-4.

Table 8-4. Fraction of total injected tracer amounts that sorbed to the PEEK tubing. Decay corrected data taken from Widestrand et al. (2010b, Table 3-11).

Na-22	Cl-36	Co-57	Ni-63	Cd-109	Ag-110m
0.1 %	–	7 %	–	6 %	11 %
Ba-133	Cs-137	Gd-153	Ra-226	Np-237	
3 %	0.2 %	15 %	–	16 %	

The activity of each tracer found in the PEEK tubing is provided in the Excel file:

- Excel file: Accompanying data, Spreadsheet: Activity at termination

Note that the activity of the tubing was not investigated for Cl-36, Ni-63 and Ra-226. The modelling groups may, at their own discretion, estimate the amount of sorbed activity for these tracers based on data from analogue radionuclides (if such exist) in Table 8-4.

Figure 8-4. *The epoxy resin adhering to the PEEK lid, protecting the fracture surface during overcoring. Reproduced from Nilsson et al. (2010, Figure 2-8).*

As discussed above an epoxy resin was injected in the stub section (cf. Figure 8-4) and into the slim hole upon termination of the experiment. This epoxy cured and was, by some processes, contaminated by radionuclides. As can be seen in Figure 8-4, some rock or fracture mineral fragments got stuck to the epoxy resin.

The epoxy disc in Figure 8-4 was sampled by so-called B-samples, drilled at the positions of the corresponding A-samples and numbered accordingly. The tracer activities in five of the B-samples (B1, B6, B8, B9, and B17) were measured and reported for some radionuclides (Nilsson et al. 2010, Sections 2.2.2 and 3.5). In some instances the B-samples were parted into two subsamples. Raw data on the total activities in the five B-samples, including unpublished data sets for two subsamples, are given in the Excel file:

- Excel file: Task 9B-2 Accompanying data, Spreadsheet: Activities in Epoxy samples

The Excel file also contains unpublished raw data for four samples collected from the epoxy that was injected into the slim hole. In the spreadsheet the samples are denoted as D-E samples with the same number as the D-core they correspond to.

Comment:
Epoxy sample activities are provided in Appendix 4.

Each B-sample has a diameter of 24 mm and makes up about 1.8 % of the surface area of the Ø177 mm epoxy disk. Accordingly, these samples could not be a basis for a complete understanding of the radionuclide distribution in the epoxy resin. The primary aim of investigating the B-samples was to study if radionuclides were present on the epoxy resin surface. From the results, it could be concluded that radionuclides were present in the epoxy resin, and also in the PEEK material that had been in contact with the tracer cocktail.

8.4.8 Tracer losses during dismantling, overcoring, and sawing of rock samples

During the overcoring, water samples were collected and analysed for Na-22 and Cs-137. Only low activities were measured at some occasions. The results are reported in Nilsson et al. (2010, Appendix 2). Losses during sawing of the drill cores into slices were estimated to an approximate average of 1 % for Ba-133 and Cs-137. For Na-22, two samples had an average loss of 7 % and for the remaining nine samples losses were below the detection limit (Nilsson et al. 2010, Section 2.3).

8.5 Deliverables and reporting of Task 9B-2

At the Task Force #34 meeting in Prague, it was decided to incorporate Task 9B-1 results into the Task 9B-2 reporting. As such, no separate delivery is formally expected for Task 9B-1.

8.5.1 Deliverables and performance measures

It was discussed at Task Force #34 meeting in Prague whether or not we should define a detailed framework for the deliverables of Task 9B-2, and also if we should define a number of numerical performance measures for the subtask. There was a general understanding that this eventually must be done (in practice at the upcoming Task 9 workshop in autumn 2016). However, at this point in time the treatment of Task 9B still has a preliminary character and no detailed deliverables and performance measures could be agreed upon. To rectify this situation, the modelling groups are asked to suggest deliverables and quantitative performance measures for Task 9B at the Task 9 workshop in Finland on the 26th to 27th of October 2016. Modellers are also asked to suggest ways of investigating different types of uncertainty.

On a general note Task 9B-2 revolves around three main deliverables:

1. Modelling of anomalous penetration profiles for the six Task 9B-1 radionuclides Na-22, Cl-36, Co-57, Ni-63, Ba-133, and Cs-137.
2. Modelling of the distribution of the Task 9B-2 radionuclides between the tracer cocktail and rock matrix. This is of special importance for Cd-109, Ag-110m, Gd-153, Ra-226 and Np-237 that display a very limited penetration depth;
3. Performing mass-balance calculations to evaluate the plausibility of the delivered experimental data.

Penetration profiles

Concerning the anomalous penetration profiles, a few possible deliverables are discussed below. However, each modelling group may choose to suggest other and/or more detailed deliverables at the Task 9 workshop in autumn 2016.

- Prior to the Task Force #34 meeting in Prague, the modelling groups were asked to send data on their inversely modelled tracer penetration profiles for individual drill cores. This was done in terms of the decay corrected activity per gram of rock slice (Bq/g) for the rock slices of the four Task 9B-1 drill cores. In Task 9B-2 we have delivered data for an extended set of analysed drill cores, for an extended set of tracers. If aiming to deliver tracer penetration profiles for all these tracers, for all drill cores, this would amount to a great number of penetration profiles. Hence, the modelling groups may make justified choices of limited subsets of modelled penetration profiles.
- An alternative option is to base the inversely modelled penetration profiles on statistical information from many drill cores. In a simple case, some kind of averaged penetration profiles may form the bases of the inversely modelled penetration profiles. Statistically more complex manners of comparing the inversely modelled penetration profiles with the experimentally obtained ones may be deployed at the discretion of the modelling groups. Such a treatment may lead to both central and alternative predictions that can be used in later mass-balance considerations.

- The modelling groups may also choose to model the solute transport as penetration in three dimensions, incorporating justified bits of experimental data from a chosen number of drill cores.

Distribution of tracers between cocktail and rock matrix

Concerning the distribution of tracers between the tracer cocktail and rock matrix, the obvious deliverable would be a partitioning coefficient of some kind. The simplest set of data would represent the time-varying ratio of the tracer activity in the rock vs. that in the tracer cocktail. However, by using the solute transport approaches developed when investigating the penetration profiles, a K_d-value or corresponding partitioning coefficient could be obtained for each tracer. The partitioning coefficient would not necessarily need to be linear and time- and space-independent. For tracers with developed penetration profiles, the reproduction of these profiles should aid in assigning partitioning coefficients. For tracers that have only penetrated to shallow depths (into the first or second slice), the absence of tracers in deeper rock (relative to the tracers' detection limits) must be acknowledged when estimating the partitioning coefficients.

Furthermore, it is encouraged that modelling groups tackle the question of speciation in both the aqueous phase tracer cocktail (i.e. without the influence of the mineral surfaces' functional groups) and in the rock matrix, where the mineral surfaces may greatly impact the speciation. Deliverables could, for example, be percentages of different species in the tracer cocktail as well as in the rock matrix (both in the pore water or sorbed to mineral surfaces). Concerning the aqueous phase speciation calculations in the tracer cocktail, the results could be compared with those from PHREEQC modelling reported in Widestrand et al. (2010b, Section 3.1). This could (preferably) be done for all nine tracers included in Task 9B-2, or for a chosen subset of tracers.

Mass-balance calculations

Concerning mass-balance calculations, an important deliverable is to see whether the measured or estimated tracer amounts, distributed on different parts of the system, add up to 100 % of the injected amount (if correcting for decay). If not explanations are needed. This makes the recovery an important performance measure. It is also important to make uncertainty estimates of the tracer amounts in the different parts of the system.

The mass-balance approach may give higher or lower confidence in the solute transport modelling performed within Task 9B-2. Different degrees of confidence may be given to different tracers. It may also give insights in the plausibility that the LTDE-SD experiment, or similar future experiments, can deliver experimental data suitable for solute transport modelling in the rock matrix.

8.5.2 Description of the model and the handling of processes, features, etc.

The main objective of Task 9B coincides with the overall objective of Task 9, which is to increase the realism in solute transport modelling in the rock mass. Accordingly we aim to go beyond the standard codes that are traditionally used in, for example, performance assessment. Instead we should, if possible, develop models that better describe the observed solute transport. Important inclusions in these models are heterogeneity and the detailed incorporation of relevant features, events, and processes. The preparing of the model(s) used in the Task 9B suite of subtasks, and the choices made, should be described using the following guidelines.

The conceptual model used, and how it is incorporated in the computational code, should be described in a transparent manner. It is encouraged to make detailed references to documents providing a comprehensive background on such issues, if such are available.

A very important part of the reporting is presenting how the model has handled different features, events, and processes. These include the experimental conditions; the perceived chain of events in the tracer test; supporting data; etc. In most modelling, a simplified representation of the reality is incorporated. Typical simplifications are neglecting features, events, and processes, or streamlining them so that they fit in a reasonably simple mathematical representation. Other efforts may involve simplifying geometrical constraints; boundary conditions; the initial state; supporting data; etc.

In this respect it is important to both describe processes, conditions, data, and other features that are incorporated in the models, as well as describing those which are knowingly neglected or simplified. Unless the handling is self-evident, steps taken when simplifying the real system should be justified and the impact of the simplification should be discussed.

As part of the Task Force #34 meeting in Prague there was an uncertainty workshop, although it was originally intended to focus on Task 8 modelling. As input to this workshop a document was prepared with the title "A Framework for Comparative Analyses and Conceptual Uncertainty Evaluation", which later was developed to a paper (Finsterle et al. 2018). It is recommended to read this paper for inspiration.

8.5.3 Reporting of 9B-2

Preliminary reporting

Task 9B-2 has a broader aim than Task 9B-1 and as stated earlier, the larger Task 9 group could not agree on detailed deliverables and numerical performance measures at the Task Force #34 meeting in Prague. Accordingly, preliminary reporting on Task 9B-2 should focus on describing the used model (see guidelines in Section 8.5.2) and presenting preliminary results on a free format. In doing this it is useful to start from the template for reporting of Task 9A, which can be found on the Task Force website:

- Word file[6]: Template for reporting of Task 9A, 2015-06-15

The preliminary reporting should be sent to the task evaluator prior to the Task 9 workshop in Finland on the 26th to 27th of October, 2016 (preferably two weeks ahead). The delivery may be accompanied by numerical data in an Excel file, at the discretion of the modelling group.

Preliminary results from Task 9B-1 were presented at the Task Force #34 meeting in Prague and numerical data were delivered to the evaluator as inserted in an Excel template that can be found on the Task Force website:

- Excel file: Template for delivering data Task 9B-1, 151123.xlsx

If the modelling group has made significant modifications to the code or model which alters the penetration profiles, this template may be revisited and updated with new data for comparison. If so, the updated file could be part of the preliminary reporting to the evaluator.

Final reporting

Most likely the entire suite of Task 9B subtasks will be finally reported in a combined report, where each modelling group prepares their own separate report. Probably the suite of 9B task descriptions (in an edited version) will be published in a separate report to which references can be made. The exact path forward remains to be discussed and decided upon.

Modelling groups are of course free to produce additional more detailed reports or to publish in the open literature. Please provide a copy of any paper submitted to the Task Force Secretary so that publications of the different modelling groups and experimenters can be coordinated.

[6] At the time of writing this task description, the downloadable word file has, for no apparent, reason the file name 005_template.doc

8.6 Documentation of Task 9B-1 and 9B-2

Task 9B-1

The following documents relating to the Task 9B are presently available at the SKB Task Force website[7]:

- *Task 9B-1 Description* (2015-11-26)
- *Task Description 9B-1 Appendix 1* (2015-11-25): A word document containing some additional descriptions of the rock samples; including photos and autoradiographs of high resolution.
- *Evolution of pH and Eh in LTDE-SD*: Numerical data on the redox and pH evolution in the tracer cocktail, in a Microsoft Excel spreadsheet.
- *Template for delivering data Task 9B-1* (2015-11-23): An Excel file wherein numerical data (deliverables) should be inserted.
- *Lab program supporting LTDE-SD (Vilks et al. 2005)*: Scientific report on laboratory work on LTDE-SD samples made in Canada.
- *Errata for Task Description 9B-1 of 2015-11-26*: Released on 2016-04-21.
- *LTDE-SD Timeline, Core Storage, and Decay Correction:* Document with a refined experimental timeline that could be used to estimate the diffusive transport in the A- and D-core samples after the termination of the in-situ in-diffusion experiment. Data can also be used, if needed, to undo/ recalculate the decay correction in the delivered results in Table 2-3 to Table 2-12 of the task description for Task 9B-1, and similar results for Task 9B-2.

Task 9B-2

The following documents are, or will be, available on the website:

- This present task description.
- Excel-files with additional data compilations for Task 9B-2:
  - *Rock matrix data:* Partitioning data on, and tracer activities in, rock slices.
  - *Tracer cocktail data:* Data on injected amounts, tracer cocktail concentrations, and sample masses.
  - *Accompanying data:* Data on experimental setup, retrieved tracer amounts at termination, contamination, etc.
- A word document with high resolution photos of an expanded set of cores and individual slices, as well as autoradiographs.

For requesting additional information or documentation, please send an e-mail to both

- Martin Löfgren (martin.lofgren@niressa.se), and
- Kersti Nilsson (Kersti.nilsson@geosigma.se)

Please do not hesitate to ask questions, as we have been assigned to deal with such requests. You may also request a telephone, Skype or Facetime meeting in order to receive additional explanations or help.

[7] http://www.skb.se/taskforce/member-area/modelling-tasks/

9 9B-2: Looking ahead

There will be a Task 9 workshop in autumn 2016, between the 26th and 27th of October in Finland. This workshop gives the opportunity to present any preliminary results on Task 9B-2. At the workshop we should also decide on deliverables, performance measures, and uncertainty analyses of Task 9B-2.

As decided at the Task Force #34 meeting in Prague, the Task 9B suite of subtasks will contain a third subtask; Task 9B-3. This subtask will deal with predictive modelling of penetration profiles in three A-cores and two D-cores samples (cf. Table 8-1), with respect to the radionuclides Cl-36, Ni-63, Ba-133, and Cs-137. The tracer activities of the individual slices of these cores were never measured within the LTDE-SD campaign, but have recently been measured to facilitate Task 9B-3. Task 9B-3 will be launched at the autumn 2016 workshop.

At the workshop, additional input may be available from the characterisation of minerals and pore structure by X-ray microtomography and ^{14}C-PMMA autoradiography of new LTDE-SD rock samples.

Looking even further ahead, the Task Force #35 meeting will be held in spring 2017 (tentatively in Sweden). It would be preferable if final results of the Task 9B suite of subtasks could be presented here. Furthermore, it is envisioned that a new task, Task 9C, will be launched at this meeting. This task will concern the predictive modelling of the through diffusion experiment (TDE) of the REPRO camping in Finland. Although Task 9C will not be launched at the autumn workshop in 2016, we will give some information on the task (and perhaps even an outline of the Task 9C task description).

10 9B-3: Introduction and background

Task 9B-3 is a continuation of Task 9B-1 and Task 9B-2, which are detailed in previous task descriptions. The general idea of Task 9B-3 is to use the models developed in Task 9B-1 and 9B-2 and perform predictive modelling of penetration profiles in the rock matrix.

As is well known, the LTDE-SD campaign involves an in-situ tracer test from a borehole drilled from a niche in the Äspö tunnel at a depth of 410 m, followed by overcoring and sampling of the surrounding rock matrix. The sampling was made by drilling into the overcored rock volume and extracting core samples. All cores were sliced, but not all were fully analysed, as part of the main LTDE-SD campaign.

Five cores that were not fully analysed in the main LTDE-SD campaign have been analysed in a campaign carried out during 2016. Three A-cores (A4, A11, and A13) and two D-cores (D15 and D16) are part of this campaign (cf. Figure 10-1). Analyses have been performed in respect to their Na-22, Cl-36, Ni-63, Ba-133, and Cs-137 activities and have resulted in numerous penetration profiles. These penetration profiles will be subjected to predictive modelling within Task 9B-3, and the recently obtained data will not be revealed prior to the subtask. However, there is one set of data that is already reported for these cores, relating to Cs-137 surface activities (cf. Section 12.4), that may be used as input to the modelling.

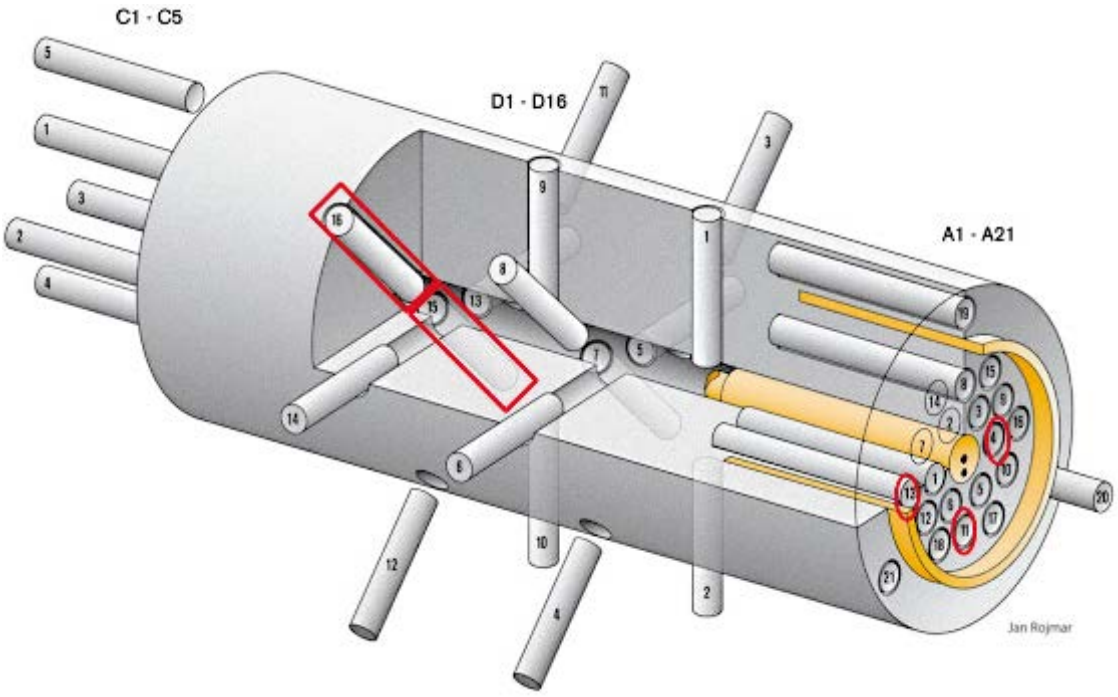

Figure 10-1. *Illustration of the sampling of the overcored rock volume in LTDE-SD. The drill cores A4, A11, and A13 of the ongoing campaign are marked by red circles at the fracture surface. Cores D15 and D16 are marked by red rectangles.*

11 9B-3: Specifics of the new analyses

Sample preparations including drilling, slicing, and crushing were performed within the main campaign of LTDE-SD and the individual samples have been stored in plastic bottles since then.

The new analyses have been performed at VKTA - Radiation Protection, Analytic & Disposal Inc, Dresden, Germany. Na-22, Ba-133, and Cs-137 activities were measured during spring 2016 by γ-ray spectrometry on crushed samples. Measurements of Cl-36 and Ni-63 activities were performed during autumn 2016, using Liquid Scintillation Counting (LSC) after chemical separation on crushed samples.

Table 11-1 lists the rock slices that are analysed in the new campaign, as well as the analysed tracers for each slice. The number of analysed slices in each drill core was reduced from 12 to 7 or 8, in order to be able to analyse more cores. As can be seen Na-22, Ba-133, and Cs-137 activities have been analysed for all selected slices. All five tracers are only analysed for two of the slices while for most slices, analyses are made for either Cl-36 or Ni-63, in addition to Na-22, Ba-133, and Cs-137.

Table 11-1. Mapping of tracers analysed for each slice in the recent campaign.

Core	Slice	Cl-36	Ni-63	Na-22, Ba-133 & Cs-137	Core	Slice	Cl-36	Ni-63	Na-22, Ba-133 & Cs-137
A4	A4.1	X		X	D15	D15.1	X	X	X
(crushed	A4.2	X		X	(crushed	D15.2		X	X
samples)	A4.3	X		X	samples)	D15.3	X		X
	A4.5	X		X		D15.5	X		X
	A4.7	X		X		D15.7	X		X
	A4.9	X		X		D15.9	X		X
	A4.12	X		X		D15.12	X		X
A11	A11.1		X	X	D16	D16.1		X	X
(crushed	A11.2		X	X	(crushed	D16.2		X	X
samples)	A11.3		X	X	samples)	D16.3		X	X
	A11.4		X	X		D16.4		X	X
	A11.5			X		D16.5			X
	A11.7			X		D16.7			X
	A11.9			X		D16.9			X
	A11.12			X		D16.12			X
A13	A13.1	X	X	X					
(crushed	A13.2		X	X					
samples)	A13.3		X	X					
	A13.5	X		X					
	A13.7	X		X					
	A13.9	X		X					
	A13.12	X		X					

12 9B-3: Specifics of the new cores

The choice of drill core samples included in the new campaign, out of those not previously analysed, was made according to the following criteria:

1. Cubic sawn samples – i.e. the mantel of the drill core sample should have been removed before crushing, as it may have become contaminated during the drilling.
2. Good quality of the autoradiographs obtained prior to crushing.

This resulted in a selection of crushed samples only.

12.1 Positions of drill cores

The positions of all core samples of LTDE-SD are provided in illustrations in Nilsson et al. (2010, Section 3.2) and in even more detail below. Core samples A4, A11, and A13 have been drilled from the fracture surface in parallel with the slimhole. The locations of the three drill cores in relation to other A-cores are illustrated in Figure 12-1. The in-situ alignment of the overcored rock volume was as described in the figure. The positions of the D15 and D16 cores are provided in Figure 12-2. These two drill cores come from the far end of the slimhole, close to the tracer inlet (cf. Nilsson et al. 2010, Figure 1-3).

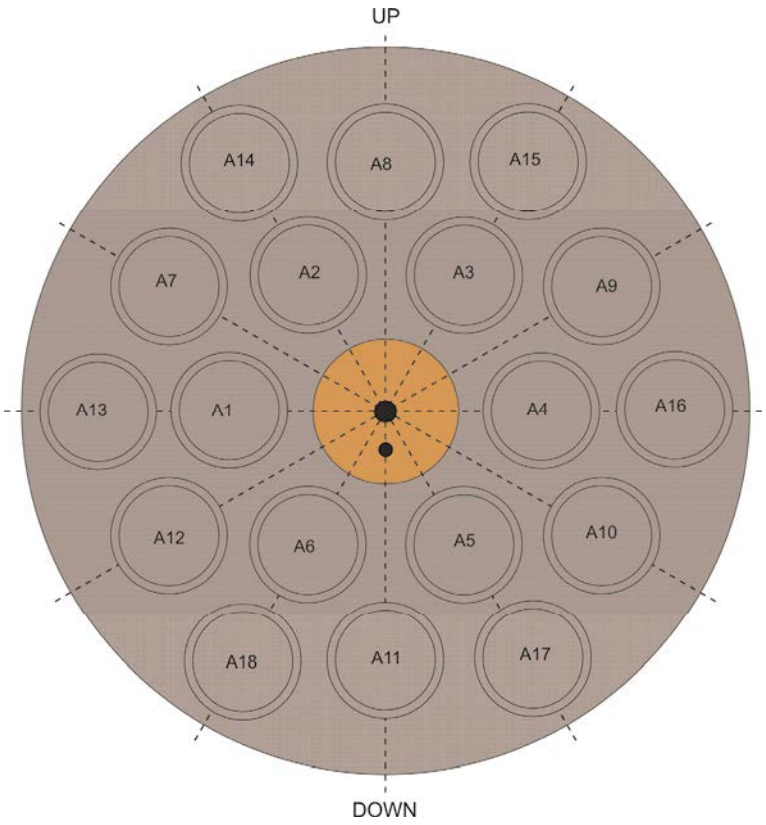

Figure 12-1. *Sampling strategy for extraction of 18 small diameter drill cores on the 177mm diameter core stub. Core samples A1 – A6 are set in a ring with radius 37.5 mm from centre of large diameter core. Samples A7 – A12 are set in a ring with radius 59.0 mm and samples A13 – A18 in a ring with 69 mm radius.*

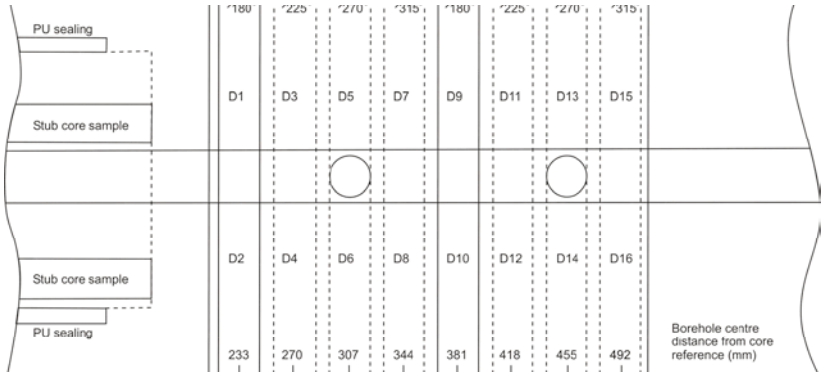

D-core sample	Length from core stub (m)
D1/D2	0.233
D3/D4	0.27
D5/D6	0.307
D7/D8	0.344
D9/D10	0.381
D11/D12	0.418
D13/D14	0.455
D15/D16	0.492

Figure 12-2. *Sampling strategy for D-core samples. The cores are distributed in 8 cuts, with 2 cores in each cut. The cuts are revolved 45 degrees to each other.*

12.2 Partitioning of the drill cores

Table 12-1 to Table 12-5 give information on the partitioning of the five drill cores of the ongoing campaign.

Table 12-1. Information on the partitioning of core sample A4.

Slice	Weight (g)	Mean length (mm)	Centre distance to surface (mm)*
A4.1	0.7896	1.9	0.95
A4.2	0.4567	1.0	2.7
A4.3	0.3923	0.7	3.9
A4.4	1.7327	3.0	6.0
A4.5	1.8073	3.1	9.4
A4.6	1.6113	2.7	13
A4.7	3.5520	5.8	17
A4.8	3.6137	5.6	23
A4.9	3.2235	5.0	29
A4.10	5.7985	10.0	37
A4.11	5.7082	10.0	47
A4.12	5.5855	10.0	57

*Assumed 0.3 mm loss in cutting

Table 12-2. Information on the partitioning of core sample A11.

Slice	Weight (g)	Mean length (mm)*	Centre distance to surface (mm)*
A11.1	1.0850	2.0	1.0
A11.2	0.7157	1.4	3.0
A11.3	0.5643	1.1	4.6
A11.4	1.5965	2.9	6.9
A11.5	1.7217	3.1	10
A11.6	1.6734	2.9	13
A11.7	2.9885	5.3	18
A11.8	3.1307	5.2	23
A11.9	3.1142	5.5	29
A11.10	8.4441	10.0	37
A11.11	8.4774	10.0	47
A11.12	7.8838	10.0	58

*Assumed 0.3 mm loss in cutting

Table 12-3. Information on the partitioning of core sample A13.

Slice	Weight (g)	Mean length (mm)*	Centre distance to surface (mm)*
A13.1	1.6391	1.7	0.85
A13.2	0.6688	1.3	2.7
A13.3	0.4801	1.1	4.2
A13.4	1.6921	2.8	6.4
A13.5	1.9459	3.1	9.7
A13.6	2.0366	3.3	13
A13.7	2.9788	4.7	17
A13.8	2.9441	4.6	22
A13.9	3.3034	5.3	28
A13.10	6.7755	10.0	36
A13.11	6.0375	10.0	46
A13.12	6.5095	10.0	56

*Assumed 0.3 mm loss in cutting

Table 12-4. Information on the partitioning of core sample D15.

Slice	Weight (g)	Mean length (mm)*	Centre distance to surface (mm)*
D15.1	1.2556	1.1	0.55
D15.2	0.5263	0.8	1.8
D15.3	0.7887	1.1	3.1
D15.4	2.2636	3.2	5.5
D15.5	2.2097	3.1	9.0
D15.6	2.2160	3.1	12
D15.7	3.5762	5.1	17
D15.8	3.6028	5.1	22
D15.9	3.6828	5.4	28
D15.10	6.7990	10.0	36
D15.11	6.5961	10.0	46
D15.12	7.4150	10.0	56

*Assumed 0.3 mm loss in cutting

Table 12-5. Information on the partitioning of core sample D16.

Slice	Weight (g)	Mean length (mm)	Centre distance to surface (mm)*
D16.1	1.4326	1.8	0.90
D16.2	0.7543	1.1	2.7
D16.3	0.7999	1.1	4.1
D16.4	2.0169	2.8	6.3
D16.5	2.4412	3.4	9.7
D16.6	2.2177	3.1	13
D16.7	3.4268	4.9	18
D16.8	3.3372	4.7	23
D16.9	3.4684	4.9	28
D16.10	7.2194	10.0	36
D16.11	5.4527	10.0	46
D16.12	6.4558	10.0	56

*Assumed 0.3 mm loss in cutting

12.3 Geological description of the drill cores

In Appendix 1, geological descriptions of the concerned core samples are provided. No autoradiographs are provided, due to the predictive nature of Task 9B-3. In this task description the photos of Appendix 1 are of low resolution. A high resolution version of Appendix 1 can be downloaded from the Task Force website (data delivery #16).

Comment:
The geological characterisation of data delivery #16 is provided in Appendix 8.
The results of analysis of the 9B-3 drill cores are provided in Appendix 2 together with previously reported data.

12.4 Surface activity of samples

In Nilsson et al. (2010) the decay corrected surface activity of Cs-137 is illustrated (cf. Figure 12-3 and Figure 12-4), also for core samples A4, A11, A13, D15, and D16. This concerns the total surface activity per drill core sample, measured on the whole core immediately after they were drilled from the overcored rock volume. In the measurement the surface that had contacted the tracer cocktail was placed closest to the detector.

The modelling groups may use this information on the surface activity, in some manner, to bootstrap the predicted penetration curves.

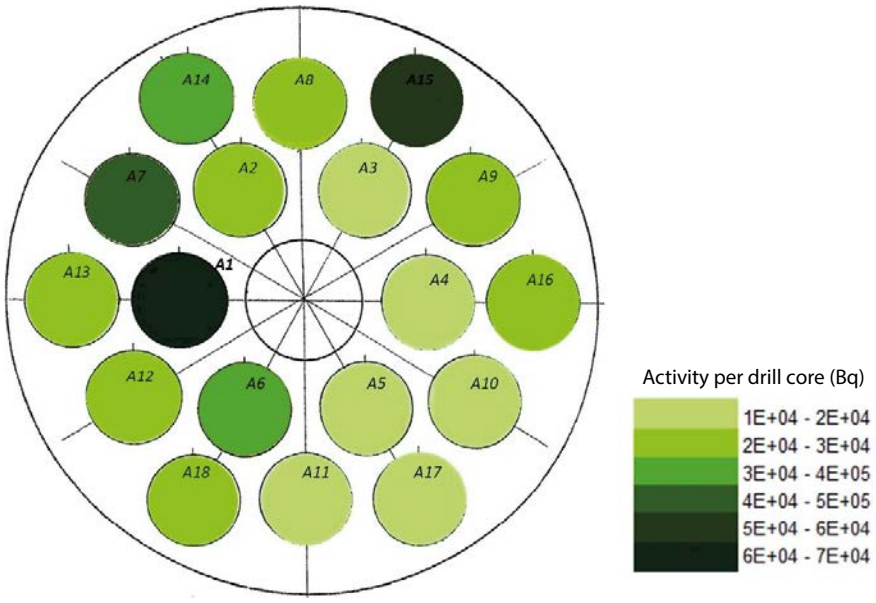

Figure 12-3. *Tracer surface distribution of Cs-137 on the stub surface, measured with γ-spectrometry on the whole rock cores. The circle in the centre represents the slimhole. Reproduced from Nilsson et al. (2010, Figure 3-4).*

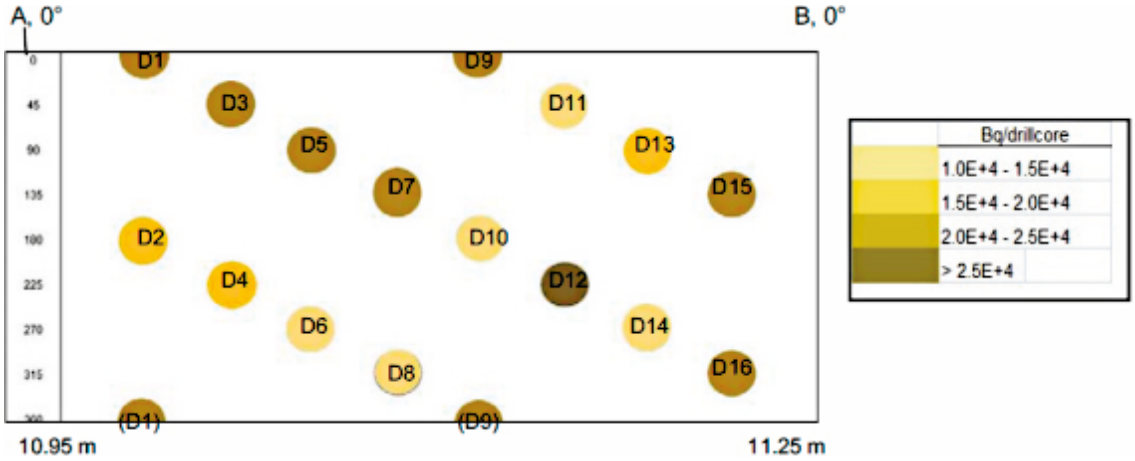

Figure 12-4. *Plan view of the surface distribution of ^{137}Cs, measured with γ-spectrometry on whole rock cores, in the test section in the 36 mm borehole. The relatively low activity in D14 might be due to a remaining epoxy layer during the measurement which in turn gave a longer distance to the detector. Excerpt from Nilsson et al. (2010, Figure 3-6).*

13 9B-3: Reporting and deliverables of Task 9B

13.3 Reporting of Task 9B

Modelling groups should present modelling results of Task 9B-3 at the Task Force spring meeting TF #35 (May 16-18, 2017 in Sweden), together with results of the other subtasks of 9B.

At the Helsinki Workshop (October 26-27, 2016) it was decided to integrate the reporting of the three subparts of Task 9B (i.e. 9B-1, 9B-2, and 9B-3). This means that each modelling group should deliver a single report that covers the entire Task 9B. If it suits the modelling group, and if feasible, the reporting could include a manuscript suitable for publication in a scientific journal (for example a summary of the modelling work or descriptions of a novel methodology). Alternatively the report could form the basis for a later publication in the open literature, which is encouraged by the SKB Task Force.

A template for SKB reports is available on the Task Force website (data delivery #13). The outline is to be decided by the authors, although headings relating to performance measures (cf. Section 13.2) are suggested.

In order to allow the evaluation of the different modelling group's work, it is necessary that the following topics are addressed in the report (the level of detail is at the discretion of the modelling group):

- Short description of the code, including key equations solved in the model (e.g. conservation of solute mass including diffusion and sorption). Approach used for the fitting procedure.
- Geometry, dimensions, grid (discretization) used in the model.
- Initial and boundary conditions, in terms of tracer concentrations (activities).
- Parameters (D_e, K_d, porosities or other equivalent parameters) plus their spatial variation (heterogeneity), for the possible different tracers and cases reported. References for parameter values taken from the reports or from other literature. Also volumes of water in the source reservoir.
- Results, roughly according to Excel-template distributed prior to Task 9B-1, including tracer profiles in the rock (activity vs. penetration depth) and tracer concentrations in the source water (activity vs. time).
- Discussion/conclusions.

Note that some of the bullets overlap with the requests in Section 13.2.

A draft of the report should be delivered to the evaluator by end of August 2017. Thereafter it will be reviewed by the evaluator (with input from others). Comments from the evaluator (and any other reviewers) will be provided by the end of November 2017. After revisions, the final report should be published in early 2018 (if a group instead choses the manuscript options, a suitable time plan should be communicated).

All three task descriptions of 9B will be compiled by the principal investigators to a public SKB report that will be published prior to the TF #35 meeting in May 2017. When reporting, references to the setup of the task; experimental design; and other issues can be made to this report. Moreover, in 2017/2018 a standalone evaluation report of Task 9B will be prepared.

Comment:
The Task 9B time plan has been updated.

13.2 Performance measures of Task 9B

At the Helsinki Workshop it was decided against setting up numerical performance measures for Task 9B. Instead it was decided to focus on system description and conceptual understanding, and the incorporation of this understanding in the actual model. For this reason we suggest the following headings as part of your report:

True system

Please describe your conceptual understanding of the true system with regard to radionuclide transport in rock in general and, if needed, in the LTDE-SD experiment in particular. What processes are dominant, significant, and subordinate? Which features and events need to be considered? Note that your system description and conceptual understanding does not necessarily need to be quantified or described by equations and developed theories, but may be described in a qualitative fashion.

Reified model

Describe your reified model, which is your best conceivable (even hypothetical) model if you did not need to worry about computational limitations, the time and manpower it would take to perform it, etc. What features, events, and processes (FEPs) out of those described under the true system heading would you neglect and why?

Actual model

Describe your actual model, with its benefits and limitations. Which features, events, and processes have been included or discarded; and on what grounds? Even when including certain FEPs, there are usually underlying assumptions, simplification, limitations, restrictions and constraints. Which are the most important ones and can their impact be predicted? Note that the actual model is often limited by computational power, limitations in the computational code, manpower, time, etc. and that such limitations may be valid justifications for your choices.

Alternative models

Sometimes the nature of some uncertainties is such that alternative models are needed to describe the true system behaviour; or to question or disprove the hypotheses examined with the actual model. Is there a need for such alternative models? This discussion can start from actual alternative models, if such have been set up, or be held from a qualitative point of view without actually setting up the alternative models.

Limitations in experimental observations

Are there limitations in the experimental setup or performance that make the experimental results insensitive to the transport processes that we intend to study? Which are they, how serious are they, and is there a work-around?

The modelling groups are encouraged to consult the document “A Framework for Comparative Analyses and Conceptual Uncertainty Evaluation”, which may be found on the Task Force website under Task 8, data delivery #21. The document was later developed into a paper (Finsterle et al. 2018).

13.3 Deliverables of Task 9B-3

Concerning Task 9B-3 in particular, the deliverables should focus on penetration profiles that can be compared to the experimental data. The experimental data will be given as the decay corrected activity per mass of rock, within the analysed slices. The decay correction will be performed with the LTDE-SD tracer injection date (2006-09-27) as reference. The value and experimental uncertainty will be provided for each data point, unless the value is below the detection threshold. In that case the detection threshold is reported. In the experimentally obtained penetration profiles, decay corrected activity data per unit of mass will be inserted on the (logarithmic) y-axis. On the x-axis will be the penetration depth, given as the centre distance to surface as provided for the individual slices in Table 12-1 to Table 12-5. This format can be used by the modelling groups as a guideline for delivering numerical data to the evaluator. However, data on other reasonable formats can also be delivered.

Figure 13-1 shows an example of an experimental penetration profile (in blue diamonds), taken from Nilsson et al. (2010). This particular penetration profile is for Na-22 in core sample A10. Each data point is assigned an error bar and the detection limit of the analysis is indicated by the two large error bars starting from the x-axis at penetration depth beyond 5 cm. The pink curve represents a penetration profile, as inversely modelled by Nilsson et al. (2010).

In doing the predictive modelling, the same rock parameters (if independent of the tracer) should be used for the individual cores and/or slices for all five tracers. This is to assure internal consistence in the modelling. Preferably the predicted penetration profiles should encompass some kind of uncertainty range.

Numerical results (i.e. full tracer profiles) should be delivered to the evaluator Josep Soler in an Excel-file two weeks prior to the TF #35 meeting, at the latest. This can be done in a similar manner as for Task 9B-1 and 9B-2.

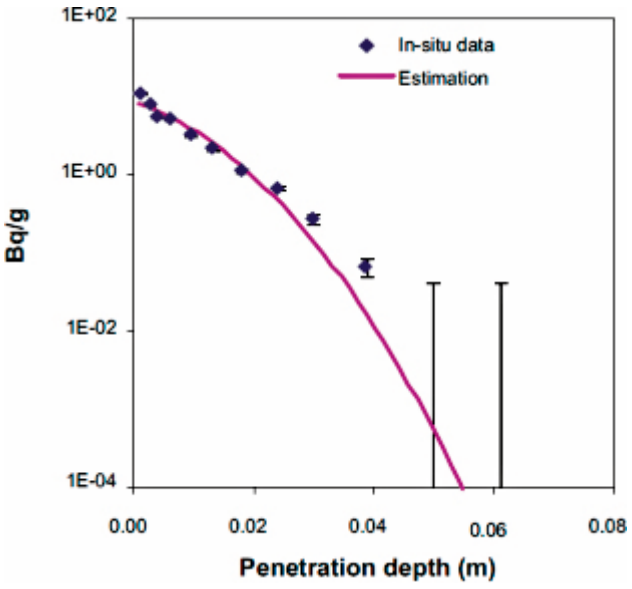

Figure 13-1. *Na-22 activity versus penetration depth in core sample A10. Reproduced from Nilsson et al. (2010, Figure 4-21).*

References

SKB's (Svensk Kärnbränslehantering AB) publications can be found at www.skb.com/publications.

Byegård J, Johansson H, Andersson P, Hansson K, Winberg A, 1999. Äspö Hard Rock Laboratory. Test plan for the long term diffusion experiment. SKB IPR-99-36, Svensk Kärnbränslehantering AB.

Finsterle S, Lanyon B, Åkesson M, Baxter S, Bergström M, Bockgård N, Dershowitz W, Dessirier B, Frampton A, Fransson Å, Gens A, Gylling B, Hančilová I, Holton D, Jarsjö J, Kim J-S, Kröhn K-P, Malmberg D, Pulkkanen V-M, Sawada A, Sjöland A, Svensson U, Vidstrand P, Viswanathan H, 2018. Conceptual uncertainties in modelling the interaction between engineered and natural barriers of nuclear waste repositories in crystalline rock. In Norris S, Neeft E A C, Neeft M (eds). Multiple roles of clays in radioactive waste confinement. London: Geological Society. (Special publications 482), 261–283.

Li C, 2001. Äspö Hard Rock Laboratory. Long-Term Diffusion Experiment. Microscopic observation of disturbance in drill core samples from KA3065A02 and KA3065A03. SKB IPR-01-03, Svensk Kärnbränslehantering AB.

Löfgren M, Neretnieks I, 2006. Through-electromigration: a new method of investigating pore connectivity and obtaining formation factors. Journal of Contaminant Hydrology 87, 237–252.

Nilsson K, Byegård J, Selnert E, Widestrand H, Höglund S, Gustafsson E, 2010. Äspö Hard Rock Laboratory. Long Term Sorption Diffusion Experiment (LTDE-SD). Results from rock sample analyses and modelling. SKB R-10-68, Svensk Kärnbränslehantering AB.

Vilks P, Miller N H, Stanchell F W, 2005. Laboratory program supporting SKB's Long Term Diffusion Experiment. Report 06819-REP-01300-10111-R00, Atomic Energy of Canada Limited.

Voutilainen M, Siitari-Kauppi M, Sardini P, Lindberg A, Timonen J. 2012. Pore-space characterization of an altered tonalite by X-ray computed microtomography and the ^{14}C-labeled-polymethylmethacrylate method. Journal of Geophysical Research 117, B01201. doi:10.1029/2011JB008622|

Wass E, 2005. LTDE Long-Term Diffusion Experiment. Hydraulic conditions of the LTDE experimental volume – results from Pre-Tests 0.1–6. SKB IPR-05-25, Svensk Kärnbränslehantering AB.

Widestrand H, Byegård J, Börjesson S, Bergelin A, Wass E, 2006. LTDE Long-Term Diffusion Experiment. Functionality tests with short-lived radionuclides 2005. SKB IPR-06-05, Svensk Kärnbränslehantering AB.

Widestrand H, Byegård J, Selnert E, Skålberg M, Höglund S, Gustafsson E, 2010a. Äspö Hard Rock Laboratory. Long Term Sorption Diffusion Experiment (LTDE-SD). Supporting laboratory program – Sorption diffusion experiments and rock material characterisation. With supplement of adsorption studies on intact rock samples from the Forsmark and Laxemar site investigations. SKB R-10-66, Svensk Kärnbränslehantering AB.

Widestrand H, Byegård J, Kronberg M, Nilsson K, Höglund S, Gustafsson E, 2010b. Äspö Hard Rock Laboratory. Long Term Sorption Diffusion Experiment (LTDE-SD). Performance of main in-situ experiment and results from water phase measurements. SKB R-10-67, Svensk Kärnbränslehantering AB.

Winberg A, Hermanson J, Tullborg E-L, Andersson P, Carlsten S, Rouhiainen P, Nilsson G, Gustafsson C, 2000. Äspö Hard Rock Laboratory. Evaluation of fracture candidates in boreholes KA2865A01 and KA3065A02. Location of experimental site for the long term diffusion experiment. SKB IPR-00-27, Svensk Kärnbränslehantering AB.

Winberg A, Hermanson J, Tullborg, E-L, Staub I, 2003. Äspö Hard Rock Laboratory. Long-Term Diffusion Experiment. Structural model of the LTDE site and detailed description of the characteristics of the experimental volume including target structure and intact rock section. SKB IPR-03-51, Svensk Kärnbränslehantering AB.

Appendix 1

Additional information on LTDE-SD

Timeline of LTDE-SD

Table A1-1 gives the dates of important events of the in-situ phase of LTDE-SD; its termination; the overcoring and sample extraction; and sample analyses. The table is part of data delivery #8.

Table A1-1. Information on dates for events with potential impact on diffusion during the course of the experiment, until analysis of the sliced rock samples.

Date	Event	Comments
2006-09-27	Tracer cocktail injection	22 radionuclides, circulation of the water in the test section (flow rate c. 15 mL/min)
2007-04-12	Termination of in-diffusion phase	Exchange of radionuclides in water for isopropyl alcohol
2007-04-12	Epoxy injection	Protection from flushing away radionuclides and mechanical damage during over coring
2007-04-27	Borehole left open with stub exposed	Water flushing may have caused desorption of radionuclides from the surface
2007-04-30 to 2007-05-02	Over core drilling of the experiment section	After removal and dismantling of the borehole equipment
2007-05-04	Core transported to Clab/Simpevarp	Core covered with heavy plastic foil to prevent drying
2008-08-03	Epoxy coating of the core	Performed in order to avoid cross-contamination
2008-08-06	Cutting of the core	Performed in order to facilitate drilling of the core samples
2007-08-08	Drilling of core samples	D1/D2, D9/D10, D5/D6, D13/D14 and D3/D4. All rock cores placed in plastic bags, see Figure A1-1 below.
2007-08-09	Drilling of core samples	D11/D12, D7/D8, D15/D16, A16, A10, A4 and A17
2007-08-10	Drilling of core samples	A5, A9, A11, A15, A3, A8, A14, A2, A6
2007-08-13	Drilling of core samples	A1, A18, A12, A13, A7, A19, A20, A21
2007-08-14	Drilling of epoxy covered PEEK lid samples	B15
2007-08-15	Drilling of epoxy covered PEEK lid samples	B15, B8, B14 and B9
2007-08-20	Drilling of epoxy covered PEEK lid samples	B3
2007-08-22	Drilling of epoxy covered PEEK lid samples	B2 and B16
2007-09-04	Drilling of epoxy covered PEEK lid samples	B7, B4, B10, B17, B5, B11, B6, B18, B1, B12 and B13
2007-10-25 to 2007-10-26	Slicing 1-10 mm	Performed at Helsinki University; A3, A7
2007-11-01	Slicing 1-10 mm	D10
2007-11-02	Slicing 1-10 mm	D9
2007-11-08	Slicing 1-10 mm	D1, D2
2007-11-15	Slicing 1-10 mm	D3, D4
2007-11-16	Slicing 1-10 mm	D5
2007-11-20	Square-cut 3 cm pieces	A2, A9
2007-11-21	Square-cut 3 cm pieces	A1, A11
2007-11-22	Slicing 1- 10 mm	A12
2007-11-25	Slicing 1- 10 mm	A3
2007-11-27	Slicing 1- 10 mm	A5
2007-12	Square-cut 3 cm pieces	A13, A14, A15, A16, A17, D8, D11, D13, D14, D16
2007-12	Slicing 1- 10 mm	
2007-12-04	Square-cut 3 cm pieces	A4
2007-12-05	Square-cut 3 cm pieces	A6
2007-12-09	Slicing 1-10 mm	A10
2007-12-10	Square-cut 3 cm pieces	A8, D6, D12
2007-12-10	Slicing 1-10 mm	A18
2007-12-11	Slicing 1-10 mm	D7
2008-01-05	Square-cut 3 cm pieces	D15
2008-02 to 2008-03	Slicing 1- 10 mm	A1, A2, A4, A6, A8, A9, A11, A13, A14, A15, A16, A17, D6, D8, D11, D12, D13, D14, D15, D16
2008-10-24 to 2010-04-16	HPGe and LSC analyses of rock samples	Performed at Baslab/Clab/Simpevarp

Core storage

Between drilling of the individual core samples from the larger overcored piece of rock and slicing the core samples, they were placed in plastic bags (see Figure A1-1). This was mainly done to avoid cross-contamination.

Decay correction

The formula for decay correcting is:

$$A_0 = (A_t \cdot e^{kt}) \qquad \text{Eq A1-1}$$

where A_t is the raw, (uncorrected) count at time t, A_0 is the count at time 0 (the decay corrected counts), e is the natural exponential function, k is the decay constant (or "lambda"), and t is the elapsed time. The decay constant is:

$$k = \frac{\ln(2)}{t_{½}} \qquad \text{Eq A1-2}$$

where $t_{½}$ is the half-life of the radioactive material of interest. This means that if one, for some reason, wants to know the activity of any radionuclide at another time than the results in the Task 9B-1 description, all given as the activity on the injection date, the values have to be recalculated:

$$A_t = A_0 \cdot e^{\left(-\ln 2 \cdot \frac{t}{t_{½}}\right)} \qquad \text{Eq A1-3}$$

where *A0* is the activity on 2006-09-27 (injection date), given in the Task 9B-1 description, *At* is the uncorrected activity on any date (t) and $t_{½}$ is the half-life of the radioactive nuclide.

Figure A-1. *Rock core samples contained in thin plastic bags, mainly to avoid cross-contamination during cutting, drilling and storage of rock core samples. Plastic bags were not primarily used to prevent drying of the pore water and air was not evacuated from them during storage.*

Appendix 2

Rock matrix data

This appendix tabulates data on the partitioning of the core samples and on their activity. The data corresponds to those tabulated in Sections 4.3.3 and 4.4.2 and are part of data delivery #11. Data in Sections 4.3.3 (partitioning data), 4.4.2 (activity data) and 12.2 (partitioning data) for core samples A4, A6, A9, A11, A13, D12, D13, D15 and D16 are not reproduced below.

Partitioning of core samples

In all tables on the partitioning of core samples, a 0.3 mm loss is assumed in the cutting of each slice when summing the sample length and when calculating the centre distance to surface.

Table A2-1. Information on the partitioning of core sample A1.

Slice	Weight (g)	Mean length (mm)	Centre distance to surface (mm)
A1.1	1.3869	5.0	2.5
A1.2	0.1531	0.7	5.7
A1.3	0.1778	0.8	6.7
A1.4	1.1330	3.1	9.0
A1.5	0.9415	2.7	12.2
A1.6	0.7087	3.0	15.4
A1.7	2.9220	6.4	20.4
A1.8	2.6552	5.3	26.6
A1.9	2.4880	5.3	32.2
A1.10	8.7488	10.0	40.2
A1.11	6.4426	10.0	50.5
A1.12	7.0701	10.0	60.8
Sum	34.8277	65.8	

Table A2-2. Information on the partitioning of core sample A5.

Slice	Weight (g)	Mean length (mm)	Centre distance to surface (mm)
A5.1	1.7242	3.5	1.8
A5.2	0.9095	1.0	4.3
A5.3	0.9598	0.8	5.5
A5.4	3.5015	3.1	7.7
A5.5	3.9991	3.2	11.1
A5.6	3.7507	2.9	14.4
A5.7	7.1556	4.7	18.5
A5.8	6.1214	5.4	23.9
A5.9	6.6172	12.4	33.0
A5.10	13.0803	12.1	45.6
A5.11	12.0770	12.1	58.0
A5.12	13.6226	11.8	70.2
Sum	73.5189	76.1	

Table A2-3. Information on the partitioning of core sample A8.

Slice	Weight (g)	Mean length (mm)	Centre distance to surface (mm)
A8.1	0.4658	1.3	0.7
A8.2	0.1206	0.6	1.9
A8.3	0.1091	0.8	2.9
A8.4	2.9793	5.8	6.5
A8.5	1.0313	2.4	10.9
A8.6	0.9747	2.0	13.4
A8.7	3.0277	6.3	17.9
A8.8	1.8053	3.8	23.2
A8.9	2.6900	5.2	28.0
A8.10	6.1075	10.0	35.9
A8.11	5.9523	10.0	46.2
A8.12	6.8785	10.0	56.5
Sum	32.1421	61.5	

Table A2-4. Information on the partitioning of core sample A10.

Slice	Weight (g)	Mean length (mm)	Centre distance to surface (mm)
A10.1	1.7242	2.0	1.0
A10.2	0.9095	0.8	2.7
A10.3	0.9598	0.9	3.8
A10.4	3.5015	3.0	6.0
A10.5	3.9991	3.4	9.4
A10.6	3.7507	3.2	13.0
A10.7	7.1556	6.1	17.9
A10.8	6.1214	5.3	23.9
A10.9	6.6172	6.0	29.9
A10.10	13.0803	11.0	38.7
A10.11	12.0770	10.5	49.7
A10.12	13.6226	11.8	61.2
Sum	73.5189	67.1	

Table A2-5. Information on the partitioning of core sample A12.

Slice	Weight (g)	Mean length (mm)	Centre distance to surface (mm)
A12.1	1.6275	2.1	1.1
A12.2	0.7728	1.3	3.1
A12.3	0.4098	0.6	4.3
A12.4	2.0114	3.1	6.5
A12.5	2.0484	3.1	9.9
A12.6	2.1368	3.2	13.3
A12.7	3.4867	5.1	17.7
A12.8	4.4821	6.4	23.7
A12.9	8.7417	12.1	33.2
A12.10	8.6585	11.9	45.5
A12.11	9.8807	13.0	58.2
A12.12	7.8458	11.2	70.6
Sum	52.1022	76.2	

Table A2-6. Information on the partitioning of core sample A15.

Slice	Weight (g)	Mean length (mm)	Centre distance to surface (mm)
A15.1	1.8378	3.3	1.7
A15.2	0.9200	1.1	4.2
A15.3	0.7731	0.9	5.5
A15.4	2.4592	2.9	7.7
A15.5	2.4844	3.0	11.0
A15.6	2.0958	2.6	14.1
A15.7	4.7111	5.9	18.6
A15.8	4.0369	5.2	24.5
A15.9	3.9243	5.5	30.2
A15.10	8.5466	11.0	38.7
A15.11	8.3040	10.1	49.6
A15.12	8.4305	10.0	60.0
Sum	48.52367	65.0	

Table A2-7. Information on the partitioning of core sample A16.

Slice	Weight (g)	Mean length (mm)	Centre distance to surface (mm)
A16.1	0.7745	1.5	0.8
A16.2	0.7377	0.9	2.3
A16.3	0.6947	0.8	3.4
A16.4	2.1423	2.8	5.5
A16.5	2.1073	2.8	8.6
A16.6	2.4203	3.2	11.9
A16.7	3.8668	5.2	16.4
A16.8	4.1759	5.9	22.3
A16.9	3.7027	5.4	28.2
A16.10	6.4353	10.6	36.5
A16.11	6.5712	10.5	47.3
A16.12	6.4991	10.7	58.2
Sum	40.1278	63.6	

Table A2-8. Information on the partitioning of core sample A17.

Slice	Weight (g)	Mean length (mm)	Centre distance to surface (mm)
A17.1	1.3125	2.2	1.1
A17.2	0.5598	1.3	3.1
A17.3	1.3270	2.1	5.1
A17.4	1.3733	2.5	7.7
A17.5	1.1508	2.4	10.4
A17.6	2.8878	4.7	14.2
A17.7	3.6938	5.6	19.7
A17.8	3.5148	5.3	25.4
A17.9	6.4239	10.0	33.3
A17.10	7.1303	10.0	43.6
A17.11	7.0128	10.0	53.9
A17.12	7.2422	20.0	69.2
Sum	43.629	79.2	

Table A2-9. Information on the partitioning of core sample A20.

Slice	Weight (g)	Mean length (mm)	Centre distance to surface (mm)
A20.1	3.9267	1.3	0.6
A20.2	2.2504	3.1	3.1
A20.3	0.7466	0.9	5.4
A20.4	2.2916	3.1	7.7
A20.5	2.4728	3.3	11.2
A20.6	2.6909	3.6	15.0
A20.7	4.0895	5.8	20.0
A20.8	4.0282	6.1	26.2
A20.9	7.4551	10.0	34.6
A20.10	7.1467	10.0	44.9
A20.11	6.8613	10.0	55.2
A20.12	7.1596	20.0	70.5
A20.13	7.1596	20.0	90.8
A20.14	8.8789	20.0	111.1
Sum	80.2556	127.8	

Table A2-10. Information on the partitioning of core sample D1.

Slice	Weight (g)	Mean length (mm)	Centre distance to surface (mm)
D1.1	1.0432	1.7	0.8
D1.2	0.4778	1.2	2.5
D1.3	0.3577	1.0	3.9
D1.4	1.3405	2.9	6.2
D1.5	1.4529	3.1	9.4
D1.6	1.5177	3.4	13.0
D1.7	2.5726	4.7	17.3
D1.8	2.4332	5.2	22.6
D1.9	2.4570	4.7	27.8
D1.10	6.4661	9.7	35.3
D1.11	5.9160	9.8	45.4
D1.12	5.5858	9.6	55.4
Sum	31.6205	60.2	

Table A2-11. Information on the partitioning of core sample D5.

Slice	Weight (g)	Mean length (mm)	Centre distance to surface (mm)
D5.1	1.2647	1.7	0.9
D5.2	1.0347	1.6	2.8
D5.3	0.6468	0.9	4.3
D5.4	1.6631	2.5	6.3
D5.5	2.0366	2.8	9.2
D5.6	1.7036	2.7	12.2
D5.7	3.5907	5.0	16.3
D5.8	3.6961	4.9	21.6
D5.9	3.2159	4.7	26.7
D5.10	7.1824	10.4	34.5
D5.11	6.6082	9.6	44.8
D5.12	7.0078	10.4	55.1
Sum	39.6506	60.3	

Table A2-12. Information on the partitioning of core sample D6.

Slice	Weight (g)	Mean length (mm)	Centre distance to surface (mm)
D6.1	1.1832	1.6	0.8
D6.2	0.3906	1.0	2.4
D6.3	0.2257	1.0	3.7
D6.4	1.3932	3.0	6.0
D6.5	1.6082	2.9	9.2
D6.6	1.7817	3.0	12.4
D6.7	2.4397	4.6	16.5
D6.8	2.6615	4.8	21.5
D6.9	2.7167	4.8	26.6
D6.10	6.3513	10.5	34.5
D6.11	5.5905	9.9	45.1
D6.12	6.8664	10.1	55.4
Sum	33.2087	60.4	

Table A2-13. Information on the partitioning of core sample D7.

Slice	Weight (g)	Mean length (mm)	Centre distance to surface (mm)
D7.1	1.9235	2.4	1.2
D7.2	0.6444	0.9	3.2
D7.3	0.6872	1.0	4.4
D7.4	1.8983	2.6	6.4
D7.5	2.1063	2.8	9.4
D7.6	2.1256	3.1	12.7
D7.7	3.4498	4.7	16.9
D7.8	3.3135	4.8	22.0
D7.9	3.5413	4.8	27.1
D7.10	7.4132	9.8	34.7
D7.11	7.0340	9.4	44.6
D7.12	7.2199	9.6	54.5
Sum	41.357	59.3	

Table A2-14. Information on the partitioning of core sample D8.

Slice	Weight (g)	Mean length (mm)	Centre distance to surface (mm)
D8.1	1.2337	1.2	0.6
D8.2	1.2809	1.7	2.3
D8.3	1.1014	1.5	4.1
D8.4	1.6415	2.3	6.3
D8.5	2.7509	3.6	9.5
D8.6	2.5922	3.2	13.3
D8.7	4.1468	5.2	17.8
D8.8	3.7619	4.5	22.9
D8.9	4.1046	5.2	28.0
D8.10	6.4145	10.6	36.3
D8.11	6.2298	10.7	47.2
D8.12	7.0412	9.6	57.7
Sum	42.2994	62.5	

Table A2-15. Information on the partitioning of core sample D14.

Slice	Weight (g)	Mean length (mm)	Centre distance to surface (mm)
D14.1	2.8469	1.5	0.8
D14.2	0.6244	0.9	2.3
D14.3	0.5934	0.9	3.5
D14.4	2.2197	3.3	5.9
D14.5	2.0447	3.1	9.4
D14.6	2.08	3.1	12.8
D14.7	2.8557	4.4	16.9
D14.8	3.4193	5.1	21.9
D14.9	3.6137	5.3	27.4
D14.10	9.4408	11.6	36.1
D14.11	8.4455	10.2	47.3
D14.12	8.4573	10.4	57.9
Sum	46.6414	63.1	

Activities per slice

The tables below provide the tracer activity of the individual slices of the A and D core samples, where measured. The note n.a. stands for not available. The uncertainty is reported as 2s, except for Cl-36 and Ni-63 (Task 9B-1 and 9B-2) for which the method uncertainty (m.u.) from the leaching procedure is included.

Comment (March 2020):
Values highlighted with yellow are updated or commented.
Comments are added to some values.
These updates may also be found in the Excel file “Task 9B-2 Rock matrix data_update 20200221_1” (Data Delivery 40).

Table A2-10. Tracer activity in slices from the A1 core, per grams of rock.

Slice	Na-22 (Bq/g)	Na-22 2δ (Bq/g)	Cl-36 (Bq/g)	Cl-36 m.u. (Bq/g)	Co-57 (Bq/g)	Co-57 2δ (Bq/g)	Ni-63 (Bq/g)	Ni-63 m.u. (Bq/g)	Ba-133 (Bq/g)	Ba-133 2δ (Bq/g)	Cs-137 (Bq/g)	Cs-137 2δ (Bq/g)
A1.1	2.23E+01	1.60E+00	n.a.		1.30E+03	1.44E+01	1.07E+04	9.56E+02	8.13E+02	5.73E+00	9.91E+03	1.73E+01
A1.2	1.63E+01	2.08E+00	n.a.		<1.52E+01		<8E+00		2.16E+01	1.40E+00	9.03E+01	2.34E+00
A1.3	1.36E+01	1.83E+00	n.a.		<1.24E+01		<8E+00		5.00E+00	1.25E+00	7.53E+00	9.06E−01
A1.4	9.44E+00	5.23E−01	n.a.		<2.30E+00		n.a.		<3.93E−01		8.71E−01*	1.64E−01
A1.5	6.67E+00	4.26E−01	n.a.		<3.90E+00		n.a.		<3.41E−01		9.68E−01*	1.48E−01
A1.6	4.84E+00	4.64E−01	n.a.		<5.29E+00		n.a.		5.31E−01	2.38E−01	1.40E+00*	1.99E−01
A1.7	2.58E+00	1.81E−01	n.a.		<9.57E−01		n.a.		<1.45E−01		4.65E−01*	6.66E−02
A1.8	9.16E−01	1.41E−01	n.a.		<1.22E+00		n.a.		<1.57E−01		2.97E−01*	6.43E−02
A1.9	7.22E−01	1.52E−01	n.a.		<1.10E+00		n.a.		1.78E−01*	7.72E−02	9.75E−01*	8.84E−02
A1.10	6.56E−01	6.44E−02	n.a.		<4.60E−01		n.a.		<7.61E−02		1.39E−01*	2.95E−02
A1.11	<2.33E−01		n.a.		<5.73E−01		n.a.		<9.53E−02		1.23E−01*	3.70E−02
A1.12	1.52E+00	1.31E−01	n.a.		<1.26E+00		n.a.		<1.44E−01		5.55E−01*	5.22E−02

Slice	Cd-109 (Bq/g)	Cd-109 2δ (Bq/g)	Ag-110m (Bq/g)	Ag-110m 2δ (Bq/g)	Gd-153 (Bq/g)	Gd-153 2δ (Bq/g)	Ra-226 (Bq/g)	Ra-226 2δ (Bq/g)	Np-237 (ng/g)	Np-237 2δ (ng/g)
A1.1	5.15E+03	1.65E+02	2.11E+02	1.01E+01	4.99E+02	3.84E+01	1.60E+02	1.23E+01	3.52E+01	3.3E+00
A1.2	<1.74E+02		<2.95E+01		<8.40E+01		<9.14E+00		n.a.	
A1.3	<1.40E+02		<3.37E+01		<7.40E+01		<7.87E+00		n.a.	
A1.4	<3.15E+01		<7.22E+00		<1.30E+01		<1.24E+00		n.a.	
A1.5	<3.71E+01		<7.82E+00		<2.50E+01		<1.49E+00		n.a.	
A1.6	<5.10E+01		<1.18E+01		<3.34E+01		<1.98E+00		n.a.	
A1.7	<1.23E+01		<1.48E+00		<6.43E+00		<4.79E−01		n.a.	
A1.8	<1.35E+01		<2.66E+00		<6.95E+00		<1.00E+00		n.a.	
A1.9	<1.42E+01		<2.72E+00		<7.33E+00		<5.63E−01		n.a.	
A1.10	<5.76E+00		<1.05E+00		<2.46E+00		<1.00E+00		n.a.	
A1.11	<7.58E+00		<1.10E+00		<3.81E+00		<1.00E+00		n.a.	
A1.12	<1.38E+01		<3.68E+00		<8.45E+00		<1.00E+00		n.a.	

*Concentration below the background estimated for the crushed core samples (based on measurements of blank sample A20).

Table A2-11. Tracer activity in slices from the A4 core (9B-3), per grams of rock.

Slice	Na-22 (Bq/g)	Na-22 2δ (Bq/g)	Cl-36 (Bq/g)	Cl-36 2δ (Bq/g)	Ni-63 (Bq/g)	Ni-63 2δ (Bq/g)	Ba-133 (Bq/g)	Ba-133 2δ (Bq/g)	Cs-137 (Bq/g)	Cs-137 2δ (Bq/g)
A4.1	< 1.1E+02		1.22E+01	2.60E+00	n.a		4.20E+02	1.00E+02	8.80E+03	1.40E+03
A4.2	2.00E+01	1.20E+01	2.28E+00	4.80E−01	n.a		6.20E+01	1.40E+01	8.00E+02	1.20E+02
A4.3	5.70E+00	2.60E+00	1.24E+00	2.80E−01	n.a		1.06E+01	2.20E+00	4.40E+01	8.00E+00
A4.5	3.90E+00	1.00E+00	6.60E−01	1.40E−01	n.a		3.20E−02*	2.00E−02	3.50E−01*	8.00E−02
A4.7	2.80E+00	8.00E−01	9.60E−01	2.00E−01	n.a		3.40E−02*	2.00E−02	4.10E−01*	8.00E−02
A4.9	2.20E+00	6.00E−01	6.80E−01	1.60E−01	n.a		1.10E−01*	2.40E−02	1.32E+00*	2.20E−01
A4.12	4.10E−01	1.80E−01	1.77E−01	4.80E−02	n.a		2.20E−02*	1.20E−02	1.85E−01*	4.40E−02

*Concentration below the background estimated for the crushed core samples (based on measurements of blank sample A20).

Table A2-12. Tracer activity in slices from the A5 core, per grams of rock.

Slice	Na-22 (Bq/g)	Na-22 2δ (Bq/g)	Cl-36 (Bq/g)	Cl-36 m.u. (Bq/g)	Co-57 (Bq/g)	Co-57 2δ (Bq/g)	Ni-63 (Bq/g)	Ni-63 m.u. (Bq/g)	Ba-133 (Bq/g)	Ba-133 2δ (Bq/g)	Cs-137 (Bq/g)	Cs-137 2δ (Bq/g)
A5.1	1.15E+01	3.84E−01	n.a.		2.51E+03	8.56E+00	n.a.		2.60E+02	1.13E+00	3.98E+03	3.19E+00
A5.2	n.a.		n.a.		n.a.		n.a.		n.a.		n.a.	
A5.3	3.73E+00	2.68E−01	n.a.		<2.16E+00		n.a.		1.07E+00	1.24E−01	3.35E+00	2.49E−01
A5.4	4.03E+00	1.49E−01	n.a.		<5.52E−01		n.a.		<8.04E−02		1.89E−01**	3.43E−02
A5.5	3.12E+00	1.24E−01	n.a.		<6.49E−01		n.a.		5.09E−02	2.41E−02	7.45E−02**	2.76E−02
A5.6	2.82E+00	1.23E−01	n.a.		<6.19E−01		n.a.		<6.68E−02		3.05E−01**	3.33E−02
A5.7	1.43E+00	6.02E−02	n.a.		<3.13E−01		n.a.		<3.37E−02		3.37E−02**	1.37E−02
A5.8	1.09E+00	5.97E−02	n.a.		<2.96E−01		n.a.		<4.13E−02		4.47E−02**	1.62E−02
A5.9	1.40E+00	7.71E−02	n.a.		<4.56E−01		n.a.		<4.80E−02		<4.02E−02	
A5.10	7.81E−01	3.45E−02	n.a.		<1.99E−01		n.a.		<2.38E−02		<1.84E−02	
A5.11	1.14E+00	4.21E−02	n.a.		<2.66E−01		n.a.		<2.98E−02		<2.14E−02	
A5.12	1.17E+00	4.00E−02	n.a.		<2.37E−01		n.a.		<2.70E−02		<1.98E−02	

Slice	Cd-109 (Bq/g)	Cd-109 2δ (Bq/g)	Ag-110m (Bq/g)	Ag-110m 2δ (Bq/g)	Gd-153 (Bq/g)	Gd-153 2δ (Bq/g)	Ra-226 (Bq/g)	Ra-226 2δ (Bq/g)	Np-237 (ng/g)	Np-237 2δ (ng/g)
A5.1	3.28E+03	6.89E+01	1.49E+02	5.22E+00	3.70E+02	2.71E+01	6.34E+01	9.16E−01	n.a.	
A5.2	n.a.		n.a.		n.a.		n.a.		n.a.	
A5.3	<2.17E+01		<4.17E+00		<1.41E+01		<1.46E+00		n.a.	
A5.4	<8.07E+00		<1.15E+00		<4.91E+00		<4.00E−01		n.a.	
A5.5	<7.06E+00		<1.66E+00		<1.22E+01		<3.50E−01		n.a.	
A5.6	<7.39E+00		<1.79E+00		<4.55E+00		<3.73E−01		n.a.	
A5.7	<3.70E+00		<9.08E−01		<2.07E+00		<1.96E−01		n.a.	
A5.8	<4.23E+00		<9.52E−01		<2.36E+00		<2.29E−01		n.a.	
A5.9	<5.03E+00		<9.30E−01		<2.72E+00		<2.12E−01		n.a.	
A5.10	<2.20E+00		<5.12E−01		<1.32E+00		<1.07E−01		n.a.	
A5.11	<2.75E+00		<6.05E−01		<1.65E+00		<1.16E−01		n.a.	
A5.12	<2.40E+00		<5.80E−01		1.42E+01	5.52E+00	<1.03E−01		n.a.	

**Concentration below the background estimated for sliced core samples.

Table A2-13. Tracer activity in slices from the A6 core, per grams of rock.

Slice	Na-22 (Bq/g)	Na-22 2δ (Bq/g)	Cl-36 (Bq/g)	Cl-36 m.u. (Bq/g)	Co-57 (Bq/g)	Co-57 2δ (Bq/g)	Ni-63 (Bq/g)	Ni-63 m.u. (Bq/g)	Ba-133 (Bq/g)	Ba-133 2δ (Bq/g)	Cs-137 (Bq/g)	Cs-137 2δ (Bq/g)
A6.1	3.47E+01	2.08E+00	9.33E+00	5.14E−01	2.28E+03	2.06E+01	1.28E+04	1.14E+03	8.95E+02	7.74E+00	2.53E+04	2.99E+01
A6.2	4.57E+01	2.07E+00	6.36E+00	3.56E−01	9.24E+01	8.79E+00	1.31E+03	1.17E+02	5.41E+01	3.60E+00	7.82E+03	1.46E+01
A6.3	1.49E+01	2.33E+00	3.88E+00	2.31E−01	<1.33E+01		1.63E+01	2.74E+00	2.59E+00	1.31E+00	1.55E+02	3.00E+01
A6.4	1.53E+01	5.08E−01	1.89E+00	1.05E−01	<1.27E+00		4.48E+00*	5.82E−01	1.95E+00	1.53E−01	1.67E+00*	1.39E−01
A6.5	1.01E+01	4.08E−01	1.18E+00	6.61E−02	<1.20E+00		<4E+00		<2.47E−01		8.00E−01*	1.13E−01
A6.6	6.96E+00	3.21E−01	1.31E+00	7.29E−02	<1.20E+00		n.a.		<1.85E−01		5.49E−01*	9.73E−02
A6.7	4.61E+00	2.03E−01	7.69E−01	4.29E−02	<3.82E−01		n.a.		<1.24E−01		5.12E−01*	6.20E−02
A6.8	3.18E+00	1.78E−01	7.83E−01	4.37E−02	1.14E+00*	3.13E−01	n.a.		1.52E−01*	6.42E−02	1.82E+00*	9.04E−02
A6.9	1.96E+00	1.09E−01	6.71E−01	3.72E−02	<3.74E−01		n.a.		<7.93E−02		3.93E−01*	3.99E−02
A6.10	1.75E+00	9.81E−02	4.65E−01	2.59E−02	<3.70E−01		n.a.		<8.33E−02		3.03E−01*	3.56E−02
A6.11	1.64E+00	9.74E−02	3.55E−01	1.98E−02	<4.49E−01		n.a.		<7.73E−02		1.83E−01*	2.42E−02
A6.12	2.08E+00	1.18E−01	3.73E−01	2.10E−02	<5.66E−01		n.a.		1.35E−01*	4.85E−02	3.52E−01*	3.30E−02

Slice	Cd-109 (Bq/g)	Cd-109 2δ (Bq/g)	Ag-110m (Bq/g)	Ag-110m 2δ (Bq/g)	Gd-153 (Bq/g)	Gd-153 2δ (Bq/g)	Ra-226 (Bq/g)	Ra-226 2δ (Bq/g)	Np-237 (ng/g)	Np-237 2δ (ng/g)
A6.1	6.18E+03	2.40E+02	2.02E+02	1.10E+01	8.68E+02	1.36E+02	1.86E+02	7.46E+00	3.76E+01	3.6E+00
A6.2	8.53E+02	1.16E+02	<1.22E+01		<9.64E+01		3.13E+01	3.63E+00	n.a.	
A6.3	<1.70E+02		<3.65E+01		<8.60E+01		<8.78E+00		n.a.	
A6.4	<1.72E+01		<2.10E+00		<7.17E+00		<9.02E−01		n.a.	
A6.5	<1.56E+01		<2.36E+00		<6.32E+00		<8.55E−01		n.a.	
A6.6	<1.55E+01		<3.75E+00		<9.20E+00		<6.95E−01		n.a.	
A6.7	<8.29E+00		<1.42E+00		<3.03E+00		<4.37E−01		n.a.	
A6.8	<9.01E+00		<5.88E−01		<3.31E+00		<4.64E−01		n.a.	
A6.9	<5.29E+00		<6.24E−01		<1.84E+00		<1.00E+00		n.a.	
A6.10	<5.63E+00		<7.95E−01		<2.31E+00		<1.00E+00		n.a.	
A6.11	<6.11E+00		<7.68E−01		<2.45E+00		<1.00E+00		n.a.	
A6.12	<7.75E+00		<8.31E−01		<3.52E+00		<1.00E+00		n.a.	

*Concentration below the background estimated for the crushed core samples (based on measurements of blank sample A20).

Table A2-14. Tracer activity in slices from the A8 core, per grams of rock.

Slice	Na-22 (Bq/g)	Na-22 2δ (Bq/g)	Cl-36 (Bq/g)	Cl-36 m.u. (Bq/g)	Co-57 (Bq/g)	Co-57 2δ (Bq/g)	Ni-63 (Bq/g)	Ni-63 m.u. (Bq/g)	Ba-133 (Bq/g)	Ba-133 2δ (Bq/g)	Cs-137 (Bq/g)	Cs-137 2δ (Bq/g)
A8.1	7.49E+01	4.63E+00	n.a.		1.60E+02	1.33E+01	2.48E+03	2.21E+02	2.21E+02	5.71E+00	4.59E+03	2.01E+01
A8.2	3.60E+02	8.21E+00	n.a.		1.66E+01	7.88E+00	<8E+00		5.98E+01	2.35E+00	3.11E+02	4.31E+00
A8.3	2.82E+01	3.10E+00	n.a.		4.01E+01	7.58E+00	<8E+00		7.04E+00	1.31E+00	4.70E+01	1.96E+00
A8.4	4.65E+00	2.26E−01	n.a.		<7.83E−01		n.a.		2.07E−01*	7.24E−02	1.18E+00*	8.41E−02
A8.5	2.85E+00	3.60E−01	n.a.		<2.68E+00		n.a.		<4.12E−01		1.63E+00*	3.94E−01
A8.6	2.15E+00	3.64E−01	n.a.		<2.92E+00		n.a.		<4.31E−01		1.20E+00*	1.92E−01
A8.7	1.43E+00	1.45E−01	n.a.		<1.06E+00		n.a.		<1.44E−01		7.66E−01*	1.09E−01
A8.8	1.21E+00	1.97E−01	n.a.		<1.65E+00		n.a.		<2.36E−01		1.06E+00*	1.16E−01
A8.9	8.47E−01	1.28E−01	n.a.		<1.13E+00		n.a.		<1.63E−01		1.30E+00*	9.27E−02
A8.10	<1.25E−01		n.a.		<6.27E−01		n.a.		<1.02E−01		2.61E−01*	4.24E−02
A8.11	<1.24E−01		n.a.		<5.98E−01		n.a.		1.36E−01*	5.03E−02	8.99E−01*	5.87E−02
A8.12	2.44E−01	6.11E−02	n.a.		<5.87E−01		n.a.		<9.13E−02		2.85E−01*	3.93E−02

Slice	Cd-109 (Bq/g)	Cd-109 2δ (Bq/g)	Ag-110m (Bq/g)	Ag-110m 2δ (Bq/g)	Gd-153 (Bq/g)	Gd-153 2δ (Bq/g)	Ra-226 (Bq/g)	Ra-226 2δ (Bq/g)	Np-237 (ng/g)	Np-237 2δ (ng/g)
A8.1	8.90E+02	1.70E+02	<5.78E+01		<3.38E+02		3.89E+01	4.18E+00	n.a.	
A8.2	2.78E+02	9.77E+01	<3.83E+01		<9.65E+01		<1.16E+01		n.a.	
A8.3	<1.69E+02		<2.69E+01		<8.29E+01		<1.28E+01		n.a.	
A8.4	<1.26E+01		<1.89E+00		<5.56E+00		<4.70E−01		n.a.	
A8.5	<3.33E+01		<3.06E+00		<1.47E+01		<1.36E+00		n.a.	
A8.6	<3.53E+01		<6.57E+00		<1.49E+01		<1.44E+00		n.a.	
A8.7	<1.17E+01		<1.78E+00		<5.29E+00		<4.62E−01		n.a.	
A8.8	<2.04E+01		<3.57E+00		<9.91E+00		<7.75E−01		n.a.	
A8.9	<1.36E+01		<2.07E+00		<6.75E+00		<1.00E+00		n.a.	
A8.10	<7.99E+00		<1.15E+00		<2.96E+00		<2.29E−01		n.a.	
A8.11	<8.18E+00		<1.04E+00		<3.42E+00		<1.00E+00		n.a.	
A8.12	<7.07E+00		<1.21E+00		<2.99E+00		<1.00E+00		n.a.	

*Concentration below the background estimated for the crushed core samples (based on measurements of blank sample A20).

Table A2-15. Tracer activity in slices from the A9 core, per grams of rock.

Slice	Na-22 (Bq/g)	Na-22 2δ (Bq/g)	Cl-36 (Bq/g)	Cl-36 m.u. (Bq/g)	Co-57 (Bq/g)	Co-57 2δ (Bq/g)	Ni-63 (Bq/g)	Ni-63 m.u. (Bq/g)	Ba-133 (Bq/g)	Ba-133 2δ (Bq/g)	Cs-137 (Bq/g)	Cs-137 2δ (Bq/g)
A9.1	2.03E+01	2.84E+00	8.30E+00	4.61E−01	2.43E+03	2.89E+01	1.56E+04	1.39E+03	7.18E+02	9.86E+00	1.16E+04	3.26E+01
A9.2	9.92E+00	4.32E−01	1.62E+00	2.85E−01	<5.32E+00		<8E+00		2.48E+01	1.04E+00	1.79E+02	2.30E+00
A9.3	8.10E+00	1.62E+00	1.09E+00	9.79E−02	<1.31E+01		<8E+00		5.97E+00	9.65E−01	1.24E+01	1.22E+00
A9.4	4.58E+00	2.83E−01	7.66E−01	6.33E−02	<8.53E−01		n.a.		2.75E−01*	8.90E−02	7.13E−01*	8.64E−02
A9.5	3.51E+00	3.79E−01	5.50E−01	3.64E−02	<1.73E+00		n.a.		<3.41E−01		6.96E−01*	1.47E−01
A9.6	2.40E+00	2.55E−01	4.38E−01	5.63E−02	<1.15E+00		n.a.		<1.95E−01		5.23E−01*	9.98E−02
A9.7	6.00E−01[1)]	2.35E−01	4.35E−01	2.50E−02	<1.12E+00		n.a.		<9.74E−02		2.69E−01*	5.28E−03
A9.8	<2.76E−01[1)]		3.15E−01	2.14E−02	<1.24E+00		n.a.		1.04E−01*	4.23E−03	3.27E−01*	6.35E−03
A9.9	4.07E−01[1)]	2.47E−01	4.34E−01	2.52E−02	1.32E+00*	6.08E−01	n.a.		<1.13E−01		3.16E−01*	4.60E−03
A9.10	<8.35E−02[2)]		3.11E−01	1.85E−02	<5.68E−01		n.a.		<5.89E−02		9.15E−01*	4.26E−03
A9.11	1.30E−01	4.93E−02	1.57E−01	9.32E−03	<5.38E−01		n.a.		<6.90E−02		9.29E−02*	2.41E−02
A9.12	<1.54E−01		9.34E−02	8.43E−03	<8.46E−01		n.a.		<1.20E−01		5.83E−01*	5.18E−02

Slice	Cd-109 (Bq/g)	Cd-109 2δ (Bq/g)	Ag-110m (Bq/g)	Ag-110m 2δ (Bq/g)	Gd-153 (Bq/g)	Gd-153 2δ (Bq/g)	Ra-226 (Bq/g)	Ra-226 2δ (Bq/g)	Np-237 (ng/g)	Np-237 2δ (ng/g)
A9.1	6.23E+03	2.96E+02	4.08E+02	2.53E+01	1.14E+03	6.85E+01	1.58E+02	7.64E+00	3.99E+01	3.8E+00
A9.2	<7.94E+01		<9.18E+00		<3.90E+01		<5.73E+00		n.a.	
A9.3	<1.33E+02		<2.27E+01		<1.01E+02		<8.06E+00		n.a.	
A9.4	<1.11E+01		<1.54E+00		<4.93E+00		<8.85E-01		n.a.	
A9.5	<2.09E+01		<5.11E+00		<1.05E+01		<1.74E+00		n.a.	
A9.6	<1.37E+01		<2.59E+00		<6.68E+00		<1.13E+00		n.a.	
A9.7	<1.11E+01		<2.31E+00		<5.31E+00		<4.57E-01		n.a.	
A9.8	<1.20E+01		<2.02E+00		<2.64E+00		<5.08E-01		n.a.	
A9.9	<1.25E+01		<2.61E+00		<6.43E+00		<5.25E-01		n.a.	
A9.10	<6.97E+00		<1.23E+00		<3.14E+00		<2.00E-01		n.a.	
A9.11	<7.18E+00		<1.19E+00		<3.69E+00		<1.00E+00		n.a.	
A9.12	<9.12E+00		<1.67E+00		<4.63E+00		<2.60E-01		n.a.	

*Concentration below the background estimated for the crushed core samples (based on measurements of blank sample A20).

1)Re-analysed after leaching, including wash liquid.

2)Re-analysed after leaching, excluding wash liquid

Table A2-16. Tracer activity in slices from the A10 core, per grams of rock.

Slice	Na-22 (Bq/g)	Na-22 2δ (Bq/g)	Cl-36 (Bq/g)	Cl-36 m.u. (Bq/g)	Co-57 (Bq/g)	Co-57 2δ (Bq/g)	Ni-63 (Bq/g)	Ni-63 m.u. (Bq/g)	Ba-133 (Bq/g)	Ba-133 2δ (Bq/g)	Cs-137 (Bq/g)	Cs-137 2δ (Bq/g)
A10.1	1.15E+01	3.90E−01	n.a.		2.12E+03	8.78E+00	n.a.		3.62E+02	1.32E+00	4.75E+03	3.68E+00
A10.2	8.40E+00	4.14E−01	n.a.		<7.54E+00		n.a.		4.98E+01	6.64E−01	6.09E+02	1.70E+00
A10.3	5.84E+00	3.37E−01	n.a.		<2.98E+00		n.a.		9.29E+00	2.51E−01	5.11E+01	4.89E−01
A10.4	5.46E+00	1.74E−01	n.a.		<9.90E−01		n.a.		8.21E−01	5.62E−02	2.56E+00	6.96E−02
A10.5	3.44E+00	1.32E−01	n.a.		<7.02E−01		n.a.		1.09E−01*	3.99E−02	3.11E−01*	3.48E−02
A10.6	2.31E+00	1.19E−01	n.a.		<8.46E−01		n.a.		8.28E−02*	3.80E−02	2.43E−01*	3.50E−02
A10.7	1.19E+00	5.80E−02	n.a.		<4.27E−01		n.a.		<4.30E−02		1.39E−01*	1.76E−02
A10.8	6.93E−01	5.42E−02	n.a.		<4.75E−01		n.a.		<4.22E−02		9.28E−02*	1.88E−02
A10.9	2.82E−01	4.04E−02	n.a.		<4.29E−01		n.a.		<4.22E−02		7.63E−02*	1.70E−02
A10.10	6.80E−02	1.83E−02	n.a.		<1.40E−01		n.a.		<2.48E−02		5.07E−02*	9.85E−03
A10.11	<4.25E−02		n.a.		<2.39E−01		n.a.		<2.65E−02		4.90E−02*	1.04E−02
A10.12	<4.23E−02		n.a.		<2.52E−01		n.a.		<2.49E−02		5.57E−02*	9.77E−03

Slice	Cd-109 (Bq/g)	Cd-109 2δ (Bq/g)	Ag-110m (Bq/g)	Ag-110m 2δ (Bq/g)	Gd-153 (Bq/g)	Gd-153 2δ (Bq/g)	Ra-226 (Bq/g)	Ra-226 2δ (Bq/g)	Np-237 (ng/g)	Np-237 2δ (ng/g)
A10.1	7.81E+03	8.05E+01	1.33E+02	1.13E+01	9.77E+02	3.04E+01	7.98E+01	1.01E+00	n.a.	
A10.2	<7.59E+01		<7.48E+00		<5.19E+01		5.04E+00	4.55E−01	n.a.	
A10.3	<3.26E+01		<6.52E+00		<2.20E+01		<1.46E+00		n.a.	
A10.4	<1.04E+01		<1.25E+00		<6.55E+00		<4.00E−01		n.a.	
A10.5	<8.51E+00		<1.55E+00		<5.40E+00		<3.50E−01		n.a.	
A10.6	<8.83E+00		<1.86E+00		<5.63E+00		<3.73E−01		n.a.	
A10.7	<4.42E+00		<1.00E+00		<2.56E+00		<1.96E−01		n.a.	
A10.8	<4.93E+00		<9.78E−01		<2.88E+00		<2.29E−01		n.a.	
A10.9	<4.62E+00		<8.03E−01		<2.83E+00		<2.12E−01		n.a.	
A10.10	<2.49E+00		<5.92E−01		<1.56E+00		<1.07E−01		n.a.	
A10.11	<2.69E+00		<5.15E−01		<1.69E+00		<1.16E−01		n.a.	
A10.12	<2.62E+00		<4.56E−01		<2.53E+00		<1.03E−01		n.a.	

*Concentration below the background estimated for the crushed core samples (based on measurements of blank sample A20).

Table A2-17. Tracer activity in slices from the A11 core (9B-3), per grams of rock.

Slice	Na-22 (Bq/g)	Na-22 2δ (Bq/g)	Cl-36 (Bq/g)	Cl-36 2δ (Bq/g)	Ni-63 (Bq/g)	Ni-63 2δ (Bq/g)	Ba-133 (Bq/g)	Ba-133 2δ (Bq/g)	Cs-137 (Bq/g)	Cs-137 2δ (Bq/g)
A11.1	9.70E+00	2.80E+00	n.a.		6.50E+03	1.60E+03	2.58E+02	3.80E+01	4.20E+03	6.00E+02
A11.2	6.00E+00	2.60E+00	n.a.		1.10E+01	2.60E+00	2.20E+01	4.00E+00	2.40E+02	3.60E+01
A11.3	5.50E+00	2.00E+00	n.a.		2.20E+00*	6.00E-01	5.20E+00	1.00E+00	2.48E+01	4.20E+00
A11.4	5.00E+00	1.60E+00	n.a		1.37E+00*	3.60E-01	1.03E+00	2.40E-01	2.55E+00	4.80E-01
A11.5	4.40E+00	1.40E+00	n.a.		n.a.		1.00E-01*	6.00E-02	1.90E-01*	6.00E-02
A11.7	2.80E+00	8.00E-01	n.a.		n.a.		3.60E-01*	1.00E-01	4.20E+00	8.00E-01
A11.9	8.40E-01	3.40E-01	n.a.		n.a.		5.80E-01	1.60E-01	8.30E+00	1.40E+00
A11.12	2.30E-01	1.40E-01	n.a		n.a.		<2.30E-02		9.50E-02*	2.40E-02

*Concentration below the background estimated for the crushed core samples (based on measurements of blank sample A20).

Table A2-18. Tracer activity in slices from the A12 core, per grams of rock.

Slice	Na-22 (Bq/g)	Na-22 2δ (Bq/g)	Cl-36 (Bq/g)	Cl-36 m.u. (Bq/g)	Co-57 (Bq/g)	Co-57 2δ (Bq/g)	Ni-63 (Bq/g)	Ni-63 m.u. (Bq/g)	Ba-133 (Bq/g)	Ba-133 2δ (Bq/g)	Cs-137 (Bq/g)	Cs-137 2δ (Bq/g)
A12.1	1.59E+01	1.09E+00	5.89E+00	3.55E−01	2.87E+03	1.40E+01	n.a.		5.81E+02	4.10E+00	7.64E+03	1.32E+01
A12.2	6.13E+00	3.95E−01	1.06E+00	6.64E−02	3.72E+01	3.16E+00	n.a.		3.06E+01	6.02E−01	4.92E+02	1.66E+00
A12.3	4.82E+00	5.75E−01	8.12E−01	5.79E−02	< 1.38E+01		n.a.		1.81E+00	3.39E−01	6.89E+00	3.40E−01
A12.4	5.33E+00	2.44E−01	7.87E−01	4.82E−02	< 1.07E+00		n.a.		2.59E−01**	7.78E−02	9.95E−01**	7.07E−02
A12.5	3.37E+00	2.01E−01	5.47E−01	3.38E−02	9.80E−02**	1.97E−02	n.a.		2.72E−01**	7.49E−02	2.52E+00	9.36E−02
A12.6	1.55E+00	1.51E−01	4.24E−01	2.64E−02	< 1.19E+00		n.a.		< 1.26E−01		1.11E−01**	5.13E−02
A12.7	7.32E−01	7.35E−02	3.39E−01	2.09E−02	< 6.17E−01		n.a.		< 7.32E−02		8.47E−02**	2.83E−02
A12.8	2.27E−01	4.91E−02	2.40E−01	1.49E−02	< 5.43E−01		n.a.		< 6.00E−02		1.12E−01**	2.41E−02
A12.9	< 5.19E−02		1.47E−01	9.07E−03	< 2.57E−01		n.a.		< 2.82E−02		< 2.54E−02	
A12.10	< 5.08E−02		1.08E−01	6.70E−03	< 3.45E−01		n.a.		< 3.50E−02		< 2.91E−02	
A12.11	< 6.29E−02		1.37E−01	8.41E−03	< 2.64E−01		n.a.		< 3.02E−02		< 2.44E−02	
A12.12	< 6.12E−02		1.63E−01	1.00E−02	< 3.98E−01		n.a.		< 3.90E−02		< 3.16E−02	

Slice	Cd-109 (Bq/g)	Cd-109 2δ (Bq/g)	Ag-110m (Bq/g)	Ag-110m 2δ (Bq/g)	Gd-153 (Bq/g)	Gd-153 2δ (Bq/g)	Ra-226 (Bq/g)	Ra-226 2δ (Bq/g)	Np-237 (ng/g)	Np-237 2δ (ng/g)
A12.1	5.22E+03	1.34E+02	2.12E+02	8.43E+00	6.44E+02	2.75E+01	1.30E+02	3.19E+00	n.a.	
A12.2	< 1.68E+02		< 1.95E+01		< 1.03E+02		3.60E+00	4.83E−01	n.a.	
A12.3	< 1.45E+02		< 2.83E+01		< 9.09E+01		< 3.42E+00		n.a.	
A12.4	< 1.42E+01		< 2.46E+00		< 8.35E+00		< 6.96E−01		n.a.	
A12.5	< 1.44E+01		< 2.48E+00		< 8.16E+00		< 6.83E−01		n.a.	
A12.6	< 1.30E+01		< 2.13E+00		< 7.46E+00		< 6.55E−01		n.a.	
A12.7	< 7.43E+00		< 1.75E+00		< 4.14E+00		< 4.02E−01		n.a.	
A12.8	< 6.18E+00		< 1.28E+00		< 3.61E+00		< 3.12E−01		n.a.	
A12.9	< 3.19E+00		< 6.48E−01		< 1.84E+00		< 1.60E−01		n.a.	
A12.10	< 3.37E+00		< 7.16E−01		2.80E+00	9.30E−01	< 1.62E−01		n.a.	
A12.11	< 2.94E+00		< 6.17E−01		< 1.70E+00		< 1.42E−01		n.a.	
A12.12	< 3.79E+00		< 7.74E−01		< 2.15E+00		< 1.78E−01		n.a.	

**Concentration below the background estimated for sliced core samples.

Table A2-19. Tracer activity in slices from the A13 core (9B-3), per grams of rock. Updated with analyses performed 2016-2017.

Slice	Na-22 (Bq/g)	Na-22 2δ (Bq/g)	Cl-36 (Bq/g)	Cl-36 2δ (Bq/g)	Ni-63 (Bq/g)	Ni-63 2δ (Bq/g)	Ba-133 (Bq/g)	Ba-133 2δ (Bq/g)	Cs-137 (Bq/g)	Cs-137 2δ (Bq/g)
A13.1	<2.20E+01		2.70E+00	6.00E-01	1.55E+04	3.80E+03	9.50E+02	1.40E+02	5.40E+03	8.00E+02
A13.2	5.80E+01	2.60E+00	n.a.		4.70E-01*	1.60E-01	1.59E+00	4.80E-01	2.90E+00	8.00E-01
A13.3	5.40E+00	2.20E+00	n.a.		1.32E+00*	3.40E-01	3.60E+00	8.00E-01	4.70E+00	1.00E+00
A13.5	2.90E+00	1.00E+00	4.40E-01	1.00E-01	n.a.		1.00E-01*	6.00E-02	8.70E-01*	2.00E-01
A13.7	3.10E-01	1.40E-01	2.40E-01	6.00E-02	n.a.		5.00E-02*	2.00E-02	7.20E-01*	1.40E-01
A13.9	<2.10E-01		1.02E-01	3.20E-02	n.a.		8.00E-02*	3.60E-02	7.80E-01*	1.60E-01
A13.12	<1.00E-01		5.70E-02	2.60E-02	n.a.		3.50E-02*	1.60E-02	3.70E-01*	8.00E-02

*Concentration below the background estimated for the crushed core samples (based on measurements of blank sample A20).

Table A2-20. Tracer activity in slices from the A15 core, per grams of rock.

Slice	Na-22 (Bq/g)	Na-22 2δ (Bq/g)	Cl-36 (Bq/g)	Cl-36 m.u. (Bq/g)	Co-57 (Bq/g)	Co-57 2δ (Bq/g)	Ni-63 (Bq/g)	Ni-63 m.u. (Bq/g)	Ba-133 (Bq/g)	Ba-133 2δ (Bq/g)	Cs-137 (Bq/g)	Cs-137 2δ (Bq/g)
A15.1	2.40E+01	1.26E+00	n.a.		1.53E+03	1.16E+01	n.a.		5.85E+02	4.31E+00	1.27E+04	1.62E+01
A15.2	5.61E+00	3.44E−01	n.a.		<3.70E+00		n.a.		1.50E+01	3.50E−01	7.77E+01	7.29E−01
A15.3	4.76E+00	3.42E−01	n.a.		<3.37E+00		n.a.		9.30E+00	3.42E−01	4.50E+01	6.19E−01
A15.4	1.57E+01	3.28E−01	n.a.		2.28E+00**	2.95E−01	n.a.		5.28E+00	1.91E−01	9.30E+00	1.78E−01
A15.5	3.26E+00	1.79E−01	n.a.		<1.23E+00		n.a.		<1.00E−01		1.56E−01**	4.24E−02
A15.6	2.39E+00	1.76E−01	n.a.		<9.94E−01		n.a.		<1.22E−01		1.51E−01**	4.91E−02
A15.7	1.61E+00	8.57E−02	n.a.		9.24E−01**	4.91E−02	n.a.		<1.83E−01		1.05E+00**	4.61E−02
A15.8	4.01E−01	5.81E−02	n.a.		<5.52E−01		n.a.		<4.36E−02		7.07E−02**	2.19E−02
A15.9	1.86E−01	5.10E−02	n.a.		<5.72E−01		n.a.		<4.44E−02		1.50E−01**	2.26E−02
A15.10	<1.52E−01		n.a.		<3.56E−01		n.a.		<9.93E−02		<9.00E−02	
A15.11	6.17E−02	2.34E−02	n.a.		<4.00E−01		n.a.		<3.10E−02		<2.43E−02	
A15.12	1.44E−01	2.95E−02	n.a.		<2.83E−01		n.a.		<2.97E−02		5.28E−02**	1.14E−02

Slice	Cd-109 (Bq/g)	Cd-109 2δ (Bq/g)	Ag-110m (Bq/g)	Ag-110m 2δ (Bq/g)	Gd-153 (Bq/g)	Gd-153 2δ (Bq/g)	Ra-226 (Bq/g)	Ra-226 2δ (Bq/g)	Np-237 (ng/g)	Np-237 2δ (ng/g)
A15.1	5.32E+03	1.43E+02	2.12E+02	1.02E+01	8.70E+02	3.03E+01	1.58E+02	3.68E+00	n.a.	
A15.2	<4.92E+01		<6.37E+00		<1.69E+01		<1.52E+00		n.a.	
A15.3	<6.73E+01		<5.01E+00		<2.22E+01		<1.81E+00		n.a.	
A15.4	<2.50E+01		<3.09E+00		<7.14E+00		<7.28E−01		n.a.	
A15.5	<1.11E+01		<3.30E+00		<7.84E+00		<5.64E−01		n.a.	
A15.6	<1.31E+01		<1.30E+00		<1.13E+01		<6.68E−01		n.a.	
A15.7	<1.01E+01		<8.94E−01		<3.60E+00		<2.97E−01		n.a.	
A15.8	<6.60E+00		<1.54E+00		<4.22E+00		<3.47E−01		n.a.	
A15.9	<6.82E+00		<1.57E+00		<4.23E+00		<3.57E−01		n.a.	
A15.10	<5.53E+00		<8.82E−01		<1.58E+00		<1.79E−01		n.a.	
A15.11	<3.92E+00		<6.70E−01		<2.37E+00		<1.69E−01		n.a.	
A15.12	<3.74E+00		<9.94E−01		<2.31E+00		<1.66E−01		n.a.	

**Concentration below the background estimated for sliced core samples.

Table A2-21. Tracer activity in slices from the A16 core, per grams of rock. A layer of epoxy covers 100 % of the first slice.

Slice	Na-22 (Bq/g)	Na-22 2δ (Bq/g)	Cl-36 (Bq/g)	Cl-36 m.u. (Bq/g)	Co-57 (Bq/g)	Co-57 2δ (Bq/g)	Ni-63 (Bq/g)	Ni-63 m.u. (Bq/g)	Ba-133 (Bq/g)	Ba-133 2δ (Bq/g)	Cs-137 (Bq/g)	Cs-137 2δ (Bq/g)
A16.1***	1.49E+01	1.68E+00	5.26E+00	3.19E−01	6.31E+03	2.96E+01	n.a.		6.22E+02	6.49E+00	1.14E+04	2.32E+01
A16.2	1.10E+01	5.01E−01	2.02E+00	1.25E−01	<8.58E+00		n.a.		8.16E+01	8.91E−01	9.41E+02	2.35E+00
A16.3	1.72E+01	6.39E−01	2.20E+00	1.37E−01	<3.73E+00		n.a.		6.55E+00	2.68E−01	7.63E+00	3.66E−01
A16.4	3.74E+00	1.95E−01	4.10E−01	2.64E−02	<1.48E+00		n.a.		7.54E+00	1.48E−01	2.92E+01	2.72E−01
A16.5	3.86E+00	1.99E−01	3.85E−01	2.49E−02	<9.11E−01		n.a.		<1.21E−01		1.32E−01**	5.16E−02
A16.6	2.54E+00	1.51E−01	3.29E−01	2.13E−02	<9.98E−01		n.a.		<1.06E−01		1.94E−01**	4.52E−02
A16.7	1.03E+00	7.59E−02	2.72E−01	1.72E−02	<6.10E−01		n.a.		<6.35E−02		9.38E−02**	2.58E−02
A16.8	4.93E−01	5.63E−02	2.72E−01	1.71E−02	<5.07E−01		n.a.		<5.84E−02		7.69E−02**	2.33E−02
A16.9	2.27E−01	5.05E−02	2.09E−01	1.36E−02	<6.25E−01		n.a.		<6.53E−02		1.19E−01**	2.72E−02
A16.10	8.66E−02	3.11E−02	1.29E−01	8.31E−03	<3.86E−01		n.a.		<3.90E−02		<3.52E−02	
A16.11	<6.60E−02		6.45E−02	4.63E−03	<3.79E−01		n.a.		<4.12E−02		<3.43E−02	
A16.12	<6.64E−02		4.60E−02	3.67E−03	<3.96E−01		n.a.		<4.39E−02		<3.65E−02	

Slice	Cd-109 (Bq/g)	Cd-109 2δ (Bq/g)	Ag-110m (Bq/g)	Ag-110m 2δ (Bq/g)	Gd-153 (Bq/g)	Gd-153 2δ (Bq/g)	Ra-226 (Bq/g)	Ra-226 2δ (Bq/g)	Np-237 (ng/g)	Np-237 2δ (ng/g)
A16.1***	9.68E+03	2.44E+02	4.48E+02	2.08E+01	1.53E+03	5.29E+01	1.88E+02	8.01E+00	n.a.	
A16.2	<9.29E+01		<7.72E+00		<5.89E+01		8.69E+00	6.09E−01	n.a.	
A16.3	<3.83E+01		<7.29E+00		<2.45E+01		<2.02E+00		n.a.	
A16.4	<1.55E+01		<2.95E+00		<9.21E+00		<1.00E−01		n.a.	
A16.5	<1.23E+01		<3.22E+00		<7.39E+00		<6.64E−01		n.a.	
A16.6	<1.04E+01		<2.68E+00		<6.17E+00		<5.78E−01		n.a.	
A16.7	<6.75E+00		<1.49E+00		<3.84E+00		<3.62E−01		n.a.	
A16.8	<6.13E+00		<1.31E+00		<3.57E+00		<3.35E−01		n.a.	
A16.9	<6.79E+00		<1.18E+00		<4.03E+00		<3.78E−01		n.a.	
A16.10	<4.02E+00		<8.17E−01		<2.41E+00		<2.18E−01		n.a.	
A16.11	<4.04E+00		<9.38E−01		<2.37E+00		<2.13E−01		n.a.	
A16.12	<4.33E+00		<1.05E+00		<2.58E+00		<2.15E−01		n.a.	

**Concentration below the background estimated for sliced core samples.

***A layer of epoxy covers 100 % of the first slice.

Table A2-22. Tracer activity in slices from the A17 core, per grams of rock.

Slice	Na-22 (Bq/g)	Na-22 2δ (Bq/g)	Cl-36 (Bq/g)	Cl-36 m.u. (Bq/g)	Co-57 (Bq/g)	Co-57 2δ (Bq/g)	Ni-63 (Bq/g)	Ni-63 m.u. (Bq/g)	Ba-133 (Bq/g)	Ba-133 2δ (Bq/g)	Cs-137 (Bq/g)	Cs-137 2δ (Bq/g)
A17.1	1.26E+01	1.27E+00	5.75E+00	3.18E−01	1.16E+03	1.15E+01	6.89E+03	6.13E+02	3.54E+02	3.91E+00	4.67E+03	1.21E+01
A17.2	8.78E+00	4.32E−01	1.82E+00	1.07E−01	<2.40E+00		1.33E+02	1.21E+01	1.36E+01	4.92E−01	9.61E+01	1.10E+00
A17.3	5.96E+00	3.32E−01	1.16E+00	6.64E−02	<8.36E−01		<4E+00		1.32E+00	1.30E−01	7.19E+00	2.10E−01
A17.4	4.47E+00	3.31E−01	9.08E−01	5.30E−02	<1.21E+00		n.a.		2.75E−01*	1.26E−01	1.02E+00*	1.34E−01
A17.5	4.04E+00	3.46E−01	7.18E−01	4.38E−02	<1.16E+00		n.a.		<3.17E−01		8.11E−01*	1.51E−01
A17.6	3.05E+00	1.90E−01	5.62E−01	3.22E−02	<7.45E−01		n.a.		<1.30E−01		3.63E−01*	8.83E−02
A17.7	4.08E+00	1.91E−01	5.02E−01	2.88E−02	<8.49E−01		n.a.		<1.13E−01		3.16E−01*	5.22E−02
A17.8	1.09E+00	1.09E−01	4.28E−01	2.48E−02	<5.22E−01		n.a.		<1.02E−01		2.26E−01*	4.81E−02
A17.9	6.12E−01	7.08E−02	3.71E−01	3.17E−02	<3.68E−01		n.a.		<8.35E−02		7.73E−02*	3.35E−02
A17.10	1.63E−01	5.16E−02	1.95E−01	1.15E−02	<3.05E−01		n.a.		<7.11E−02		5.65E−02*	2.16E−02
A17.11	1.36E−01	4.91E−02	1.26E−01	8.00E−03	<2.70E−01		n.a.		<7.27E−02		6.21E−02*	2.28E−02
A17.12	<8.59E−02		8.27E−02	5.77E−03	<3.22E−01		n.a.		<7.21E−02		9.19E−02*	2.22E−02

Slice	Cd-109 (Bq/g)	Cd-109 2δ (Bq/g)	Ag-110m (Bq/g)	Ag-110m 2δ (Bq/g)	Gd-153 (Bq/g)	Gd-153 2δ (Bq/g)	Ra-226 (Bq/g)	Ra-226 2δ (Bq/g)	Np-237 (ng/g)	Np-237 2δ (ng/g)
A17.1	8.79E+03	1.41E+02	2.60E+02	1.26E+01	6.47E+02	2.68E+01	5.82E+01	2.76E+00	5.82E+01	5.5E+00
A17.2	<3.31E+01		<4.97E+00		<1.39E+01		<2.50E+00		n.a.	
A17.3	<1.20E+01		<2.21E+00		<5.07E+00		<1.06E+00		n.a.	
A17.4	<1.75E+01		<1.84E+00		<5.88E+00		<1.02E+00		n.a.	
A17.5	<2.00E+01		<2.68E+00		<6.87E+00		<1.22E+00		n.a.	
A17.6	<1.06E+01		<1.39E+00		<3.70E+00		<4.85E−01		n.a.	
A17.7	<1.03E+01		<1.73E+00		<5.06E+00		<3.79E−01		n.a.	
A17.8	<6.98E+00		<7.46E−01		<2.72E+00		<3.98E−01		n.a.	
A17.9	<5.48E+00		<3.20E−01		<2.25E+00		<1.00E+00		n.a.	
A17.10	<4.84E+00		<6.95E−01		<1.60E+00		<1.00E+00		n.a.	
A17.11	<5.02E+00		<4.61E−01		<1.49E+00		<1.00E+00		n.a.	
A17.12	<4.93E+00		<4.50E−01		<1.88E+00		<1.00E+00		n.a.	

*Concentration below the background estimated for the crushed core samples (based on measurements of blank sample A20).

Table A2-23. Tracer activity in slices from the A20 core, per grams of rock.

Slice[3)]	Na-22 (Bq/g)	Na-22 2δ (Bq/g)	Cl-36 (Bq/g)	Cl-36 m.u. (Bq/g)	Co-57 (Bq/g)	Co-57 2δ (Bq/g)	Ni-63 (Bq/g)	Ni-63 m.u. (Bq/g)	Ba-133 (Bq/g)	Ba-133 2δ (Bq/g)	Cs-137 (Bq/g)	Cs-137 2δ (Bq/g)
A20.1	<1.46E−01		<1E−01		<6.58E−01		n.a.		6.31E−02	2.63E−02	6.32E−01	3.40E−02
A20.2	<1.65E−01		<2E−01		<1.15E+00		n.a.		<9.12E−02		1.55E−01	4.24E−02
A20.3	<5.01E−01		<7E−01		<3.05E+00		n.a.		<2.89E−01		7.36E−01	1.36E−01
A20.4	<3.25E−01		<2E−01		<1.40E+00		n.a.		<1.17E−01		4.40E−01	5.31E−02
A20.5	<1.47E−01		<2E−01		<1.36E+00		n.a.		<8.07E−01		2.76E−01	4.59E−02
A20.6	<1.71E−01		<2E−01		<1.27E+00		n.a.		<8.36E−02		1.70E−01	4.07E−02
A20.7	<1.24E−01		<1E−01		<8.53E−01		n.a.		<7.36E−02		1.45E−01	3.13E−02
A20.8	<1.33E−02		<1E−01		<8.07E−01		n.a.		<6.77E−02		1.33E−01	3.15E−02
A20.9	<6.61E−02		<7E−02		1.35E+00	2.68E−01	n.a.		1.23E−01	2.22E−02	1.13E+00	3.36E−02
A20.10	<6.47E−02		<7E−02		<1.40E+00		n.a.		1.35E−01	3.26E−02	1.32E+00	4.30E−02
A20.11	<7.01E−02		<7E−02		2.47E+00	7.28E−01	n.a.		1.95E−01	3.67E−02	1.71E+00	7.07E−02
A20.12	<1.16E−01		<7E−02		<9.31E−01		n.a.		9.75E−02	4.77E−02	2.69E−01	3.94E−02
A20.13	<6.57E−02		<6E−02		<4.10E−01		n.a.		<5.08E−02		2.00E−01	2.12E−02
A20.14	<6.66E−02		<6E−02		<4.74E−01		n.a.		5.99E−02	2.56E−02	2.45E−01	2.30E−02

[3)]Outside the experimental volume.

Table A2-24. Tracer activity in slices from the A20 core, per grams of rock.

Slice[3)]	Cd-109 (Bq/g)	Cd-109 2δ (Bq/g)	Ag-110m (Bq/g)	Ag-110m 2δ (Bq/g)	Gd-153 (Bq/g)	Gd-153 2δ (Bq/g)	Ra-226 (Bq/g)	Ra-226 2δ (Bq/g)	Np-237 (ng/g)	Np-237 2δ (ng/g)
A20.1	< 6.14E+00		< 1.65E+00		< 4.05E+00		< 3.57E−01		n.a.	
A20.2	< 1.10E+01		< 2.66E+00		< 7.71E+00		< 6.22E−01		n.a.	
A20.3	< 3.32E+01		< 9.08E+00		< 2.27E+01		< 1.88E+00		n.a.	
A20.4	< 1.28E+01		< 2.56E+00		< 9.31E+00		< 6.11E−01		n.a.	
A20.5	< 1.29E+01		< 2.95E+00		< 9.38E+00		< 5.66E−01		n.a.	
A20.6	< 1.18E+01		< 1.10E+00		< 8.65E+00		< 5.20E−01		n.a.	
A20.7	< 8.35E+00		< 2.09E+00		< 5.65E+00		< 3.42E−01		n.a.	
A20.8	< 8.34E+00		< 1.99E+00		< 5.71E+00		< 3.48E−01		n.a.	
A20.9	< 4.69E+00		< 8.08E−01		< 3.01E+00		< 1.88E−01		n.a.	
A20.10	< 6.26E+00		< 1.63E+00		< 3.64E+00		< 1.96E−01		n.a.	
A20.11	< 6.70E+00		< 1.66E+00		< 3.83E+00		< 2.04E−01		n.a.	
A20.12	< 1.10E+01		< 2.67E+00		< 9.12E+00		< 1.00E+00		n.a.	
A20.13	< 5.64E+00		< 1.23E+00		< 3.85E+00		< 1.58E−01		n.a.	
A20.14	< 5.78E+00		< 5.22E−01		< 4.01E+00		< 1.63E−01		n.a	

[3)]Outside the experimental volume.

Table A2-25. Tracer activity in slices from the D1 core, per grams of rock.

Slice	Na-22 (Bq/g)	Na-22 2δ (Bq/g)	Cl-36 (Bq/g)	Cl-36 m.u. (Bq/g)	Co-57 (Bq/g)	Co-57 2δ (Bq/g)	Ni-63 (Bq/g)	Ni-63 m.u. (Bq/g)	Ba-133 (Bq/g)	Ba-133 2δ (Bq/g)	Cs-137 (Bq/g)	Cs-137 2δ (Bq/g)
D1.1	4.63E+01	2.49E+00	-		8.39E+02	2.02E+01	5.25E+03	4.68E+02	8.79E+02	6.96E+00	1.21E+04	2.20E+01
D1.2	3.08E+01	1.22E+00	1.48E+00	1.50E−01	<2.76E+00		3.43E+01	3.99E+00	1.49E+01	6.00E−01	1.41E+02	1.43E+00
D1.3	1.90E+01	1.16E+00	9.17E−01	6.40E−02	<3.02E+00		1.21E+01	2.30E+00	1.41E+00	3.85E−01	6.10E+00	4.31E−01
D1.4	1.37E+01	5.12E−01	1.06E+00	8.25E−02	<1.10E+00		n.a.		<2.99E−01		4.71E−01*	1.25E−01
D1.5	8.25E+00	3.98E−01	5.75E−01	3.40E−02	4.41E+00	6.05E−01	n.a.		4.00E−01	1.34E−01	4.45E+00	2.00E−01
D1.6	2.97E+00	6.27E−01	4.58E−01	5.03E−02	<1.04E−01		n.a.		<2.40E−01		5.92E−01*	1.10E−01
D1.7	1.21E+00	1.39E−01	3.04E−01	1.84E−02	<5.25E−01		n.a.		<1.44E−01		6.06E−01*	7.49E−02
D1.8	6.54E−01	1.29E−01	1.77E−01	1.60E−02	<9.85E−01		n.a.		<1.61E−01		7.49E−01*	8.08E−02
D1.9	<2.42E−01		1.51E−01	1.10E−02	<6.40E−01		n.a.		1.84E−01*	7.20E−02	1.10E+00*	8.86E−02
D1.10	1.03E−01	4.95E−02	1.07E−01	8.28E−03	<3.59E−01		n.a.		<7.53E−02		1.94E−01*	3.52E−02
D1.11	<1.43E−01		8.54E−02	5.91E−03	<6.19E−01		n.a.		<9.50E−02		1.89E−01*	4.18E−02
D1.12	<1.37E−01		7.78E−02	8.03E−03	<6.65E−01		n.a.		1.38E−01	5.37E−02	6.91E−01*	5.67E−02

Slice	Cd-109 (Bq/g)	Cd-109 2δ (Bq/g)	Ag-110m (Bq/g)	Ag-110m 2δ (Bq/g)	Gd-153 (Bq/g)	Gd-153 2δ (Bq/g)	Ra-226 (Bq/g)	Ra-226 2δ (Bq/g)	Np-237 (ng/g)	Np-237 2δ (ng/g)
D1.1	4.14E+03	1.89E+02	<4.20E+01		5.71E+02	4.27E+01	1.80E+02	8.14E+00	1.70E+01	1.6E+00
D1.2	<3.94E+01		<6.73E+00		<1.59E+01		<2.93E+00		n.a.	
D1.3	<4.04E+01		<6.18E+00		<1.37E+01		<3.91E+00		n.a.	
D1.4	<1.84E+01		<1.94E+00		<6.38E+00		<1.04E+00		n.a.	
D1.5	<1.67E+01		<2.70E+00		<6.15E+00		<9.64E−01		n.a.	
D1.6	<1.54E+01		<2.94E+00		<5.67E+00		<9.22E−01		n.a.	
D1.7	<9.58E+00		<1.32E+00		<2.93E+00		<5.44E−01		n.a.	
D1.8	<1.27E+01		<2.47E+00		<5.34E+00		<5.75E−01		n.a.	
D1.9	<9.80E+00		<1.36E+00		<3.61E+00		<5.70E−01		n.a.	
D1.10	<5.23E+00		<7.44E−01		<1.93E+00		<1.00E+00		n.a.	
D1.11	<7.83E+00		<1.52E+00		<3.19E+00		<2.37E−01		n.a.	
D1.12	<8.36E+00		<1.16E+00		<3.44E+00		<2.51E−01		n.a.	

*Concentration below the background estimated for the crushed core samples (based on measurements of blank sample A20).

Table A2-26. Tracer activity in slices from the D5 core, per grams of rock.

Slice	Na-22 (Bq/g)	Na-22 2δ (Bq/g)	Cl-36 (Bq/g)	Cl-36 m.u. (Bq/g)	Co-57 (Bq/g)	Co-57 2δ (Bq/g)	Ni-63 (Bq/g)	Ni-63 m.u. (Bq/g)	Ba-133 (Bq/g)	Ba-133 2δ (Bq/g)	Cs-137 (Bq/g)	Cs-137 2δ (Bq/g)
D5.1	5.85E+01	2.17E+00	n.a.		2.18E+03	1.47E+01	n.a.		6.97E+02	5.08E+00	9.11E+03	1.63E+01
D5.2	2.02E+01	5.53E−01	n.a.		<5.10E+00		n.a.		2.77E+01	4.57E−01	3.14E+02	1.15E+00
D5.3	1.52E+01	6.18E−01	n.a.		<4.10E+00		n.a.		3.06E+00	2.51E−01	2.64E+01	4.38E−01
D5.4	4.21E+00	7.60E−02	n.a.		5.54E−01**	6.36E−02	n.a.		5.31E−01	2.18E−02	1.71E+00	3.21E−02
D5.5	9.06E+00	3.00E−01	n.a.		<1.49E+00		n.a.		<1.60E−01		3.77E−01**	6.45E−02
D5.6	5.06E+00	2.57E−01	n.a.		<2.04E+00		n.a.		<1.64E−01		<1.48E−01	
D5.7	1.76E+00	3.35E−02	n.a.		9.87E−02**	2.82E−02	n.a.		2.34E−01**	1.02E−02	1.30E+00	1.86E−02
D5.8	8.83E−01	8.01E−02	n.a.		<5.59E−01		n.a.		<7.31E−02		<6.16E−02	
D5.9	2.89E−01	7.08E−02	n.a.		<7.99E−01		n.a.		<7.79E−02		<6.77E−02	
D5.10	1.48E−02	4.81E−03	n.a.		<2.94E−02		n.a.		<6.50E−03		<6.06E−03	
D5.11	<7.31E−02		n.a.		<4.55E−01		n.a.		<4.61E−02		<3.45E−02	
D5.12	<6.87E−02		n.a.		<4.21E−01		n.a.		<4.47E−02		3.70E−02	

Slice	Cd-109 (Bq/g)	Cd-109 2δ (Bq/g)	Ag-110m (Bq/g)	Ag-110m 2δ (Bq/g)	Gd-153 (Bq/g)	Gd-153 2δ (Bq/g)	Ra-226 (Bq/g)	Ra-226 2δ (Bq/g)	Np-237 (ng/g)	Np-237 2δ (ng/g)
D5.1	3.76E+03	1.50E+02	<3.10E+01		3.58E+02	3.17E+01	1.41E+02	5.88E+00	n.a.	
D5.2	<5.21E+01		<6.64E+00		<3.44E+01		1.65E+00	3.15E−01	n.a.	
D5.3	<4.03E+01		<9.23E+00		<2.69E+01		<2.16E+00		n.a.	
D5.4	3.90E+00	9.11E−01	<2.62E−01		<6.22E−01		<8.42E−01		n.a.	
D5.5	<1.52E+01		<3.18E+00		<9.22E+00		<6.87E−01		n.a.	
D5.6	<1.68E+01		<4.52E+00		<3.61E−01		<8.22E−01		n.a.	
D5.7	1.71E+00	4.50E−01	<7.72E−02		<3.12E−01		<3.90E−01		n.a.	
D5.8	<7.67E+00		<1.60E+00		<4.23E+00		<3.79E−01		n.a.	
D5.9	<8.63E+00		<1.81E+00		<4.80E+00		<4.35E−01		n.a.	
D5.10	<4.45E−01		<4.73E−02		<1.61E−01		<1.95E−01		n.a.	
D5.11	<4.61E+00		<1.09E+00		<2.77E+00		<2.12E−01		n.a.	
D5.12	<4.36E+00		<9.37E−01		<2.63E+00		<2.00E−01		n.a.	

**Concentration below the background estimated for sliced core samples.

Table A2-27. Tracer activity in slices from the D6 core, per grams of rock.

Slice	Na-22 (Bq/g)	Na-22 2δ (Bq/g)	Cl-36 (Bq/g)	Cl-36 m.u. (Bq/g)	Co-57 (Bq/g)	Co-57 2δ (Bq/g)	Ni-63 (Bq/g)	Ni-63 m.u. (Bq/g)	Ba-133 (Bq/g)	Ba-133 2δ (Bq/g)	Cs-137 (Bq/g)	Cs-137 2δ (Bq/g)
D6.1	2.66E+01	6.93E−01	n.a.		2.19E+03	1.28E+01	3.66E+03	3.26E+02	5.47E+02	2.04E+00	6.78E+03	5.29E+00
D6.2	2.13E+01	1.02E+00	n.a.		< 9.13E+00		2.91E+01	3.59E+00	2.36E+01	7.28E−01	2.71E+02	1.82E+00
D6.3	1.83E+01	1.30E+00	n.a.		1.16E+01	5.61E+00	< 8E+00		3.43E+00	6.31E−01	4.58E+01	1.07E+00
D6.4	8.79E+00	3.68E−01	n.a.		< 2.55E+00		< 4E+00		< 2.62E−01		1.73E+00	1.19E−01
D6.5	1.39E+01	4.17E−01	n.a.		< 2.41E+00		6.19E+00*	7.30E−01	< 2.59E−01		4.64E+00	1.50E−01
D6.6	5.07E+00	2.53E−01	n.a.		< 1.96E+00		n.a.		< 1.94E−01		3.58E−01*	7.54E−02
D6.7	2.67E+00	1.68E−01	n.a.		< 1.49E+00		n.a.		< 1.63E−01		1.15E+00*	7.59E−02
D6.8	1.05E+00	1.22E−01	n.a.		< 1.36E+00		n.a.		2.25E−01*	< 7.06E−02	4.94E+00	1.91E−01
D6.9	4.17E−01	1.02E−01	n.a.		< 1.30E+00		n.a.		< 1.35E−01		2.58E+00	1.44E−01
D6.10	< 1.53E−01		n.a.		< 1.04E+00		n.a.		< 1.42E−01		4.06E−01*	5.16E−02
D6.11	< 1.90E−01		n.a.		< 1.44E+00		n.a.		< 1.56E−01		2.98E−01*	5.52E−02
D6.12	< 1.24E−01		n.a.		< 1.18E+00		n.a.		< 1.28E−01		1.64E−01*	4.44E−02

Slice	Cd-109 (Bq/g)	Cd-109 2δ (Bq/g)	Ag-110m (Bq/g)	Ag-110m 2δ (Bq/g)	Gd-153 (Bq/g)	Gd-153 2δ (Bq/g)	Ra-226 (Bq/g)	Ra-226 2δ (Bq/g)	Np-237 (ng/g)	Np-237 2δ (ng/g)
D6.1	3.44E+03	1.16E+02	< 1.47E+01		1.41E+02	6.85E+01	1.14E+02	1.56E+00	1.76E+01	1.7E+00
D6.2	< 9.74E+01		< 1.50E+01		< 5.62E+01		< 3.58E+00		n.a.	
D6.3	< 1.23E+02		< 2.82E+01		< 7.12E+01		< 6.20E+00		n.a.	
D6.4	< 2.47E+01		< 5.07E+00		< 1.63E+01		< 1.00E+00		n.a.	
D6.5	< 2.32E+01		< 5.55E+00		< 1.57E+01		< 8.71E−01		n.a.	
D6.6	< 1.91E+01		< 4.52E+00		< 1.24E+01		< 7.86E−01		n.a.	
D6.7	< 1.57E+01		< 2.26E+00		< 9.48E+00		< 5.74E−01		n.a.	
D6.8	< 1.47E+01		< 6.98E+00		< 8.81E+00		< 5.26E−01		n.a.	
D6.9	< 1.39E+01		< 2.81E+00		< 8.60E+00		< 5.15E−01		n.a.	
D6.10	< 1.39E+01		< 2.89E+00		< 1.01E+01		< 1.00E+00		n.a.	
D6.11	< 1.58E+01		< 3.03E+00		< 1.15E+01		< 1.00E+00		n.a.	
D6.12	< 1.27E+01		< 1.80E+00		< 9.47E+00		< 1.00E+00		n.a.	

*Concentration below the background estimated for the crushed core samples (based on measurements of blank sample A20).

Table A2-28. Tracer activity in slices from the D7 core, per grams of rock.

Slice	Na-22 (Bq/g)	Na-22 2δ (Bq/g)	Cl-36 (Bq/g)	Cl-36 m.u. (Bq/g)	Co-57 (Bq/g)	Co-57 2δ (Bq/g)	Ni-63 (Bq/g)	Ni-63 m.u. (Bq/g)	Ba-133 (Bq/g)	Ba-133 2δ (Bq/g)	Cs-137 (Bq/g)	Cs-137 2δ (Bq/g)
D7.1	2.26E+01	1.16E+00	6.08E−01	3.73E−02	2.66E+03	1.29E+01	n.a.		6.67E+02	3.87E+00	6.60E+03	1.13E+01
D7.2	2.04E+01	6.88E−01	−		5.48E+01	6.12E+00	n.a.		1.39E+02	1.30E+00	2.10E+03	3.76E+00
D7.3	1.84E+01	6.37E−01	6.63E−01	4.30E−02	1.38E+01	3.36E+00	n.a.		1.51E+01	5.58E−01	5.21E+02	1.81E+00
D7.4	2.20E+01	4.63E−01	4.38E−01	2.74E−02	6.06E+00	8.81E−01	n.a.		6.36E−01	1.14E−01	2.20E+01	2.98E−01
D7.5	1.49E+01	3.67E−01	5.14E−01	3.18E−02	1.83E+00**	6.95E−01	n.a.		<1.57E−01		5.39E−01**	6.55E−02
D7.6	9.84E+00	3.02E−01	3.90E−01	2.44E−02	<1.36E+00		n.a.		<1.46E−01		2.10E−01**	5.83E−02
D7.7	4.51E+00	1.57E−01	3.58E−01	2.21E−02	<5.23E−01		n.a.		<8.29E−02		7.18E−02**	2.93E−02
D7.8	1.90E+00	1.13E−01	3.08E−01	1.91E−02	<6.01E−01		n.a.		<7.43E−02		<6.12E−02	
D7.9	6.47E−01	7.60E−02	3.57E−01	2.19E−02	<6.07E−01		n.a.		<6.91E−02		5.64E−02**	2.74E−02
D7.10	1.25E−01	3.12E−02	4.26E−01	2.58E−02	<3.66E−01		n.a.		<3.53E−02		<3.24E−02	
D7.11	<6.32E−02		2.89E−01	1.76E−02	<3.71E−01		n.a.		<3.14E−02		<3.30E−02	
D7.12	<5.80E−02		2.55E−01	1.56E−02	<3.07E−01		n.a.		<3.72E−02		<3.18E−02	

Slice	Cd-109 (Bq/g)	Cd-109 2δ (Bq/g)	Ag-110m (Bq/g)	Ag-110m 2δ (Bq/g)	Gd-153 (Bq/g)	Gd-153 2δ (Bq/g)	Ra-226 (Bq/g)	Ra-226 2δ (Bq/g)	Np-237 (ng/g)	Np-237 2δ (ng/g)
D7.1	4.61E+03	1.16E+02	<2.95E+01		2.66E+02	2.43E+01	1.08E+02	4.46E+00	n.a.	
D7.2	<1.33E+02		<8.89E+00		<8.47E+01		6.57E+00	8.09E−01	n.a.	
D7.3	<6.89E+01		<8.72E+00		<4.35E+01		<2.04E+00		n.a.	
D7.4	<1.88E+01		<3.76E+00		1.19E+01	3.49E+00	<7.38E−01		n.a.	
D7.5	<1.49E+01		<3.34E+00		<8.96E+00		<6.65E−01		n.a.	
D7.6	<1.40E+01		<2.64E+00		<8.30E+00		<6.59E−01		n.a.	
D7.7	<8.31E+00		<1.84E+00		<5.73E+00		<4.06E−01		n.a.	
D7.8	<8.26E+00		<1.33E+00		<5.61E+00		<4.23E−01		n.a.	
D7.9	<7.54E+00		3.18E+00	1.43E+00	<5.25E+00		<3.95E−01		n.a.	
D7.10	<3.89E+00		<7.27E−01		<2.34E+00		<1.89E−01		n.a.	
D7.11	<3.80E+00		<7.39E−01		<2.33E+00		<1.99E−01		n.a.	
D7.12	<3.64E+00		<7.29E−01		<2.20E+00		<1.94E−01		n.a.	

**Concentration below the background estimated for sliced core samples.

Table A2-29. Tracer activity in slices from the D8 core, per grams of rock.

Slice	Na-22 (Bq/g)	Na-22 2δ (Bq/g)	Cl-36 (Bq/g)	Cl-36 m.u. (Bq/g)	Co-57 (Bq/g)	Co-57 2δ (Bq/g)	Ni-63 (Bq/g)	Ni-63 m.u. (Bq/g)	Ba-133 (Bq/g)	Ba-133 2δ (Bq/g)	Cs-137 (Bq/g)	Cs-137 2δ (Bq/g)
D8.1	3.07E+01	6.99E−01	n.a.		3.02E+03	1.29E+01	n.a.		4.79E+02	1.92E+00	8.21E+03	5.46E+00
D8.2	1.88E+01	4.79E−01	n.a.		<3.60E+00		n.a.		2.86E+00	1.79E−01	4.27E+01	3.87E−01
D8.3	2.64E+01	6.05E−01	n.a.		<7.19E+00		n.a.		4.91E+01	5.96E−01	5.42E+02	1.47E+00
D8.4	1.35E+01	4.15E−01	n.a.		<3.27E+00		n.a.		2.33E−01**	1.08E−01	1.14E+00**	9.64E−02
D8.5	7.42E+00	2.38E−01	n.a.		<1.33E+00		n.a.		1.70E−01**	6.10E−02	1.66E−01**	4.93E−02
D8.6	3.52E+00	1.78E−01	n.a.		<2.68E+00		n.a.		<1.17E−01		2.02E−01**	5.13E−02
D8.7	9.33E−01	7.46E−02	n.a.		<7.48E−01		n.a.		<5.59E−02		1.14E−01**	2.40E−02
D8.8	3.64E−01	6.69E−02	n.a.		<8.13E−01		n.a.		<5.76E−02		2.36E−01**	5.83E−02
D8.9	1.29E−01	4.79E−02	n.a.		<7.14E−01		n.a.		<5.16E−02		1.39E−01**	2.45E−02
D8.10	7.51E−02	3.65E−02	n.a.		<5.27E−01		n.a.		<4.61E−02		<3.85E−02	
D8.11	<7.64E−02		n.a.		<5.41E−01		n.a.		<4.69E−02		<3.95E−02	
D8.12	<6.93E−02		n.a.		<5.12E−01		n.a.		<4.11E−02		<3.48E−02	

Slice	Cd-109 (Bq/g)	Cd-109 2δ (Bq/g)	Ag-110m (Bq/g)	Ag-110m 2δ (Bq/g)	Gd-153 (Bq/g)	Gd-153 2δ (Bq/g)	Ra-226 (Bq/g)	Ra-226 2δ (Bq/g)	Np-237 (ng/g)	Np-237 2δ (ng/g)
D8.1	3.89E+03	1.12E+02	<1.12E+01		2.90E+02	6.95E+01	1.20E+02	1.54E+00	n.a.	
D8.2	<2.86E+01		<6.20E+00		<2.00E+01		<1.09E+00		n.a.	
D8.3	<7.10E+01		<7.51E+00		<4.81E+01		3.18E+00	4.08E−01	n.a.	
D8.4	<2.18E+01		<5.02E+00		<1.44E+01		<1.27E+00		n.a.	
D8.5	<1.29E+01		<2.67E+00		<8.45E+00		<8.53E−01		n.a.	
D8.6	<1.31E+01		<3.53E+00		<1.14E+01		<5.09E−01		n.a.	
D8.7	<7.35E+00		<1.84E+00		<6.66E+00		<5.40E−01		n.a.	
D8.8	<8.08E+00		<1.87E+00		<4.95E+00		<3.38E−01		n.a.	
D8.9	<7.32E+00		<1.78E+00		<4.47E+00		<3.72E−01		n.a.	
D8.10	<5.23E+00		<9.76E−01		<3.61E+00		<3.41E−01		n.a.	
D8.11	<5.34E+00		<1.33E+00		<3.65E+00		<2.18E−01		n.a.	
D8.12	<4.72E+00		<1.01E+00		3.21E+00	9.65E−01	<2.25E−01		n.a.	

**Concentration below the background estimated for sliced core samples.

Table A2-30. Tracer activity in slices from the D12 core, per grams of rock.

Slice	Na-22 (Bq/g)	Na-22 2δ (Bq/g)	Cl-36 (Bq/g)	Cl-36 m.u. (Bq/g)	Co-57 (Bq/g)	Co-57 2δ (Bq/g)	Ni-63 (Bq/g)	Ni-63 m.u. (Bq/g)	Ba-133 (Bq/g)	Ba-133 2δ (Bq/g)	Cs-137 (Bq/g)	Cs-137 2δ (Bq/g)
D12.1	2.25E+01	1.03E+00	n.a.		5.13E+03	2.69E+01	6.72E+03	5.99E+02	9.97E+02	4.14E+00	1.65E+04	1.41E+01
D12.2	1.88E+01	9.72E−01	n.a.		7.43E+01	8.05E+00	2.53E+02	2.39E+01	9.64E+01	1.46E+00	1.17E+03	4.17E+00
D12.3	1.52E+01	6.70E−01	n.a.		1.71E+01	3.29E+00	3.71E+01	4.41E+00	2.05E+01	5.72E−01	2.69E+02	1.57E+00
D12.4	1.40E+01	4.91E−01	n.a.		7.00E+00	1.76E+00	1.32E+01	1.31E+00	2.21E−00	2.14E−01	3.41E+01	4.85E−01
D12.5	1.41E+01	5.56E−01	n.a.		<3.68E+00		8.61E+00	9.11E−01	<3.30E−01		9.79E−01*	1.42E−01
D12.6	9.65E+00	4.72E−01	n.a.		<3.93E+00		n.a.		<3.54E−01		5.62E−01*	1.39E−01
D12.7	7.31E+00	2.58E−01	n.a.		<1.60E+00		n.a.		<1.79E−01		3.04E−01*	6.13E−02
D12.8	3.71E+00	1.97E−01	n.a.		<1.62E+00		n.a.		<1.94E−01		1.96E−01*	6.09E−02
D12.9	1.74E+00	1.32E−01	n.a.		<1.32E+00		n.a.		<1.46E−01		2.27E−01*	5.25E−02
D12.10	7.00E−01	9.14E−02	n.a.		<1.29E+00		n.a.		<1.38E−01		1.17E−01*	4.74E−02
D12.11	<1.87E−01		n.a.		<1.43E+00		n.a.		<1.78E−01		7.28E−01*	7.05E−02
D12.12	<1.55E−01		n.a.		<1.38E+00		n.a.		<1.53E−01		2.27E−01*	5.49E−02

Slice	Cd-109 (Bq/g)	Cd-109 2δ (Bq/g)	Ag-110m (Bq/g)	Ag-110m 2δ (Bq/g)	Gd-153 (Bq/g)	Gd-153 2δ (Bq/g)	Ra-226 (Bq/g)	Ra-226 2δ (Bq/g)	Np-237 (ng/g)	Np-237 2δ (ng/g)
D12.1	1.06E+04	2.47E+02	<3.41E+01		<2.86E+02		2.37E+02	3.30E+00	2.45E+01	2.3E+00
D12.2	<1.70E+02		<1.86E+01		<9.89E+01		9.18E+00	2.27E+00	n.a.	
D12.3	<7.29E+01		<9.88E+00		<4.23E+01		<2.29E+00		n.a.	
D12.4	<3.47E+01		<5.63E+00		<2.21E+01		<1.21E+00		n.a.	
D12.5	<3.53E+01		<1.01E+01		<2.38E+01		<1.41E000		n.a.	
D12.6	<3.64E+01		<7.40E+00		<2.49E+01		<1.48E+00		n.a.	
D12.7	<1.73E+01		<3.18E+00		<1.05E+01		<5.78E−01		n.a.	
D12.8	<1.75E+01		<2.25E+00		<1.03E+01		1.33E+00	1.12E−01	n.a.	
D12.9	<1.40E+01		<2.57E+00		<8.41E+00		<1.00E+00		n.a.	
D12.10	<1.37E+01		<2.68E+00		<1.04E+01		<1.00E+00		n.a.	
D12.11	<1.75E+01		<3.20E+00		<1.33E+01		<1.00E+00		n.a.	
D12.12	<1.55E+01		<2.96E+00		<1.20E+01		<1.00E+00		n.a.	

*Concentration below the background estimated for the crushed core samples (based on measurements of blank sample A20).

Table A2-31. Tracer activity in slices from the D13 core, per grams of rock.

Slice	Na-22 (Bq/g)	Na-22 2δ (Bq/g)	Cl-36 (Bq/g)	Cl-36 m.u. (Bq/g)	Co-57 (Bq/g)	Co-57 2δ (Bq/g)	Ni-63 (Bq/g)	Ni-63 m.u. (Bq/g)	Ba-133 (Bq/g)	Ba-133 2δ (Bq/g)	Cs-137 (Bq/g)	Cs-137 2δ (Bq/g)
D13.1	2.58E+01	2.28E+00	8.74E−01	5.21E−02	1.45E+03	1.93E+01	6.41E+03	5.71E+02	8.16E+02	7.89E+00	9.29E+03	2.43E+01
D13.2	n.a		n.a		n.a		3.28E+03	3.04E+01	n.a		n.a	
D13.3	1.87E+01	1.67E+00	5.44E−01	6.50E−02	1.38E+01	3.83E+00	7.44E+01	7.39E+00	5.14E+01	1.61E+00	6.84E+02	4.80E+00
D13.4	1.65E+01	6.29E−01	6.31E−01	3.72E−02	<3.42E+00		1.60E+01	1.54E+00	9.83E+00	4.28E−01	2.66E+02	1.65E+00
D13.5	1.38E+01	5.09E−01	6.90E−01	4.10E−02	<1.42E+00		7.01E+00**	8.15E−01	4.13E−01	1.42E−01	8.81E+00	2.68E−01
D13.6	1.06E+01	4.33E−01	5.74E−01	3.20E−02	<1.19E+00		n.a		<2.72E−01		1.17E+00**	1.29E−01
D13.7	6.69E+00	2.90E−01	5.12E−01	2.96E−02	<7.76E−01		n.a		<1.85E−01		6.77E−01**	8.35E−02
D13.8	3.56E+00	2.60E−01	5.09E−01	3.00E−02	<9.22E−01		n.a		<2.14E−01		1.01E+00**	1.13E−01
D13.9	1.16E+00	8.75E−02	2.86E−01	1.66E−02	<3.54E−01		n.a		9.32E−02**	3.49E−02	7.18E−01**	4.60E−02
D13.10	1.63E−01	4.82E−02	1.61E−01	1.01E−02	<3.92E−01		n.a		<7.00E−02		3.05E−01**	3.51E−02
D13.11	<8.19E−02		1.77E−01	1.13E−02	<6.12E−01		n.a		<5.15E−02		2.04E−01**	2.69E−02
D13.12	9.05E−02[2)]	4.12E−02	2.75E−01	1.59E−02	<3.14E−01		n.a		1.08E−01**	3.96E−02	3.20E−01**	2.01E−02

Slice	Cd-109 (Bq/g)	Cd-109 2δ (Bq/g)	Ag-110m (Bq/g)	Ag-110m 2δ (Bq/g)	Gd-153 (Bq/g)	Gd-153 2δ (Bq/g)	Ra-226 (Bq/g)	Ra-226 2δ (Bq/g)	Np-237 (ng/g)	Np-237 2δ (ng/g)
D13.1	8.55E+03	2.31E+02	<5.02E+01		4.54E+02	4.75E+01	1.59E+02	1.01E+01	2.31E+01	2.2E+00
D13.2	n.a		n.a		n.a		n.a		n.a.	
D13.3	<9.84E+01		<1.26E+01		<4.28E+01		<6.83E+00		n.a.	
D13.4	<3.98E+01		<5.34E+00		<1.71E+01		1.19E+00	4.22E−01	n.a.	
D13.5	<1.89E+01		<2.06E+00		<7.05E+00		<1.02E+00		n.a.	
D13.6	<1.72E+01		<1.25E+00		<5.02E+00		<9.39E−01		n.a.	
D13.7	<1.19E+01		<6.96E+00		<4.41E+00		<6.42E−01		n.a.	
D13.8	<1.45E+01		<1.53E+00		<4.86E+00		<7.94E−01		n.a.	
D13.9	<4.94E+00		<5.57E−01		<1.79E+00		<2.69E−01		n.a.	
D13.10	<5.30E+00		<9.91E−01		<2.28E+00		<2.48E−01		n.a.	
D13.11	<7.11E+00		<1.57E+00		<3.42E+00		<2.89E−01		n.a.	
D13.12	<5.26E+00		<9.51E−01		<1.96E+00		<1.00E+00		n.a.	

**Concentration below the background estimated for sliced core samples.

2)Re-analysed after leaching, excluding wash liquid

Table A2-32. Tracer activity in slices from the D14 core, per grams of rock.

Slice	Na-22 (Bq/g)	Na-22 2δ (Bq/g)	Cl-36 (Bq/g)	Cl-36 m.u. (Bq/g)	Co-57 (Bq/g)	Co-57 2δ (Bq/g)	Ni-63 (Bq/g)	Ni-63 m.u. (Bq/g)	Ba-133 (Bq/g)	Ba-133 2δ (Bq/g)	Cs-137 (Bq/g)	Cs-137 2δ (Bq/g)
D14.1***	1.59E+01	8.11E−01	5.13E+00	3.09E−01	5.25E+03	1.40E+01	n.a.		4.10E+02	2.65E+00	5.90E+03	8.80E+00
D14.2	2.00E+01	7.14E−01	1.17E+00	7.67E−02	1.11E+02	1.78E+01	n.a.		7.53E+01	9.23E−01	8.34E+02	2.40E+00
D14.3	1.87E+01	7.04E−01	1.06E+00	7.05E−02	<1.94E+01		n.a.		2.18E+01	5.03E−01	1.70E+02	1.12E+00
D14.4	1.94E+01	4.02E−01	7.79E−01	4.82E−02	6.30E+00	7.77E−01	n.a.		1.85E+00	1.09E−01	2.66E+02	4.11E+00
D14.5	1.46E+01	3.64E−01	8.70E−01	5.37E−02	3.74E+00	7.12E−01	n.a.		<1.72E−01		1.86E−01**	6.39E−02
D14.6	9.09E+00	2.94E−01	6.73E−01	4.19E−02	<2.80E+00		n.a.		<1.56E−01		2.02E−01**	5.84E−02
D14.7	3.89E+00	1.57E−01	7.34E−01	4.51E−02	<1.23E+00		n.a.		<1.04E−01		1.31E−01**	3.94E−02
D14.8	1.57E+00	9.94E−02	5.89E−01	3.63E−02	<8.73E−01		n.a.		<7.21E−02		9.50E−02**	3.20E−02
D14.9	<1.77E−01		5.48E−01	3.38E−02	<1.24E+00		n.a.		<7.30E−02		8.99E−02**	1.76E−02
D14.10	<6.21E−02		2.90E−01	1.77E−02	<3.87E−01		n.a.		<3.15E−02		<2.59E−02	
D14.11	<5.37E−02		3.43E−01	2.10E−02	<1.09E+00		n.a.		<3.54E−02		2.90E−02**	1.23E−02
D14.12	1.03E−01	2.61E−02	4.00E−01	2.43E−02	<2.92E−01		n.a.		<3.58E−02		<2.95E−02	

Slice	Cd-109 (Bq/g)	Cd-109 2δ (Bq/g)	Ag-110m (Bq/g)	Ag-110m 2δ (Bq/g)	Gd-153 (Bq/g)	Gd-153 2δ (Bq/g)	Ra-226 (Bq/g)	Ra-226 2δ (Bq/g)	Np-237 (ng/g)	Np-237 2δ (ng/g)
D14.1***	2.87E+03	9.33E+01	5.19E+01	4.66E+00	4.40E+02	2.06E+01	9.74E+01	2.10E+00	n.a.	
D14.2	<2.50E+02		<1.27E+01		<1.88E+02		6.98E+00	9.59E−01	n.a.	
D14.3	<1.51E+02		<1.12E+01		<1.14E+02		<2.36E+00		n.a.	
D14.4	<1.61E+01		<3.04E+00		<9.65E+00		<6.31E−01		n.a.	
D14.5	<1.54E+01		<4.51E+00		<9.07E+00		<6.85E−01		n.a.	
D14.6	<1.41E+01		<3.34E+00		<8.46E+00		<6.73E−01		n.a.	
D14.7	<1.04E+01		<1.14E+00		<6.08E+00		<4.90E−01		n.a.	
D14.8	<8.27E+00		<1.26E+00		<4.90E+00		<4.09E−01		n.a.	
D14.9	<7.72E+00		<1.61E+00		<1.73E−01		<3.87E−01		n.a.	
D14.10	<3.08E+00		<5.03E−01		<1.79E+00		<1.48E−01		n.a.	
D14.11	<3.40E+00		<6.79E−01		<3.80E+00		<1.66E−01		n.a.	
D14.12	<3.43E+00		<7.50E−01		<2.03E+00		<1.66E−01		n.a.	

**Concentration below the background estimated for sliced core samples.

***A layer of epoxy covers 100 % of the first slice.

Table A2-33. Tracer activity in slices from the D15 core (9B-3), per grams of rock.

Slice	Na-22 (Bq/g)	Na-22 2δ (Bq/g)	Cl-36 (Bq/g)	Cl-36 2δ (Bq/g)	Ni-63 (Bq/g)	Ni-63 2δ (Bq/g)	Ba-133 (Bq/g)	Ba-133 2δ (Bq/g)	Cs-137 (Bq/g)	Cs-137 2δ (Bq/g)
D15.1	<3.20E+01		7.10E−01	2.00E−01	2.60E+03	6.00E+02	6.70E+02	1.20E+02	1.11E+04	1.60E+03
D15.2	1.60E+01	6.00E+00	n.a.		2.20E+02	6.00E+01	4.80E+01	8.00E+00	7.50E+02	1.20E+02
D15.3	1.02E+01	3.00E+00	2.60E−01	6.00E−02	n.a		7.00E+00	1.40E+00	1.07E+02	1.60E+01
D15.5	7.17E+00	1.58E+00	2.00E−01	6.00E−02	n.a.		6.50E−02*	3.20E−02	6.80E−01*	1.40E−01
D15.7	1.53E+00	0.46E−01	2.10E−01	6.00E−02	n.a.		4.10E−01	2.60E−02	5.20E−01*	1.00E−01
D15.9	<2.20E−01		1.73E−01	4.60E−02	n.a.		1.09E−01*	4.00E−02	9.60E−01*	1.80E−01
D15.12	<8.20E−02		8.10E−02	3.20E−02	n.a.		3.50E−02*	1.40E−02	3.50E−01*	6.00E−02

*Concentration below the background estimated for the crushed core samples (based on measurements of blank sample A20).

Table A2-34. Tracer activity in slices from the D16 core (9B-3), per grams of rock.

Slice	Na-22 (Bq/g)	Na-22 2δ (Bq/g)	Cl-36 (Bq/g)	Cl-36 2δ (Bq/g)	Ni-63 (Bq/g)	Ni-63 2δ (Bq/g)	Ba-133 (Bq/g)	Ba-133 2δ (Bq/g)	Cs-137 (Bq/g)	Cs-137 2δ (Bq/g)
D16.1	<7.60E+01		n.a.		6.40E+03	1.60E+03	1.20E+03	2.00E+02	1.24E+04	1.80E+03
D16.2	1.92E+01	4.60E+00	n.a.		9.60E+01	2.40E+01	3.10E+01	6.00E−00	3.80E+02	6.00E+01
D16.3	1.91E+01	4.60E+00	n.a.		5.80E+00*	1.40E+00	5.40E+00	1.00E+00	7.00E+01	1.00E+01
D16.4	1.16E+01	2.60E+00	n.a.		1.19E+00*	3.00E−01	4.40E−01	1.40E−01	3.70E+00	6.00E−01
D16.5	6.30E+00	1.60E+00	n.a.		n.a.		6.70E−02*	4.40E−02	9.00E−01*	2.00E−01
D16.7	1.22E+00	4.80E−01	n.a.		n.a.		8.30E−02*	3.60E−02	8.00E−01*	1.60E−01
D16.9	2.70E−01	1.80E−01	n.a.		n.a.		4.60E−02*	2.40E−02	5.00E−01*	1.00E−01
D16.12	<1.47E−01		n.a.		n.a.		4.40E−02*	2.20E−02	4.10E−01*	1.00E−01

*Concentration below the background estimated for the crushed core samples (based on measurements of blank sample A20).

Table A2-35. Tracer activity per gram in first additional slice from the A8 core, mainly consisting of epoxy.

Slice	Ni-63 (Bq/g)	Ni-63 m.u. (Bq/g)	Np-237 (ng/g)	Np-237 2δ (ng/g)
A8.P***	8.10E+03	7.21E+02	3.91E+01	3.7E+00

*** Consists mainly of epoxy.

Appendix 3

Tracer cocktail data

The data of this appendix is part of data delivery #11.

Injected amount of tracers in the tracer cocktail

The amounts of tracer that was injected in the LTDE-SD experiment are provided in Table A3-1.

Table A3-1. Amounts of tracer injected in the tracer cocktail, with uncertainty estimates.

Tracer	Injected amount (Bq)	Uncertainty 2δ (Bq)	Comments
Na-22	3.17E+06	9.4E+04	
Cl-36	5.90E+06	1.1E+05	
Co-57	1.89E+07	4.6E+05	
Ni-63	3.04E+07	2.8E+06	
Ba-133	1.78E+06	3.5E+04	
Cs-137	8.80E+06	2.2E+05	
Cd-109	2.71E+07	2.4E+06	
Ag-110m	4.69E+05	1.0E+04	Value in Widestrand et al. (2010b) is incorrect
Gd-153	4.30E+06	2.3E+05	
Ra-226	1.49E+05	8.3E+03	
Tracer	Injected amount (ng)	Uncertainty 2σ (ng)	
Np-237	3.14E+05	1.7E+04	

Mass of sampled tracer cocktail

Sampling of the tracer cocktail was carried out by extracting samples, without replacing the extracted volume. The initial volume of the tracer cocktail was 1150 ± 50 mL. Table A3-2 gives the dates of sample extraction, the samples' mass, and the total tracer cocktail volume remaining after the sample extraction. In total 203.9 g of tracer was sampled throughout the experiment.

Table A3-2. Data on sampled tracer cocktail.

Sample number	Date	Extracted mass (g)	Total volume after sampling (mL)
1	2006-09-27	9.7455	1140
2	2006-09-27	1.2343	1139
3	2006-09-27	9.6181	1129
4	2006-09-27	0.9323	1128
5	2006-09-28	9.7733	1119
6	2006-09-29	10.0335	1109
7	2006-10-04	9.9131	1099
8	2006-10-11	9.172	1090
9	2006-10-25	9.4126	1080
10	2006-11-08	9.6852	1070
11	2006-11-22	9.0384	1061
12	2006-11-22	5.4432	1056
13	2006-11-22	5.2043	1051
-	2006-11-30	4	1047
14	2006-12-06	9.5193	1037
15	2006-12-20	9.5364	1028
16	2007-01-08	9.6239	1018
17	2007-01-24	9.9886	1008
18	2007-02-07	9.4264	999

Sample number	Date	Extracted mass (g)	Total volume after sampling (mL)
19	2007-02-21	9.9499	989
21	2007-03-07	9.6937	979
23	2007-03-21	9.4287	970
24	2007-04-04	9.0202	961
25	2007-04-04	4.8362	956
26	2007-04-04	4.7517	951
27	2007-04-04	4.9126	946

Tracer activities in cocktail

Table A3-3. Data on tracer cocktail samples, with activity and uncertainty of activity.

Sample number	Date	Time after injection (h/d)	Comments	Na-22 (Bq/mL)	Na-22 2δ (Bq/mL)
3	2006-09-27	2 h	All data are decay corrected to the time for tracer injection	3.20E+03	1.01E+02
5	2006-09-28	14 h		3.14E+03	9.89E+01
6	2006-09-29	44 h		3.10E+03	9.76E+01
7	2006-10-04	7 d		3.02E+03	9.54E+01
8	2006-10-11	14 d		3.03E+03	9.57E+01
9	2006-10-25	28 d		2.96E+03	9.35E+01
10	2006-11-08	42 d		2.86E+03	9.03E+01
11	2006-11-22	56 d		2.66E+03	8.59E+01
12	2006-11-22	56 d	Filtered sample		
13	2006-11-22	56 d	Cation exchanged		
-	2006-11-30		pH sample		
14	2006-12-06	70 d		3.09E+03	9.76E+01
15	2006-12-20	84 d		2.70E+03	8.53E+01
16	2007-01-08	103 d		2.74E+03	8.65E+01
17	2007-01-24	119 d		2.81E+03	8.88E+01
18	2007-02-07	133 d		2.60E+03	8.27E+01
19	2007-02-21	147 d		2.89E+03	9.19E+01
21	2007-03-07	161 d		2.88E+03	9.16E+01
23	2007-03-21	175 d		2.83E+03	9.03E+01
24	2007-04-04	189 d		2.94E+03	9.35E+01
25	2007-04-04	189 d	Filtered sample		
26	2007-04-04	189 d	Cation exchanged		
27	2007-04-04	189 d	Anion exchanged		

Table A3-4. Data on tracer cocktail samples, with activity and uncertainty of activity.

Sample number	Cl-36 (Bq/mL)	Cl-36 2δ (Bq/mL)	Co-57 (Bq/mL)	Co-57 2δ (Bq/mL)	Ni-63 (Bq/mL)	Ni-63 2δ (Bq/mL)
3	5.35E+03	1.03E+02	1.36E+04	3.35E+02	2.22E+04	2.16E+01
5	5.09E+03	9.78E+01	7.03E+03	1.75E+02	1.53E+04	1.80E+01
6	5.09E+03	9.84E+01	3.62E+03	9.14E+01	1.49E+04	1.77E+01
7	5.04E+03	9.72E+01	2.63E+02	1.35E+01	1.40E+04	1.71E+01
8	4.98E+03	9.60E+01	1.71E+02	1.21E+01	1.33E+04	1.68E+01
9	5.25E+03	1.01E+02	9.83E+01	1.11E+01	9.70E+03	1.43E+01
10	5.00E+03	9.60E+01	8.87E+01	1.08E+01	1.19E+04	1.58E+01
11	5.09E+03	9.78E+01	8.70E+01	1.12E+01	1.17E+04	1.57E+01
12						
13						
–						
14	5.12E+03	9.84E+01	1.00E+02	1.14E+01	1.15E+04	1.56E+01
15	5.06E+03	9.72E+01	8.94E+01	1.00E+01	1.08E+04	1.51E+01
16	5.05E+03	9.72E+01	9.90E+01	1.02E+01	1.06E+04	1.50E+01
17	5.04E+03	9.72E+01	1.10E+02	1.05E+01	1.01E+04	1.46E+01
18	5.22E+03	1.00E+02	1.22E+02	1.01E+01	9.24E+03	5.32E+00
19	5.18E+03	9.90E+01	1.36E+02	1.14E+01	8.91E+03	5.50E+00
21	5.25E+03	1.01E+01	1.47E+02	1.14E+01	8.72E+03	5.17E+00
23	5.15E+03	9.84E+01	1.52E+02	1.16E+01	8.39E+03	5.08E+00
24	5.13E+03	9.84E+01	1.61E+02	1.18E+01	7.90E+03	4.92E+00
25						
26						
27						

Table A3-5. Data on tracer cocktail samples, with activity and uncertainty of activity.

Sample number	Ba-133 (Bq/mL)	Ba-133 2δ (Bq/mL)	Cs-137 (Bq/mL)	Cs-137 2δ (Bq/mL)	Cd-109 (Bq/g)	Cd-109 2δ (Bq/g)
3	1.45E+03	3.47E+01	7.07E+03	1.78E+02	2.15E+04	1.93E+03
5	1.39E+03	3.36E+01	5.87E+03	1.48E+02	1.01E+04	9.49E+02
6	1.30E+03	3.13E+01	5.33E+03	1.35E+02	9.03E+03	8.48E+02
7	1.23E+03	2.97E+01	4.56E+03	1.16E+02	8.24E+03	7.70E+02
8	1.21E+03	2.95E+01	4.18E+03	1.06E+02	8.38E+03	7.81E+02
9	1.18E+03	2.92E+01	3.72E+03	9.50E+01	7.81E+03	7.32E+02
10	1.13E+03	2.78E+01	3.48E+03	8.89E+01	7.05E+03	6.64E+02
11	1.24E+03	3.38E+01	3.53E+03	9.06E+01	6.61E+03	6.34E+02
12						
13						
–						
14	1.19E+03	2.90E+01	3.44E+03	8.89E+01	6.67E+03	6.40E+02
15	1.06E+03	2.60E+01	2.96E+03	7.61E+01	5.61E+03	5.39E+02
16	1.01E+03	2.51E+01	2.94E+03	7.58E+01	5.53E+03	5.39E+02
17	1.09E+03	2.69E+01	2.99E+03	7.71E+01	5.31E+03	5.20E+02
18	9.60E+02	2.33E+01	2.68E+03	6.93E+01	4.47E+03	4.47E+02
19	1.06E+03	2.62E+01	2.89E+03	7.49E+01	4.58E+03	4.69E+02
21	1.01E+03	2.51E+01	2.86E+03	7.41E+01	4.58E+03	4.66E+02
23	1.01E+03	2.51E+01	2.82E+03	7.33E+01	4.39E+03	4.53E+02
24	1.03E+03	2.55E+01	2.90E+03	7.52E+01	4.31E+03	4.50E+02
25						
26						
27						

Table A3-6. Data on tracer cocktail samples, with activity and uncertainty of activity.

Sample number	Ag-110m (Bq/g)	Ag-110m 2δ (Bq/g)	Gd-153 (Bq/g)	Gd-153 2δ (Bq/g)	Ra-226 (Bq/g)	Ra-226 2δ (Bq/g)
3	2.35E+02	5.82E+00	3.08E+03	1.62E+02	1.03E+02	8.33E+00
5	1.33E+01	7.46E-01	1.39E+02	1.03E+01	8.27E+01	7.33E+00
6	1.98E+00	3.83E-01	4.55E+01	6.61E+00	7.48E+01	6.00E+00
7	< 1.25E+00		2.11E+01	5.46E+00	7.32E+01	6.62E+00
8	< 1.16E+00		1.70E+01	6.06E+00	6.87E+01	6.35E+00
9	< 1.72E+00		1.72E+01	5.28E+00	6.63E+01	6.00E+00
10	< 1.26E+00		1.95E+01	3.67E+00	6.02E+01	5.84E+00
11	< 1.32E+00		1.38E+01	4.64E+00	5.71E+01	5.39E+00
12						
13						
-						
14	< 1.16E+00		1.28E+01	4.85E+00	6.09E+01	6.62E+00
15	< 1.79E+00		< 1.06E+01		-	-
16	< 1.29E+00		1.13E+01	4.90E+00	5.72E+01	7.03E+00
17	< 9.80E-01		< 1.02E+01		6.33E+01	6.03E+00
18	< 1.26E+00		1.48E+01	4.98E+00	6.42E+01	6.50E+00
19	< 1.38E+00		1.97E+01	4.00E+00	5.13E+01	5.11E+00
21	< 1.97E+00		1.39E+01	3.72E+00	5.30E+01	5.19E+00
23	< 8.07E-01		1.71E+01	4.12E+00	5.71E+01	6.17E+00
24	< 1.76E+00		1.31E+01	3.70E+00	6.21E+01	6.87E+00
25						
26						
27						

Table A3-7. Data on tracer cocktail samples, with activity and uncertainty of activity.

Sample number	Np-237 (ng/g)	Np-237 2δ (ng/g)
3	2.72E+02	2.98E+01
5	2.30E+02	2.52E+01
6	2.22E+02	2.43E+01
7	2.23E+02	2.45E+01
8	2.14E+02	2.35E+01
9	2.45E+02	2.68E+01
10	2.09E+02	2.30E+01
11	2.20E+02	2.41E+01
12		
13		
-		
14	2.08E+02	2.28E+01
15	2.00E+02	2.19E+01
16	2.03E+02	2.23E+01
17	2.03E+02	2.23E+01
18	1.95E+02	2.14E+01
19	1.98E+02	2.17E+01
21	1.94E+02	2.13E+01
23	1.81E+02	1.99E+01
24	1.68E+02	1.84E+01
25		
26		
27		

Appendix 4

Accompanying data on LTDE-SD

The data of this appendix is part of data delivery #11 and concerns 1) geometries of the experimental setup; 2) data on tracer activities at the termination of the in-situ phase; and 3) activities of the so-called B samples and D-E samples, which were taken from the epoxy injected at the fracture surface and in the slim hole, respectively, upon termination to protect the rock surfaces. The tracer activity data presented below in this appendix were confirmed and updated in data delivery #24. Data for "Activity in PEEK tubing" in Table A4-3 is updated, as well as headings and clarifications in Tables A4-2 and A4-4 to A4-7, according to data delivery #24.

Experimental geometries

Various information on the geometries of the experimental setup are displayed in Table A4-1, as well as in Figures A4-1 to A4-5.

Table A4-1. Data on the experimental geometries.

Description	Data	Uncertainty (+/−)	Unit	Comment
Rock areas in contact with the tracer cocktail				
Diameter of the ”stub section”	177	1	mm	
Diameter of the ”slim hole section”	36	0.5	mm	The dummy in the ”slim hole section” contains four holes, therefore the total volume is presented below
Length of the ”slim hole section”	300	1	mm	See above
Diameter of analysed rock cores	24	0.2	mm	
Length of analysed rock cores	See data in Appendix 2	1	mm	
Other test volume measures				
Volume of the ”stub section”	80	13	mL	
Volume of the ”slim hole section”	148	1	mL	
Aperture between the stub section fracture surface and the PEEK lid	3.25 (2-4)	0.52	mm	(2-4) refers to the measured minimum and maximum values
Downward dip of drillhole KA3065A03	−4.5		°	
Position of the test section; from borehole length	10.74		m	
Position of the test section; to borehole length	11.23		m	
Diameter of the slim hole PEEK dummy	26.0	0.1	m	
Inner diameter of PEEK tubing	3.2	0.26	mm	
Total length of PEEK tubing	140	5	m	
Maximum volume of the pressure regulation cylinder	402	5	mL	
Volume of other equipment components	27	11	mL	

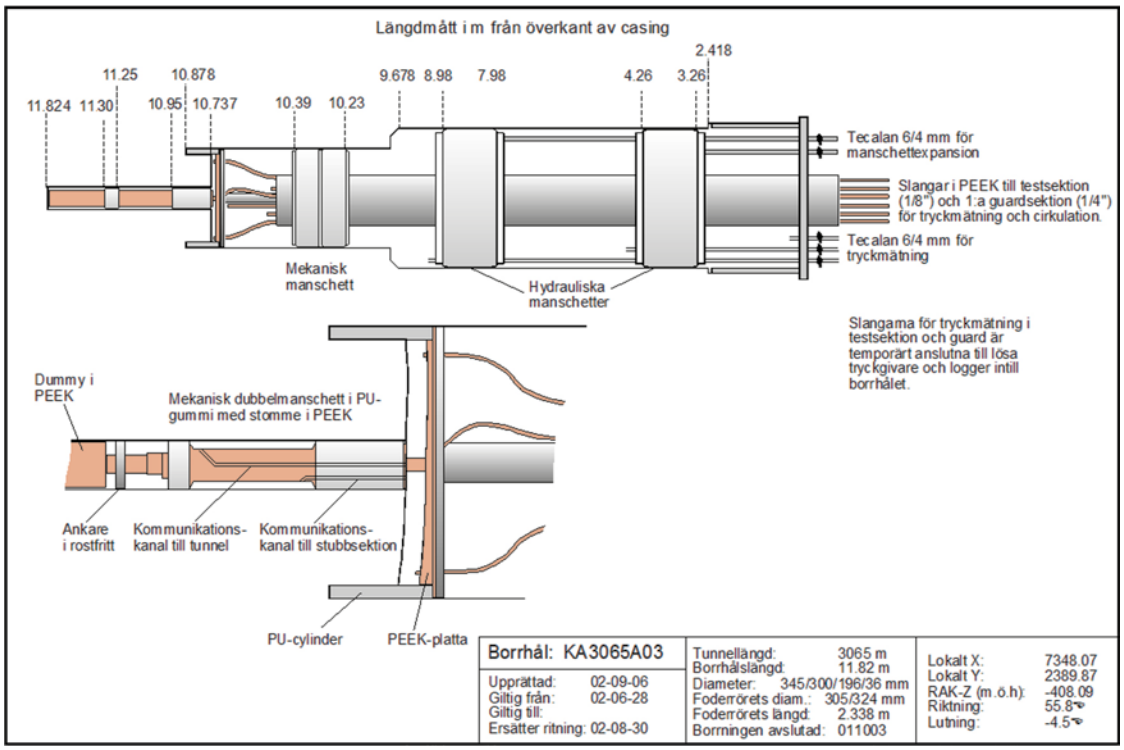

Figure A4-1. *Drillhole installations in KA3065A03, displaying packer positions: 3.26-4.26 m drillhole length from top of casing (TOC); hydraulic packers. 7.98-8.98 m drillhole length from TOC; hydraulic packers. 10.23-10.39 m drillhole length from TOC; mechanical packer. 10.737-10.95 m and 11.25-11.30 m drillhole length from TOC; mechanical double packer delimiting the slim hole section. Measures according to instrument drawing no 3-2054.*

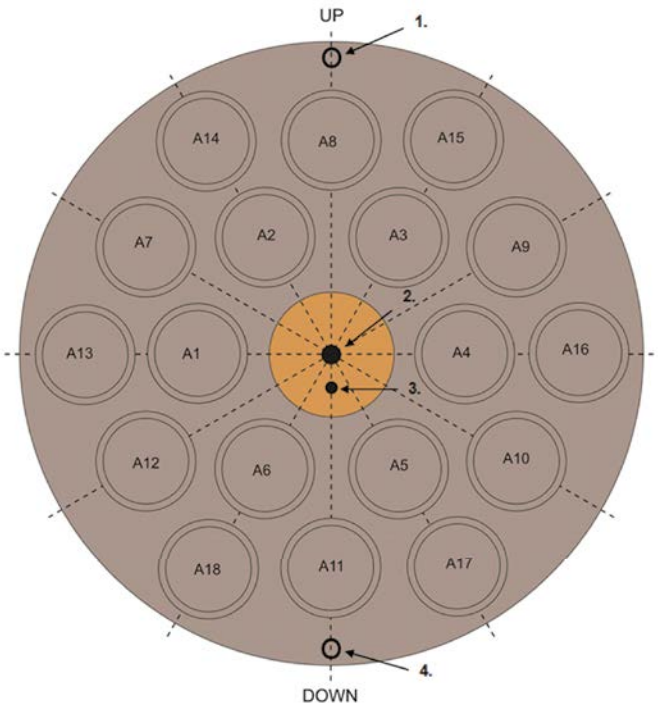

1. Outlet from stub section
2. Inlet to slim hole section
3. Outlet from slim hole section
4. Inlet to stub section

Figure A4-2. *Locations of tracer cocktail inlets and outlets, relative to the A-core positions.*

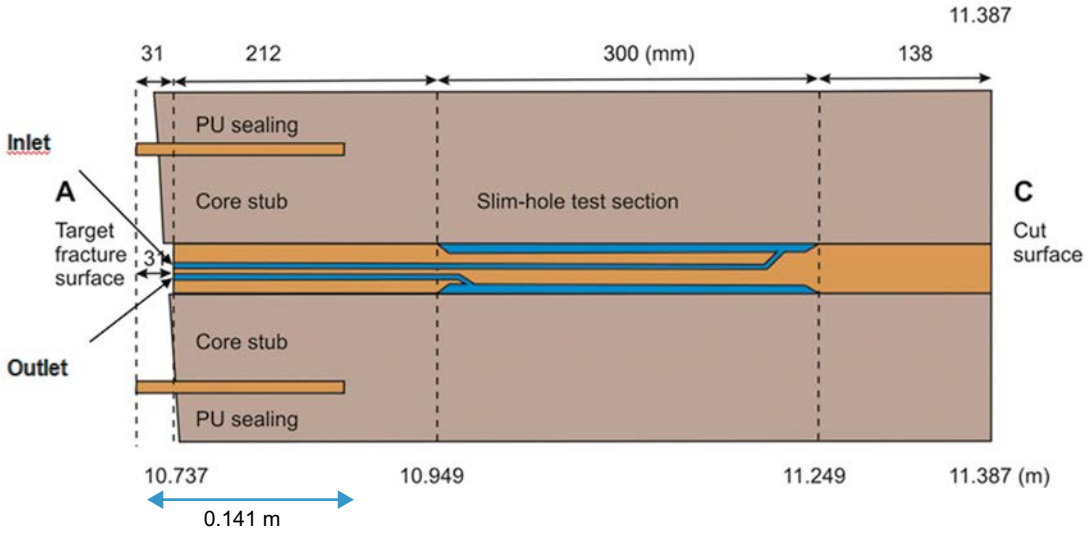

Figure A4-3. *Locations of tracer cocktail inlets and outlets in slimhole. The length of the PU sealing is 0.141 m.*

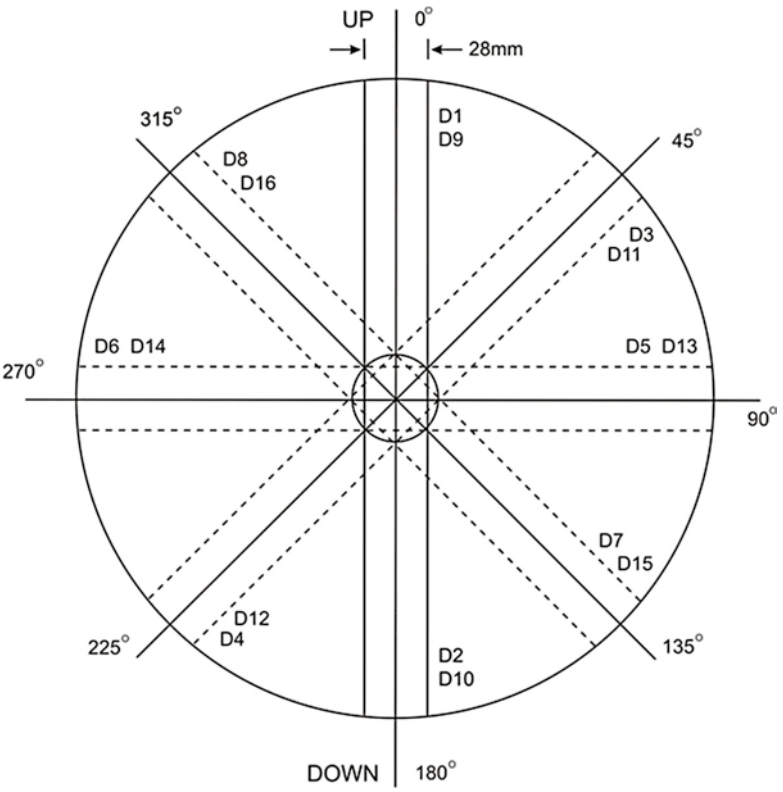

Figure A4-4. *Locations of the D-cores, profile perpendicular to KA3065A03.*

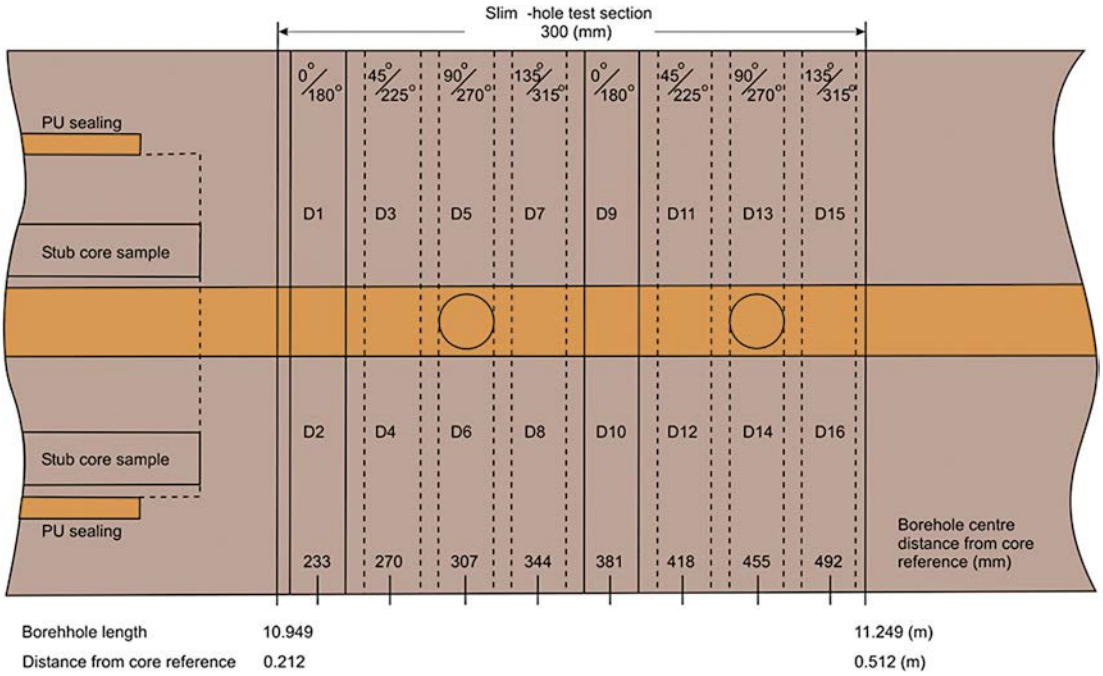

Figure A4-5. *Locations of the D-cores, profile along KA3065A03.*

Tracer activity at termination

The activities in Tables A4-2 and A4-3 relates to the activity in water remaining in the equipment by the time terminating the experimental in-situ phase as well as the experiment groundwater present in the experiment section, flushed out using iso-propanol during the iso-propanol exchange. Five different equipment components (including the pressure regulation cylinder) were emptied of water on the day before termination (Widestrand et al. 2010b, Section 2.4.1). The water (including rinsing water) was collected in five different vessels and analysed separately. The sums of the five total activities of the different nuclides are reported as "Water phase, emptied from equipment components" in Table A4-2. The water phase including the major part of the experiment groundwater and the whole volume of the isopropanol samples collected during the iso-propanol exchange is reported as "Water phase including iso-propanol used at the exchange". This fraction may also include tracer that was desorbed from the rock surfaces and dissolved in the iso-propanol.

Table A4-2. Tracer activity in experiment groundwater present in equipment and in the experiment groundwater present in the experiment section, flushed out using iso-propanol. n.a. means not available.

Tracer	Water phase, emptied from equipment components (Bq)	Uncertainty 2δ/Bq	Water phase including iso-propanol used at the exchange (Bq)	Uncertainty 2δ/Bq
Na-22	8.04E+05	3.23E+03	1.75E+06	1.24E+04
Cl-36	n.a.		n.a.	
Co-57	6.70E+04	1.52E+03	4.98E+04	8.21E+03
Ni-63	n.a.		n.a.	
Ba-133	2.82E+05	1.30E+03	5.56E+05	4.95E+03
Cs-137	7.99E+05	2.18E+03	1.72E+06	8.44E+03
Cd-109	1.18E+06	2.75E+04	2.84E+06	1.04E+05
Ag-110m	<5.55E+03		<1.78E+04	
Gd-153	<1.65E+04		<3.72E+04	
Ra-226	n.a.		n.a.	
Np-237 (ng)	n.a.		3.96E+03	3.76E+02

Table A4-3. Tracer activity in the iso-propanol/epoxy slurry and in tubing, where n.a. means not available.

Tracer	Total amount from epoxy/ isopropanol slurry, upper phase* (Bq)	Uncertainty 2δ (Bq)	Activity in PEEK tubing (Bq)**	Uncertainty 2δ (Bq)
Na-22	1.72E+05	9.13E+03	7.47E+03	2.15E+02
Cl-36	n.a.		n.a.	
Co-57	2.91E+04	1.41E+03	1.92E+06	1.13E+06
Ni-63	n.a.		n.a.	
Ba-133	2.93E+04	1.58E+03	1.02E+05	4.85E+04
Cs-137	1.73E+05	9.14E+03	3.77E+04	2.76E+04
Cd-109	1.68E+05	1.05E+04	2.26E+06	1.01E+06
Ag-110m	< 7.81E+02		1.18E+05	1.31E+04
Gd-153	< 1.73E+03		9.21E+05	4.14E+05
Ra-226	n.a.		n.a.	
Np-237 (ng)	3.59E+02	3.42E+01	3.04E+02	2.89E+01

* Upper phase refers to the liquid phase in contrast to the cured Epoxy phase at the bottom of the flask.

** The tubings were leached with HNO_3, (diluted 1:1) and three main activity ranges were used at the updated estimation of total amounts of activities. Update according to data delivery #24.

Tracer activities of epoxy B and D-E samples

Table A4-4. Total tracer activities in the epoxy B samples, with uncertainty estimates, where n.a. means not available.

Tracer	B1 II (Bq)	2δ (Bq)	B1 (Bq)	2δ (Bq)	B6 (Bq)	2δ (Bq)
Na-22	5.88E+00	-	2.50E+01	2.64E+00	5.21E+01	3.19E+00
Cl-36	n.a.		n.a.		n.a.	
Co-57	7.31E+03	4.52E+02	1.82E+04	1.12E+03	9.94E+03	6.13E+02
Ni-63	n.a.		n.a.		n.a.	
Ba-133	1.91E+01	1.42E+00	2.84E+02	1.71E+01	1.50E+02	8.91E+00
Cs-137	6.24E+01	3.89E+00	7.81E+02	4.82E+01	1.05E+03	6.01E+01
Cd-109	2.30E+03	3.09E+02	6.28E+03	8.11E+02	3.12E+03	3.98E+02
Ag-110m	2.45E+02	1.69E+01	3.26E+03	1.91E+02	3.38E+03	1.95E+02
Gd-153	< 2.04E+02		2.90E+03	2.25E+02	1.03E+03	8.00E+01
Ra-226	n.a.		n.a.		n.a.	
Np-237 (ng)	2.80E+01	2.66E+00	9.03E+01	8.58E+00	2.13E+01	2.02E+00

Table A4-5. Tracer activities in the epoxy B samples, with uncertainty estimates, where n.a. means not available.

Tracer	B8 (Bq)	2δ (Bq)	B8 II PEEK (Bq)	2δ (Bq)	B9 (Bq)	2δ (Bq)
Na-22	5.44E+00	8.89E-01	6.62E+00	1.02E+00	2.85E+01	2.48E+00
Cl-36	n.a.		n.a.		n.a.	
Co-57	2.86E+03	1.78E+02	1.21E+04	7.46E+02	9.02E+03	5.57E+02
Ni-63	n.a.		n.a.		n.a.	
Ba-133	6.28E+01	4.03E+00	2.68E+01	1.71E+00	7.63E+01	4.81E+00
Cs-137	2.65E+02	1.55E+01	4.80E+01	3.05E+00	1.00E+02	6.09E+00
Cd-109	1.73E+03	2.34E+02	1.83E+03	2.57E+01	3.05E+03	4.02E+02
Ag-110m	2.77E+02	1.92E+01	3.48E+02	2.28E+01	6.82E+02	4.23E+01
Gd-153	8.91E+02	7.32E+01	2.83E+02	3.56E+01	6.78E+02	5.92E+01
Ra-226	n.a.		n.a.		n.a.	
Np-237 (ng)	n.a.		n.a.		n.a.	

Table A4-6. Tracer activities in the epoxy B and D-E samples, with uncertainty estimates, where n.a. means not available.

Tracer	B17 (Bq)	2δ (Bq)	D-E1 (Bq)	2δ (Bq)	D-E6 (Bq)	2δ (Bq)
Na-22	8.09E+01	5.93E+00	5.83E+01	4.28E+00	3.01E+01	1.88E+00
Cl-36	n.a.		n.a.		n.a.	
Co-57	1.21E+04	7.50E+02	1.78E+05	1.09E+04	2.54E+04	1.57E+03
Ni-63	n.a.		n.a.		n.a.	
Ba-133	1.08E+02	6.84E+00	1.29E+03	7.65E+01	3.40E+02	2.02E+01
Cs-137	2.17E+02	1.30E+01	8.33E+02	4.81E+01	6.93E+02	3.98E+01
Cd-109	4.97E+03	6.50E+02	3.86E+04	4.90E+03	4.80E+03	6.10E+02
Ag-110m	6.36E+03	3.70E+02	1.28E+03	7.76E+01	2.07E+02	1.27E+01
Gd-153	1.36E+03	1.10E+02	1.81E+04	1.38E+03	1.53E+03	1.18E+02
Ra-226	n.a.		n.a.		n.a.	
Np-237 (ng)	5.22E+01	4.96E+00	n.a.		5.73E+01	5.44E+00

Table A4-7. Tracer activities in the epoxy D-E samples, with uncertainty estimates, where n.a. means not available.

Tracer	D-E12 (Bq)	2δ (Bq)	D-E13 (Bq)	2δ (Bq)
Na-22	3.03E+01	2.61E+00	4.04E+01	3.24E+00
Cl-36	n.a.		n.a.	
Co-57	9.11E+04	5.62E+03	1.26E+05	7.76E+03
Ni-63	n.a.		n.a.	
Ba-133	5.98E+02	3.57E+01	4.78E+02	2.86E+01
Cs-137	2.73E+03	1.57E+02	1.40E+03	8.08E+01
Cd-109	1.17E+04	1.51E+03	1.43E+04	1.85E+03
Ag-110m	7.38E+02	4.79E+01	6.28E+02	4.05E+01
Gd-153	6.40E+03	4.95E+02	6.83E+03	5.30E+02
Ra-226	n.a.		n.a.	
Np-237 (ng)	n.a.		1.18E+02	1.12E+01

Appendix 5

Geological characterisation of core D6

The geological characterisation of core sample D6 is taken from data delivery #12. The data delivery also provided geological characterisations of numerous of other samples. However, for these other samples the geological characterisations are already reported in Nilsson et al. (2010).

Mineralogy:

Quartz, K-feldspar, plagioclase, biotite, chlorite, titanite, hematite/magnetite and epidote.

K-feldspar to varying extent albitized, biotite partially altered to chlorite and plagioclase is partially saussuritized, i.e. altered to epidote, sericite and albite.

Fractures:

Thin sealed fractures (with irregular outshoots) at 2.5, 3.5 and 4.5 cm respectively, at an angle of 65° to the borehole axis.

Wall rock alteration:

Faint to weak alteration, 0-6 cm (i.e. near the slimhole).

Autoradiographs and photos of the first 1-4 core slices, for which the base of the slice is approximately 16 mm.

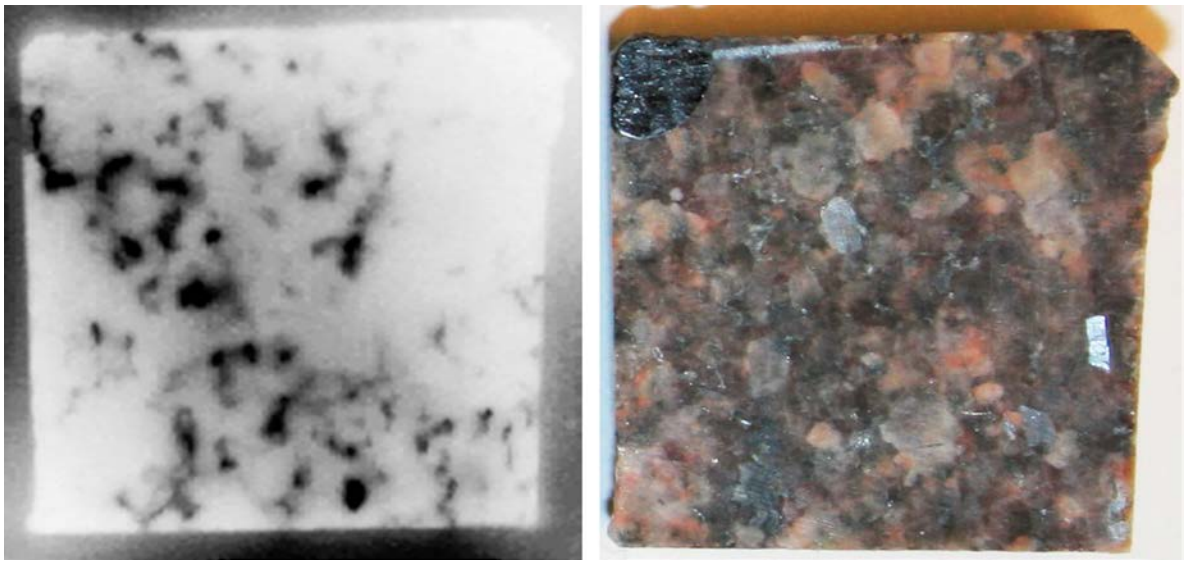

D6.1. *No comments.*

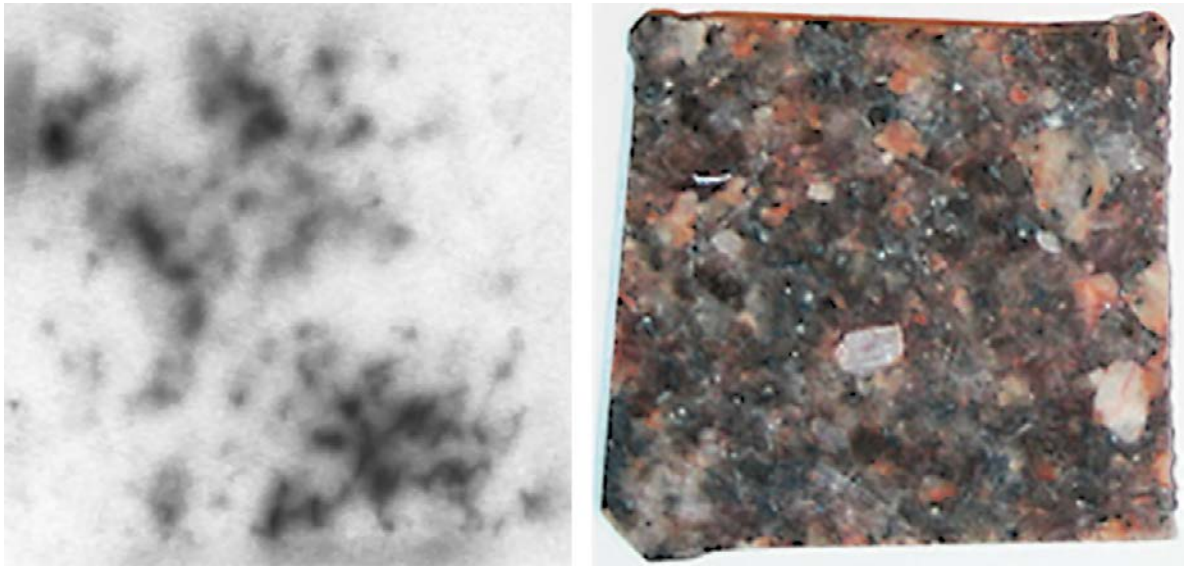

D6.2. *No comments.*

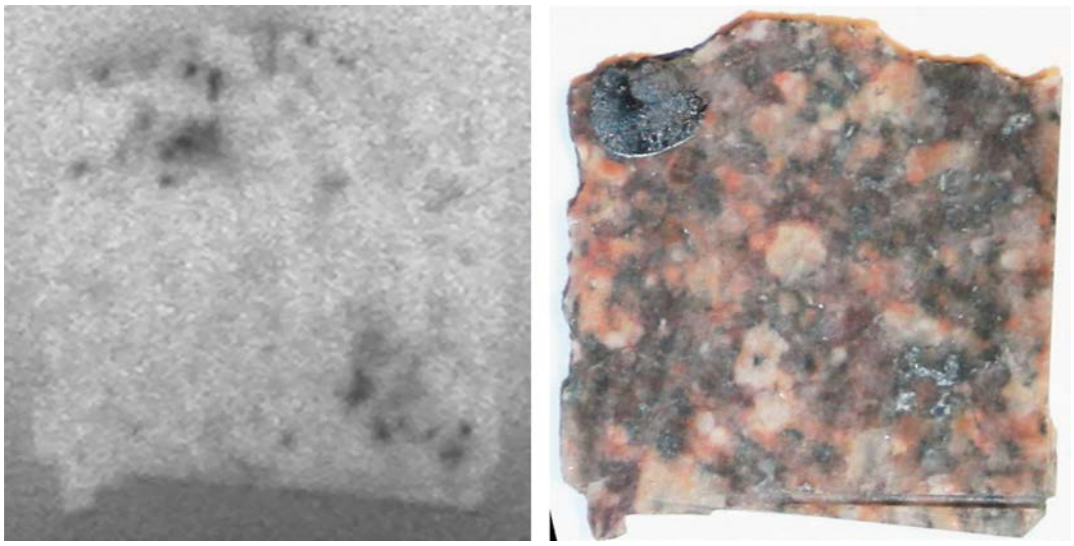

D6.3. *No comments.*

D6.4. *No comments.*

Appendix 6

Description of a sample from the LTDE-SD project

Henrik Drake, 2016-09-15

General

The specimen is made up of a large rock piece from a drill core with 3 smaller holes drilled into it (DH-1, DH-2, DH-3, see Figure A6-1). The uppermost part of the rock piece represents a fracture plane ("A") and has a thick mylonite/cataclasite with calcite fragments closest to the hydrothermally altered, red-stained, wall rock and chlorite/clay minerals and calcite on the outermost part. The brown-coloured cataclasite is more common than the light green-coloured mylonite. There is also another major open fracture ("B"). This fracture has a partial cover of secondary minerals (calcite, chlorite, clay minerals). There are also numerous sealed and partly open fractures, mainly with secondary K-feldspar, calcite and chlorite filling. One of them can be seen in DH-2 of Figure A6-1 below. The rock specimen was cut with a rock saw in order to prepare thin sections for microscopy investigation of the wall rock (point-counting and SEM), and of the mineral filling/coating lining fracture "A" (a thin section was prepared perpendicular to the fracture). Larger rock pieces from the outermost part of the sawed part were ground by a swing mill and analysed for chemical composition by ALS, Luleå, Sweden.

Detailed descriptions of the geological characteristics of the wall rock, of the filling/coating of fracture "A" and a detailed description of the intercepts in each of the three boreholes are given below.

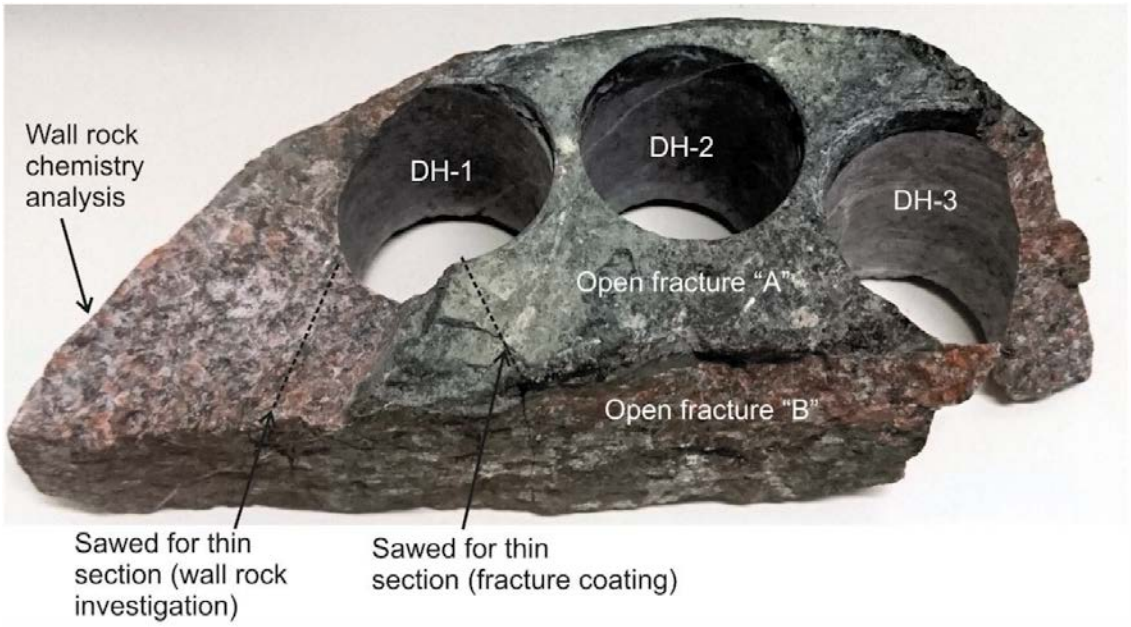

Figure A6-1. *Photograph of the core piece, with the three boreholes indicated (DH-1, DH-2, DH-3). Width of the whole piece is about 16 cm.*

General feature of the wall rock

Mineralogical observations

The wall rock is hydrothermally altered and reddish coloured compared to fresh rock. The alteration is evident throughout the rock of the whole specimen and there is no significant change in alteration intensity between different parts of the specimen, except that microfracturing seems to be more intense close to the main fracture. The rock is highly heterogeneous, with large variation in amount of Fe-Mg-minerals (biotite and chlorite) and quartz+feldspars. The general alteration feature is that plagioclase has been altered (pseudomorphic replacement) to secondary feldspars (albite and adularia), epidote and sericite. The adularia contains fine-grained hematite crystals giving it a red colour. Biotite has altered to chlorite (+titanite, and some fluorite). Magnetite has been partly or completely replaced by hematite. The altered rock commonly has micro-fractures.

Modal composition

The modal composition was determined by point counting. The volume percent is listed in Table A6-1 along with data from Widestrand et al. (2010a). The composition is very similar to the samples from Widestrand et al. (2010a), and is in line with a granodiorite composition.

Table A6-1. Modal composition of a rock sample from this study (see position in Figure A6-1), along with reference data from Widestrand et al. (2010a).

Mineral	This study	A02, Unaltered rock sample of Ävrö granodiorite (adjacent to rock sample A02:5)	A03 #10,strongly altered rock (Ävrö granodiorite), mylonitic/ cata-clasitic rock and fracture	A03 #14, slightly redstained Ävrö granodiorite	Ävrö granodiorite within the Trans-port laboratory programme*
	vol.%	vol.%	vol.%	vol.%	vol.%
Quartz	32.4	30.6	33.2	35.2	30.4
Plagioclase	3	3.0		13.0	33.2***
Sauss. Plag.	29.8	27.6		13.2	
Sericitised Plag*			16.3		
K-feldspar	29.4	28.6	30.8	31.8	25.8
Biotite	0.2	5.8		3.0	2.2
Chlorite	2	1.8	3.6	2.0	3.6
Titanite	0.4	1.0		0.4	0.4
Epidote	2	0.6	13.1	0.6	2.8
Opaque	0.4	1.0		0.6	0.4
Hornblende					0.6
Apatite	0.2	–**	0.2	0.2	
Calcite			2.6		
Allanite			0.2		
Muscovite	0.4				

* Data from rock sample KLX02 753.80 (Oskarshamn Site Investigation).

** less than 0.2 percent.

*** The plagioclase is to some extent saussuritized, although not determined in percentage.

Chemistry

The chemical composition of the wall rock sampled in the current project is compared in Table A6-2 to the chemical composition listed in Widestrand et al. (2010, Table 2-1). The sample in this project is very similar in composition to the earlier measurements from A02 and A03, but has slightly higher Si and K, and lower Ca, which likely is due to the small sample volume used in combination with the very heterogeneous rock and can be explained by a slightly higher quartz (and K-feldspar) and lower plagioclase content of the studied rock sample.

Table A6-2. Chemical composition of the altered rock in this project and reference data from R-10-66 (Widestrand et al. 2010a).

Element	Unit	This project	A02:6 (R-10-66)	A03:1 Batch 1 (R-10-66)
SiO2	%	73.2	68.5	69.5
Al2O3	%	13.9	14.4	14.1
CaO	%	0.75	2.06	1.77
Fe2O3	%	2.10	3.01	2.44
K2O	%	5.66	4.73	5.1
MgO	%	0.684	1.03	0.775
MnO	%	0.024	0.0454	0.0385
Na2O	%	3.00	3.26	3.08
P2O5	%	0.110	0.152	0.121
TiO2	%	0.348	0.436	0.346
Sum	%	99.80	97.6	97.3
LOI	%	0.5	0.6	0.6
Ba	mg/kg	1780	1540	1660
Be	mg/kg	1.29	1.84	1.69
Co	mg/kg	6.71	< 6	< 6
Cr	mg/kg	381	21.6	17.5
Cs	mg/kg		2.51	2.05
Cu	mg/kg		55.1	< 6
Ga	mg/kg	13.2	14.9	14
Hf	mg/kg	4.51	6.58	22
Mo	mg/kg	< 5	3.22	< 2
Nb	mg/kg	8.64	8.42	7.67
Ni	mg/kg	89	< 10	< 10
Rb	mg/kg	144	132	136
S	mg/kg		21.2	16.0
Sc	mg/kg	1.98	3.02	4.56
Sn	mg/kg		4.77	7.70
Sr	mg/kg	332	741	725
Ta	mg/kg	0.625	0.696	0.679
Th	mg/kg	9.67	3.63	3.38
U	mg/kg	4.06	2.47	3.13
V	mg/kg	27.6	37.8	31.0
W	mg/kg	0.856	0.621	0.678
Y	mg/kg	14.6	15.2	46.0
Zn	mg/kg		56.2	46.6
Zr	mg/kg	202	317	938
La	mg/kg	45.2	92.3	54.9
Ce	mg/kg	79.5	234	157
Pr	mg/kg	8.24	12.6	9.15
Nd	mg/kg	29.3	37.0	27.7
Sm	mg/kg	4.42	4.59	3.94
Eu	mg/kg	0.969	0.620	0.425
Gd	mg/kg	3.06	2.27	2.29
Tb	mg/kg	0.436	0.330	0.316
Dy	mg/kg	2.3	2.08	1.99
Ho	mg/kg	0.441	0.418	0.388
Er	mg/kg	1.15	1.13	1.11
Tm	mg/kg	0.184	0.172	0.167
Yb	mg/kg	1.18	1.19	1.08
Lu	mg/kg	0.17	0.181	0.153

General feature of the filling/coating of fracture "A"

The overall characteristics of the main fracture can be summarized as follows (Figure A6-2): The outermost part of the fracture (the open fracture "A"), is coated by secondary minerals, such as chlorite, clay minerals (corrensite, Figure A6-2, but also illite), calcite, quartz and barite (Figure A6-2). Below this coating there is a brownish to dark green, fine-grained cataclasite, generally ~5 mm in thickness. The mineralogy of this cataclasite is dominated by illite, K-feldspar (Figure A6-4), hematite (fine-grained disseminated, staining the minerals to a brownish red colour), epidote, chlorite, quartz, large scattered crystals of calcite and wall rock fragments. In the contact zone between the cataclasite and the wall rock there is a fine-grained greenish filling, of a couple of mm in thickness, but the thickness varies widely and in places this filling is absent. This greenish filling appears partly to have semi-ductile texture in parts (mylonitic), but seems to be composed of several pulses of mineralisation (Figure A6-5a), including more euhedral epidote, K-feldspar, and calcite (when calcite is present the filling is whitish in colour, Figure A6-2b), chlorite, quartz, and sulphides (pyrite and chalcopyrite). The cataclasite and mylonite resemble the K-feldspar-rich and epidote-rich cataclasite/mylonite reported in previous investigations.

The contact zone between the wall rock and the greenish filling is somewhat diffuse as several parallel veins exist, of which some penetrate the uppermost part of the wall rock (Figure A6-5b), and a network of micro-fractures penetrate the wall rock (Figure A6-5c). A later feature is thin, <1 mm, veins filled with mainly calcite and K-feldspar, and some quartz, chlorite and hematite (and some chalcopyrite, Figure A6-5d). These veins are undulating but mostly cut fracture "A" and the older coatings at 30-45°, but almost perpendicular intersection is also evident (Figure A6-2b). These sealed fractures can be reddish along the wall rock contact due to hematite-staining. There are voids in these fracture fillings, so porosity should be quite high. There are also thinner partly open fractures, << 1 mm, which also have calcite, quartz, feldspar and chlorite infilling (example in Figure A6-5a), with high porosity. In several cases the semi-open fractures may have been opened during activities in the boreholes. The mineralogical composition of the different fracture coatings and filling types was identified in a thin section (the sawed surface in the right part of Figure A6-2b).

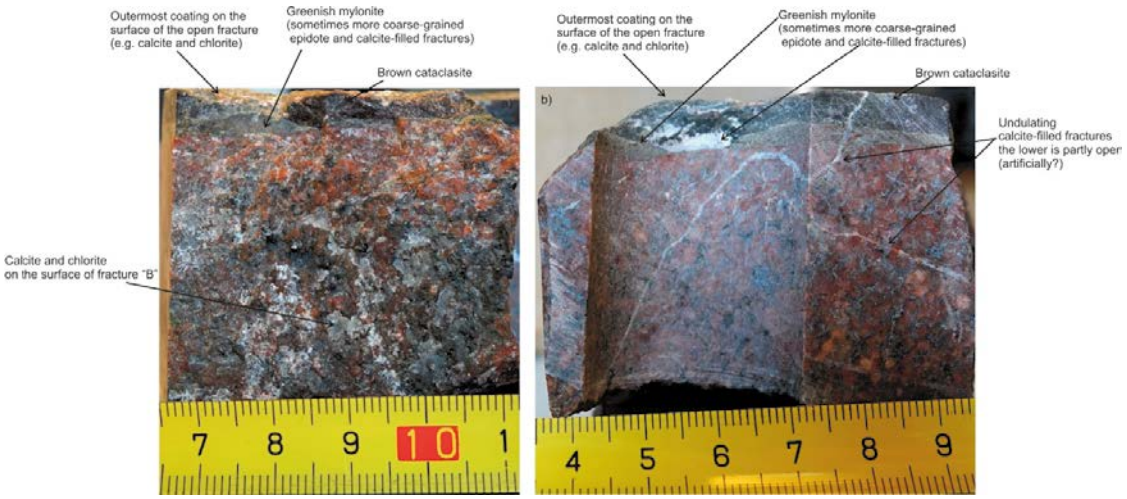

Figure A6-2. *General features of the structure as seen in (a) perpendicular to fracture B with fracture A in the upper part of the photo and in (b) which shows DH-1.*

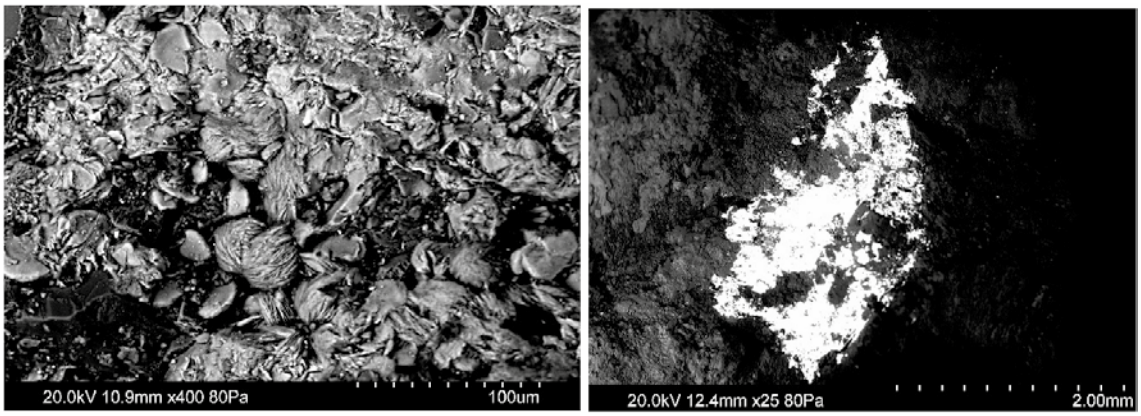

Figure A6-3. *Spherulitical clay mineral aggregates (corrensite) on the surface of fracture "A" (left). Barite (bright mineral) on the surface of fracture "A" (right).*

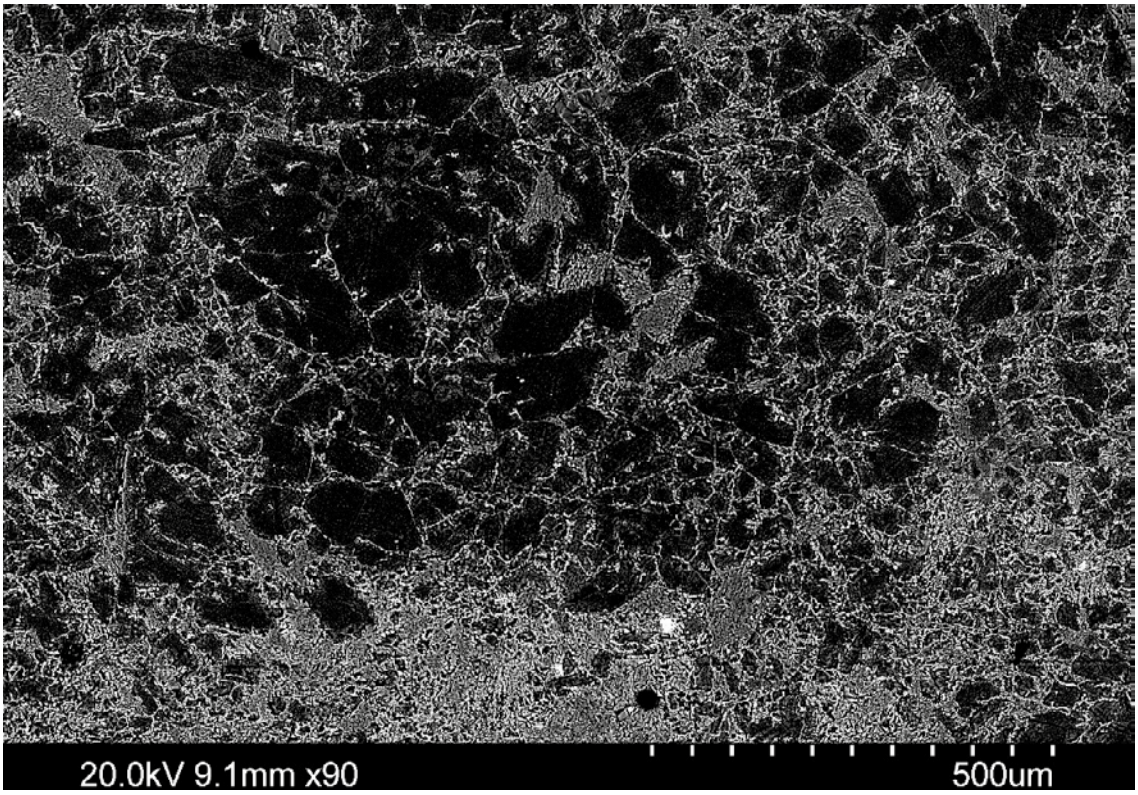

Figure A6-4. *SEM-image of cataclasite composed of illite (dark crystals), K-feldspar (grey crystals in between illite crystals) and epidote (bright aggregates, mainly in the bottom and right part of the image).*

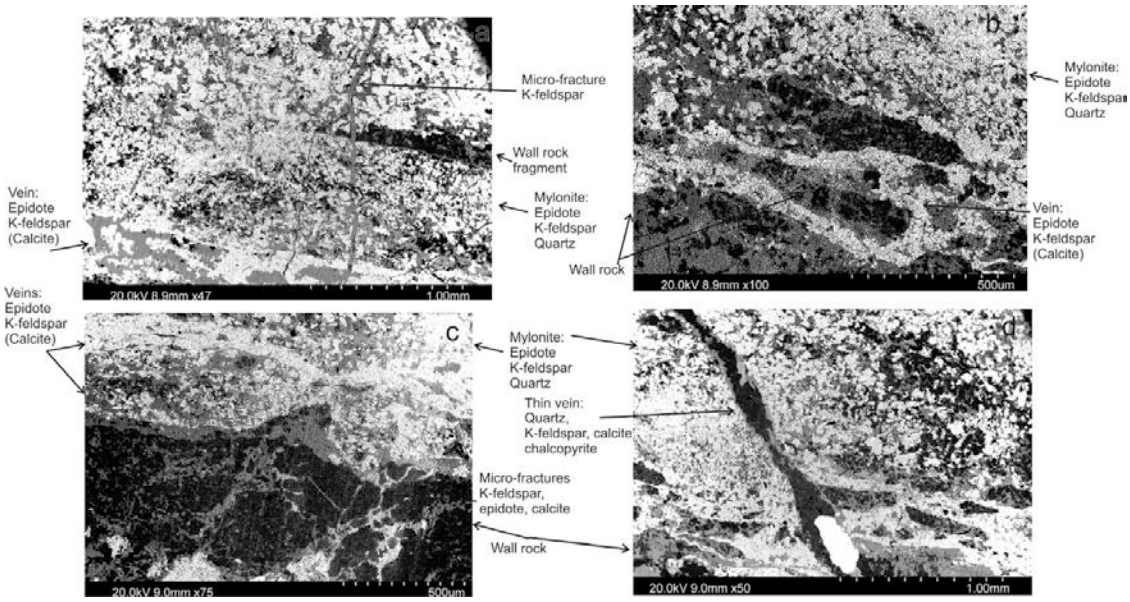

Figure A6-5. *SEM-image of (a) fine-grained greenish filling with more coarse-grained veins in the lower part, (b) penetration of the epidote/feldspar-veins into the outer parts of the wall rock, (c) micro-fractures into the wall rock from the epidote/feldspar-veins. The micro-fractures are filled with epidote, K-feldspar and calcite dominantly. (d) A fracture filled with K-feldspar, chalcopyrite (bright), calcite and quartz (dark mineral in the middle of the fracture) cutting through the epidote mylonite and vein filling.*

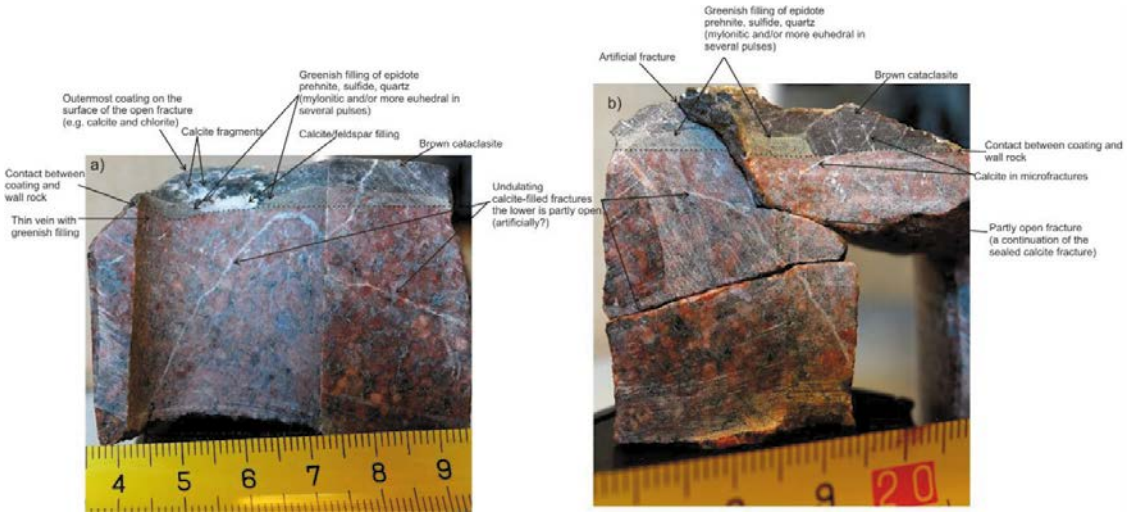

Figure A6-6. *Detailed description of DH-1, E wall (a) and W wall (b, slightly fragmented due to sawing).*

Detailed description of borehole walls

The coating thickness varies between different parts of the boreholes. In this detailed description of the different borehole walls, details in the different boreholes are described in directions N, E, S, W based on the position of the specimen in the photograph (Fig A6-1). Left part of DH-1 in Fig A6-1 is described as W, the wall furthest away from the camera as N etc. For the wall rock, the red-stained hydrothermal alteration described above is pervasive throughout the specimen and therefore the general description (above) is representative for all boreholes and not repeated below.

Detailed description of DH-1

In DH-1 the E wall (Figure A6-6a) has clay mineral-dominated coating on top of the cataclasite filling. The cataclasite filling thickness is 4-5 mm but decreases significantly to the north. There are numerous large calcite fragments within the cataclasite but also a larger calcite fracture filling between the cataclasite and the wall rock. The thickness of this calcite filling is up to 3 mm. On the N and S side of the calcite filling the greenish filling is instead placed between the wall rock and the cataclasite. The thickness of the greenish filling is 2-3 mm. The contact to the wall rock is a bit diffuse as the greenish filling is composed of several parallel bands with wall rock fragments in between. A thin calcite-feldspar-filled fracture runs through the whole E wall at about 45 degrees angle but undulates before it reaches the greenish filling (8 mm below the fracture surface).

The W wall of DH-1 (Figure A6-6b) has a very thin clay mineral coating on top of the cataclasite. The cataclasite thickness is generally 4-7 mm but decreases significantly to the N. For half of the W wall there is no greenish coating between the cataclasite and the wall rock (the N part) and there are no calcite fragments in the cataclasite at this wall. The greenish filling is ~3 mm thick when it occurs. There are a few thin calcite-filled microfractures cutting through the cataclasite at about 45 degrees angle. In the wall rock there is a notable calcite-feldspar filled fracture that splits into two parts, one being semi-parallel with the main open fracture (distance from the main fracture is 10-15 mm) and one at 45 degrees to the main fracture.

Detailed description of DH-2

Because this borehole is intact it was difficult to visualise, therefore photographs were taken in four directions (Figure A6-7). The N wall (Figure A6-7a) has a mineral coating of mainly clay minerals, feldspar, quartz, calcite and chlorite. Below this coating there is cataclasite (brown to dark green, at most 7 mm thick, i.e. distance to the wall rock contact is 7 mm) with calcite fragments. In the bottom part of the cataclasite there is a brighter green filling, with e.g. epidote, K-feldspar, quartz and chlorite, with a thickness of up to 2 mm. There is a sealed fracture filled with calcite and K-feldspar cutting the cataclasite at 45°. This fracture extends 15 mm from the main open fracture. At a distance of 25 mm from the main fracture there is a partly open microfracture.

The E wall features about the same thickness of the cataclasite (6-7 mm) as in the N wall, as well as calcite fragments within the cataclasite. In the southern part of the E wall there is no greenish filling between the cataclasite and the wall rock, and here the cataclasite changes color from dark green to dark brown. A prominent semi open fracture exists at 15-20 mm distance from the fracture surface.

The S wall has a dark brown cataclasite with a thin, partial coating on top. The cataclasite is 5 mm thick, has a few calcite fragments and a couple of microfractures that are semiperpendicular to the main fracture. In the W part of the S wall the greenish filling between the cataclasite and the wall rock appears and becomes thicker to the W. up to a couple of mm.

The W wall has calcite on the outermost part of the coating, surrounded by chlorite and clay minerals. The cataclasite is up to 8 mm thick, but in the S part of the wall it has a greenish filling of epidote in between the wall rock contact (up to 3 mm thick). In the rest of the cataclasite exposure there are abundant calcite fragments making up to 50 % of the cataclasite. A calcite/feldspar-filled fracture of 1 mm thickness runs at 45° to the main fracture and 16 mm into the wall rock from the fracture.

Detailed description of DH-3

This borehole features a partial cataclasite cover, i.e. some of the cataclasite coating has been removed, probably during drilling. The W wall and most of the N wall still have coverage of cataclasite (about 5-6 mm thickness, with a thin coating on top). The E wall is fragmented (not shown in Figure A6-8) and only has a small part (1 cm width) with cataclasite (2 mm thickness). The S wall is fragmented and has only some cataclasite to the west. The cataclasite is brownish and has no greenish filling in the contact zone to the wall rock (only in the outermost part of the SW wall, Figure A6-8) and only very few calcite fragments, in contrast to the other boreholes. There are some partly open fractures deeper into the borehole, one undulating at 15-20 mm distance to the main fracture (semi-parallel to this fracture). Another partly open fracture runs semi-perpendicularly to the main fracture. There are also calcite-filled microfractures in the cataclasite.

Overall interpretation

Fracture "A" in this investigation likely is a part of the target structure of the LTDE-SD investigations in Nilsson et al. (2010) and Widestrand et al. (2010a). However, the studied specimen has more cataclasite than the samples in Nilsson et al. (2010) and Widestrand et al. (2010a). The minerals in the greenish veins and cataclasite/mylonite in between the brownish cataclasite and the wall rock (epidote, chlorite and feldspar) and the calcite veins with chlorite and e.g. chalcopyrite+hematite, are in close resemblance to the observations in Widestrand et al. (2010a, Chapter 2) and Nilsson et al. (2010, Appendix 3). However, it seems as if the structure studied here has thicker epidote mylonite/ veins compared to the fractures in Nilsson et al. (2010) and Widestrand et al. (2010a), perhaps a matter of heterogeneity of the thickness along the structure. The thin calcite veins, with K-feldspar, chlorite, hematite, K-feldspar and chalcopyrite are nevertheless very similar in the studied specimen and the descriptions in Nilsson et al. (2010) and Widestrand et al. (2010a).

Another common feature is the very similar coating and wall rock alteration. However, this wall rock alteration feature is very common around fractures in the area and cannot be regarded as an undisputable tracer for the structure. The mineralogical and chemical composition matches quite nicely with the rock in Nilsson et al. (2010) and Widestrand et al. (2010a). The small deviations are probably due to the very small sample volume used in the chemical analysis in this study and the heterogeneity of the rock (large feldspar crystals etc.), that will have large effect on the composition.

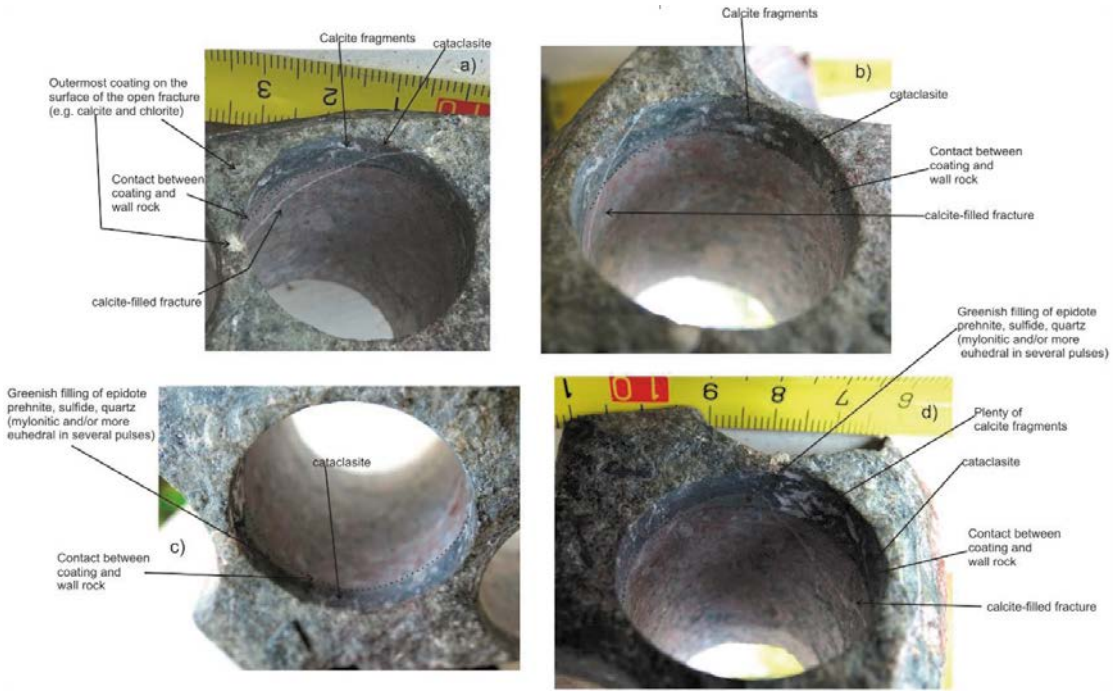

Figure A6-7. *Detailed description of DH-2, N wall (a), E wall (b), S wall (c) and W wall (d).*

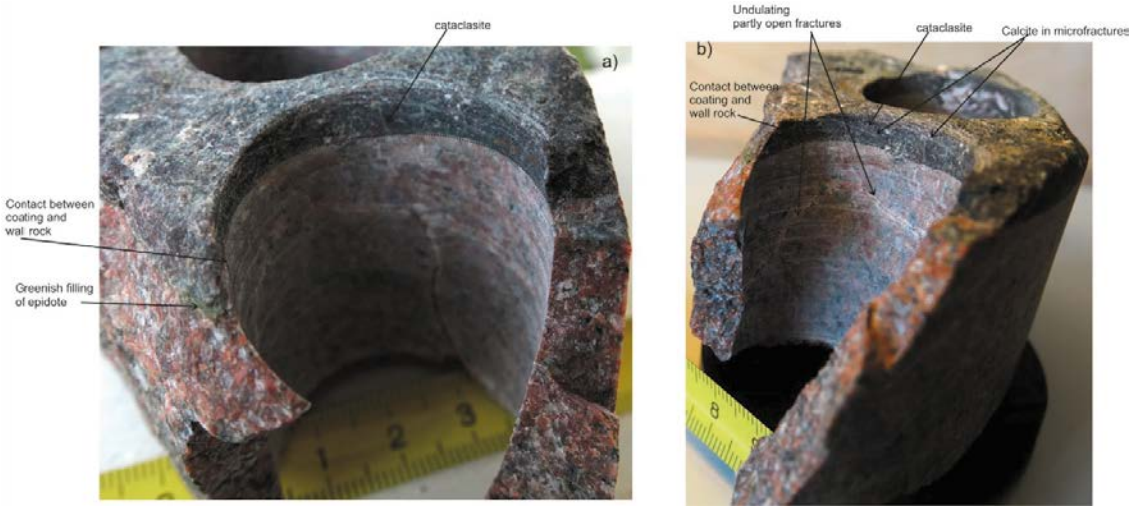

Figure A6-8. *Detailed description of DH-3, N and W wall (a) and SW wall (b).*

Appendix 7

Injected activity of Na-22

The text below corresponds to data delivery #17.

LTDE-SD (Task 9B): Update concerning tracer injection activity for ^{22}Na

Kersti Nilsson and Johan Byegård (Geosigma), 2017-03-17

Introduction

When looking at the data set for Task 9B (LTDE-SD), it was obvious that the amount of ^{22}Na present in the samples collected from the water circulating in the experiment section corresponded to a higher ^{22}Na activity than in the injected tracer cocktail, which is unreasonable. An updated value was presented at the SKB Task Force GWFTS Workshop in Helsinki in October 2016 by Johan Byegård, and is established in this memo.

Updated LTDE-SD tracer injection activity for ^{22}Na

In SKB report R-10-68 (Nilsson et al. 2010), the reported ^{22}Na injection activity was 3.2 MBq, which resulted in an unrealistic positive recovery compared with the ^{22}Na activity in the experiment section. When analysing the gamma spectrometry data again, it was discovered that the injected activity was underestimated (>20 %) since the measurements of the injection samples were performed in a geometry favouring summation effects in the HPGe measurement of ^{22}Na, see Figure A7-1 below.

Thus, the updated value for the amount of injected ^{22}Na is 3.8 MBq. In SKB Report R-10-67 (Widestrand et al. 2010), the reported recovery of ^{22}Na found in the a) water phase; b) the isopropanol solution used for removal of the water phase; c) desorbed by excess of Epoxy, was 100 %. Due to the fact that the injected amount of ^{22}Na now has been updated to a higher value, the new recovery value has been lowered to 85 %.

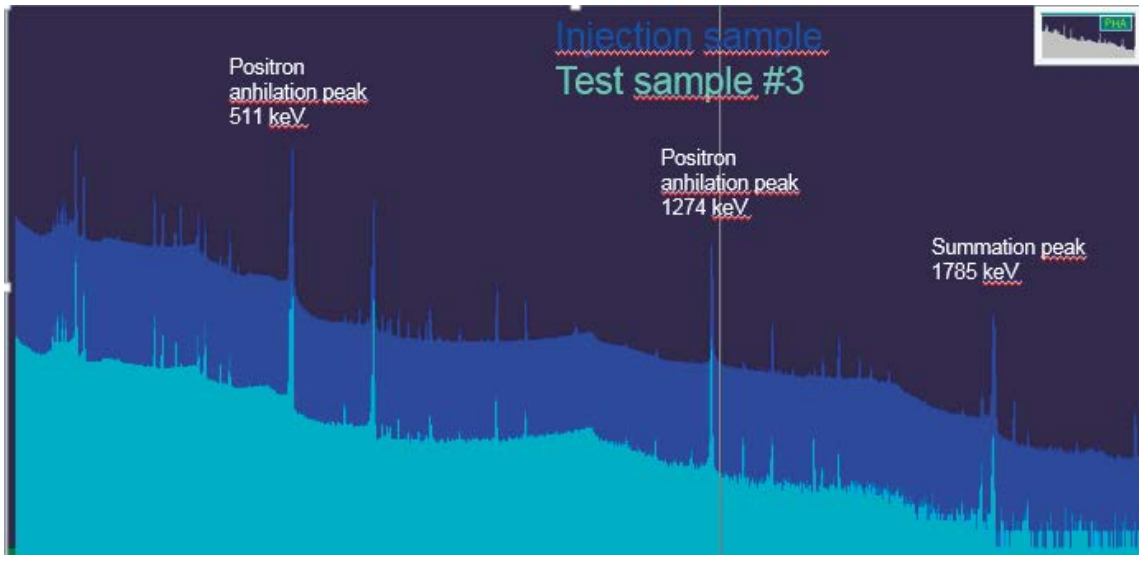

Figure A7-1. *Gamma spectrum for Test sample no 3 (light blue) compared with the injection sample (dark blue).*

Appendix 8

Geological description of the drill cores

The geological characterisation below corresponds to Appendix 1 of the Task 9B-3 description and concerns Task 9B-3 and the recently analysed core samples A4, A11, A13, D15, and D16.

The photos below are of lower resolution. A high resolution version of the appendix can be downloaded from the Task Force website (data delivery #16). In the photos of whole core samples, the exposed surface is to the right (at A). The photos of the recently analysed slices are always oriented in the same manner.

Core sample A4

General:

Remaining epoxy on the fracture surface, 100 %.

A 0-2 mm thick fracture coating covers approximately 70 % of the fracture surface.

Mineralogy:

Quartz, K-feldspar, plagioclase, biotite, chlorite, titanite, hematite/magnetite and epidote.

K-feldspar to varying extent albitized, biotite partially altered to chlorite and plagioclase is partially saussuritized, i.e. altered to epidote, sericite and albite. Titanite is probably hematite stained, visible as rusty colour around some of the mineral grains.

Fracture surface coating (A): chlorite, calcite, chalcopyrite ± pyrite ± epidote (see photo below).

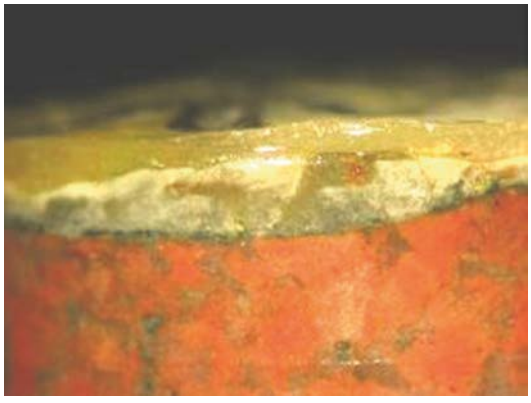

Fractures:

Two varieties of fractures:

a) Sealed, more or less parallel with the fracture surface (A). The largest one 3 cm from the fracture surface (A). These fractures form a circle around the core, but do not close the ends (see photo a) below). Red coloured according to small hematite grains in calcite.

b) Very thin sealed or partly open microfractures. Can be seen anywhere and at different orientations at the rock core (see photo b) below).

a)

b)

Wall-rock alteration:

Faint to medium degree of red staining, increasing towards the fracture surface (A).

When faint degree, merely a rust-coloured grain boundary.

Slices:

Core A4, cuboidal sample prior to further sawing into slices. 30 mm length, fracture coating to the right.

Photos of the first six A4 core slices.

A4.1. *The first rock slice is slightly irregular. Mainly consisting of fracture minerals (although the picture shows the opposite side, i.e. the wall rock side, fracture minerals are visible in the right lower corner), chiefly calcite and grains of chalcopyrite.*

A4.2. *Titanite is strongly altered, (weathered and decomposed).*

A4.3. *No specific notations*

A4.4.

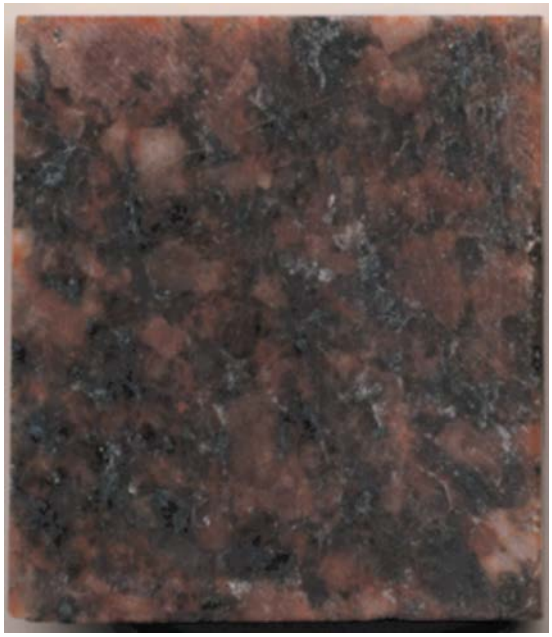

A4.5.

A4.6.

Core sample A11

General:

Epoxy covers 100 % of the fracture surface. Generally thin (≤ 0.5 mm), but irregular, fracture coating is observed at about 60 % of the fracture surface (A). Remaining 40 % seems to be without fracture coating.

Mineralogy:

Quartz, K-feldspar, plagioclase, biotite, chlorite, titanite, hematite/magnetite and epidote.

K-feldspar to varying extent albitized, biotite partially altered to chlorite and plagioclase is partially saussuritized, i.e. altered to epidote, sericite and albite. Titanite is probably hematite stained, visible as rusty colour around some of the mineral grains.

Fracture surface coating (A): Calcite and chlorite.

Fracture mineralogy for sealed and partly opened fractures: calcite, hematite, small amounts of chlorite, ± quartz (see photo b) below).

Fractures:

a) Partly open fracture at about 1.5 cm from the fracture surface (see photo a) below). Parallel (or subparallel) to (A).

b) A few sealed microfractures close to the fracture surface (A). Diagonal relative to the borehole axis.

c) Sealed and thin calcite filled fracture at 45° relative to the borehole axis.

a)

b)

Wall-rock alteration:

Red staining, from weak to medium the first 10 cm, i.e. closest to fracture surface (A) to no alteration towards (B).

Slices:

Core A11, cuboidal sample prior to further sawing into slices.30 mm length, fracture coating to the right.

Photos of the first six A11 core slices.

A11.1. *Epoxy cover on the opposite side. Grain boundaries partly porous.*

A11.2. *No specific notations.*

A11.3. *No specific notations.*

A11.4. *Few small microfractures.*

A11.5. *No specific notations.*

A11.6.

Core sample A13

General:

Epoxy covers 85 % of the fracture surface.

Fracture coating visible at about 45 % of the fracture surface, ≤0.2 mm thickness.

Mineralogy:

Quartz, K-feldspar, plagioclase, biotite, chlorite, titanite, hematite/magnetite and epidote.

K-feldspar to varying extent albitized, biotite partially altered to chlorite and plagioclase is partially saussuritized, i.e. altered to epidote, sericite and albite. Titanite is probably hematite stained, visible as rusty colour around some of the mineral grains.

Fracture surface coating: chlorite.

Fracture fillings (partly open fractures): chlorite and calcite.

Fractures:

a) 2 parallel to subparallel (to the fracture surface), partly open fractures at about 1 cm and 3 cm distance from the fracture surface (A).

b) 2 small partly open fractures cut approximately diagonal to the borehole axis at about 8 and 9 cm distance from the fracture surface (A).

Wall-rock alteration:

Faint to medium degree of oxidation (red staining).

Slices:

Core A13, cuboidal sample prior to further sawing into slices. 30 mm length, fracture coating to the right.

Photos of the first six A13 core slices.

A13.1. *No specific notations.*

A13.2.

A13.3.

A13.4.

A13.5.

A13.6.

Core sample D15

Mineralogy:

Quartz, K-feldspar, plagioclase, biotite, chlorite, titanite, hematite/magnetite and epidote.

K-feldspar to varying extent albitized, biotite partially altered to chlorite and plagioclase is partially saussuritized, i.e. altered to epidote, sericite and albite.

Fracture filling, sealed fractures: calcite and hematite ± quartz ± laumontite.

Fractures:

a) Microfractures, parallel to subparallel with the slimhole surface (A). Primarily visible in quartz and feldspars.

b) Sealed fracture visible at approximately 2.5 cm from (A), when core is rotated 0-135°. Angle, c. 60° to the borehole axis.

c) Partly open microfracture cuts the fracture described in b).

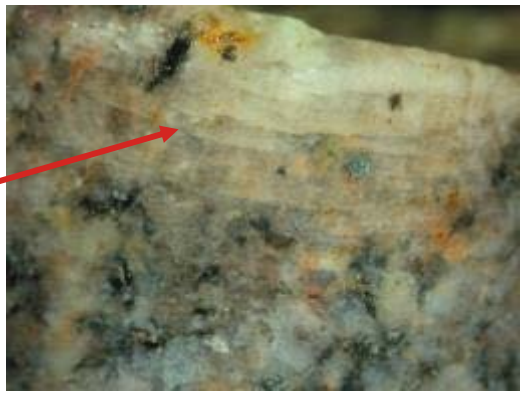

Wall-rock alteration:

Faint to weak oxidation (red staining) in the last part of rock core, c. 7–12 cm (towards B).

Slices:

Core D15, cuboidal sample prior to further sawing into slices. 30 mm length, slimhole rim to the right.

Photos of the first six D15 core slices.

D15.1.

D15.2.

D15.3.

D15.4.

D15.5.

D15.6.

Core sample D16

General:

Epoxy at the surface towards slimhole (yellow).

Mineralogy:

Quartz, K-feldspar, plagioclase, biotite, chlorite, titanite, hematite/magnetite and epidote.

K-feldspar to varying extent albitized, biotite partially altered to chlorite and plagioclase is partially saussuritized, i.e. altered to epidote, sericite and albite.

Fracture filling, sealed fractures: calcite and hematite ± quartz ±laumontite.

Fractures:

a) Partly open fracture at 6.5 cm from (A), perpendicular to the borehole axis.

b) Sealed fracture visible at approximately 0.5 cm from (B).

Wall-rock alteration:

Faint oxidation (red staining) at the last part of rock core, c. 7.5–13 cm (towards B).

Slices:

Core D16, cuboidal sample prior to further sawing into slices. 30 mm length, slimhole rim to the right.

Photos of the first six D16 core slices.

D16.1.

D16.2.

D16.3.

D16.4.

D16.5.

D16.6.

Appendix 9

Discussion on artefacts in LTDE-SD

The below text corresponds to data delivery #21.

Experimental artefacts with impact on penetration profiles, further details and discussions

Johan Byegård, Erik Gustafsson, Kersti Nilsson (Geosigma), 2017-08-28

Introduction

For the modelling of LTDE-SD results, it is of importance to be able to assess the impact of experimental artefacts as good as possible. At the Helsinki TF Workshop in October 2016, Johan Byegård (Geosigma) presented the experimentalist's views on aspects, which could be of importance, brought up earlier by Luis Moreno and Ivars Neretnieks. Accordingly, in this document the suggested artefacts are listed and an attempt is made to supply as much information as possible in order to facilitate their incorporation into further modelling. There might be more updates provided continuously during Task 9B.

The list of artefacts should not be seen as complete, and modellers are encouraged to ask more questions regarding the performance of the experiment.

Suggested important artefacts with impact on penetration profiles

Anomalous profiles with low tracer concentrations present far away from the stub/slimhole surface exist for Ba-133, Cs-137 and to some extent for Na-22 and Cl-36. The reason for absence of the other present tracers is a combination of lower activity used, sometimes higher detection limits and shorter half-lives causing decreased activity due to prolonged decay, but could of course also be due to different diffusion properties of the tracers.

A number of potential explanations for the presence of anomalous have been suggested and we will here discuss these:

Contamination from high to low activity zone

The drilling of the sample cores was made either in the direction high to low concentration or low to high concentration, see Table A9-1, and the equipment was thoroughly cleaned between drilling of each core. In addition, the cylindrical cores were, at a later stage, sawn to be square-cut in order to avoid any contamination on the drilled core surfaces (except core A10), see Figure A9-1.

Table A9-1. Summary of drilling directions for each core.

Direction low to high	Direction high to low
	A1 to A21
D1	D2
D3	D4
D5	D6
D7	D8
D9	D10
D11	D12
D13	D14
D15	D16

One hypothesis is that if there was contamination from high to low activity zone (combined with very low penetration into the inner part of the cores), the decrease of tracer concentrations would be more or less equal for all tracers, regardless of sorption strength and/or sorption mechanism. A preliminary investigation of two of the cores was made, comparing the Cs-137 (sorption presumed to be dominated by cation exchange) concentration decrease, relative to the Co-57 and Ni-63 (sorption presumed to be dominated by surface complexation) concentration decreases. The results showed a low correlation, cf. Figure A9-2, for cores A6 and A9. The detection limits of other tracers, presumed to sorb by surface complexation (i.e. Cd-109 and Gd-153), are even higher than for Co-57 and have therefore been omitted in the figures. This approach to check for contamination could possibly be taken further and be extended to comprise more cores and results.

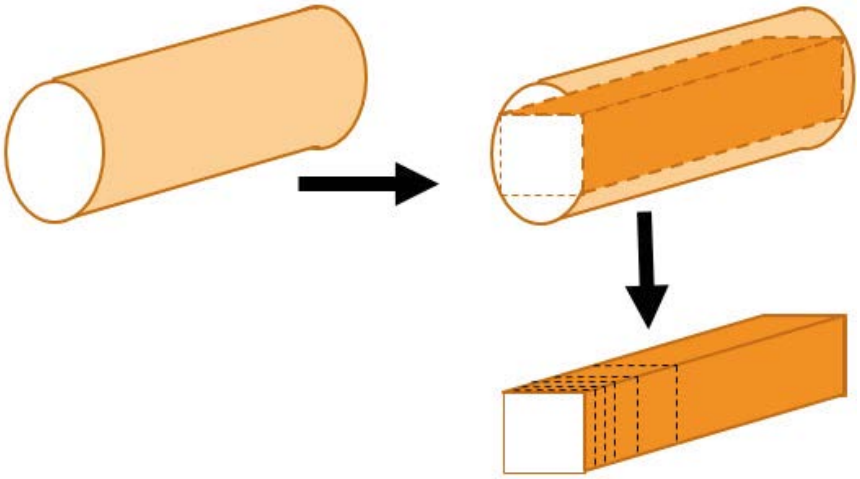

Figure A9-1. *Schematic drawing of the square-cutting into rods performed prior to slicing for the majority of the analysed A- and D-cores.*

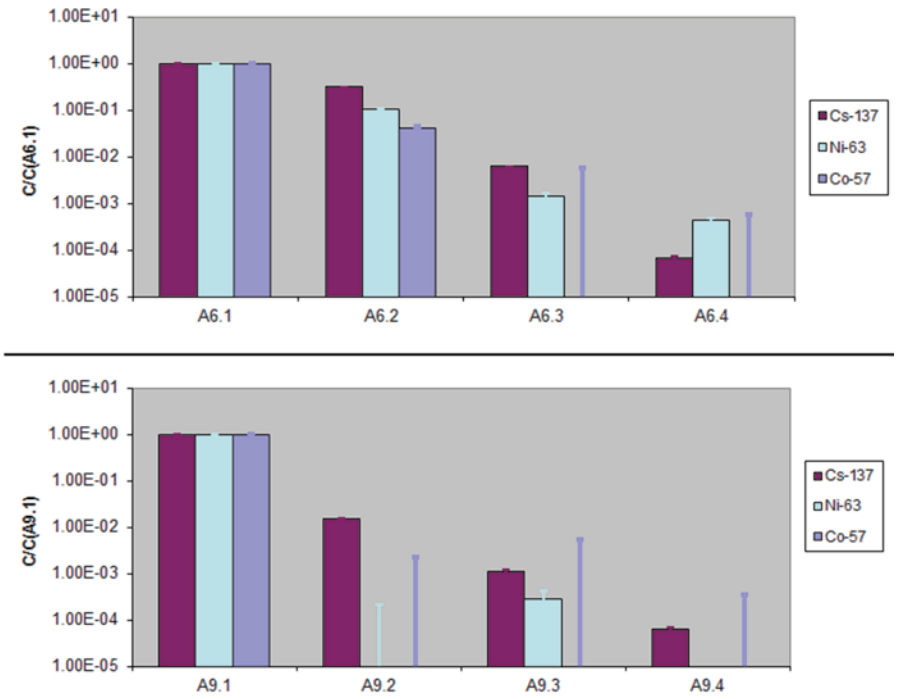

Figure A9-2. *Comparison of the relative decrease, in log scale, of Cs-137 and Ni-63 concentrations set to 1 in slice 1, followed by the three sequent slices in core A6 (top) and A9 (bottom).*

If there was contamination in the core drilling (of cylindrical cores) from high to low activity zone, one would also expect a clear difference between the tracer concentration results for the cores drilled in different directions. In Figure A9-3, the Cs-137 concentrations in cores drilled from low to high activity direction is shown on the left hand side and Cs-137 concentrations in cores drilled in the opposite direction is shown to the right. No significant difference in Cs-137 concentrations can be seen.

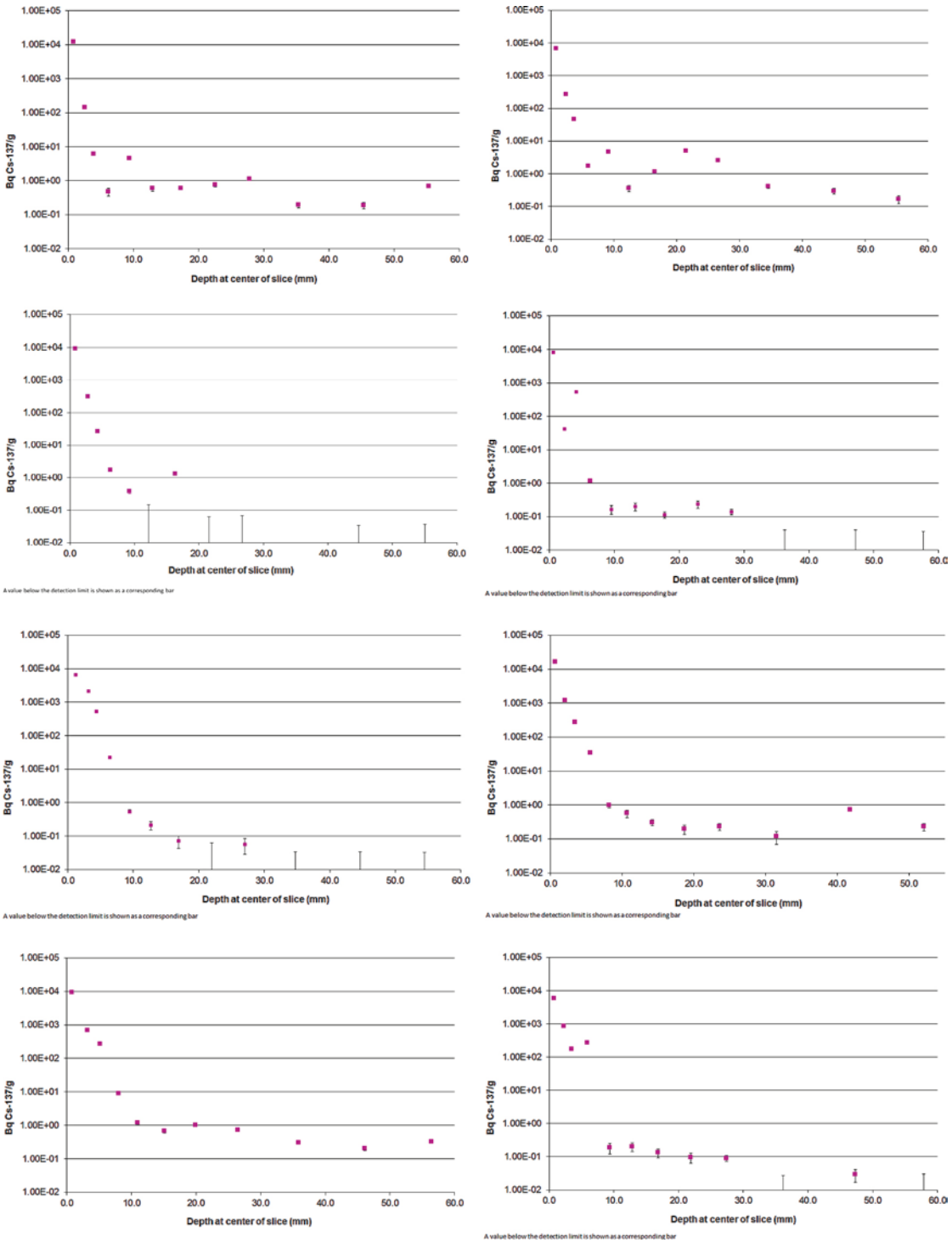

Figure A9-3. *D cores drilled from low to high activity (D1, D5, D7 and D13) to the left and from high to low activity (D6, D8, D12 and D14) to the right.*

However, since Cs-137 is present in all slices from the A20 core the presence of a low concentration contamination level due to diffuse contamination cannot be ruled out (see Figure A9-4).

Contamination in drill core A20

At the Helsinki meeting in October 2016, it was observed that the analyses of drill core A20, drilled from the outside of the polyurethane cylinder show rather high Cs-137 concentrations about four to six centimetres into the core, see Figure A9-4. In Figure A9-5, Na-22, Cl-36 (below the detection limits), Ba-133 and Cs-137 concentrations (Bq/g) are shown, normalized to the mean concentrations in slice A20:1 of the four tracers.

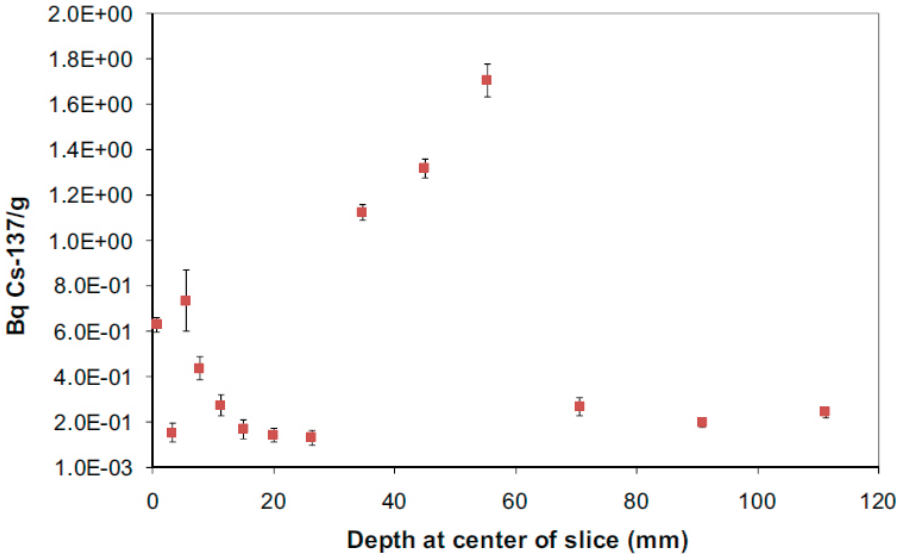

Figure A9-4. *Cs-137 in core A20 (core not exposed to the tracer solution, i.e. blank sample), presented in Nilsson et al. (2010, Appendix 11).*

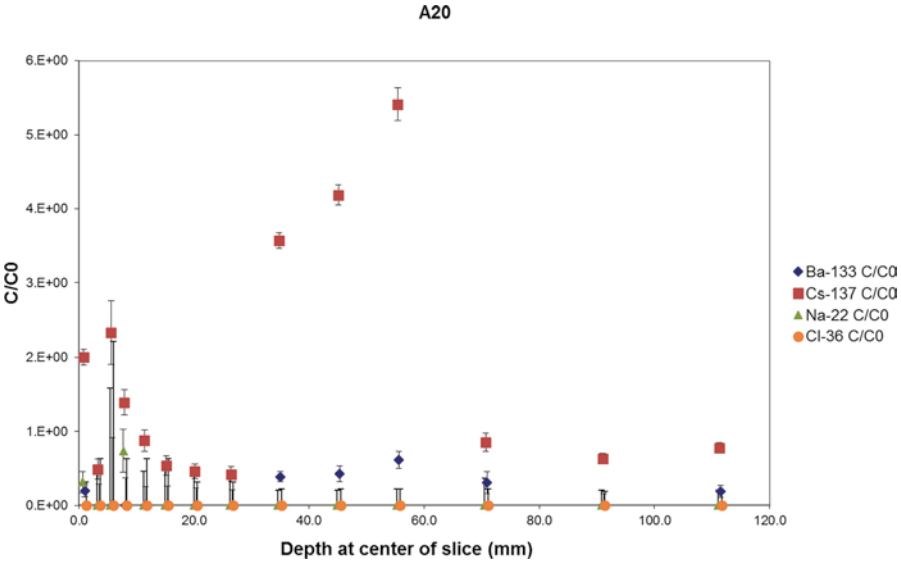

Figure A9-5. *Measured Cl-36, Na-22, Ba-133 and Cs-137 concentrations in core A20 (Bq/g), normalized to the mean tracer concentration (of all four tracers) in slice A20:1 (C_0; Bq/g). Concentrations below the detection limits for Cl-36, Na-22 and Ba-133 are shown as error bars starting on the x-axis.*

In three of the slices (number A20:9 to A20:11) at 35 to 55 mm core length, the relative Cs-137 concentration levels are elevated, and the relative Ba-133 concentration levels are slightly elevated. (Na-22 and Cl-36 concentrations are below the detection limits in these samples.) The fact that elevated relative concentrations coincide for Ba-133 and Cs-137 might point to contamination in these slices. Mean concentrations have been calculated, based on measured values in the three slices A20:9 to A20:11 (35 to 55 mm). These are displayed in Table A9-3.

However, concerning possible contamination, the procedure for slicing comprised that the cores were sliced one by one, and the flushing water was exchanged between each core. In the documentation of the mapping of the microfractures in the cores, two partly opened, thin fractures were found at a distance of 4.5 to 5.5 cm from the fracture surface. These positions correspond at least with slices A20:10 and A20:11. However, a transport route from the stub section along the border between the polyurethane cylinder and the rock matrix, is contradicted by the fact of absence of Na-22 and Cl-36 in these samples. This inconsistency is also relevant in case of contamination. A hypothesis is that the non-sorbing or very slightly sorbing tracers such as Cl-36 and Na-22 might have been flushed away together with the flushing water during the sawing of the slices. A contradiction to this is however, that Cl-36 could be found above the detection limits in all other A core samples located within the experimental volume of the stub.

The suspicion of contamination raises a question whether the presence of tracers in other slices in core A20, although at lower levels, could be caused by a diffuse contamination. In Table A9-3, a mean value or single value for the lower concentrations (present in other slices than A20:9 to A20:11) is reported for each tracer detected in core A20.

Table A9-3. Compilation of calculated mean concentrations for Na-22, Co-57, Ba-133, Cs-137 and Ra-226. Concentrations are shown from suspected major contamination, present in core A20 for penetration depths 35 to 55 mm together with concentrations calculated due to suspected minor contamination in A20, respectively.

Tracer	Concentration in A20 at penetration depth 35 to 55 mm (Bq/g)	Uncer-tainty (Bq/g)	Tracer present in slice number (35 to 55 mm)	Concentration in A20 at other penetration depths than 35 to 55 mm (Bq/g)		Uncer-tainty (Bq/g)
Na-22	-			0.17	(A20:1, A20:4)	0.14
Co-57	1.9	0.8	A20:9, A20:11	-		
Ba-133	0.15	0.07	A20:9, A20:10, A20:11	0.07	(A20:1, A20:12, A20:14)	0.06
Cs-137	1.4	0.3	A20:9, A20:10, A20:11	0.3	(A20:1-A20:8; A20:12-A20:14)	0.3
Ra-226	11	2	A20:11	-		

Interference in the analyses?

The large number of present radionuclides provides a risk for a general increase of the background level in the spectrum causing increased detection limits for radionuclides present in comparatively low concentrations. However, interference between peaks of different radionuclides is very uncommon when applying the HPGe high resolution gamma spectrometry technique. Consequently, erroneous results due to interferences of the peaks of Ba-133 and of Cs-137 from the peaks of Na-22 can be ruled out since these peaks are well separated.

For the non-gamma decaying radionuclides Cl-36 and Ni-63, measurements were performed using liquid scintillation counting (LSC). Prior to the measurements, Cl-36 was separated by AgCl(s) precipitation, after that dissolved in NH_3(aq) and thereafter measured by LSC. Ni-63 was separated by Ni-dimethylglyoxim precipitation, dissolved by 3 M HNO_3, and then measured by LSC. The results were carefully checked for interferences in the separation procedures.

Capillarity caused by drying at the surface?

Ivars Neretnieks made a presentation at TF#34 in Prague of the results from an experiment, demonstrating the effects of a drying front, using paper chromatography. The results showed that substances are indeed transported by drying at the surface. However, the direction is towards the drying front.

Drying could have taken place during two different stages after the over core drilling and before slicing of the cores.

At the stage before core drilling, this provides a gradient towards the surface for the A-cores, and not into the rock matrix. For the D-cores, the drying front is in the opposite direction (from outside of the large diameter core surrounding the slim hole test section and towards the slim hole). However, the surface of the 300 mm core is very far from the bulk of the tracers, which are present mainly at the surface of, or close to the slim hole. Consequently, a drying front is less probable to have caused any transportation of the bulk of tracers present at the stub- or slimhole surfaces into the rock matrix.

At the stage when the cores had been drilled but before slicing (stored in reasonably tight plastic bags), the most probable locations of drying fronts are very difficult to guess. However, the largest area is along the mantle of the core, while the end surfaces are smaller, which should imply a larger probability for drying fronts perpendicular the core axis. Except very close to the end surfaces, where tracer transport should be directed towards the end surface, the tracer transport would thereby not generally take place along the core length, but more or less perpendicular to the core axis.

Can "after-diffusion" during the long period after over-coring lead to the strange profiles?

The diffusion process is likely to continue after the termination of the experiment. However, it is still an open question whether after-diffusion is likely to cause the unexpected profiles or not. The times for slicing etc. are provided in the 9B-2 Task Description, Appendix "*LTDE-SD Timeline, Core Storage, and Decay Correction*" (i.e. Appendix 1 of this present report) if one wants to investigate the effects to some extent. In Figure A9-6 below, a spot check of Na-22 and Cs-137 penetration in two samples is shown. Sample A12 was sliced in November 2007 and sample A6 was sliced in February/March 2008. No other cores with different times for slicing have been compared.

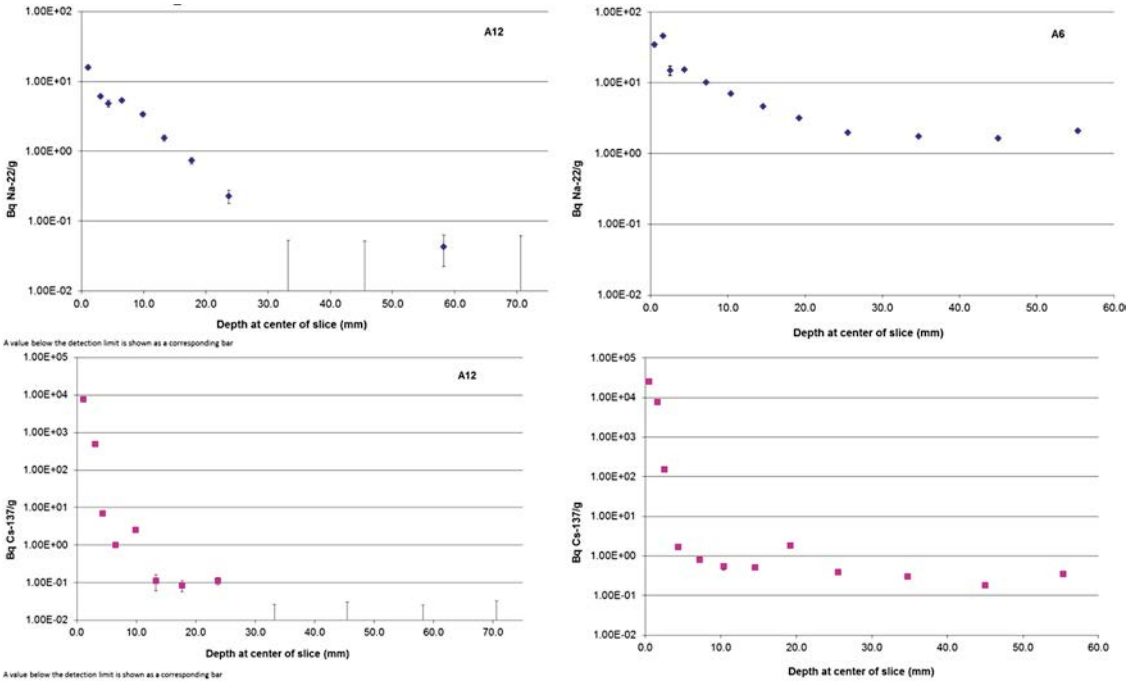

Figure A9-6. *Comparison between Na-22 (top) and Cs-137 (below) in a sample (A12, left) sliced in November 2007 and a sample (A6, right) sliced in February 2008.*

Can the multicomponent diffusion (Maxwell-Stefan) effects be important?

When planning the experiment, the intention was to not affect the chemical composition of the groundwater by addition of the tracer cocktail, i.e. not increasing the natural chemical concentrations. In cases where this was not possible, the addition of tracers was restricted to not cause a chemical elemental concentration higher than 1E-6 M.

Summary

Table A9-4. Summary of possible impacts of artefacts and suggested actions.

Section/Process	Status	Suggested action within TF
Contamination from high to low activity zone	No obvious	Rule out
Sawing slices	Roughly uniform presence of sorbing tracers in centre of A20 is suspicious? Risk of a) Diffuse contamination. b) Possibility of an alternative transport route from the stub section In both cases Na-22 and Cl-36 concentrations below the detection limit is inconsistent with the assumptions.	Cannot be ruled out. Risk of diffuse contamination at the following levels: Na-22: 0.17 Bq/g Ba-133: 0.07 Bq/g Cs-137: 0.3 Bq/g
Interferences	Unlikely for gamma spectroscopy. QA checks during scintillation counting for any such effects.	Rule out
Capillarity	Mechanism has been demonstrated but expected transport directions not consistent with possible artefacts.	Rule out?
After diffusion	Core history available for modelling of after-diffusion. Spot check comparison of Cs-137 and Na-22 in core A6 and A12 may show some differences.	Option to model
Multicomponent diffusion	Planning of cocktail to minimise changes in groundwater composition: C< 1.E-6 M	Rule out

Appendix 10

Pressures in LTDE-SD

In the Äspö Hard Rock Laboratory the hydraulic gradient is towards the tunnel system. The LTDE-SD experimental test sections (slim hole and stub) are located at about 11 metres into the rock from a niche in the main tunnel, see Figure A10-1. Outside the test sections the experimental borehole (KA3065A03) was packed off with one mechanical and two inflatable packers to avoid hydraulic gradients in the test sections, see Figure A10-2. Also, the exploration borehole KA3065A02 and all other nearby boreholes were packed off by packers. Pressures were monitored in the test sections and packed off borehole sections. An elaborate pressure regulating system (Figure A10-3) was used to keep the pressure in the test section somewhat lower than the pressure in the first guard section (P ref) to avoid advective transport of tracers from the test sections into the rock.

The hydraulic conditions were stable during the experiment, apart from short pressure disturbances mainly due to injection and sampling occasions in the borehole, see Figure A10-4. The pressure in the test section (KA3065A03a1; location seen in Figure 10-2) varied between 3580 and 3600 kPa and was kept c. 20 kPa lower than the pressure in the first guard section (KA3065A03a2). The pressure in the second guard section (KA3065A03a3) was only slightly lower, c. 1 kPa, than the pressure in the first guard section. The pressure in the third guard section (KA3065A03a4), ranging 4,26–7,98 m from the tunnel wall was lower than in the first and second guard sections but c. 2 kPa higher than in the test section (KA3065A03a1).

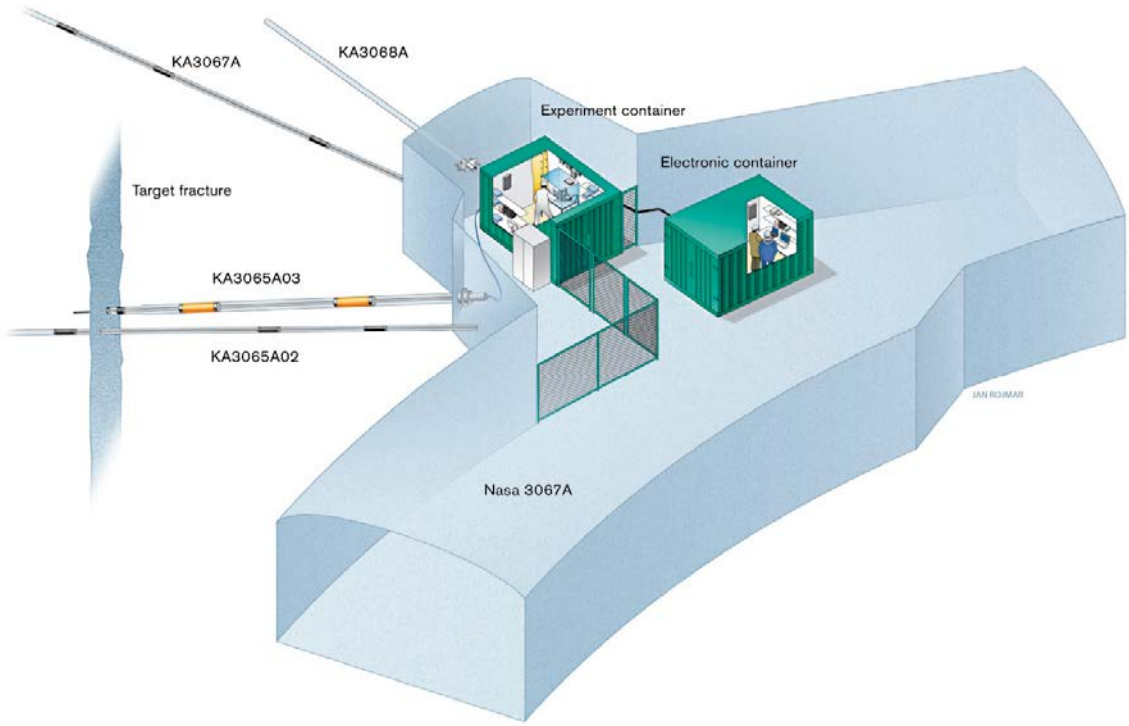

Figure A10-1. *The LTDE-SD experimental site and borehole layout in Äspö HRL.*

The LTDE-SD area is surrounded by two dominant conductive structures, NW-2 and NW-3. The conclusion from the hydraulic pre-tests (Wass 2005) was that the NW-2 and NW-3 and related structures are of vital importance for the hydraulic pressure in the LTDE-SD boreholes, therefore no drilling or opening of boreholes were allowed in these structures during the in-situ experiment. The first guard section in KA3065A03 (KA3065A03a1) and the third section in the exploration borehole (KA3065A02a3) are both interpreted to intersect NW-3. As can be seen from figures A10-4 and A10-6 the pressures in these two sections were close and well correlated. The exploration borehole (KA3065A02) reaches further into the rock than the experimental borehole and as expected the pressures in the innermost sections in KA3065A02 (KA3065A02a1 and KA3065A02a2) are respectively 26 and 10 kPa higher than in section KA3065A02a3.

Table A10-1. Pressure monitoring sections in KA3065A03.

Section	From (m)	To (m)	Comments
KA3065A03a1	10.737	11.23	Experiment section (stub and slimhole test sections).
KA3065A03a2	10.39	10.737	First guard section
KA3065A03a3	8.98	10.23	Second guard section
KA3065A03a4	4.26	7.98	Third guard section

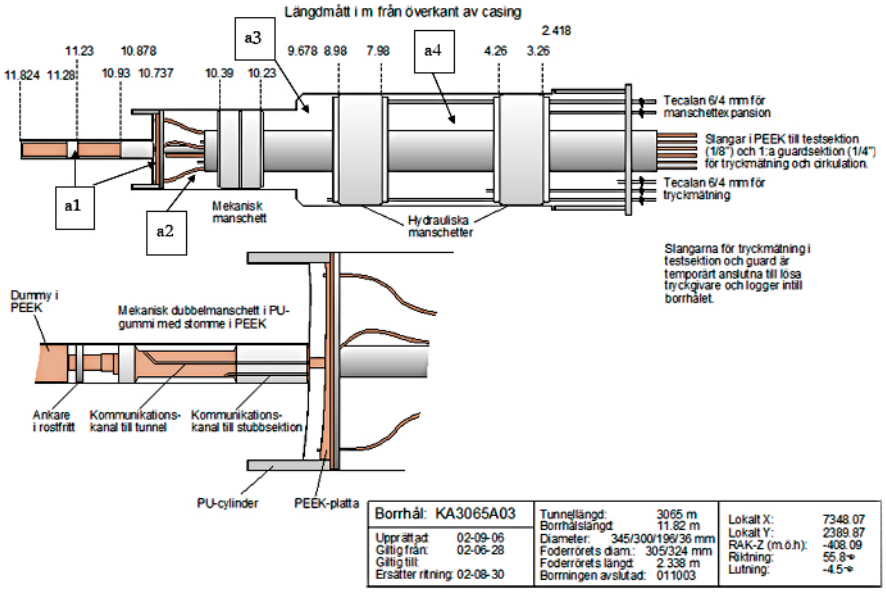

Figure A10-2. *Packer installations in KA3065A03.*

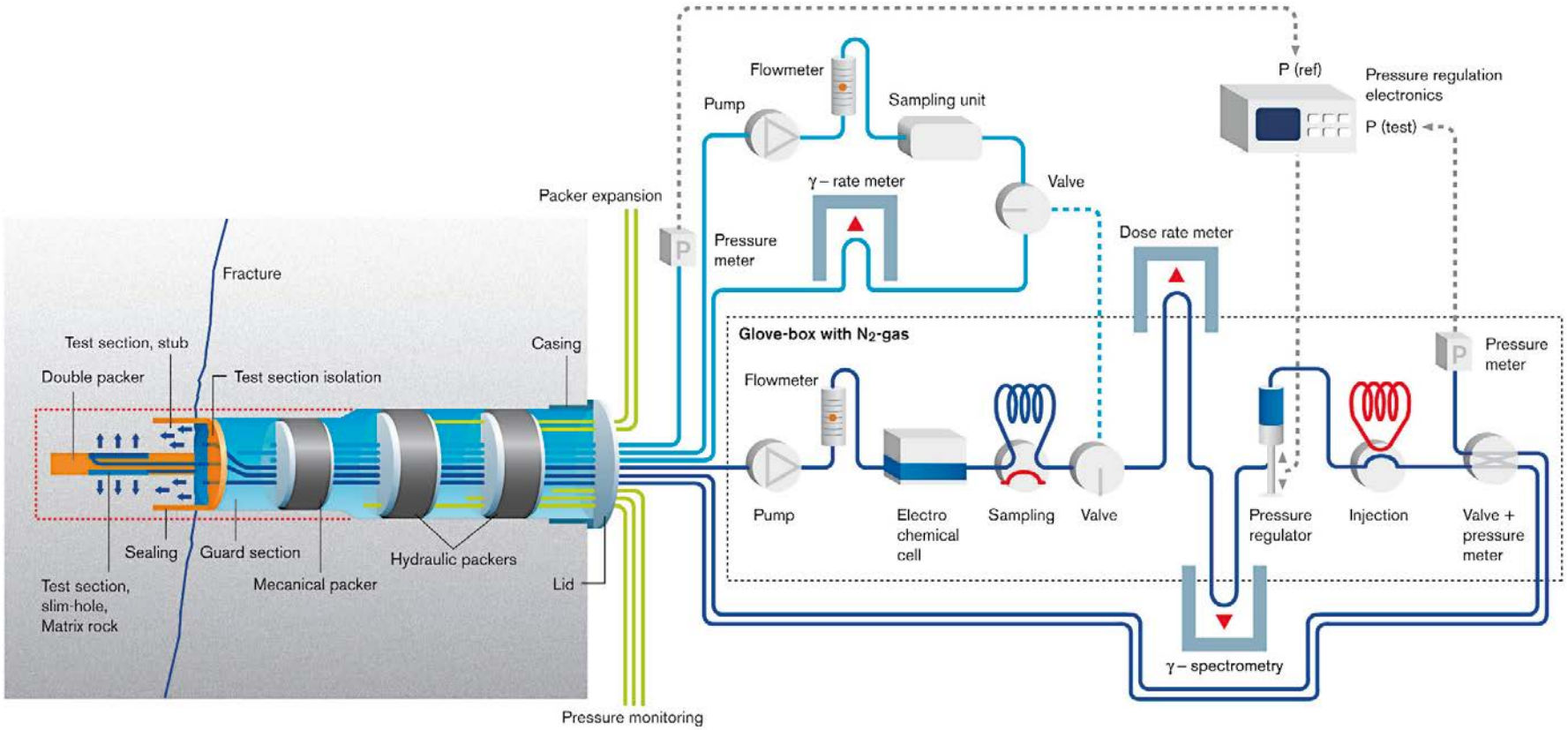

Figure A10-3. *LTDE-SD experimental set-up including packers, pressure regulation and measurement and injection/sampling possibilities.*

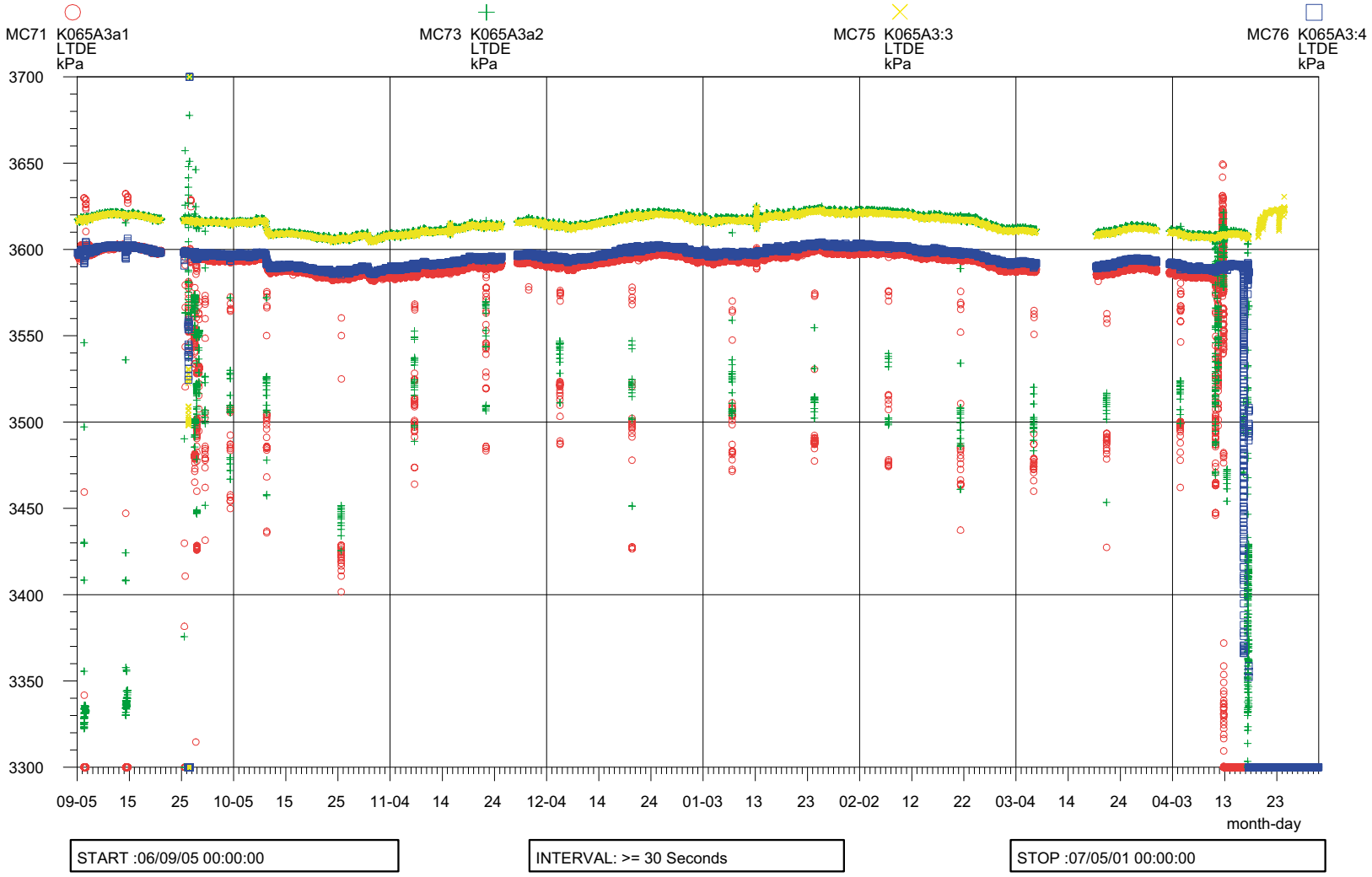

Figure A10-4. *Pressures (kPa) in the LTDE-SD Experiment borehole, KA3065A03.*

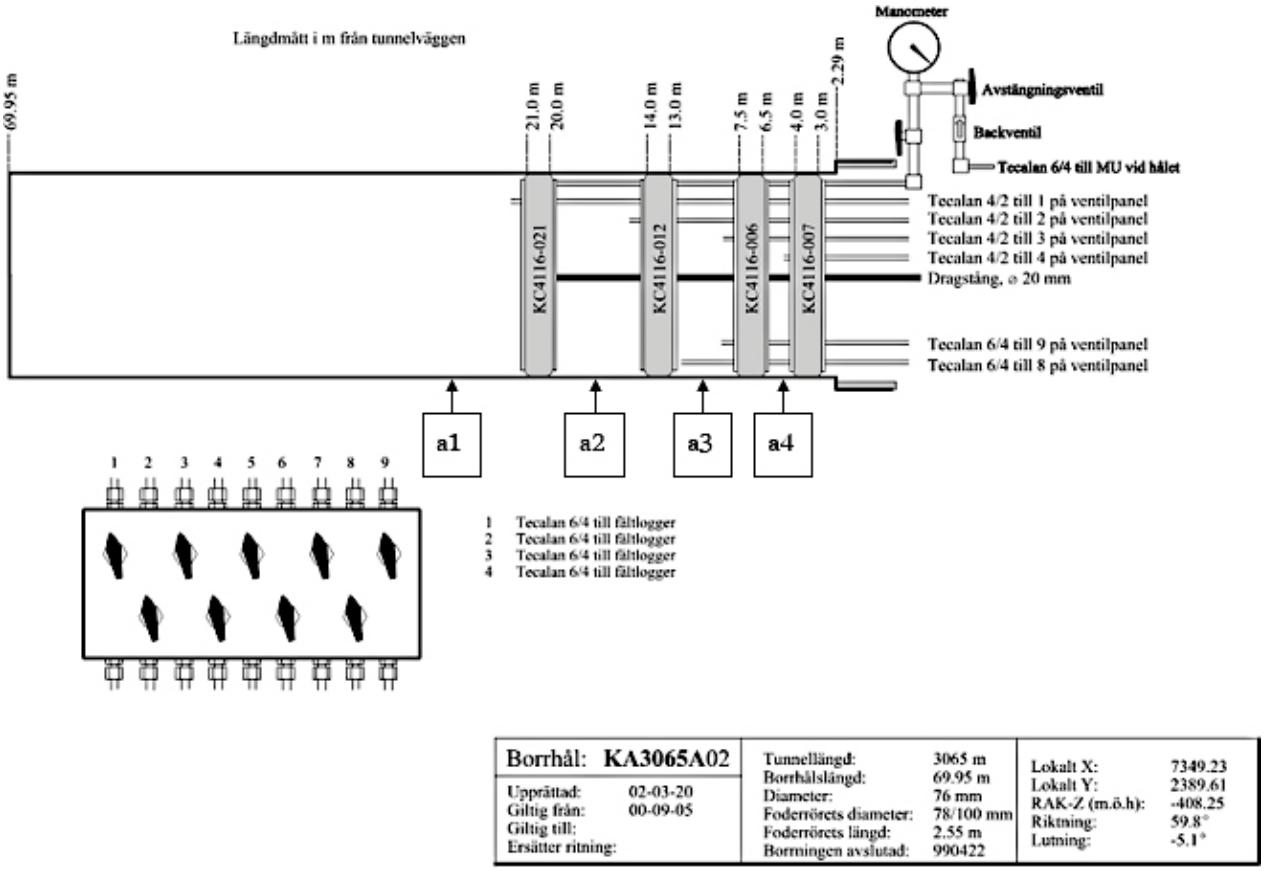

Figure A10-5. *Packer installations in KA3065A02.*

Table A10-2. Pressure monitoring sections in KA3065A02.

Section	From (m)	To (m)
KA3065A02a1	21.0	70.0
KA3065A02a2	14.0	20.0
KA3065A02a3	7.5	13.0
KA3065A02a4	4.0	6.5

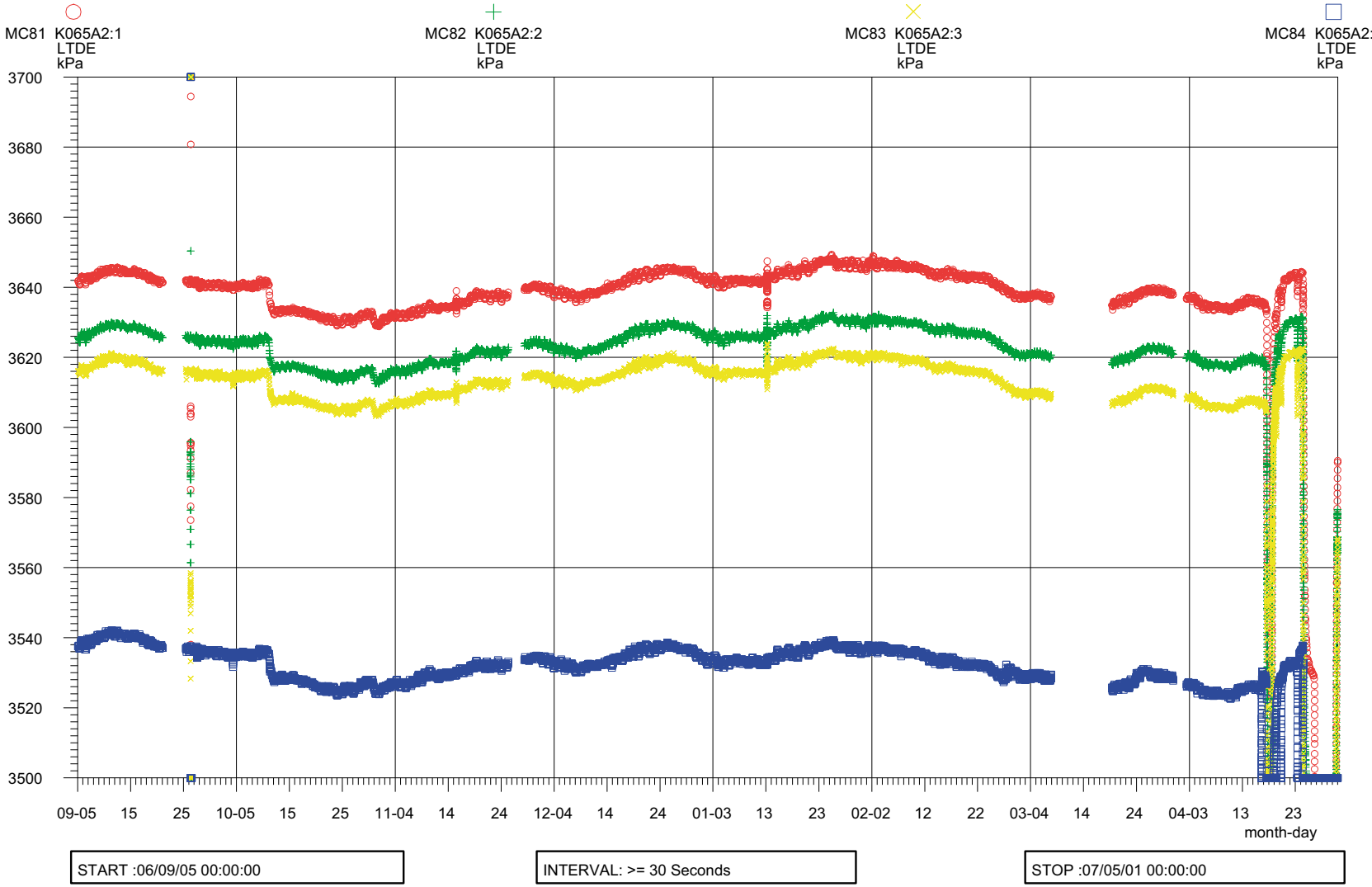

Figure A10-6. *Pressures (kPa) in the LTDE-SD exploration borehole, KA3065A02.*

Appendix 11

Concerning mass balances in LTDE-SD and potentially underestimated sorption

After the end of the circulation phase (6 months), some activities were initialized in order to prepare for over-coring of the rock. The aims of these activities were to:

- Empty the electrochemical flow cell and to study the adsorption on the flow cell (and circulation lines/tubings), i.e. to obtain information to explain the differences observed between the on-line and sample measurements.
- Remove the remaining aqueous phase containing the radioactive tracers. i.e., inject a "pure" liquid that should replace the original water phase. Isopropanol was selected as exchanging liquid, due to:
  - Expectation that a less polar liquid like isopropanol wold not cause desorption of adsorbed tracers like a more polar liquid like e.g., distilled water.
  - Expectation that flushing of the rock surfaces with isopropanol would give better adhesive properties for the Epoxy during the subsequent Epoxy injection.
- Inject Epoxy resin, with the aim to increase the mechanical strength of the rock during over-coring of the drillhole and to protect the water-rock interface of stub and slim hole test sections from flushing water used for over-core drilling.

Electrochemical flow-cell - adsorption

In Figure A11-1, the degree of sorption is shown for the tracers possible to measure using g-spectrometry; measurements were reported by comparing the activity of the tracers after the original water phase had been removed (i.e., the adsorbed amount of tracers) with the activity obtained when the flow cell was filled with water (i.e., the activity from the adsorbed amount plus the tracers present in the aqueous phase). It is shown that the tracers expected to be dominated by a strong surface complexation mechanism (e.g. Gd(III), Hf(IV), Sn(IV), Cd(II), Co(II), Ag(I)) undergo a very strong adsorption to the PEEK-lines. Based on the reported difficulties of maintaining the reducing conditions in the equipment, it is likely that iron oxide films have formed on the inside of the PEEK equipment and that the observed adsorption actually is a result of the interaction of the surface-complexation-sorbing tracers with surface deposits of iron oxides. The tracers that are expected to be dominated by a cation exchange mechanism (e.g. Na(I), Ba(II), Sr(II), Cs(I)) show none or very low interaction with PEEK surfaces which is in line with the possible explanation of equipment adsorption as a result of interaction with iron oxide.

The adsorption found for SeO_4^{2-} is more difficult to explain. It is possible that parts of the injected Se was present as (or was reduced to) SeO_3^{2-}, which from the literature is known to interact with iron oxides. The $^{226}Ra^{2+}$ is measured using its daughter radionuclide $^{214}Pb(II)$ and it is possible that the sorption is overestimated due to the fact that radioactive equilibrium was not obtained and since $^{214}Pb(II)$ is more sorbing than $^{226}Ra^{2+}$.

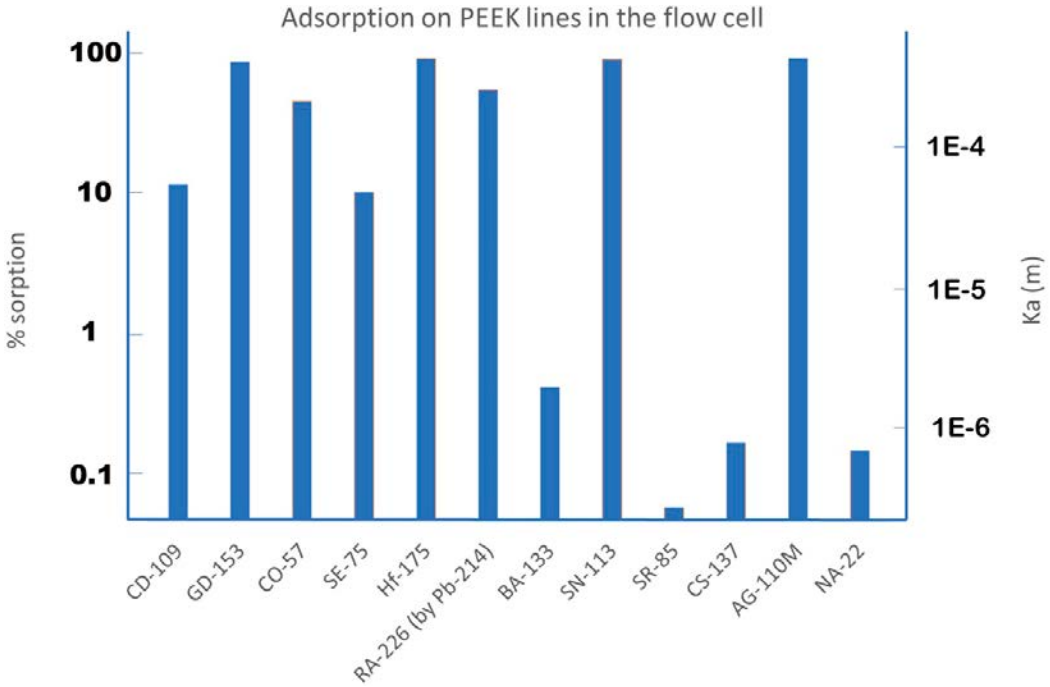

Figure A11-1. *Degree of sorption of tracers on PEEK lines/tubings in the electrochemical flow cell. The degree of sorption is given both as percentage of total amount of tracers being adsorbed as well as given as Ka (m), i.e., tracer surface concentration (Bq/m^2) divided by the tracer concentration in the water phase (Bq/m^3). The number gives the relation of tracers in the on-line measurement cell; a) the measured amount of tracers after the cell had been emptied of the tracer groundwater, divided by b) the measured amount of tracers before the cell had been emptied of tracer groundwater.*

Isopropanol injection

The injection of isopropanol aimed to remove and exchange the remaining water phase from the circulation equipment of the experiment and to prepare the rock surface to become more adherent for the Epoxy resin. (There were reasons to expect that isopropanol would cause less desorption of weakly sorbing tracers (e.g., Na-22) during the exchange process compared to e.g. an exchange performed with synthetic groundwater), cf. Figure A11-2 below, from SKB Report TR-98-18.

The results of the injection of isopropanol for the g-emitting tracers are shown in Figure A11-3. Very different behaviour is shown for the different tracers, which shows that the isopropanol injection process was not a chemically inert dissolution process but instead the different tracers were desorbed to different degrees. It was thus obvious that the isopropanol exchange suffered from the same characteristics as observed in the laboratory batch sorption experiment; desorption occurs in the isopropanol rinsing similar to what has been observed for rinsing using distilled water.

It has been assumed that the behaviour of the anion SeO_4^{2-} represents a pure dilution process (and relative concentrations higher than the one for SeO_4^{2-} represents desorption). Calculations have been performed from batch number 4 onwards. The earlier batches were excluded since these samples showed similar results for all tracers. Relating this amount of tracer to the adsorbed amount of tracer calculated from the concentration decrease gives that the following amounts of tracers were desorbed during the isopropanol rinsing: Na 29 %, Co 0.2 %, Sr 4 %, Cs 1 %, Ba < 0.3 %, Cd 0.8 %. One can observe a correlation between weaker sorption from the aqueous phase and stronger desorption in the isopropanol phase.

A comparison of the measurement of the flow cell before (corresponds to the data given in Figure A11-1) and after the isopropanol rinsing is made in Figure A11-3. It is also here obvious that the isopropanol is causing desorption of the cation exchange sorbing tracers and that tracers adsorbed by surface complexation undergo a very minor (if any) desorption during the isopropanol exchange.

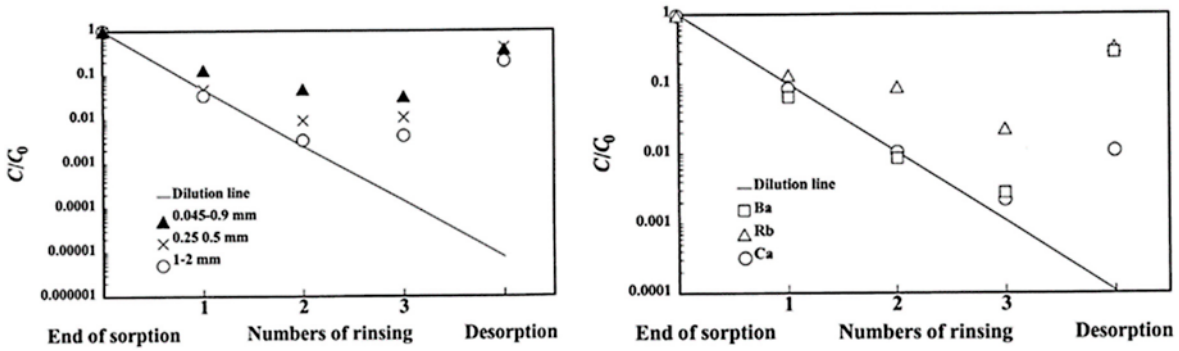

Figure A11-2. *Illustration of the desorption behaviour during rinsing processes in batch sorption/ desorption experiments (From SKB Report TR-98-18). After the sorption phase of the experiment, the crushed material was repeatedly exposed to distilled water rinsing (aimed to remove the original tracer cocktail solution) followed by an addition of desorption solution. In case of no desorption, the measured concentrations of the tracers should follow the dilution line; any deviation from that line is indicative of desorption taking place. Left: behaviour of* Cs^{+} in different *size fractions of the rock material. Right: comparison of the behaviour of* Ca^{2+}, Rb^{+} *and* Ba^{2+} *in a 1-2 mm size fraction experiment.*

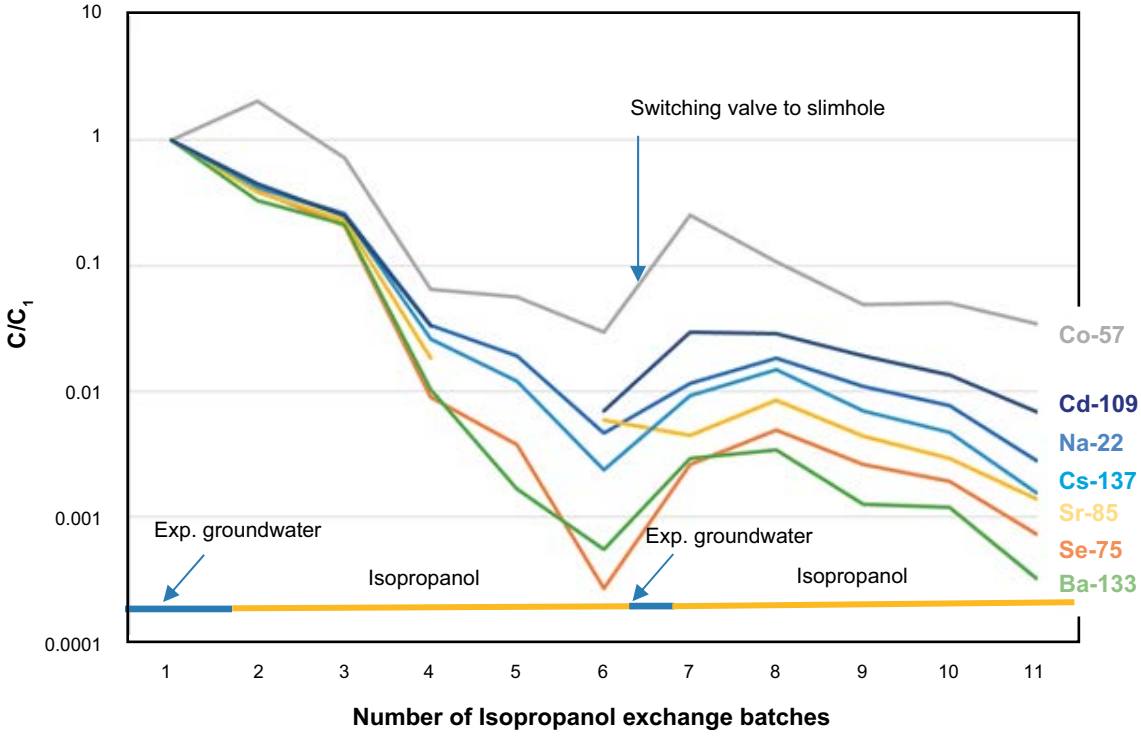

Figure A11-3. *Relative concentrations for different isopropanol batches during the isopropanol injection process.* C/C_1 *is the measured concentration of tracer divided by the concentration in the first sample. The bottom line gives the expected outcome in the different samples (each batch consisting of 330-390 ml) provided that a plug flow is obtained, i.e., whether the outflow in the different samples consists of isopropanol or experimental groundwater. Due to the experimental setup of the equipment, a switching of the valve was necessary to be performed at about the middle of the process so that also the slim section could be emptied; this is the major reason for the observed increase of the concentration in batches 6 to 7.*

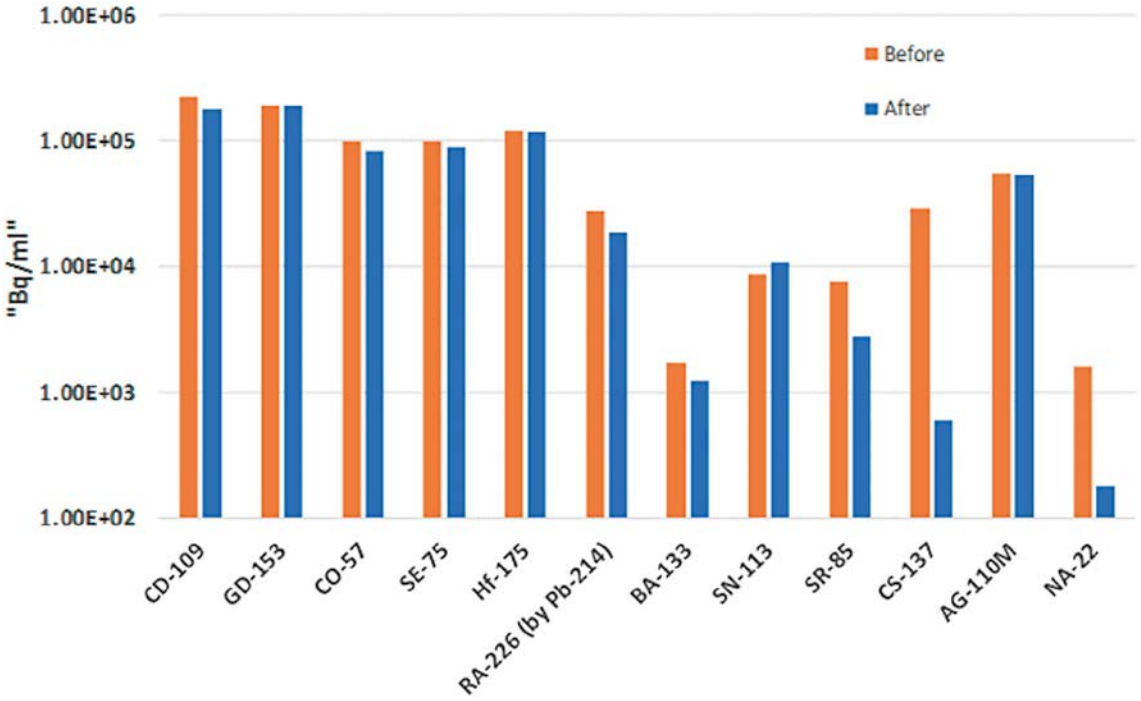

Figure A11-4. *Concentrations of tracers in the measurement on-line cell, before and after isopropanol was used for rinsing of the experimental section and had passed the on-line measurement cell.*

Injection of Epoxy resin

After the rinsing of the system with isopropanol, injection of liquid epoxy resin was performed. Before the injection, as much circulation equipment as possible was disconnected in order to ensure that filling up of the borehole sections would be obtained before the resin had cured.

When the resin had filled up the borehole and had returned through the lines to the injection point, measurements using portable equipment indicated an increased g-dose rate in the front between the isopropanol and the Epoxy resin, which was quite unexpected. Targeted measurements indicated that the activity was not in the Epoxy resin in the bottom of the sampling bottle (cf. Figure A11-5) but instead was in the entire bottle, thus indicating that the activity was transported in the Epoxy front in contact with the isopropanol.

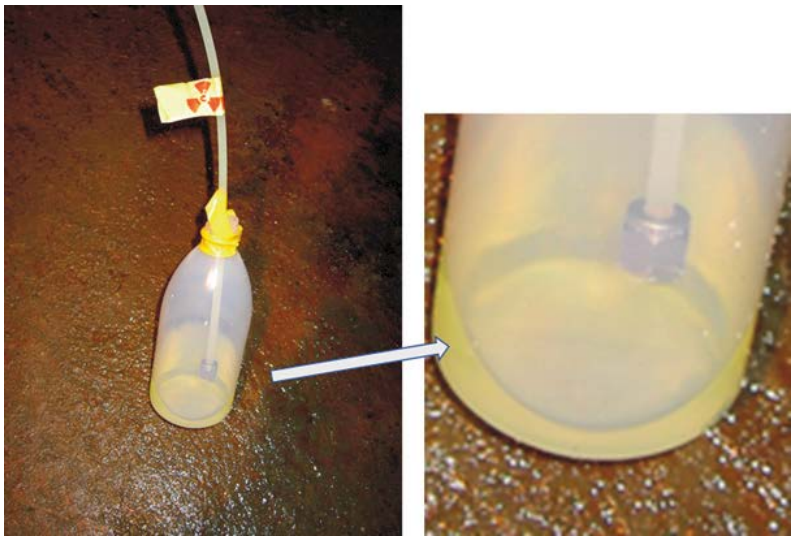

Figure A11-5. *Mixture of isopropanol and Epoxy resin leaving the slim-hole via tubings.*

During the injection of Epoxy resin, a non-aqueuos liquid, it was not expected that any desorption of the adsorbed tracers would occur. But, when adding data from the Epoxy batch to the diagram in Figure A11-3, shown in Figure A11-6, an essential increase of all tracer activities can be seen.

Possible explanation for the release of tracers by the Epoxy injection

Three different explanations/hypothesis for the increase of the relative tracer concentrations in the combined batch of Epoxy and isopropanol, seen in Figure A11-6 are addressed below:

- Mechanical processes (I)
- Mechanical processes (II) and
- Chemical processes

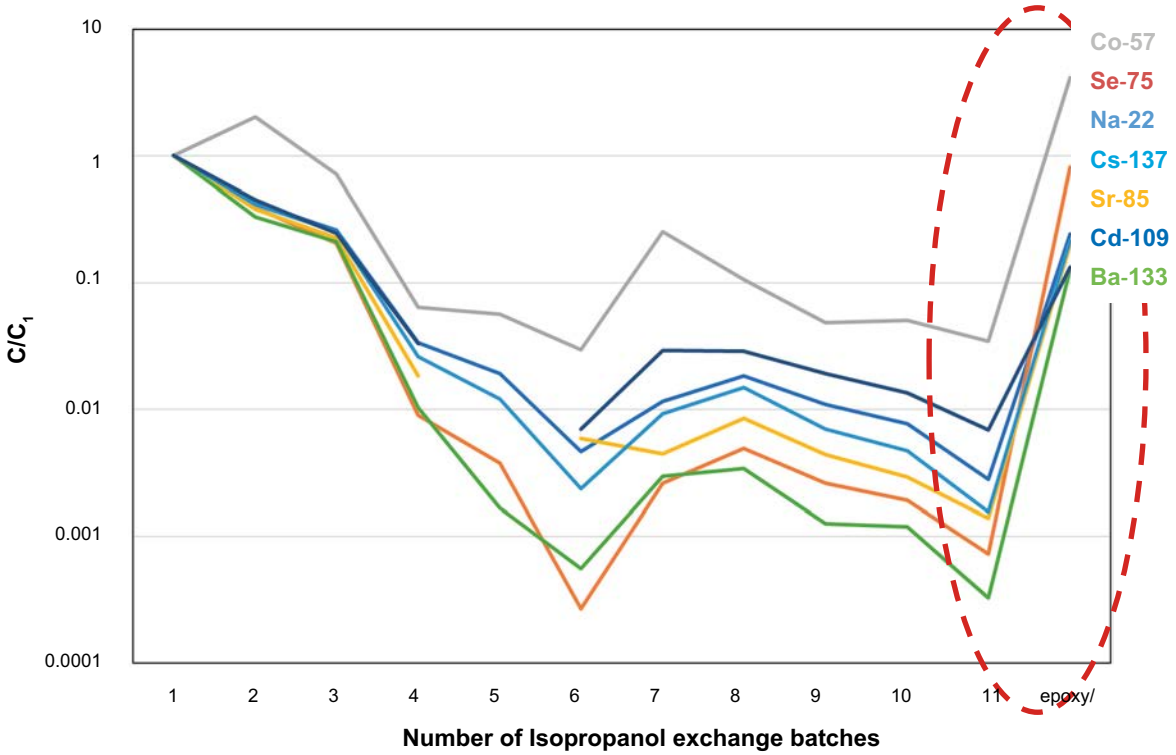

Figure A11-6. *Relative concentrations for different isopropanol batches during the isopropanol injection, including the last batch where the Epoxy front is present.*

Mechanical processes (I)

One mechanical process could be that the non-cured Epoxy solution reaches non-mixed ”pockets” (e.g. due to density differences) in the circulation line and mixes with experiment water not reached during the isopropanol exchange. In that case, the expected result would be a concentration in the Epoxy proportional to the concentration in the circulated water phase at the end of the experiment, i.e., C_{epoxy}/C_{end} would be equal for all tracers. In Figure A11-7, it is seen that this is not the case, so this hypothesis cannot be verified.

Mechanical processes (II)

A second proposed mechanical process would be that the non-cured Epoxy solution causes release of loosely consolidated micro-particles (from the rock surfaces and/or the PEEK surfaces of the equipment). In that case, the expected result would be tracer concentrations in the Epoxy proportional to the sorbed amount of tracer, i.e. A_{epoxy}/A_{ads} equal for all tracers, see Figure A11-8. However, since the values vary in orders of 6 magnitudes for the different tracers, there is no support for this hypothesis.

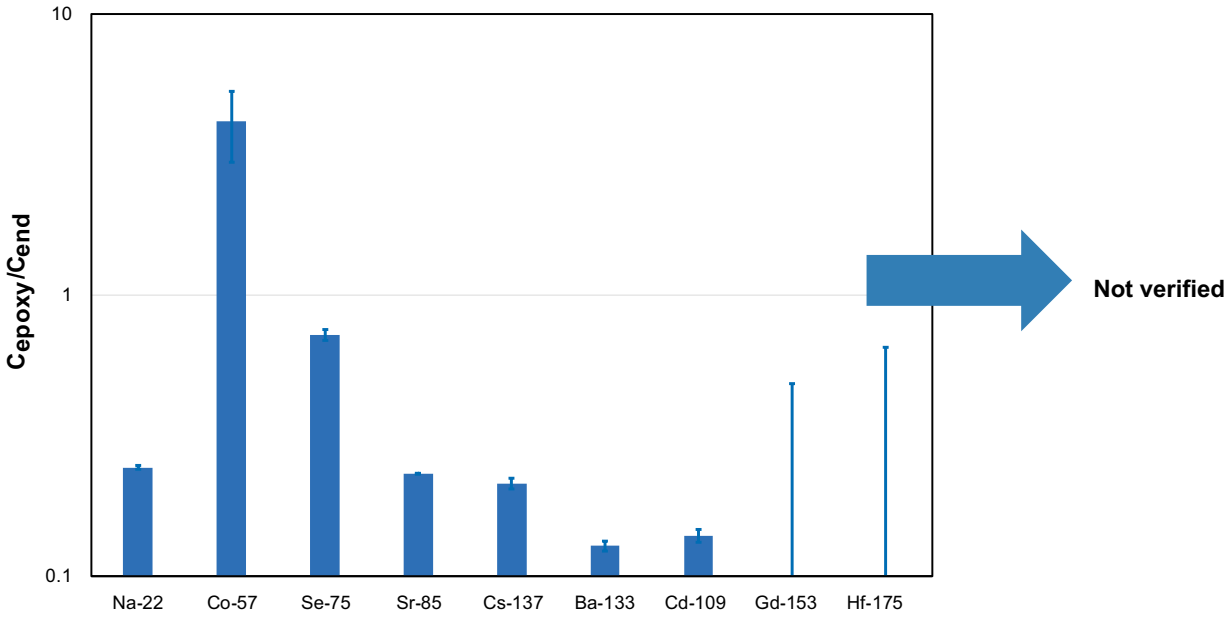

Figure A11-7. *Tracer concentrations in the isopropanol/Epoxy solution relative to the experiment water at the time of finalizsation of the experiment. If the activity in the last batch would be a result of remaining experimental section water that has mixed with the Isopropanol/Epoxy, one would expect the same ratio for all tracers, which is not the case.*

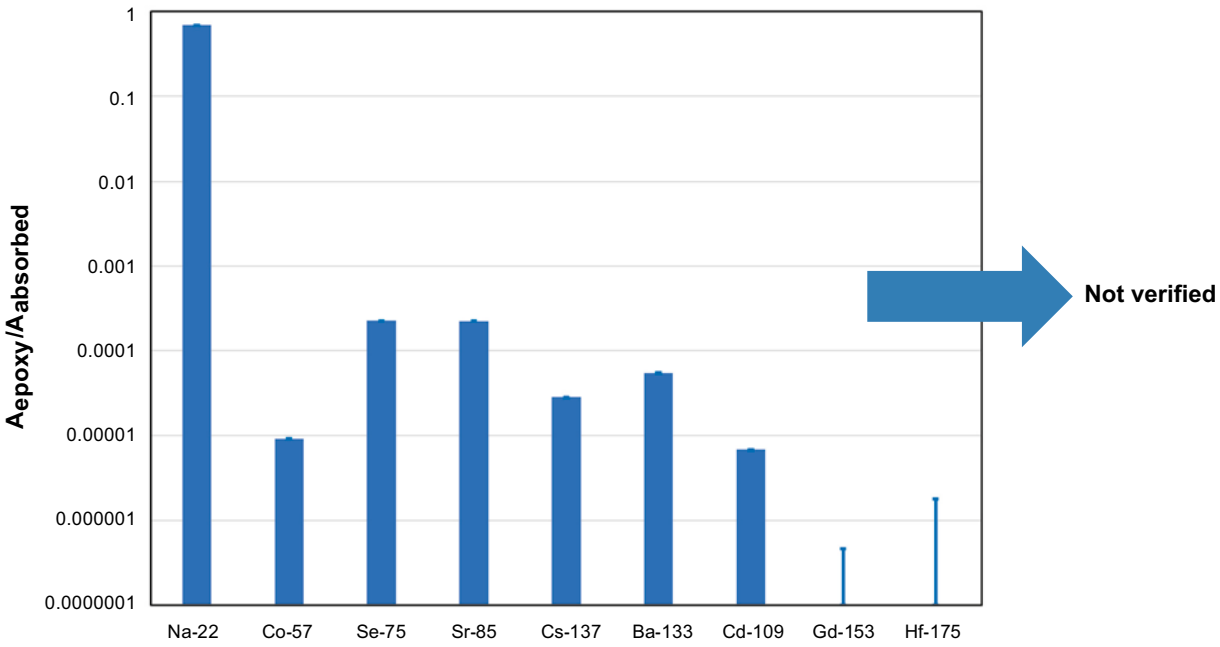

Figure A11-8. *Ratios of tracers between amounts in the isopropanol/Epoxy solution and amounts adsorbed on surfaces. A similar value for all tracers would indicate that the activity of the combined isopropanol/ Epoxy solution would be a result of loosening of consolidated solid particles that had been exposed for tracer adsorption during the circulation phase of the experiment. However, no support for this hypothesis can be found in the results.*

Chemical processes

A closer examination of the content of the Epoxy used (Epotek 301), shows that the stabilizer in the Epoxy consists of trimethyl-1,6-hexanediamine. Since amines are suspected to:

- Occupy cation exchange sites of the rock material, enabling desorption of cation exchange sites
- Form soluble complexes with tracers expected to sorb by surface complexation (e.g. cobalt), enhancing desorption of such tracers,

it is likely that an interaction process occurred when the tracer-adsorbed surfaces were exposed to the Epoxy resin. Since the desorbed tracers seem to be located in the isopropanol phase and to a lesser extent in the cured Epoxy, one explanation could be that at least some of the amine in the stabilizer was leached from the Epoxy resin into the surrounding isopropanol, making it easier for the amine to interact with rock surfaces and therefore causing desorbed tracers to be transported to the interface between the Epoxy and the isopropanol, cf. Figure A11-9.

The ratios of losses of desorbed tracers compared with adsorbed tracers during the isopropanol/Epoxy treatment is shown in Figure A11-10. The observations and conclusions made are that weakly sorbing tracers (e.g. Na-22 and Sr-85) are suspected to have been severely influenced by the isopropanol/ Epoxy treatment, but for the other tracers studied, less than 5 % is lost.

Based on these observations, one could speculate of the possibility of that significant parts of the so far non-recovered tracer of the experiment would be present in the Epoxy resin. The bottom part of this sample was never separately sampled or measured due to the finding that no significant increase of the activity in the bottom of the bottle was indicated by portable device measurement.

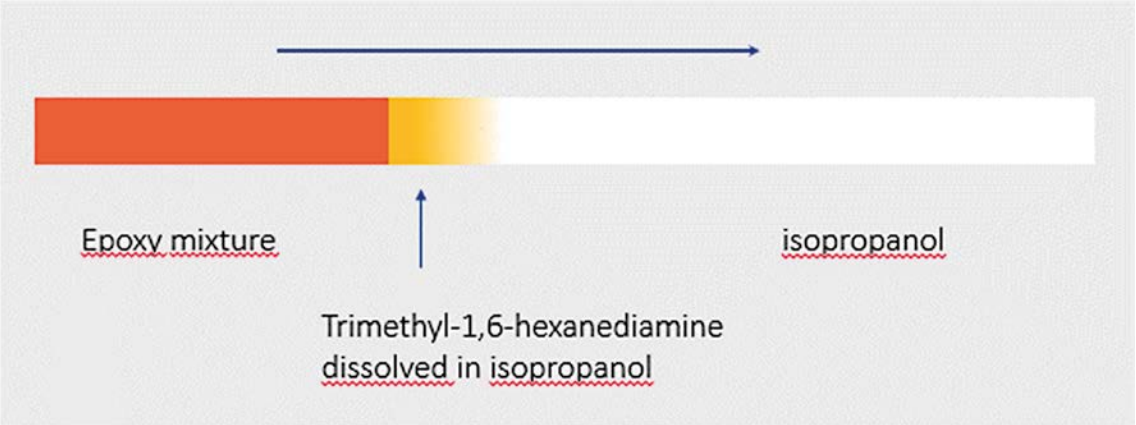

Figure A11-9. *Principal illustration of the proposed mechanism of transferring of tracers from Epoxy to isopropanol by cation exchange and surface complexation processes including trimethyl-1,6-hexanediamine. The amine is suggested to leach from the Epoxy resin to the isopropanol and thereby obtain properties to interact more strongly with the rock surfaces and desorb tracers which then will be transported in the interface of the Epoxy and the isopropanol.*

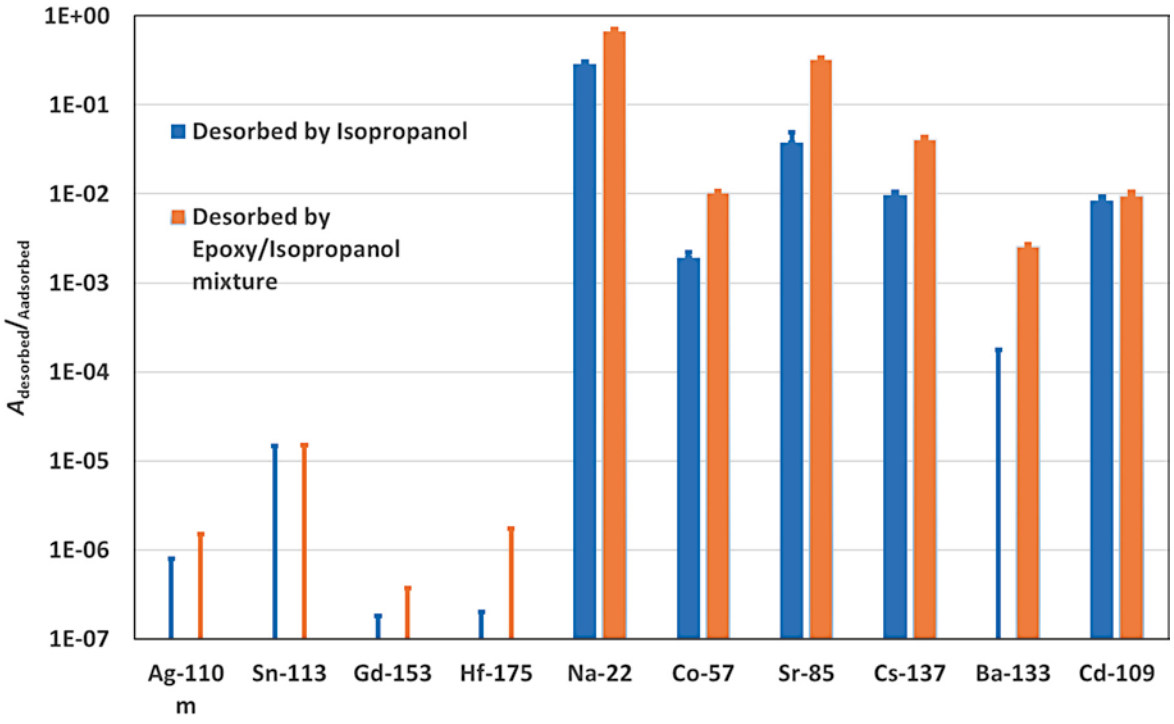

Figure A11-10. *Ratio of tracers desorbed/adsorbed by isopropanol and by isopropanol/Epoxy mixture.*

If this hypothesis would be correct:

- The non-recovered part of the tracers would have been released from their sorption sites (mechanical and/or chemical processes) by the Epoxy resin, probably by an interaction with the trimethyl-1,6-hexanediamine.
- They would have remained in cured Epoxy resin and in this case not being dissolved in the surrounding isopropanol, i.e., was missed when the sampling of the upper phase of the isopropanol/Epoxy mixture was made.

Dose rates from radionuclides tracers in the Epoxy/Isopropanol mixture

The assumption above is contradicted by the observation of the dose-rate measurement of the last bottle, indicating no significantly increased dose-rate at the Epoxy part in the bottom of the bottle. On the other hand, several of the strongly sorbing tracers (e.g. Co-57, Cd-109 and Gd-159) have low g-energies which possibly could contribute very minorly to the total dose-rate of the content of the bottle, expected to be dominated by the high g-energy radionuclides Na-22 and Cs-137, as observed in Figure A11-11 and Figure A11-12.

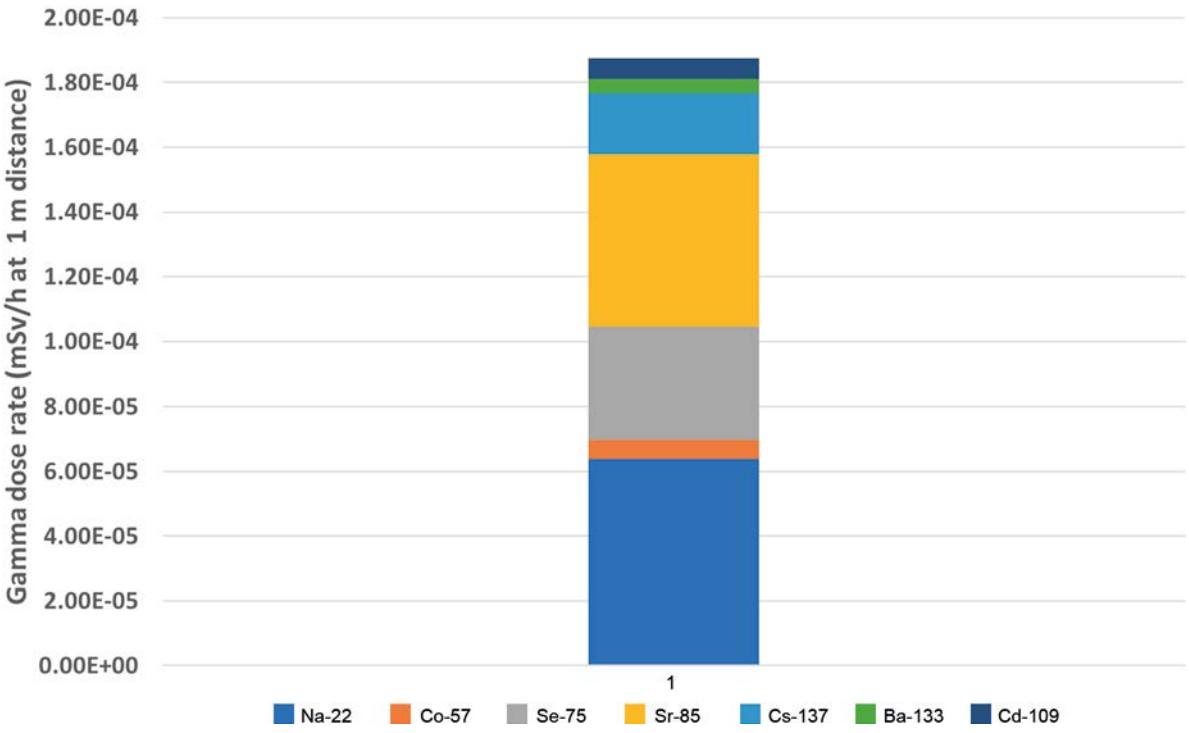

Figure A11-11. *Gamma dose rates from tracers found (by measurements) in the Epoxy/isopropanol phase.*

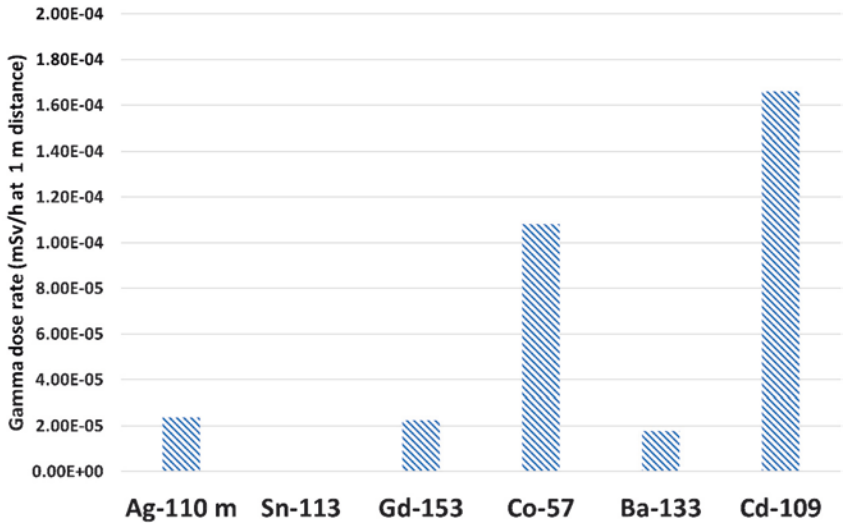

Figure A11-12. *Calculated gamma deose rate from tracers in the sampling beaker containing the interface of the isopropalnol/Epoxy IF the adsorbed part of the different tracers would have been desorbed according to the process described in the text. The adsorbed amount was calculated from the decrease of the measured concentration in the aqueous phase during the circulation phase of the experiment.*

Measurement of strongly sorbing tracers in Epoxy samples

A number of Epoxy samples were measured for gamma emitting tracers. The samples were collected both from the slim hole (for results, see Figure A11-13) and from the surface facing the fracture (for results, see Figure A11-14).

The observations and conclusions made are:

- The Epoxy injection was performed in the sequence Inlet – Slim hole – Fracture – Outlet which might cause that the tracers originally located in the slim hole may have been transported to the fracture.
- The tracer distribution is more homogeneous in fracture Epoxy than in slim hole Epoxy

The observations and the large variation of concentrations between the different samples concentration make it difficult to establish average tracer concentrations with reasonable uncertainties.

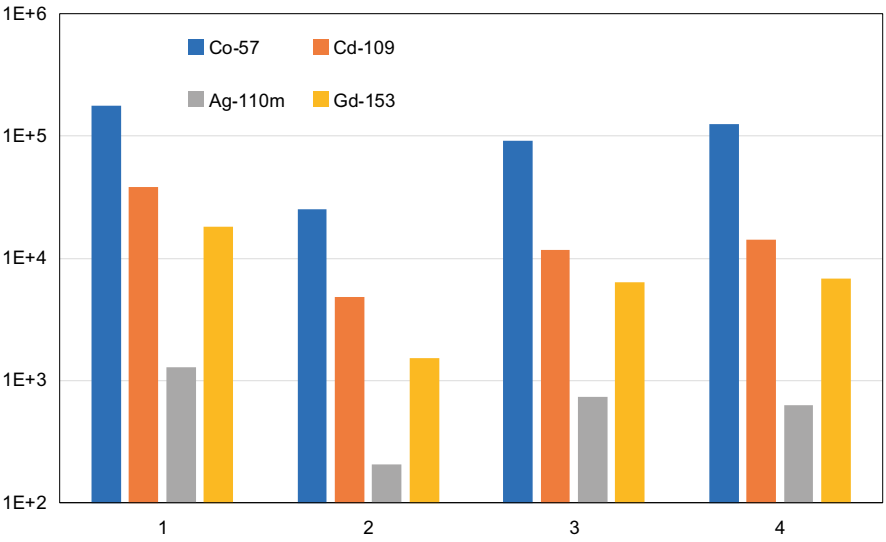

Figure A11-13. *Tracer concentrations in four slim hole Epoxy samples (Bq/g).*

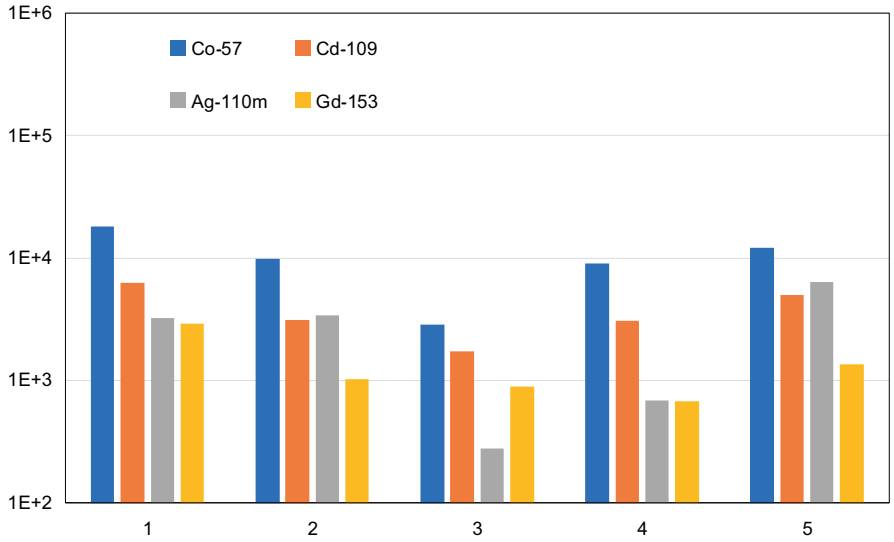

Figure A11-14. *Tracer concentrations in five fracture Epoxy samples (Bq/g).*

Summary and conclusions

It is most probable that a very large part of the Na-22 adsorbed during the circulation phase of the experiment was removed by the Epoxy and isopropanol treatment, i.e. that the core samples from the penetration studies underestimates the actual adsorption of Na-22.

Studies of the tracer content in the Epoxy samples from the fracture surface and the slim borehole has improved the mass balance for the strongly sorbing tracers; however, it is still possible that release of tracer caused by the Epoxy front has been missed and could explain some of the deficit in the mass balance still observed.

Appendix 12

Investigation of the risk of contamination during rock sampling

LTDE-SD (Task 9B): Memo; Investigation of the risk of contamination during rock sampling in the LTDE-SD experiment

Johan Byegård, Kersti Nilsson, 2019-07-11

Introduction

At the Solna TF Workshop in October 2018, it was stated that it is very likely that the anomalous penetration profiles at deeper penetration depths are a result of potential contamination during the sample preparation for at least some of the LTDE-SD radionuclides. All phases of the sampling procedure that might have been a source of contamination have been explored and will be reported in the present memo.

A Memo Part 1 "LTDE-SD (Task 9B): Memo; Updated detection and reporting limits and risk of contamination for the sorbing tracers Co-57, Ba-133, Cs-137 and Ra-226, revised due to potential contamination during the sample preparation, Part 1" with updated detection and reporting limits and levels of risk of contamination was delivered by Kersti Nilsson and Johan Byegård, January 21, 2019 as Delivery #29.

Since the present contamination investigation showed a difference between the processes for sliced only and sliced + crushed samples for the sorbing tracers, some changes and additions of limits/levels have been made in the present Memo, see Table 3-1 for a comparison. The updated levels were calculated including uncertainty, with the A20 core as a basis for crushed samples and measured values in sample slices 4 to 9 as a basis for samples only sliced. The present recommendation is to regard values below the stated levels as potential contamination.

Identification of the potential contamination sources

It was during the modelling work that the GWFTS group decided to have a closer look into the history of the cores to investigate what processes could be responsible for causing contamination and possibly the non-expected extended penetration profiles.

The following potential contamination processes were identified:

1. **Drilling of 24 mm core samples from the stub (A and D profiles)**. It is likely that the circular sawing is transferring tracers from the high tracer concentration part to the low (or none) concentration part. This can be caused by transferring of sawing dust or by desorption initiated by the sawing liquid giving an increased spreading of the tracer. The magnitude of this contamination process was checked by digital autoradiography of the surfaces of the core samples. The methods showed increased blackening at the external surfaces, indicating contamination caused by the core sample drilling.
2. **Square-cutting of core samples.** In order to remove the surface contamination caused by the core sample drilling, a square-cutting technique was applied (cf. Figure 2-1). Since this kind of cutting could not be performed using the entire drill cores, they had to be divided in to three parts lengthwise. During the square-cutting there were difficulties in isolating the high-activity external top surface of the core samples from contact with the sawing liquid. A potential contamination process was therefore identified involving spreading from the external top surface to the newly formed square surfaces through the sawing liquid.

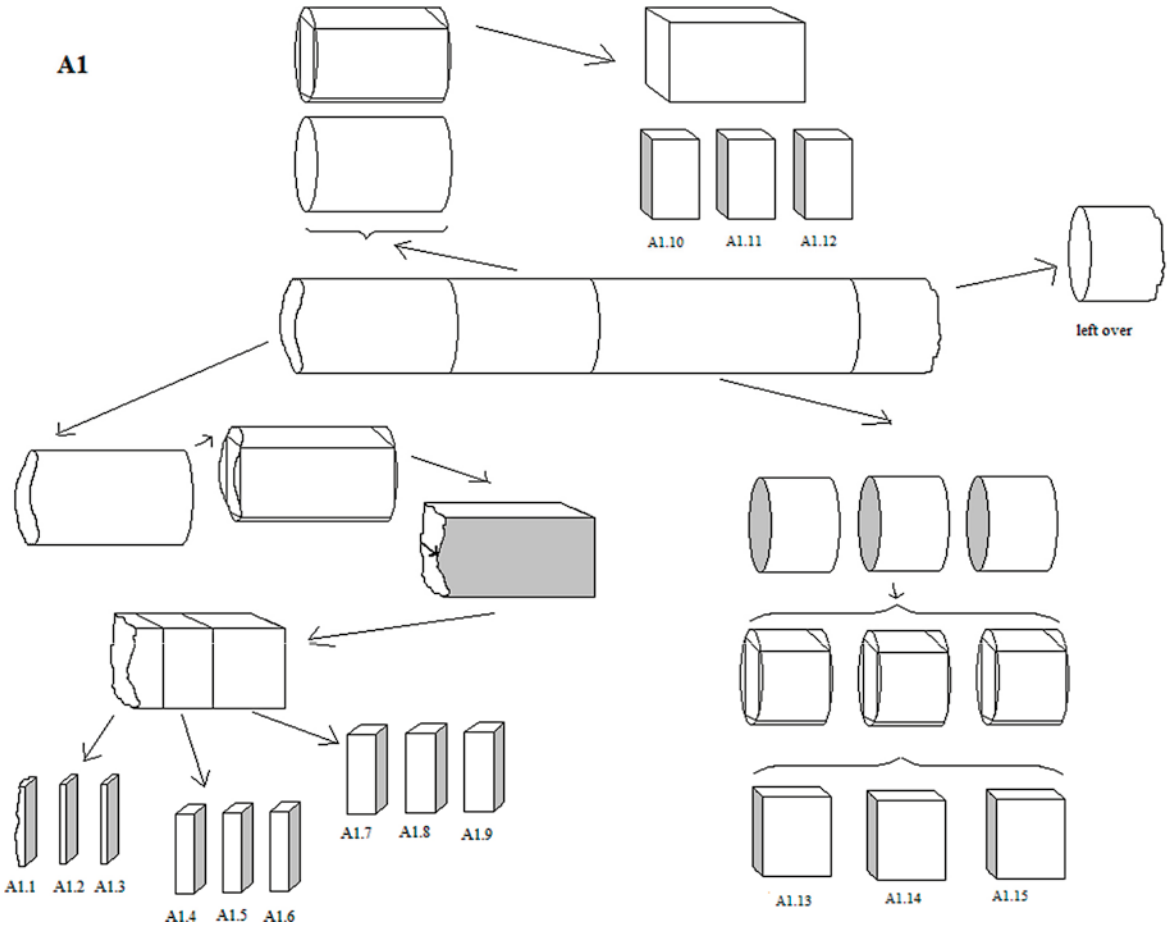

Figure 2-1. *Partition diagram of the sawing procedure of a core sample (in this example A.1) into subsamples and thereafter into cuboid shape (c. 16×16 mm) and finally thin slices (c. 3×1, 3×3, 3×5, 3×10 and 3×20 mm, see text above). The shaded areas represent surfaces exposed to autoradiographic imaging plates. The figure and figure text are copied from SKB Report R-10-68 (Nilsson et al. 2010).*

The magnitude of this this contamination process was checked by digital autoradiography of the surfaces of the core samples. Digital and X-ray film autoradiography were also applied after the core had been sliced. Both methods showed no observed increased blackening at the edges of surfaces, which showed that any contamination at least must be below the level that can be measured by autoradiography. Altogether, it was only shown by the autoradiography results that the contamination caused by the core sample drilling was significantly decreased by the square-cutting.

An important fact is that this assumed contamination process from the square-cutting will only occur in the first third of the sample core (slices 1-9), which is the only part that was square-cut together with the highly active top surface.

3) **Slicing of core samples.** After the square-cutting, the core samples were sliced into slices of different lengths. Since the slicing was always performed in the direction opposite to diffusion (from low to high tracer activities and with careful washing of the device after each sawing) this has been considered as a less probable contamination process.

4) **Crushing of core slices.** Since several of the core samples were aimed to be used for non-gamma emitting tracers, i.e., tracers that demanded dissolution of the rock material, the square-cut core materials were crushed. A potential contamination process was thus identified by the possibility that tracers were transferred between the different crushing batches.

Results of the investigation

When exploring the potential contamination, focus has been on the tracer Cs-137 due to its high dynamic range (injected in high activity, possible to measure in very low activity). Besides that, the strong adsorption of the tracer makes one expect very little (i.e., none) movement to the inner part of the core; observation of tracer there may thus be an indicator of contamination.

Besides the nuclide specific contamination of Cs-137, attention has also been paid to the blackening of the autoradiographs as a method of determining the location of the contamination. This method captures the contribution from all tracers involved, but in this case, the major part of the blackening is due to Cs-137 as well.

Drilling of core samples from the stub (A and D profiles)

The autoradiographic analyses of the external surfaces of the entire 24 mm core cylinders indicated a pattern shaped according to contamination by activity being successively transported and deposited on the core walls by the drill bit.

This suspicion of contamination on the edge of the core after the overcoring was supported by the results from the preliminary slicing of some of the cylindric cores. From these results, it became quite obvious that the blackening was concentrated on the edges and that a contamination is obtained in the drilling of the core samples.

During the investigation, it was however found that core sample A10 had no or very little visible blackening located at the edges, and that is why this core was sliced and measured without square-cutting (cf. Section 3.2). The results from Cs-137 measurements are shown in Figure 3-1 and it is obvious that the profile contains too much activity in the inner part of the core to be explained by a rock matrix diffusion process within these time frames. One can from these results conclude that the A10 sample probably represents a comparatively low contamination caused by overcoring, since the level in the A10 sample is not enough to cause blackening in the autoradiographs. Blackening was obtained for all the other entire core samples studied.

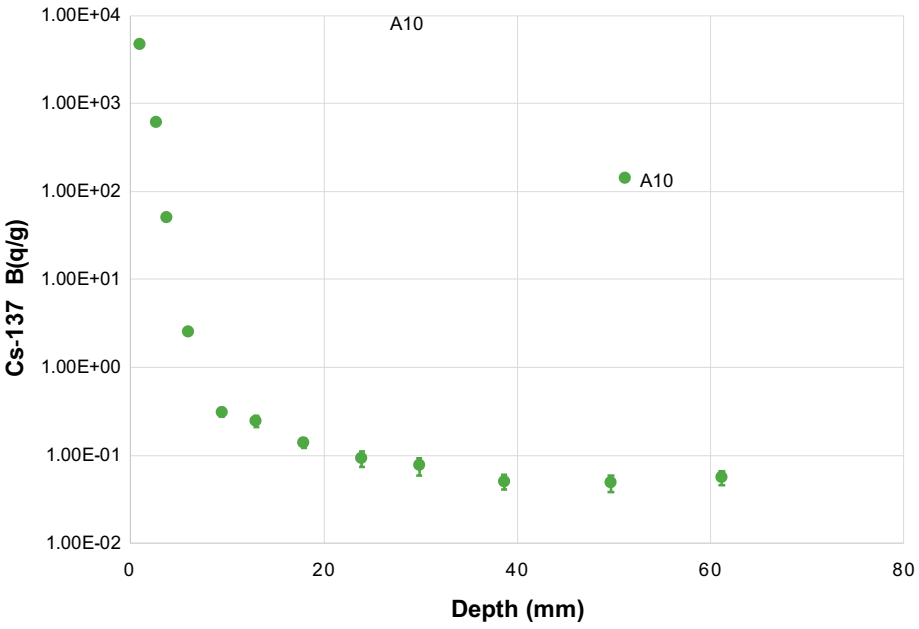

Figure 3-1. *Penetration profile measured for Cs-137 in sample A10, the only core sample which was sliced without any square-cutting applied.*

Square-cut and sliced samples

In order to remove the observed contamination from the cylindric drill cores extracted from the stub, square-cutting was applied in which the edges of the core samples were intended to be removed (cf. Figure 2-1). This lengthwise cutting was considered as impossible to perform using an entire drill core (17 cm), so it was divided into three separate rods/subsamples. The first one comprised slices 1-9, the second slices 10-12 and the third slices 13-15.

During the square-cutting, it was realised that it was difficult to isolate the high-activity external top surface of the rods from the sawing liquid when performing the lengthwise sawing. It was therefore suspected that the sawing liquid may desorb/dissolve/leach tracer from the top surface and cause them to adsorb evenly on the newly formed square surfaces of the rod, resulting in a new contamination. Since the highly active external top surface was only present in the first of the three rods, this type of contamination should therefore only occur in the first subsample of the entire core (i.e. slices 1-9) and there would be a sharp difference in activity compared with the other samples (slices 10-15).

After the square-cutting, the samples were sliced according to Figure 2-1. The slicing was always performed in the direction opposite to diffusion (from slice 15 towards slice 1 with careful cleaning of the equipment between each slice) so the process is considered less likely to have caused major contamination)

When studying the results for Cs-137 in samples exposed only to square-cutting and slicing, one can see a sharp difference between slices 9 and 10 (Figures A-17 and A-19). Before slice 10, one does not find any slice below the detection limit and from slice 10 and further into the profile there is no slice containing measurable amounts of Cs-137. It is quite obvious that the levelling out from slice 5-6 (at about 10 mm depth) to slice 9 is a result of spreading of the tracer during the square-cutting and that these values should be considered as suspicious, see Figure 3-2.

An elaborate evaluation has been made in order to make an estimation of the potential contamination level this process can cause. An average of the concentrations obtained from the sharp levelling out after the absolute first few mm up to slice number 9 was used in the estimation (cf. Figure 3-2).

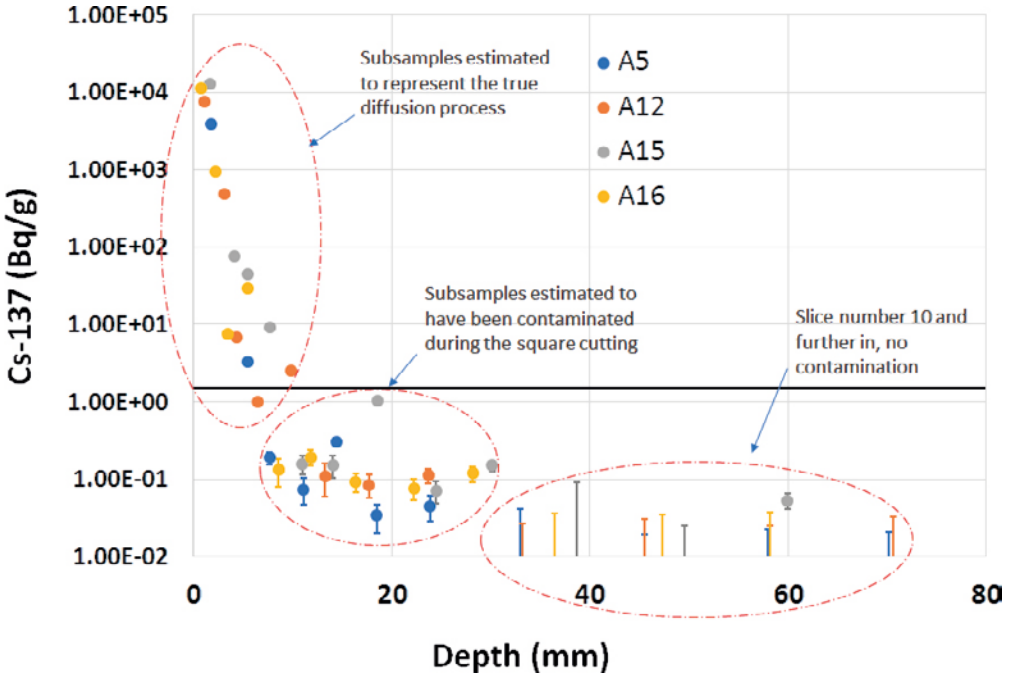

Figure 3-2. *Penetration profiles of A-samples, square-cut but not crushed. The dark grey line represents the Potential contamination level for sliced samples, see Table 3-1.*

Table 3-1. Compilation of the calculated potential contamination levels for Co-57, Ba-133 and Cs-137 in sliced and sliced + crushed samples, together with the values earlier reported in Memo 1 (Delivery #29).

Tracer	Detection limit, revised (Bq/g) (Memo 1 and 2)	Reporting limit (Bq/g) (Memo 1)	Potential contamination level for sliced samples (Bq/g)	Risk of contamination (Bq/g) (Memo 1)	Potential contamination level for sliced and crushed samples (Bq/g)
Co-57	-		3	3	3
Ba-133	-	0.4	0.3	-	0.4
Cs-137	-	1	1.5	2	2
Ra-226	1	(~~0.7~~)*	-	-	-

* Only the detection limit is valid.

Square-cut, sliced and crushed samples

After the square-cutting and slicing process, some of the sample series were selected for crushing, since they were selected for dissolving and leaching of non-gamma active tracers before measurement.

The results of Cs-137 measurements when analysing crushed samples are given in Figures A-18 and A-20. The results look quite similar to the ones without crushing except that Cs-137 is now detected in all slices, (even in slices 10-15), i.e., one can suspect that the crushing device causes contamination of the samples. One can possibly estimate that the contamination level is generally higher compared to the non-crushed samples and that the variation is somewhat higher. Besides this, the blank A20 sample is included in this group and one can from the results from that sample make a general estimation of the potential contamination levels in crushed samples. It seems that three of the slices in the A20 core possess the highest Cs-137 concentrations of all A and D inner slices, i.e., slices with depths 15 mm and deeper. It is somewhat surprising that the highest inner concentration is found in a sample that was not exposed to the tracer activity solution, but it is the opinion of the authors that this result is due to pure chance.

As for the square-cut and crushed samples, the samples representing the levelling out after the sharp decrease at the beginning have been compiled to obtain a representation of the estimated potential contamination, cf. Figure 3-3.

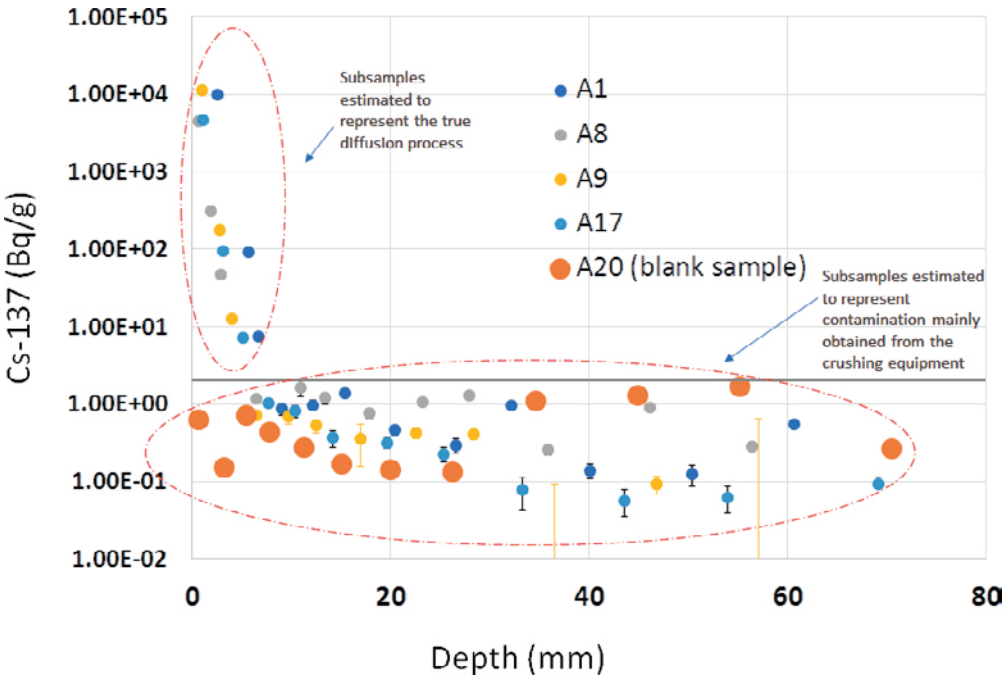

Figure 3-3. *Penetration profiles of A-samples, square-cut and thereafter crushed. The dark grey line represents the Potential contamination level for sliced and crushed samples, see Table 3-1.*

Compilation of the results and conclusions

A compilation of the penetration profiles for the most studied tracers in the LTDE-SD experiment is given in the section Additional material below.

The conclusions of the study can be summarized as:

- The sampling of the LTDE-SD stub by 24 mm core drilling is very likely to have caused contamination along the edges of the sampled drill cores.
- Square-cutting in order to remove contamination located on the edges of the cylindric drill cores succeeded.
- However, a contamination during the square-cutting is likely to have occurred due to difficulties with keeping the high-activity external top surface of the drill core isolated from the drilling liquid. This has influenced the penetration profiles in the first third of the drill core, up to slice number 9.
- For the samples which have undergone crushing, there seems to have been an additional contamination which has influenced all the slices.
- The contamination potential when studying Cs-137 (the tracer with the highest dynamic range) indicates that the inner part of the rock might have obtained a concentration ~ 1E-5 times the tracer concentration in the top surface part for the square-cut and sliced samples; corresponding number for the crushed material is ~ 1E-4. From these hypotheses, no significant contamination affecting the measured profiles is suspected for non- and weakly-sorbing tracers (e.g., Cl-36 and Na-22).
- The present recommendation is to regard values below the stated levels as potential contamination.
- Observations from the sliced and crushed A20 core played a significant role in identifying and characterising the suspected contamination (especially for crushed samples) as this core came from outside the region believed to have been unexposed to the radionuclide tracers. Inclusion of similar “blank” samples at vulnerable stages is recommended as a part of quality control of any similar studies.

Additional material

Penetration profiles of the LTDE-SD experiment sorted by their preparation history (measured as entire slices or as crushed material)

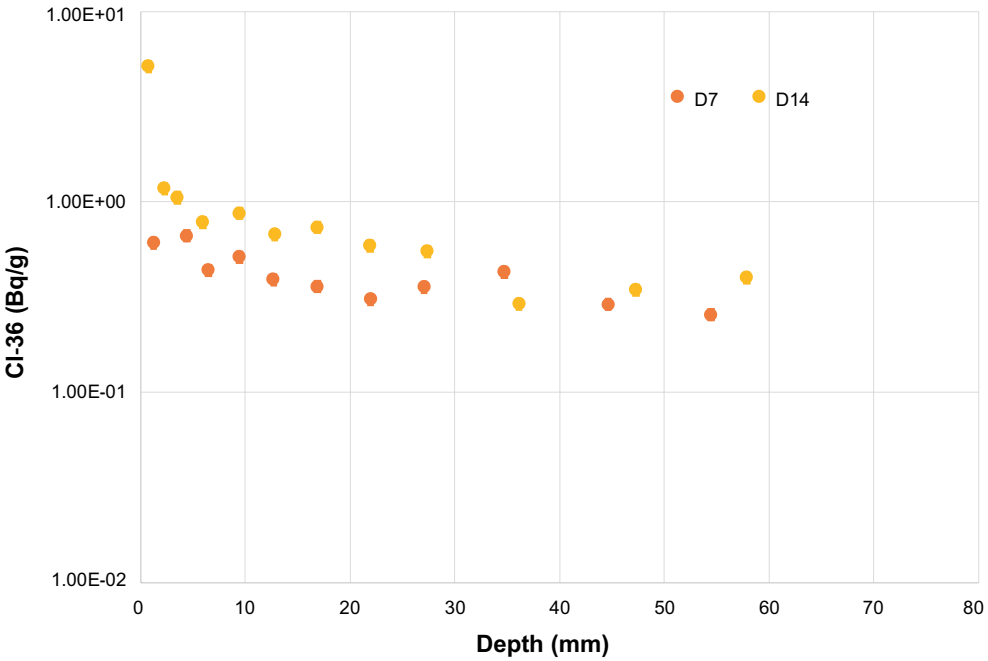

Figure A-1. *Penetration profiles of Cl-36 in D-samples, tracers leached from entire core slices and no crushing of the rock was applied.*

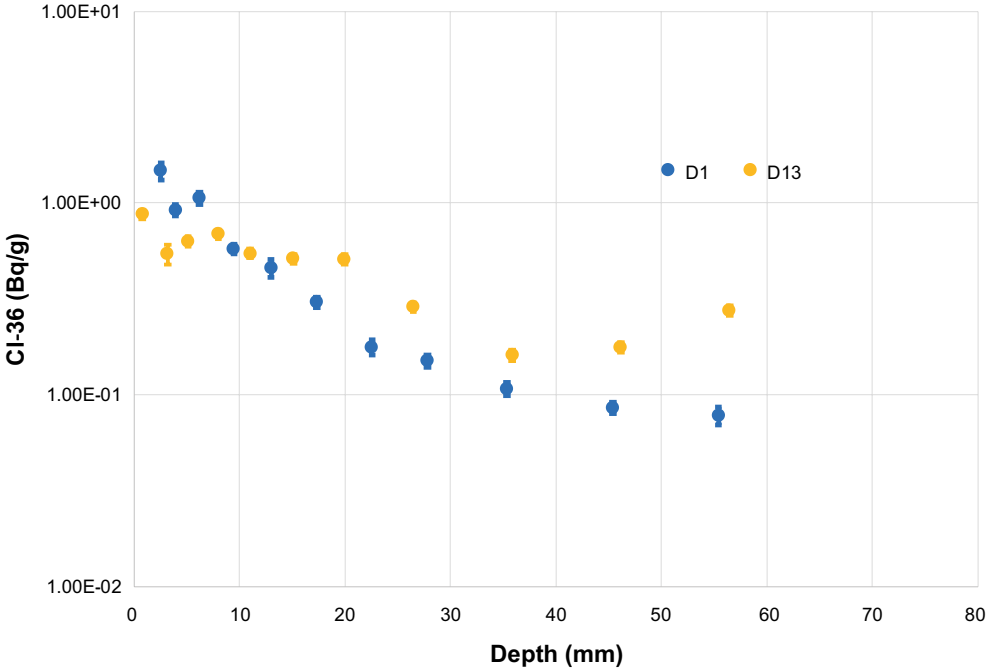

Figure A-2. *Penetration profiles of Cl-36 in D-samples, tracers leached from sliced and crushed rock core.*

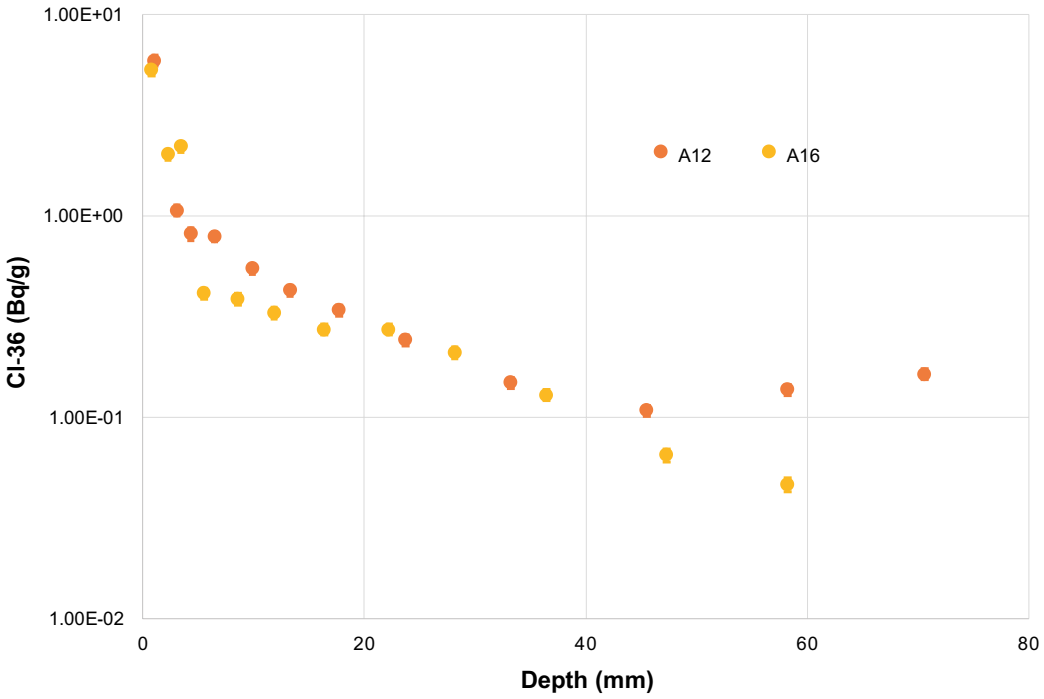

Figure A-3. *Penetration profiles of Cl-36 in A-samples, tracers leached from entire core slices and no crushing of the rock was applied.*

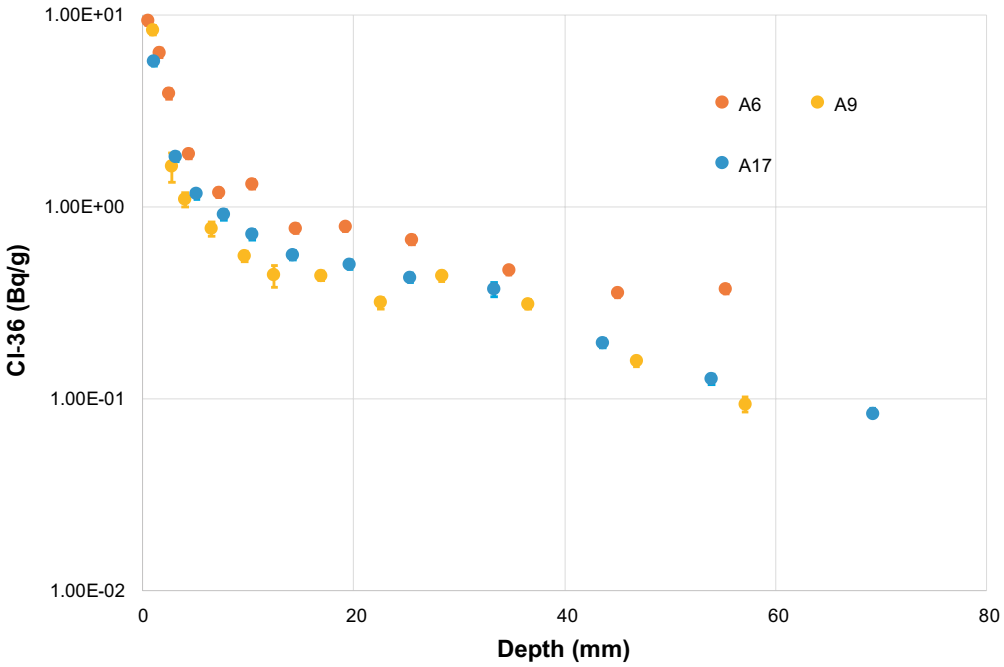

Figure A-4. *Penetration profiles of Cl-36 in A-samples, tracers leached from sliced and crushed rock core.*

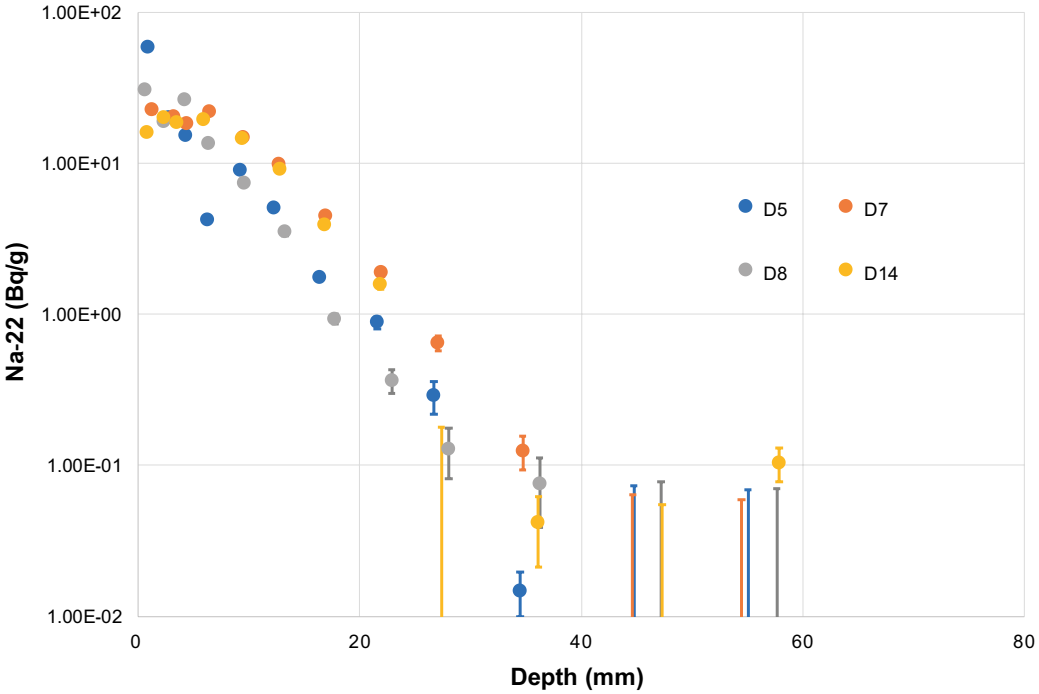

Figure A-5. *Penetration profiles of Na-22 in D-samples, tracers measured on entire core slices and no crushing of the rock was applied.*

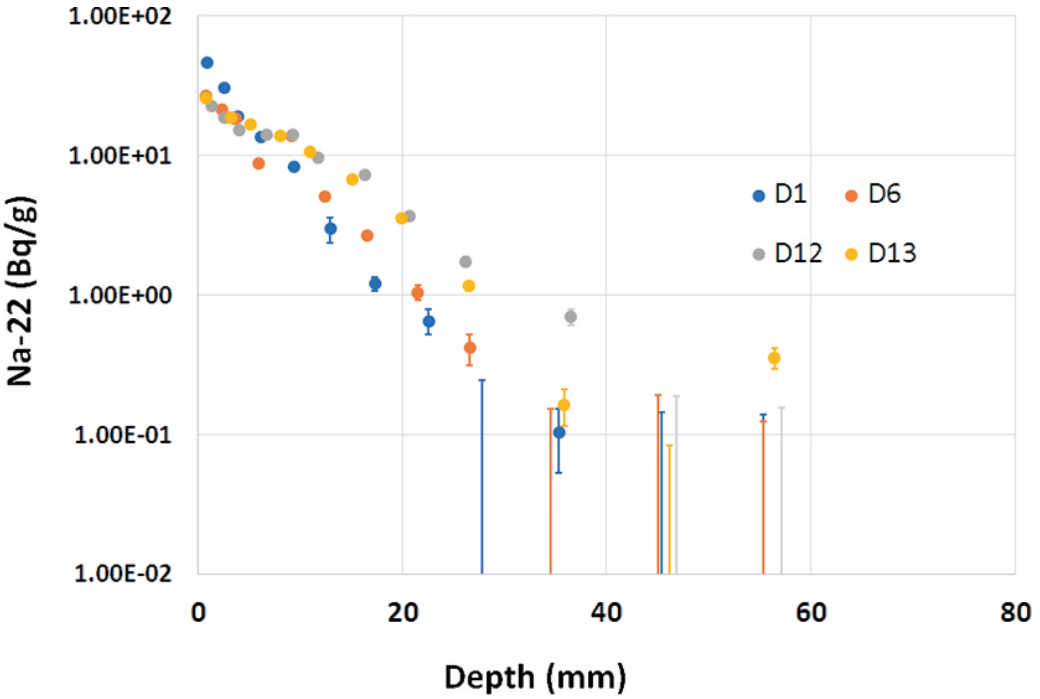

Figure A-6. *Penetration profiles of Na-22 in D-samples, tracers measured on crushed rock material, obtained from sliced drill core.*

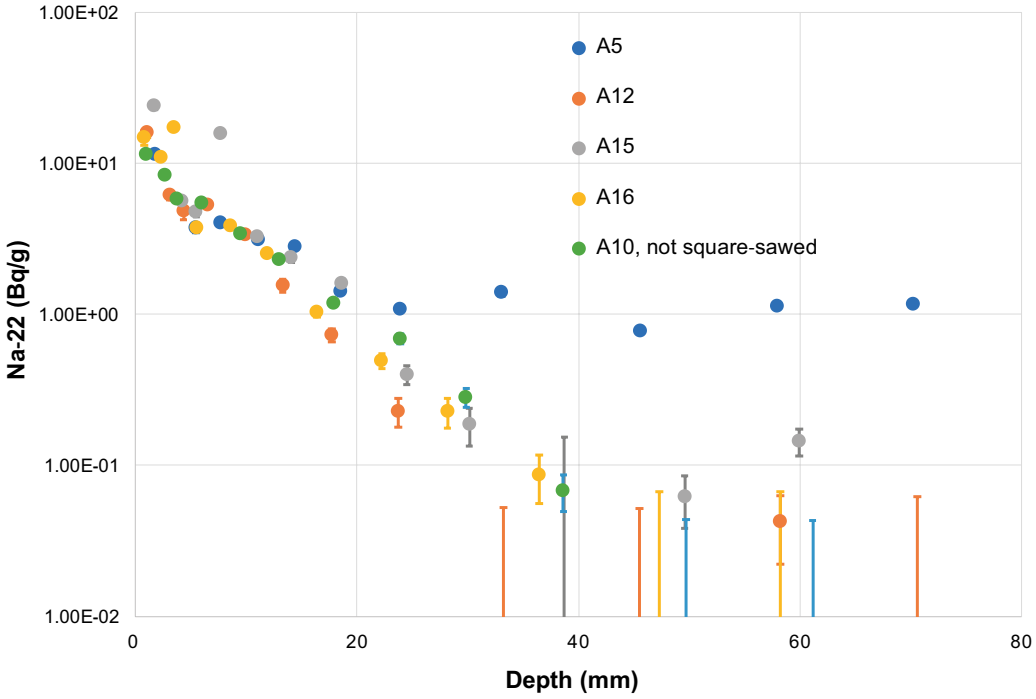

Figure A-7. *Penetration profiles of Na-22 in A-samples, tracers measured on entire core slices and no crushing of the rock was applied.*

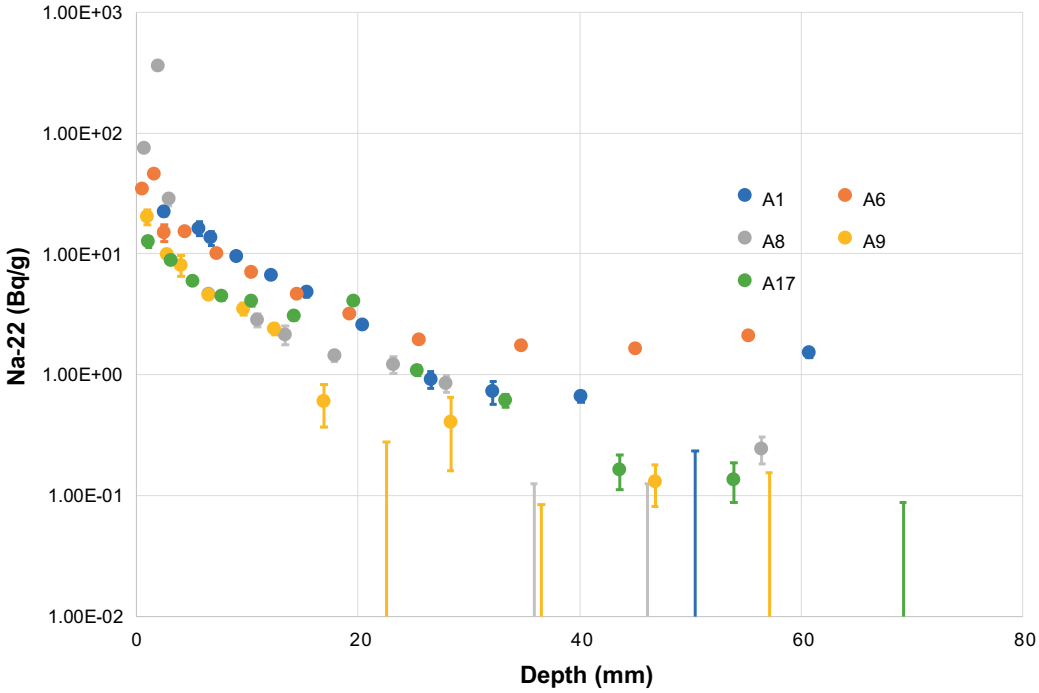

Figure A-8. *Penetration profiles of Na-22 in A-samples, tracers measured on entire core slices and no crushing of the rock was applied.*

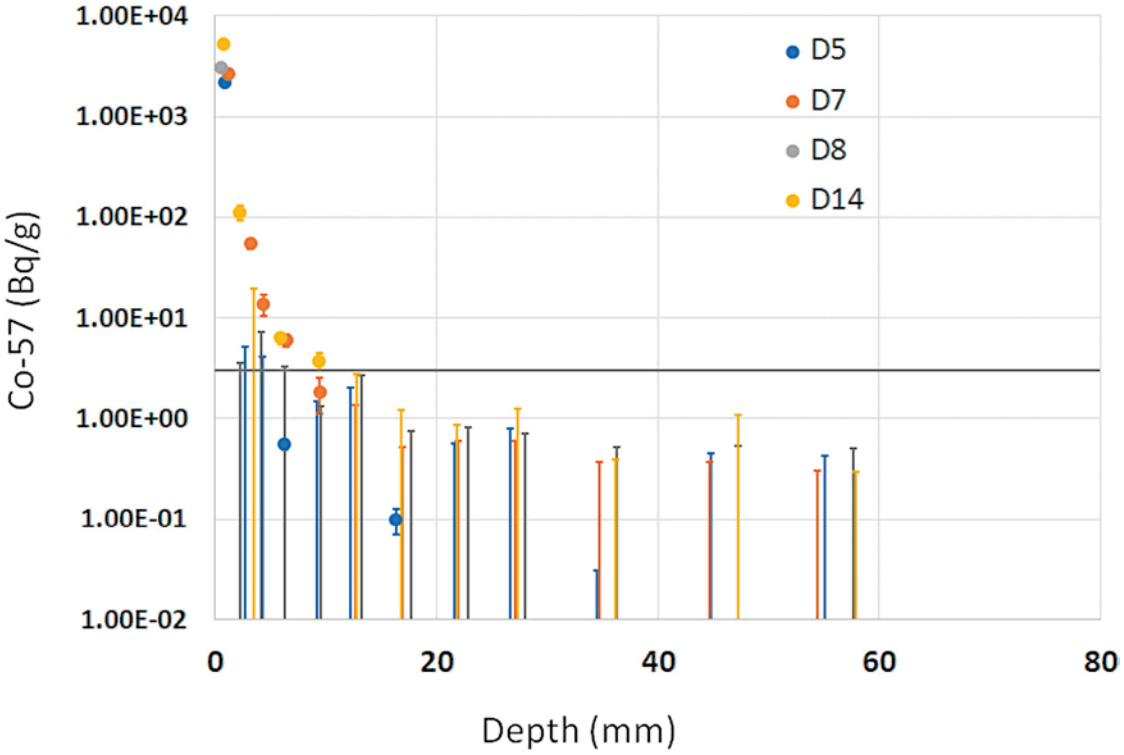

Figure A-9. *Penetration profiles of Co-57 in D-samples, tracers measured on entire core slices and no crushing of the rock was applied. The dark grey line represents the Potential contamination level for sliced samples, see Table 3-1.*

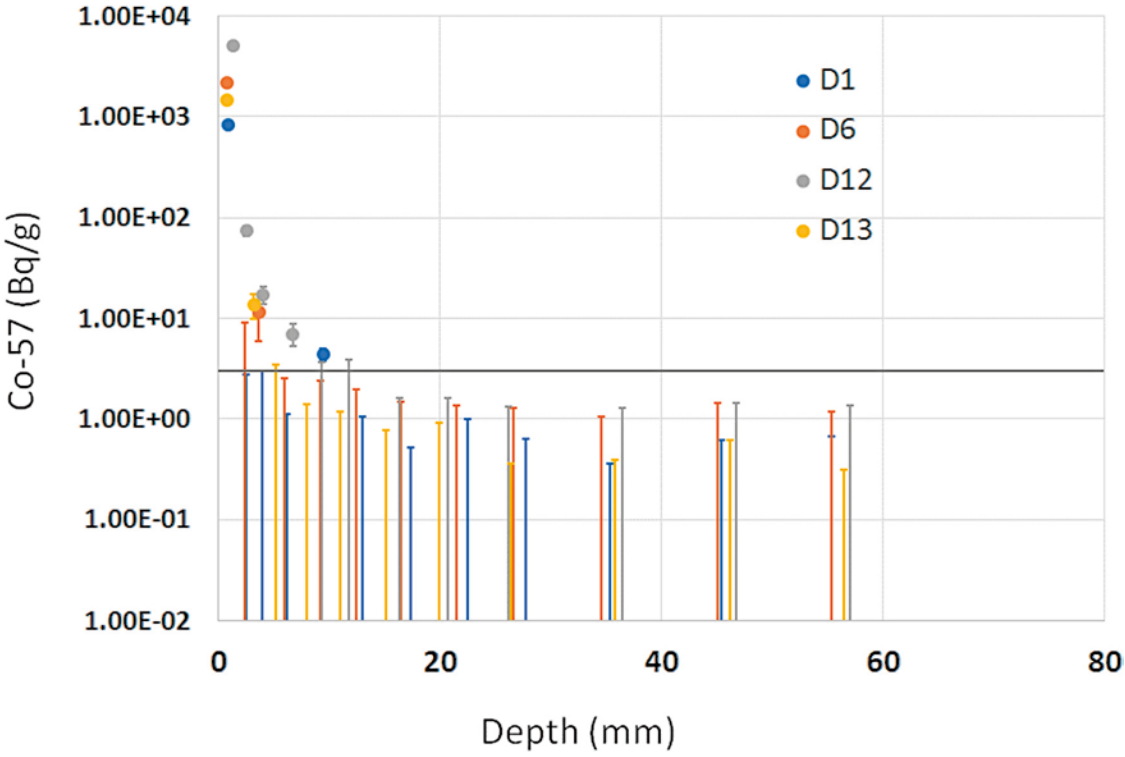

Figure A-10. *Penetration profiles of Co-57 in D-samples, tracers measured on crushed rock material, obtained from sliced drill core. The dark grey line represents the Potential contamination level for sliced and crushed samples, see Table 3-1.*

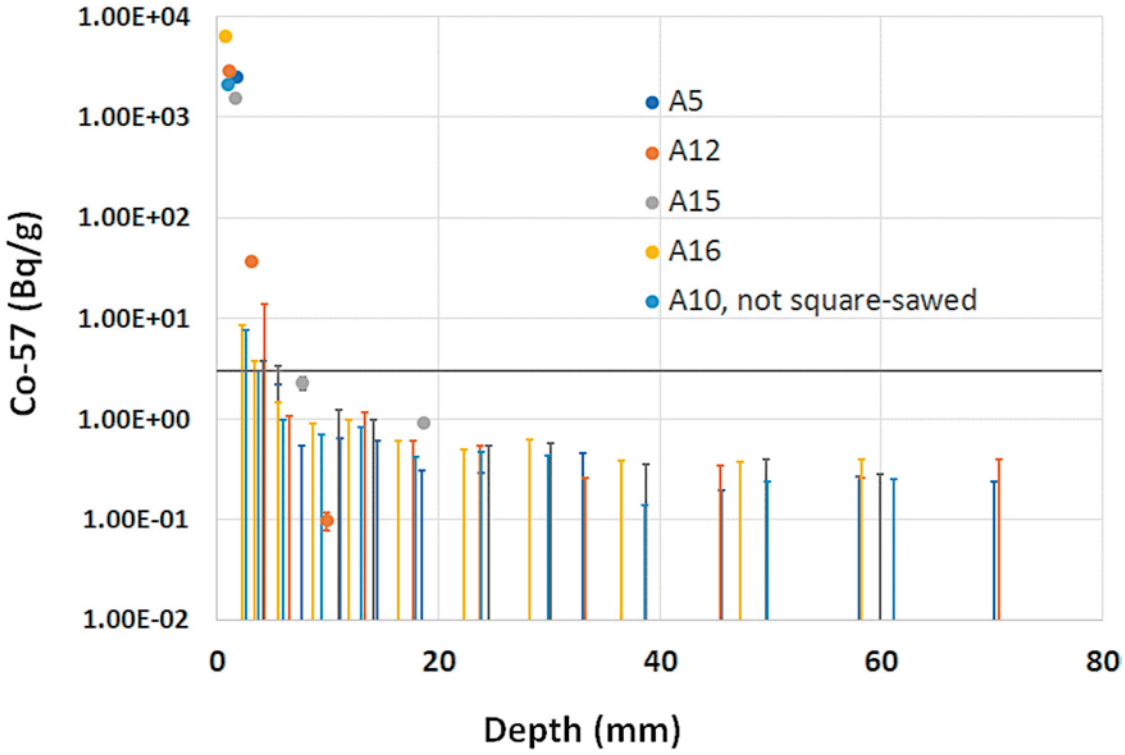

Figure A-11. *Penetration profiles of Co-57 in A-samples, tracers measured on entire core slices and no crushing of the rock was applied. The dark grey line represents the Potential contamination level for sliced samples, see Table 3-1.*

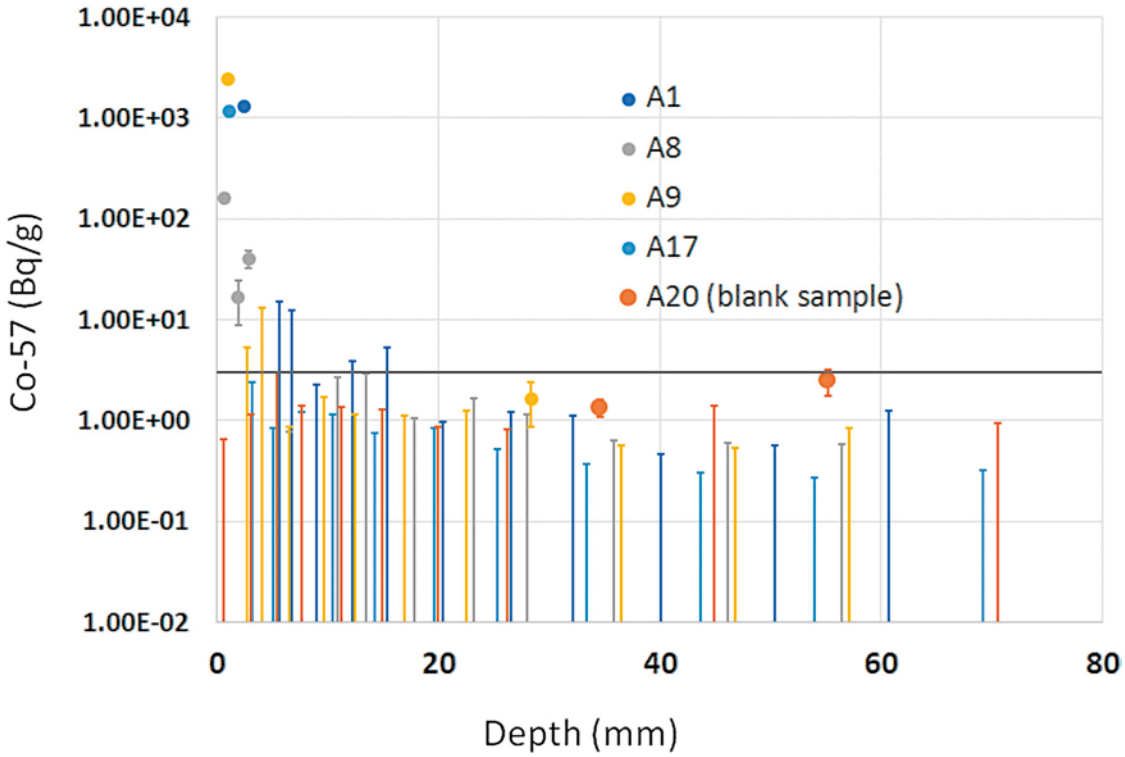

Figure A-12. *Penetration profiles of Co-57 in A-samples, tracers measured on crushed rock material, obtained from sliced drill core. The dark grey line represents the Potential contamination level for sliced and crushed samples, see Table 3-1.*

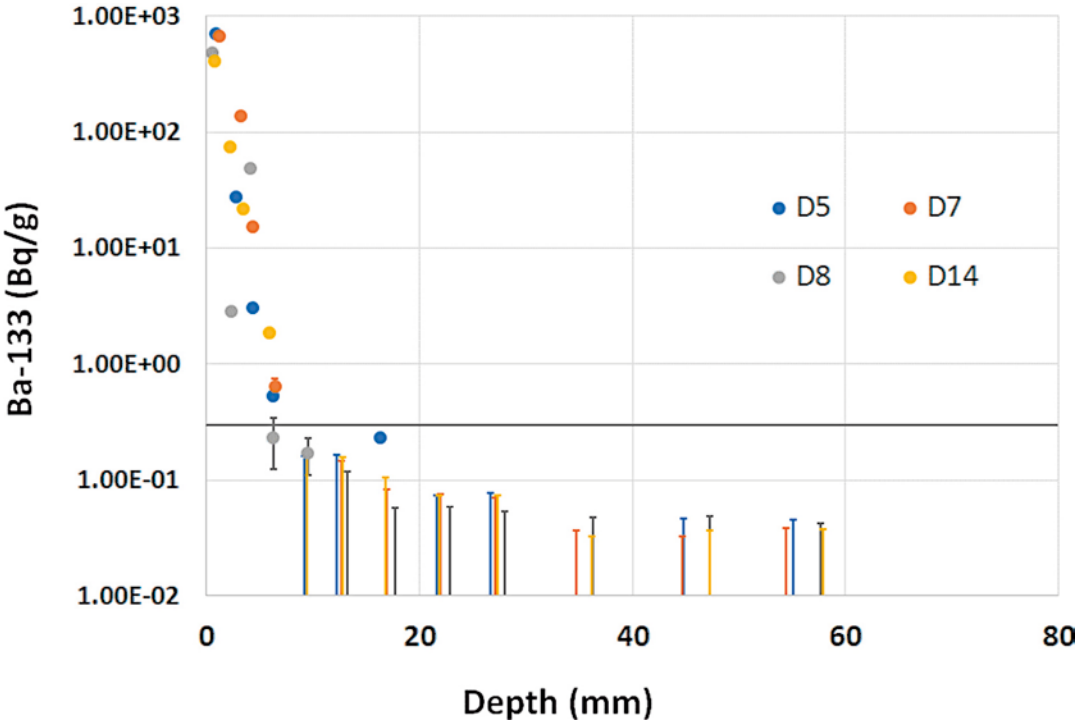

Figure A-13. *Penetration profiles of Ba-133 in D-samples, tracers measured on entire core slices and no crushing of the rock was applied. The dark grey line represents the Potential contamination level for sliced samples, see Table 3-1.*

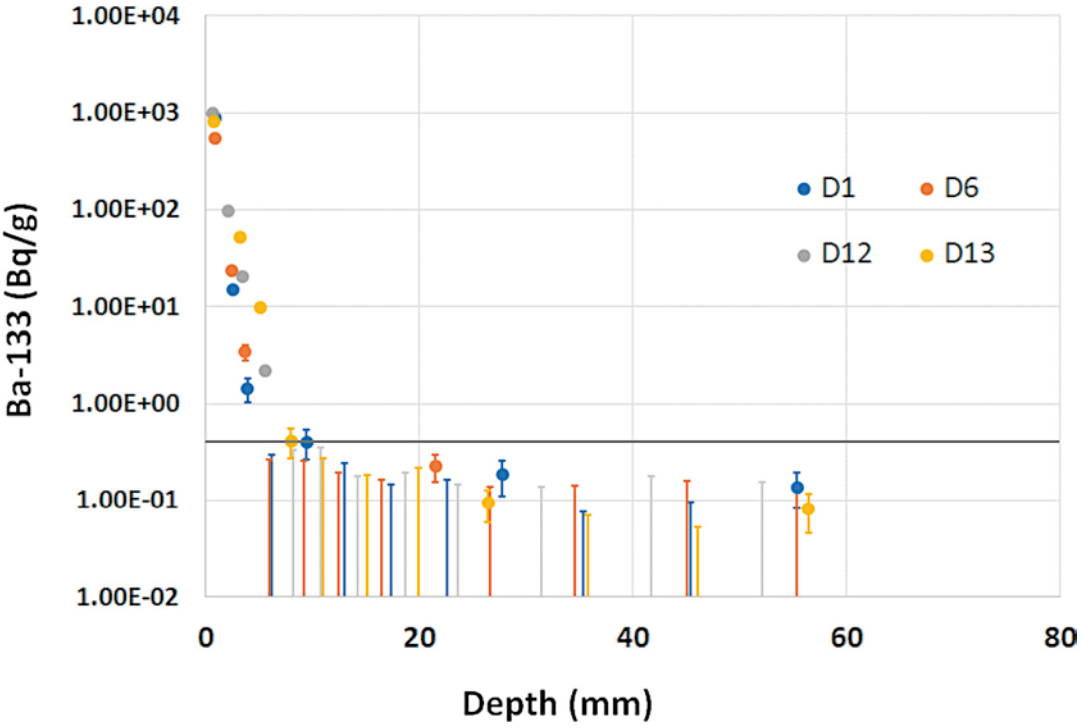

Figure A-14. *Penetration profiles of Ba-133 in D-samples, tracers measured on crushed rock material, obtained from sliced drill core. The dark grey line represents the Potential contamination level for sliced and crushed samples, see Table 3-1.*

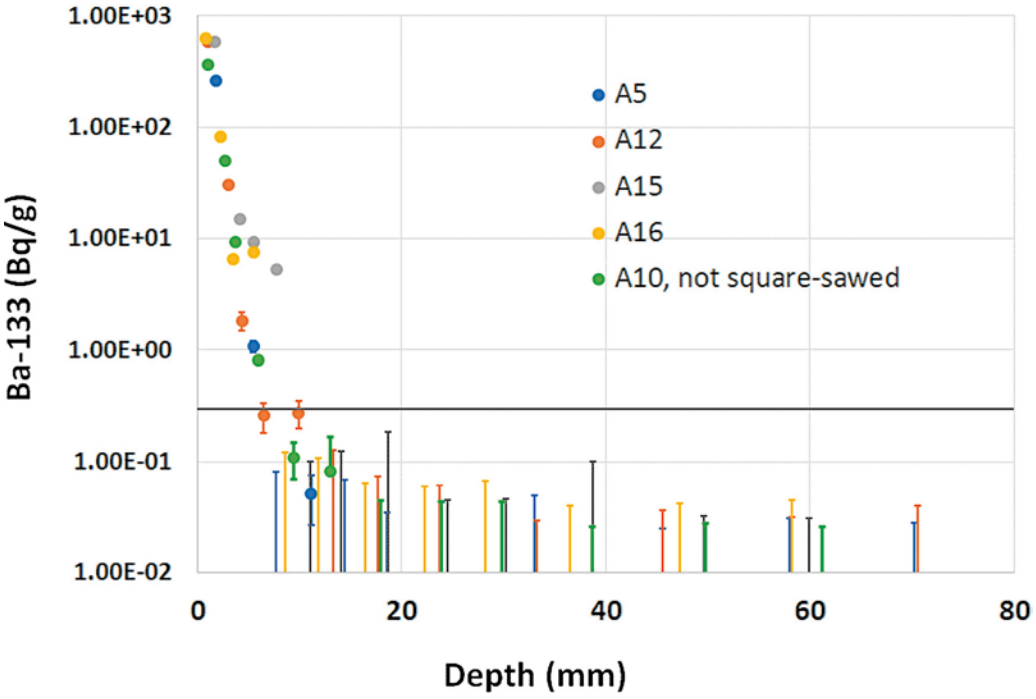

Figure A-15. *Penetration profiles of Ba-133 in A-samples, tracers measured on entire core slices and no crushing of the rock was applied. The dark grey line represents the Potential contamination level for sliced samples, see Table 3-1.*

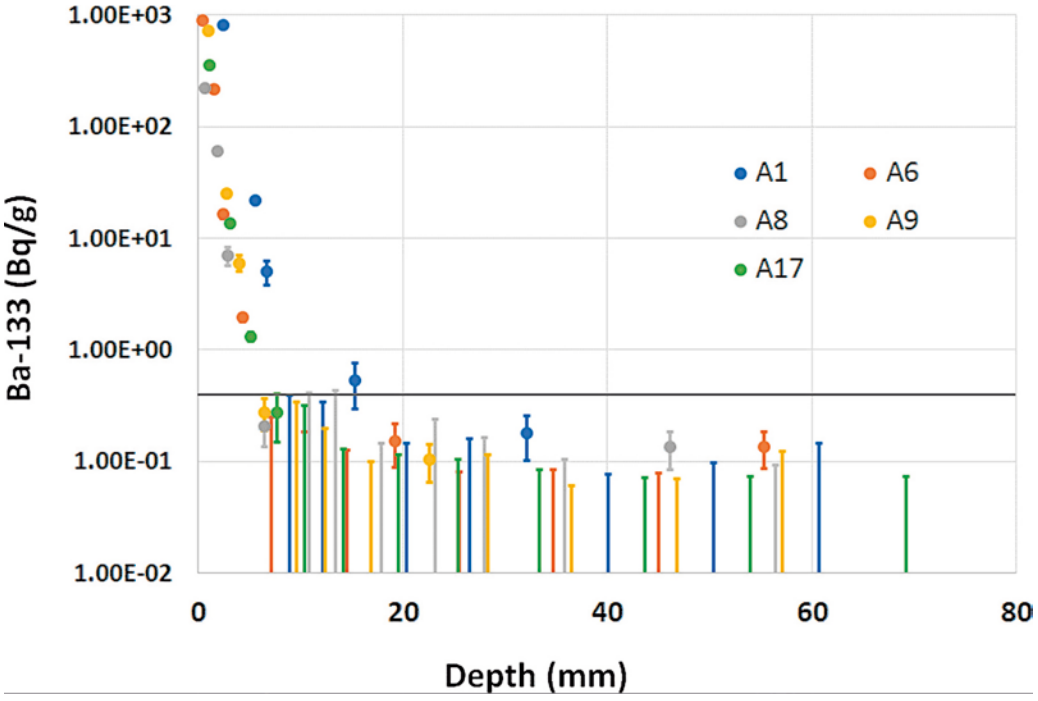

Figure A-16. *Penetration profiles of Ba-133 in A-samples, tracers measured on crushed rock material, obtained from sliced drill core. The dark grey line represents the Potential contamination level for sliced and crushed samples, see Table 3-1.*

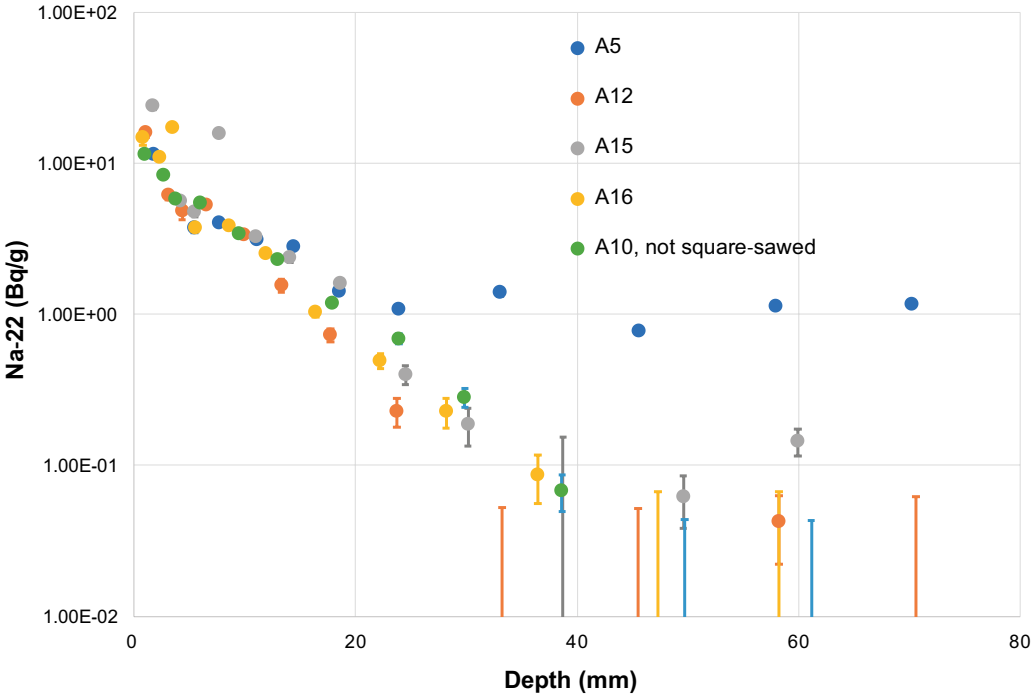

Figure A-17. *Penetration profiles of Cs-137 in D-samples, tracers measured on entire core slices and no crushing of the rock was applied. Slice 9 in each D-core (if present above detection limit) has a black border line and the dark grey line represents the Potential contamination level for sliced samples, see Table 3-1.*

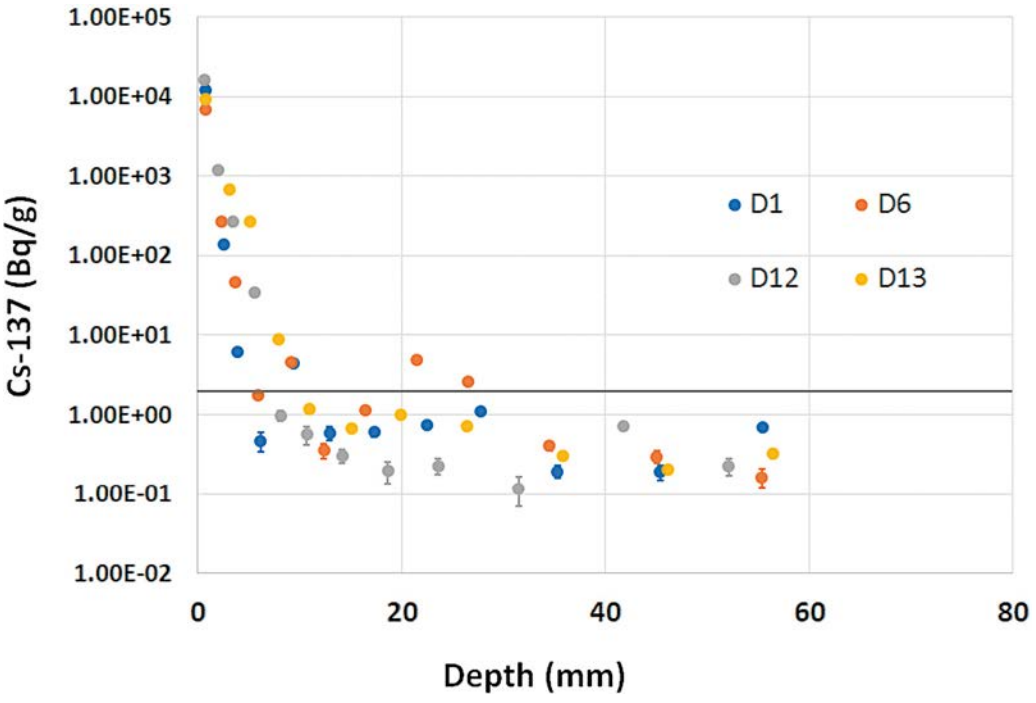

Figure A-18. *Penetration profiles of Cs-137 in D-samples, tracers measured on crushed rock material, obtained from sliced drill core. The dark grey line represents the Potential contamination level for sliced and crushed samples, see Table 3-1.*

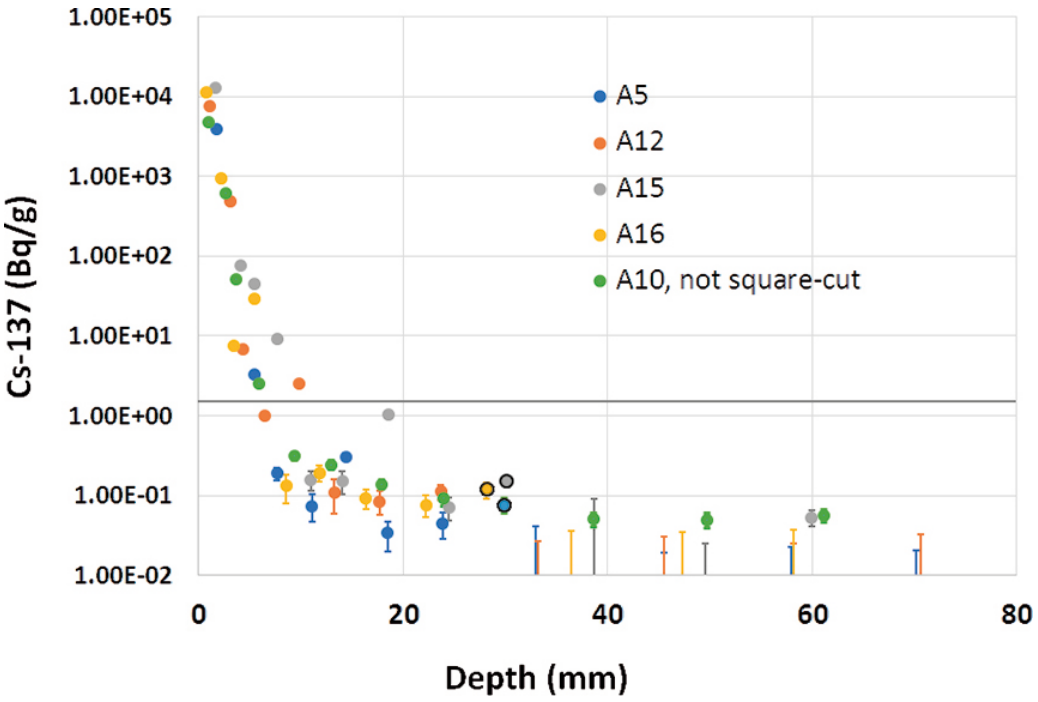

Figure A-19. *Penetration profiles of Cs-137 in A-samples, tracers measured on entire core slices and no crushing of the rock was applied. Slice 9 in each A-core (if present above detection limit) has a black border line and the dark grey line represents the Potential contamination level for sliced samples, see Table 3-1.*

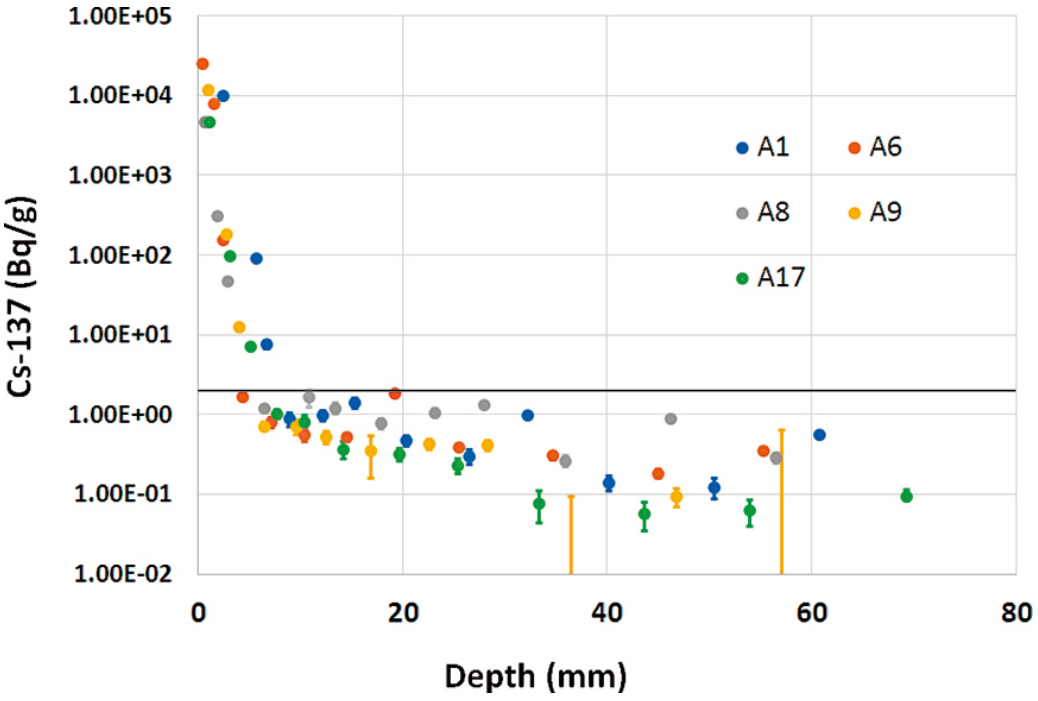

Figure A-20. *Penetration profiles of Cs-137 in A-samples, tracers measured on crushed rock material, obtained from sliced drill core. The dark grey line represents the Potential contamination level for sliced and crushed samples, see Table 3-1.*

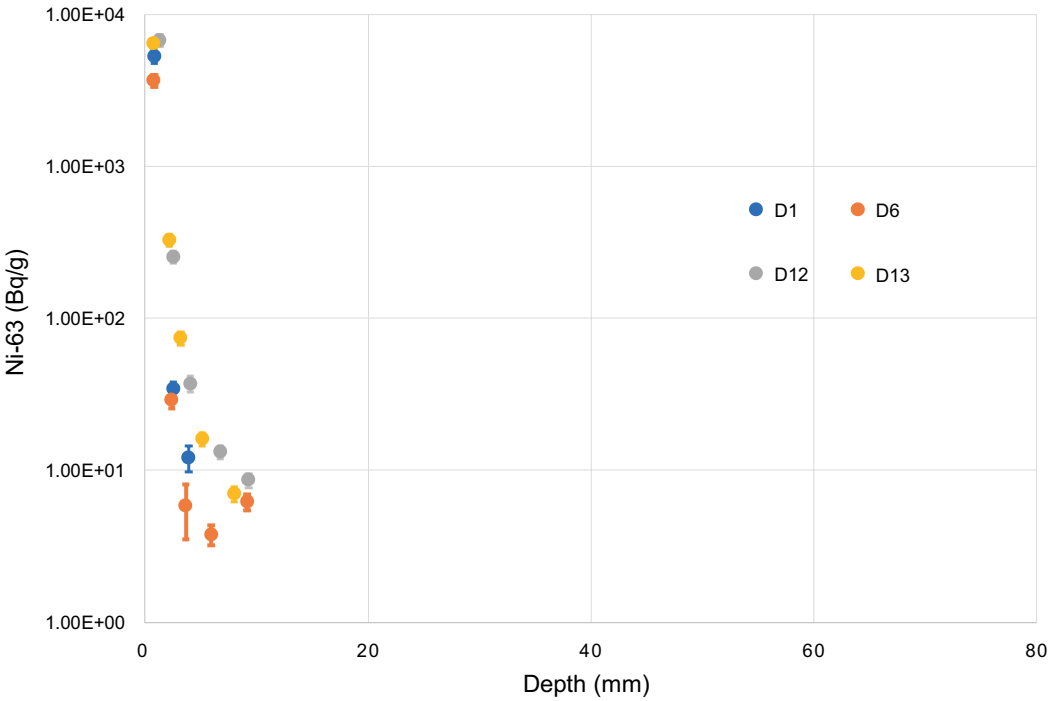

Figure A-21. *Penetration profiles of Ni-63 in D-samples, tracers measured on crushed rock material, obtained from sliced drill core.*

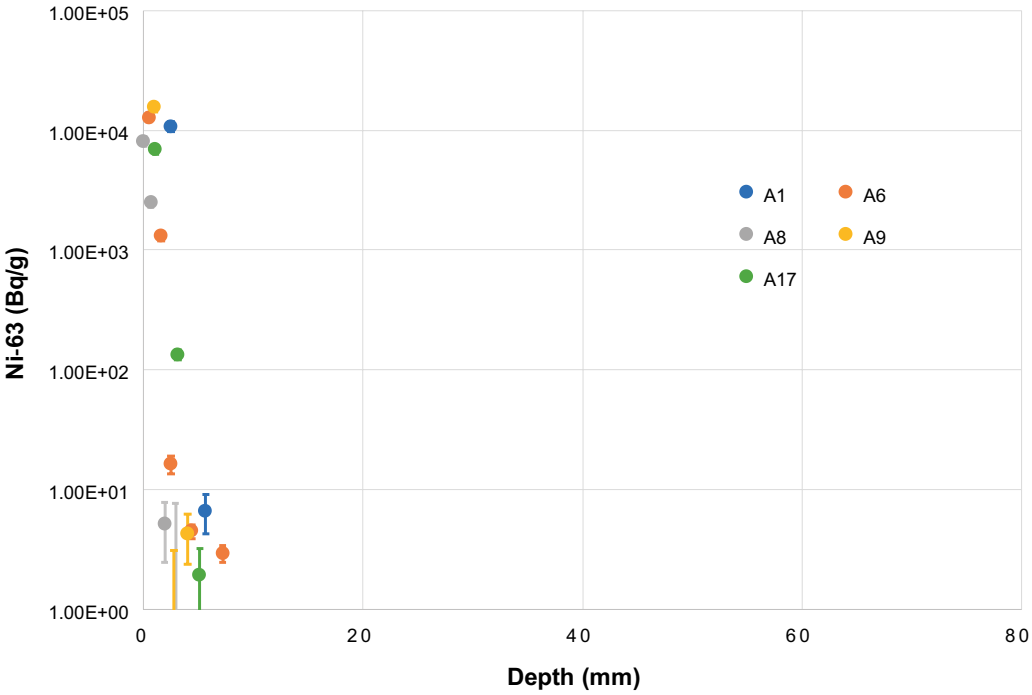

Figure A-22. *Penetration profiles of Ni-63 in A-samples, tracers measured on crushed rock material, obtained from sliced drill core.*

Arkitektkopia AB, Bromma, 2020

SKB is responsible for managing spent nuclear fuel and radioactive waste produced by the Swedish nuclear power plants such that man and the environment are protected in the near and distant future.

skb.se